THE UNIVERSITY OF QUEENSLAND

AUSTRALIA

The role of Nuclear Factor One transcription factors in cerebellar development

James Maxwell Fraser

BSc (Hons), UQ

A thesis submitted for the degree of Doctor of Philosophy at

The University of Queensland in 2020

School of Biomedical Sciences

Abstract

The cerebellum is a unique and often overlooked component of the central nervous system, with a lobular and multi-layered structure. It consists of a dense interwoven network of interacting neurons and glia with only one major output; through Purkinje neuron afferent projections. Upwards of 80% of the cells in the cerebellum are cerebellar granule neurons (CGNs). CGNs arise from highly proliferative, $MATH1^{+}$ progenitors (CGNPs) in the embryonic brain, found in a germinal region called the rhombic lip (RL). RL progenitors respond to mitogenic signals and cues initiated by transcription factors and migrate along the cerebellar anlage, forming the external granule layer (EGL). Mitogens such as Sonic Hedgehog (SHH), encourage these progenitors to proliferate in the EGL, before they differentiate and migrate inwards forming the internal granule layer (IGL). This migration results in eventual disintegration of the EGL early in postnatal development. One family of transcription factors identified to play a role in self-renewal and differentiation of stem and progenitor populations is the Nuclear Factor One (NFI) family.

NFIA, NFIB and NFIX are expressed throughout the central nervous system (CNS) and are essential for normal development. NFI-mutant mice are embryonic or postnatal lethal, with a number of developmental defects. In the cerebellum, loss of NFIX has been shown to cause delays in the development of both neurons and glia. As the cerebellum consists of almost a dozen different cell types, the first step of this thesis was to examine the cell-type specific expression of NFIX. Immunohistochemistry and co-immunofluorescence analysis revealed that NFIX is strongly expressed in proliferative progenitors in the RL, embryonic and postnatal EGL, as well as in post-mitotic CGNs in the IGL. NFIX was also expressed in Bergmann glia, and GFAP expressing astrocytes in the IGL and white matter. NFIX was expressed in stellate and basket interneurons, as well as in subpopulations of unipolar brush cells, microglia and oligodendrocytes. Interestingly, NFIX was not expressed in Purkinje neurons, despite strong NFIX expression in the ventricular and nuclear transitory zone of the embryonic cerebellum. Lastly, analysis revealed the presence of four NFIX transcript variants in isolated CGNPs. Together these findings suggest NFIX may play an extensive role in cerebellar development, especially in the maturation of CGNs.

Nfix$^{-/-}$ mice display delays in cerebellar granule neuron progenitor (CGNP) differentiation, yet the mechanisms behind this delay are yet to be determined. Using co-immunofluorescence staining with granule neuron and proliferative markers, we determined that a delay EGL differentiation is present at P15, with a higher number of proliferative and mitotically active CGNPs. Furthermore, *in vitro* analysis revealed increased proliferation of *Nfix*$^{-/-}$ neurospheres, compared to wild-type controls. As CGNPs are the cell of origin of some medulloblastomas (MB), and loss of NFIA expression has led

to poorer outcomes in mouse models of MB, we decided to look at NFIX expression in human MB cell lines. NFIX expression was markedly reduced, suggesting that NFIX is crucial for CGNP differentiation. Lastly, to identify mechanistic determinants of this developmental delay, we performed both ChIP-seq for NFIX and RNA-seq on *Nfix*$^{-/-}$ and control CGNPs at P7. Combining these data with a DNase I hypersensitive site dataset (accessible chromatin) and an RNA-seq dataset from *Math1*$^{-/-}$ CGNPs, we revealed 578 directly regulated gene targets of NFIX in CGNPs, of which 90 were co-ordinately regulated by *Math1*. One of these downstream targets was the Reelin-pathway scaffold protein *Itsn1*. We showed that like *Nfix*, loss of *Itsn1* results in a delay in CGNP differentiation, potentially exacerbated *Nfix*-mediated manipulation of *Itsn1* binding partner *Dab1*. Lastly, we also found that ITSN1 expression was downregulated in human MB cell lines. Collectively, this showed that NFI-mediation of downstream targets genes is a crucial in the regulation of CGNP differentiation,

Previous analysis has shown that NFI expression overlaps in progenitor populations in the developing CNS, suggesting a redundant, compensatory or synergistic mechanism may direct progenitor cell differentiation. Indeed, using co-immunofluorescence staining we found that NFIA and X expression overlaps in both CGNPs, postnatal CGNs and Bergmann glia throughout postnatal development. As co-expression suggests the potential for an overlapping role in development, we performed RNA-seq in *Nfia*$^{fl/fl}$; *Math1*-cre^{+} CGNPs, and compared this with our *Nfix*$^{-/-}$ RNA-seq dataset from the previous chapter, to reveal co-ordinately mis-regulated gene targets of NFIA and NFIX. Then, combining these data with a DNase I hypersensitive site dataset, and NFIX, NFIA and NFIB ChIP-seq datasets in P7 CGNPs, we reveal 304 directly regulated gene targets of NFIA and NFIX, of which 283 show co-ordinate regulation, Additionally, 282 of these contain an NFIB-associated ChIP-peak. Further examination of these targets using Gene Ontology reveal co-ordinate regulation of genes involved in nervous system development and cell differentiation, as well as a suite of other transcription factors.

Collectively, this thesis presents an in-depth characterisation of both the expression and multifaceted roles of NFI transcription factors in the postnatal cerebellum.

Declaration by author

This thesis is composed of my original work, and contains no material previously published or written by another person except where due reference has been made in the text. I have clearly stated the contribution by others to jointly-authored works that I have included in my thesis.

I have clearly stated the contribution of others to my thesis as a whole, including statistical assistance, survey design, data analysis, significant technical procedures, professional editorial advice, financial support and any other original research work used or reported in my thesis. The content of my thesis is the result of work I have carried out since the commencement of my higher degree by research candidature and does not include a substantial part of work that has been submitted to qualify for the award of any other degree or diploma in any university or other tertiary institution. I have clearly stated which parts of my thesis, if any, have been submitted to qualify for another award.

I acknowledge that an electronic copy of my thesis must be lodged with the University Library and, subject to the policy and procedures of The University of Queensland, the thesis be made available for research and study in accordance with the Copyright Act 1968 unless a period of embargo has been approved by the Dean of the Graduate School.

I acknowledge that copyright of all material contained in my thesis resides with the copyright holder(s) of that material. Where appropriate I have obtained copyright permission from the copyright holder to reproduce material in this thesis and have sought permission from co-authors for any jointly authored works included in the thesis.

Publications included in this thesis

1. **Fraser J**., Essebier A., Gronstajski R.M., Boden M., Wainwright B.J., Harvey T.J., Piper M. Cell-type specific expression of NFIX in the developing and adult cerebellum. *Brain Structure and Function 2017 Jul;222(5):2251-2270, Online Nov 2016*

2. **Fraser J.*,** Essebier A.*, Brown A., Davila R.A., Sengar A., Tu A., Ensbey K., Day B., Scott M., Gronostajski R., Wainwright B.M, Boden M, Harvey T., Piper M. 2018. Granule neuron precursor cell proliferation is regulated by NFIX and Intersectin 1 during postnatal cerebellar development. *Brain Structure and Function. March 2019, Volume 224, Issue 2, pp 811–827, Online Dec 2018*

3. **Fraser J*,** Essebier A*, Brown AS, Davila RA, Harkins D, Zalucki O, Shapiro LP, Penzes P, Wainwright BJ, Scott MP, Gronostajski RM, Bodén M, Piper M, Harvey TJ. Common Regulatory Targets of NFIA, NFIX and NFIB during Postnatal Cerebellar Development. *The Cerebellum doi: 10.1007/s12311-019-01089-3 Online Dec 2019.*

Submitted manuscripts included in this thesis

No Manuscripts submitted for publication

Other publications during candidature

1. Harris L., Zalucki O., Clément O., **Fraser J.**, Matuzelski E., Oishi S., Harvey T.J., Burne T.H.J., Heng J.I., Gronostajski R.M., Piper M. Neurogenic differentiation by hippocampal neural stem and progenitor cells is biased by NFIX expression. *Development. 2018 Feb 7;145(3). doi: 10.1242/dev.155689.*

2. Davila R.A., Harkins D., Currey L., **Fraser J**., Bowles J., Piper M. A simple, web-based repository for the management, access and analysis of micrographic images. *Journal of Molecular Histology* 2019 Dec;50(6):573-580. doi: 10.1007/s10735-019-09850-y.

Conferences

J **Fraser J.M**., Essebier A., Gronstajski R.M., Boden M., Wainwright B.J., Harvey T.J., Piper M**.** 2015. SBMS international postgraduate symposium. **Poster.**

J **Fraser J.M**., Essebier A., Gronstajski R.M., Boden M., Wainwright B.J., Harvey T.J., Piper M**.** 2016. ComBio Brisbane International Conference. **Talk.**

J **Fraser J.M**., Essebier A., Gronstajski R.M., Boden M., Wainwright B.J., Harvey T.J., Piper M**.** 2016. SBMS international postgraduate symposium. **Talk.**

J **Fraser J.M**., Essebier A., Gronstajski R.M., Boden M., Wainwright B.J., Harvey T.J., Piper M**.** 2017. SBMS international postgraduate symposium. **Poster.**

Fraser J.M., Essebier A., Brown A., Davila R.A., Sengar A., Tu A., Ensbey K., Day B., Scott M., Gronostajski R., Wainwright B.M, Boden M, Harvey T., Piper M. 2018**.** University of Otago Postgraduate Symposium. **Talk.**

Fraser J.M., Essebier A., Brown A., Davila R.A., Sengar A., Tu A., Ensbey K., Day B., Scott M., Gronostajski R., Wainwright B.M, Boden M, Harvey T., Piper M. 2018**.** ASMR postgraduate research symposium**. Poster.**

Fraser J.M. 2018. UQ Faculty of Medicine Three-minute thesis. **Talk.**

Fraser J.M., Essebier A., Brown A., Davila R.A., Sengar A., Tu A., Ensbey K., Day B., Scott M., Gronostajski R., Wainwright B.M, Boden M, Harvey T., Piper M. 2018**.** EMBL postgraduate student symposium**. Short Talk/Poster.**

Contributions by others to the thesis

Significant contributions in the form of project design and conception, overview of results and writing and proofing of manuscripts was provided by my primary Michael Piper. Other members of the Piper laboratory made contributions to the work in this thesis, in particular my co-supervisor Tracey Harvey who contributed in both conception, experimentation and analysis including purification of cells, qPCR and ChIP-seq. Alexandra Essebier performed bioinformatic analysis of RNA-seq and ChIP-seq data, provided analysis and interpretation of results and contributed figures Figure 3-6 and Figure 3-7. Figure 4-5 was also adapted from an earlier version of her work with permission. *Nfia* and *Nfib* ChIP-seq raw reads were obtained from collaborators/co-authors overseas.

Statement of parts of the thesis submitted to qualify for the award of another degree

No works submitted towards another degree have been included in this thesis

Research Involving Human or Animal Subjects

Nfix$^{+/+}$, *Nfix*$^{-/-}$ and *Nfia*$^{fl/fl}$; *Math1*-cre mice were used with approval from the University of Queensland Animal Ethics Committee (AEC approval numbers: QBI/143/16/NHMRC/ARC and QBI/149/16/ARC). *Itsn1*-deficient animals were also used in accordance with the recommendations of the Canadian Council on Animal Care and animal care regulations and policies of the Hospital for Sick Children, Toronto. All experiments were performed according to the Australian Code of Practice for the Care and Use of Animals for Scientific Purposes.

Acknowledgements

There are so many people that I need to thank for helping me through this marathon.

Firstly, to my principal supervisor Mike. Thank you for taking a chance on a microbiology student and giving me the opportunity to jump headfirst into the amazing world of developmental neurobiology. Your continual support, leadership and encouragement is all anyone could as for in a mentor and more. Additionally, thank you for fostering a research environment that encourages personal growth, scientific excellence and great friendships.

To my Associate Supervisor Tracey, and to the to the rest of the Piper lab, thank you for being such a great bunch of people and your help along the way.

I would like to thank my Associate Supervisor Brandon Wainwright for his guidance, research facility managers Shaun Walters and Luke Hammond, the QBI Animal team, members of my PhD committee and our external collaborators. I would also like to acknowledge the animals that were sacrificed as part of this research project, without of which none of this work could have proceeded.

To all my friends, thank you for keeping me sane, pushing me along and being a captive audience during my many venting sessions. To Dave, Holly and the rest of the crew, thank you for the group chats, wine and cheese nights and coffee dates. To Lachlan and Mitch, thank you for the podcast recommendations, boiled chicken and late night skype sessions. To Andy, thank you for helping to get me through Honours and my PhD, home-brews, jet-black coffees and sartorial guidance.

Lastly, I am forever indebted to my family. Dad, you ignited my passion for science at a young age with your stories, enthusiasm and wisdom. Mum, you have supported me in everything I have done, no matter the occasion. Annie, you have always been there with snippets of wisdom well beyond your years. Thank you all, and I promise I will be around more often now.

Financial support

J.F was supported by an Australian Government Research Training Program Scholarship, and this research was supported by a Cancer Council Queensland research grant.

Keywords

nfix, nfia, *intersectin 1*, cerebellum, transcription factor, medulloblastoma, granule neuron, development, neurogenesis

Australian and New Zealand Standard Research Classifications (ANZSRC)

ANZSRC code: 110902, Cellular Nervous System, 100%

Fields of Research (FoR) Classification

FoR code: 1109, Neurosciences, 100%

Table of Contents

List of Figures

List of Tables

List of abbreviations used in the thesis

ATOH1	Atonal Homologue 1
BG	Bergmann glia
BrdU	5-Bromo-2'-deoxyuridine
BMP	Bone Morphogenic Protein
BSA	Bovine Serum Albumin
CC	Corpus Callosum
CGN	Cerebellar Granule Neuron
CGNP	Cerebellar Granule Neuron Precursor
ChIP-Seq	Chromatin immunoprecipitation sequencing
CNS	Central Nervous System
DAPI	4',6-Diamidino-2-Phenylindole
DAVID	Database for Annotation, Visualization and Integrated Discovery
DCN	Deep Cerebellar Nuclei
DCX	Doublecortin
DHS	DNase I hypersensitivity
DNA	Deoxyribonucleic acid
DPI	Days Post Injection
E	Embryonic day
EdU	5-ethynyl-2'-deoxyuridine
EGL	External Granule Cell Layer
GABA	Gamma-aminobutyric acid
GBX2	Gastrulation Brain Homeobox 2
GFAP	Glial Fibrillary Acidic Protein
GNP	Granule Neuron Precursors
GO	Gene ontology
HEK298T	Human Embryonic Kidney 298T
HeLa	Henrietta Lacks uterine cell variety
HES	Hairy-Enhancer-of-Split
IGL	Internal Granule Cell Layer
IO	Inferior Olive
JAG1	Jagged-1
ITSN1	Intersectin 1
Ki67	Marker of Proliferation Ki-67
MATH1	Mouse Atonal Homologue 1

ML	Molecular layer
NeuN	RNA Binding Fox-1 Homologue 3
NFI	Nuclear Factor One
NFIA	Nuclear Factor One A
NFIB	Nuclear Factor One B
NFIC	Nuclear Factor One C
NFIX	Nuclear Factor One X
NSC	Neural Stem Cell
OTX2	Orthodenticle Homeobox 2
P	Postnatal day
PN	Purkinje Neuron
PAX	Paired-Box protein
PBS	Phosphate-buffered saline
PCL	Purkinje cell layer
PFA	Paraformaldehyde
PHH3	Phosophistone H3
PI	Post-injection
PCR	Polymerase Chain Reaction
PTCH1	Patched-1
qPCR	Quantitative Polymerase Chain Reaction
RL	Rhombic Lip
RNA	Ribonucleic acid
RNA-seq	RNA sequencing
S100β	S100 calcium-binding protein β
SEMA6A	Semaphorin 6A
SHH	Sonic hedgehog
SMAD	Mothers against Decapentaplegic Homolog
SMO	Smoothened
TAG1	Transient axonal glycoprotein 1
TBR	T-box brain protein
TF	Transcription factor
TFG-β1	Transforming Growth Factor Beta 1
UBC	Unipolar Brush Cell
VLDLR	Very low density lipoprotein receptor
VZ	Cerebellar Ventricular Zone

WM	White matter
ZIC	Zinc-finger protein of the cerebellum

Chapter 1 - **Nuclear Factor One transcription factors and the developing cerebellum.**

1.1 Scope of thesis and structure

This work conducted and constituting this thesis examines the role of the Nuclear Factor One (NFI) transcription factor family in the development of the mouse cerebellum. Primarily, this research focuses on the role of Nuclear Factor One X (*Nfix)* in the development of the most populous neuron of the cerebellum, the cerebellar granule neuron. Initially (Chapter 1), this thesis broadly reviews murine cerebellar development at a cellular level, and examines the role of transcription factors (including the *Nfi* family) in regulating stem and progenitor cell populations during neural development. Chapter 2 focuses on identifying the expression of NFIX in the embryonic and postnatal cerebellum of wild-type mice, in a number of neuronal and glial cell lineages. Next (Chapter 3), the role of *Nfix* in regulating the differentiation of cerebellar granule neuron precursors in the postnatal mouse cerebellum is explicitly examined, identifying the scaffolding protein *Intersectin 1* (ITSN1) as a directly and co-ordinately regulated target of *Nfix* and the transcription factor Mouse Atonal Homologue 1 (*Math1*). The third data chapter of this thesis (Chapter 4) investigates co-ordinate regulation of genes in these cells by *Nfia, Nfib* and *Nfix.* Lastly in Chapter 5, this thesis finishes by discussing how this new work expands on previous knowledge and repositions NFI transcription factors as central regulators of CGNP and cerebellar development.

1.2 Aims of Chapter 1

The aim of this chapter is to introduce the reader to the broad mechanisms governing both embryonic and postnatal development of the mouse cerebellum, at a gross morphological and cellular level. I aim to describe cerebellar development from two key germinal zones, the cerebellar ventricular zone (VZ) and the rhombic lip (RL), and introduce the different cell types that arise from these zones respectively; I pay particular attention to cerebellar granule neurons and their precursors. Next, I transition into identifying the role of transcription factors in regulating cerebellar development, paying particular focus to the Nuclear factor one (NFI) family. Previously, NFIs have been suggested to play a key role in promoting the differentiation of both stem and progenitor populations in the central nervous system (CNS), but this research has predominately focussed on other regions of the CNS such as the hippocampus, forebrain, corpus callosum and spinal cord. Additionally, this research is usually conducted in neural stem cells (NSCs) and glia. Thus, there is little known about the role of NFIs in the cerebellar progenitors or precursors, such as cerebellar granule neuron progenitors (CGNPs).

Early research has shown that the absence of *Nfix* in mice leads to what appears to be a delay in the differentiation or development of CGNPs, from broad histological studies suggesting that like other regions of the brain, *Nfix* regulates the differentiation of these progenitors as well. But transcription factors are far from black and white in their function- indeed the role of NFIs themselves have been shown to be very cell-type specific and may change based on the cellular context or indeed the stage of development. To address this, I aim to direct the reader to what we already know about the role of NFIs in CGNPs, specifically elaborating on proposed roles of *Nfix* in these cells and where the gaps in our knowledge lie.

1.3 Introduction

The cerebellum is a lobular, bi-hemispheric structure, situated inferior to the occipital and temporal lobes of the brain, within the posterior fossa. Historically, the cerebellum is associated with motor control, controlling functions such as the timing, co-ordination and precision of movement. However, in recent decades, the idea of the functions of the cerebellum have expanded, with prominent roles in cognition identified in humans (for an extensive review, see [1]). This multifaceted component of the brain is often overlooked in its functionality and essential role in numerous daily processes. The cerebellum is a largely unique structure in the brain, that it primarily operates with a 'feed-forward' processing system, with an immense multitude of inputs converging onto one primary output, moving in a unilateral direction [2]. Simplistically, input to the cerebellum primarily comes from mossy fibres that form excitatory synapses with cerebellar granule neurons (CGNs). These granule neurons then interact with Purkinje neurons via parallel fibres, which then in turn interact with a scarce number of deep cerebellar nuclei (DCN) embedded in the white matter. The cerebellum is also unique in that a significant proportion of its structural and morphological development occurs postnatally. Embryonic cerebellar development follows a program that has many elements, both in common and distinct to the program governing postnatal cerebellar development. Thus, to get a rounded view of cerebellar development, there is merit in investigating both embryonic and postnatal development independently. As the cerebellum is the centre of many crucial human functions, disorders and diseases during cellular development can have severely debilitating results, with disorders ranging from motor defects to devastating tumour formation [3]. Medulloblastoma, the most common primary paediatric brain tumour arises predominately in the cerebellum, with a substantial proportion having a proposed granule neuron progenitor cell of origin [4, 5]. Understanding the cell intrinsic and cell extrinsic mechanisms governing cerebellar development is essential if we are to better understand its role both in disease and as a crucial component of the brain.

1.3.1 Early embryonic development of the murine cerebellum

A significant proportion of cerebellar development occurs embryonically. In the developing embryo, the CNS is first evident as a cluster of epithelial cells, known as the neural plate. As development progresses, this plate thickens and folds dorsally to form the neural tube. The neural tube can be separated into three sections: the prosencephalon, mesencephalon and rhombencephalon, the latter of which forms the hindbrain [6]. The rhombencephalon is further divided into sections, known as rhombomeres, numbered from R0 to R7. Development of the pre-cerebellum is first evident in the mouse embryo when isthmic constriction occurs, separating the mesencephalon and the upper rhombomeres. Eventually, R0 and R1 will go on to develop into the cerebellum. Development of the early embryonic mouse cerebellum relies on the interaction of a number of different families of proteins, such as transcription factors, signalling proteins and growth factors [7]. For example, at E7.5, separation of the midbrain and hindbrain can be characterised molecularly, with expression of the transcription factors OTX2 and GBX2 confined to the upper and lower sides of the isthmus respectively [8-10]. At around E9, with the establishment of the mid-hindbrain boundary, two separate germinal zones form; the Rhombic Lip (RL) and the Ventricular Zone (VZ) and cerebellar histogenesis begins [11, 12]. The RL and VZ give rise to multiple lineages of glutamatergic and GABAergic neurons respectively. Both the RL and VZ cease to exist as germinal zones towards the end of embryogenesis (~E17.5 onwards). At around this time, the cerebellar primordium loses its smooth surface and begins to fold, a product of the formation of ‘anchoring centres’, Sonic Hedgehog (SHH) signalling and resultant CGNP proliferation [13, 14].

1.3.2 Structure of the postnatal and adult cerebellum

The adult mouse cerebellum consists of three major lobes (anterior, posterior and flocculonodular), divided into approximately 10 lobules. It has been noted that the total number of lobules and overall size of the cerebellum can vary based on the genetic background of the mouse analysed [15, 16]. The posterior lobe can further be divided into superior and inferior subdivisions. The anterior lobe consists of lobules I-V, superior posterior of lobules VI, VIIa and VIIb, inferior posterior of lobes VIIIa, VIIIb and IX, and flocculonodular lobe X [16]. From a posterior viewpoint, the vermis runs medially through the cerebellum, splitting it into two separate hemispheres. Viewing a cross section sagitally Figure 1-1), the cerebellar cortex can be broadly broken up into roughly three-four layers; the molecular layer (ML), Purkinje cell layer (PCL), internal granule layer (IGL) and the external granule layer (EGL). The latter consists of proliferative progenitor cells and is present up until the third week postnatally in mice. These progenitors eventually differentiate and migrate into the IGL. Each layer is home to a discrete population of cells that interact with one another in discrete signalling networks. In the adult cerebellum the ML is home to basket and stellate interneurons, as well as the projections of Bergmann glia and Purkinje neurons in the layers below [17-20]. Additionally, parallel fibres from granule neurons in the IGL travel up through the PCL and ML towards the pial surface where they extend tangentially. The PCL predominately contains the soma of the PNs and Bergmann glia as well as Candelabrum cells, although these have only been vaguely described in the cerebellum [20-23]. The IGL sits below the PCL and contains a multitude of cell types including: post-mitotic cerebellar granule neurons, Golgi cells, Lugaro cells, unipolar brush cells, protoplasmic astrocytes and oligodendrocytes [21, 24-26]. Importantly, it houses ascending tracts of climbing and mossy fibres as well as the descending axons of Purkinjie neurons. Below the IGL is the white matter (WM) of the cerebellum, which contains astrocytes and Deep Cerebellar Nuclei (DCN). The latter act as the primary output centres of the cerebellum, relaying information to the thalamus and descending motor tracts[27].

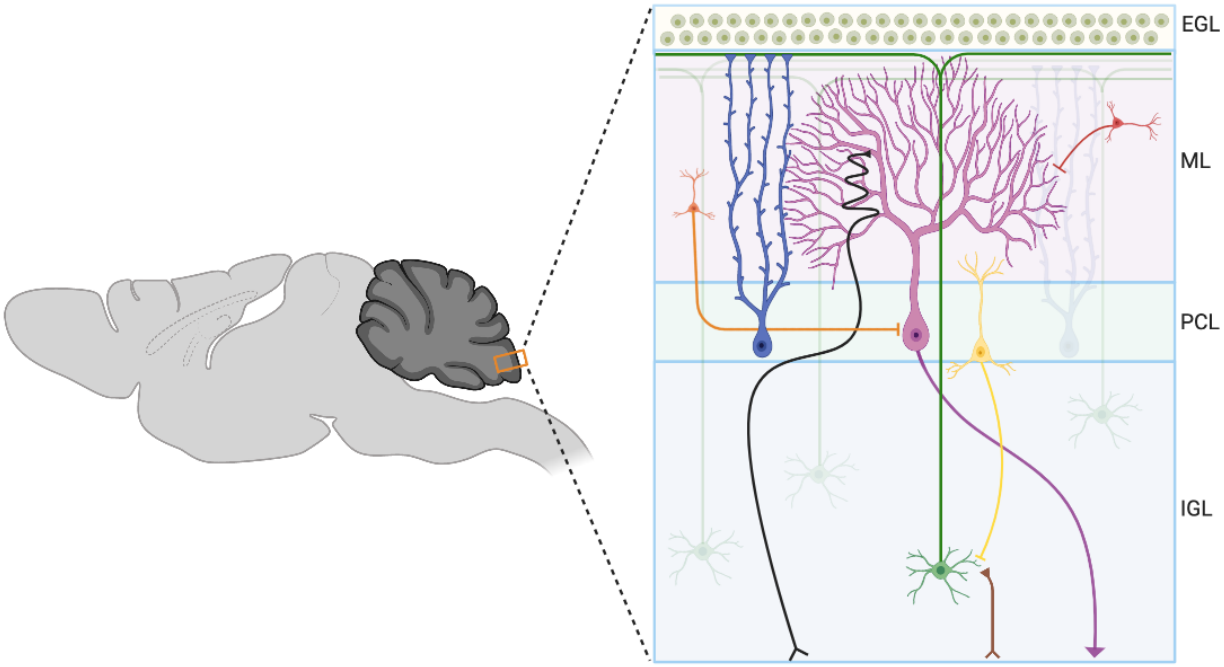

Figure 1-1 Sagittal cross section of the mouse cerebellum showing a simplified version of the cerebellar cytoarchitecture

The cerebellar cortex can broadly be divided into three or four layers, depending on the stage of development. The external granule layer (EGL) contains proliferative CGNPs (light green) which mature and migrate through to the internal granule layer (IGL). This layer is only present in adolescence and is depleted by ~P16 in normal mice. During migration, mature CGNs (dark green) extend long parallel fibers that traverse the pial surface. The molecular layer (ML) houses stellate (red) and basket (orange) inhibitory interneurons which interact with Purkinje neurons (pink) and CGN parallel fibers (dark green). The Purkinje cell layer (PCL) houses the cell bodies of Purkinje neurons and Bergmann glia (dark blue), that latter which acts as a scaffold for migratory CGNs. Golgi cells (yellow) are inhibitory interneurons generally found in the upper aspects of the IGL and interact with CGN – mossy fiber (brown) synapses. Climbing fibers (black) extend from the inferior olivary nucleus and form excitatory synapses with PNs in the ML. The sole output of the cerebellum is through long descending PN axons (pink, arrow).

1.4 Cerebellar cellular development from the ventricular zone

The cerebellar ventricular zone (VZ) is the primary germinal zone of GABAergic interneurons and DCN, Purkinje neurons and astrocytes [21, 28-31]. Cells from the ventricular zone generally follow an 'inside out' path of maturation, developing first in the ventricular zone and then in the prospective white matter (PWM) before migrating towards their terminal positions in the adult cerebellum. Progenitor cells in the VZ express the proneural bHLH transcription factors PTF1A and MASH1 during embryogenesis [28, 29, 32]. Additionally, a subset of these progenitors expressed the paired homeobox transcription factor PAX2 [29, 33, 34].

1.4.1 Golgi Cells

Golgi cells are GABAergic inhibitory interneurons and play a chief role in the organisation of spatiotemporal responses in the cerebellum. Alike with other GABAergic interneurons, Golgi cells are born out of progenitors from the VZ and undergo final maturation in the WM, as they migrate to the ML [28, 35]. They provide an inhibitory input on CGNs whilst themselves receiving inhibition from mossy fibres, which also synapse with CGNs [36, 37]. Thus, Golgi cells form both feed forward and feedback inhibitory circuits that are crucial in maintaining signalling between layers of the cerebellum [38].

1.4.2 Lugaro cells

Lugaro cells are interneurons with cell bodies located predominantly near the upper border of the IGL, just below the Purkinjie cell layer [39]. They are large GABAergic interneurons with two dendrites emerging from opposite poles of their cell body [40, 41]. Lugaro cells receive inputs from CGNs, Purkinje neurons, Basket Cells and Stellate cells. Their main axon extends from the proximal dendrite body and travels up into the ML to terminate on the dendrites of Basket and Stellate cells [41, 42]. Furthermore, they form synapses with the apical dendrites of Golgi cells. Two types of Lugaro cells have been identified in the cerebellum with slightly differing morphological characteristics, however functionality seems conserved as the two subtypes have similar synaptic connections [42].

1.4.3 Basket and stellate interneurons

Basket and stellate cells are the principal GABAergic interneurons of the molecular layer of the cerebellum [43]. Whilst both form inhibitory synapses with the secondary and tertiary dendrites of PCs, basket cells also form synapses that envelope the soma of the PC [18, 43, 44]. Additionally, Stellate cells form synapses with parallel fibres, potentially mediating synaptic efficacy in the cerebellum during motor learning [45].

1.4.4 Glia

The cerebellum is home to several main types of glia: protoplasmic velate astrocytes, oligodendrocytes and Bergmann Glia (BG). Whilst it is generally accepted that protoplasmic astrocytes, oligodendrocytes and BG develop from precursors in the VZ [46-49], the possibility of a small population of glia generated from the upper rhombic lip has been suggested, although this has yet to be proved with fate-mapping experiments [50, 51]. Interestingly, a small population of Bergmann glia has been found to arise from the postnatal EGL [52]. Furthermore, the origin of oligodendrocytes is a point of contention, with recent studies suggesting an extracerebellar point of origin [31]. BG cell bodies sit in the PCL, with long radial processes extending up through the ML to the basement membrane. These processes play a crucial role in the migration of post-mitotic granule cells from the EGL to the IGL and wrap around the dendrites of PCs in the ML [19, 20]. BG have also been suggested to act as regulators of PC and interneuron excitability in the ML [53]. Less is known about the function of velate protoplasmic astrocytes, which are found in the IGL and WM of the cerebellum [35]. It has been suggested that they play a localised role in signalling and information transfer through to the ML, through calcium-based signalling mechanisms, similar to those found in BG [54].

1.4.5 Purkinje neurons

Purkinje neurons are the largest cells in the cerebellum and are easily characterised by their shape; a large, ovular cell body located in the PCL from which extends an expansive network of dendrites up to the surface of the cerebellum. From the bottom of the soma extends a long axon that travels through the IGL to the WM, to project onto DCN [55]. In common with other GABAergic interneurons, PN are born from the ventricular zone in the developing cerebellum [34]. PNs develop between E10.5 and E12.5 in the VZ, before a majority of other GABAergic neurons and glia [48]. Early born PNs originate in the aspect of the VZ closest to the RL and migrate outwards towards the pial surface. Early during PN migration, cells form a multilayer 'Purkinje plate', in response to Reelin, initially secreted by DCNs, and then later from CGNPs in the EGL [23, 27, 56, 57]. Activation of Reelin signalling triggers PNs to disperse into a single monolayer that runs parallel to the pial surface, seen clearly in early postnatal mice [58]. Dendritic development of PCs occurs in the post-natal brain, with extensive branching of PN dendrites clearly visible in the second week postnatal. Purkinje neurons are crucial components in the complex signalling network of the cerebellum. Climbing fibres from the Inferior Olive form powerful excitatory synapses with the proximal dendrites. An interesting selection process takes place during development; initially PCs synapse with multiple climbing fibres but as development progresses, these synapses get eliminated postnatally so that in the adult brain each PC receives a single input from one CF [59, 60]. PCs receive further excitatory inputs from the interaction of CGN parallel fibres with PC dendrites near the surface of the cerebellum. Stellate and basket cells both form inhibitory synapses with distal PC dendrites, with Basket cells also synapsing on the PC soma [44].

1.5 Cerebellar development from the RL

The rhombic lip (RL) is a dorsal region of the neural tube, responsible for the generation of cerebellar glutamatergic neurons, such as cerebellar granule neurons, Unipolar Brush Cells and glutamatergic deep cerebellar nuclei [27, 30, 32]. Mouse rhombic lip precursors are identified by their expression of the bHLH transcription factor Mouse Atonal Homologue 1 (MATH1), that is in turn essential for their production [50, 61-63]. The rhombic lip is first evident from around E9 onwards, and from ~E10.5, cells begin to migrate away from the germinal zone in a stepwise manner. First, cerebellar nuclei leave the RL (E10-E12.5) followed by CGNPs (E12.5 onwards) and lastly Unipolar Brush Cells (~E14-E18). Despite the common site of origin, the developmental profile of these cells types differs greatly

1.5.1 Unipolar brush cells

Unipolar Brush Cells (UBC) are small, glutamatergic, excitatory interneurons that, like CGNs, are recipients of mossy fibre afferent outputs in the IGL of the cerebellum [64]. Slightly larger than granule cells but smaller than Golgi cells, their most striking feature is undoubtedly their solitary output- a dendritic 'brush', consisting of hundreds of fine, closely clustered dendrite branches [26]. A single mossy fibre terminal forms a giant synapse around the UBC brush, making contract with all dendrites, the largest synapse found in the CNS. UBCs can be broadly separated into two types. Type I UBCs express the calcium binding protein Calretinin whilst Type II UBCs express the metabotropic mGluR1α receptor [65].Whilst a vast majority of the immature cells in the rhombic lip are immature granule neurons, studies using the transcription factor TBR2 as a marker of UBCs have revealed that, despite previous speculation of a ventricular zone origin (VZ), UBCs are indeed produced from the MATH1$^+$ precursors in the RL [66]. Unlike CGNPs however, UBCs migrate to the IGL through the cerebellar white matter and reach their final position by P10 [66]. In their final positions, they then undergo further maturation and dendritogenesis as late as P28 in rat brains [67]. It has been noted that unlike other cells in the cerebellum, UBCs have uneven distribution, with more located in the ventral than distal lobules [68].

1.5.2 Glutamatergic Deep Cerebellar Nuclei

Deep cerebellar nuclei (DCN) are the major output sources for the cerebellum and in the adult brain, consist of a mixture of glutamatergic projection neurons and GABAergic interneurons. Glutamatergic projection neurons are the first cells generated from $Math1^{+}$ progenitors in the rhombic lip, with progenitors identified as early as E10.5 [50]. DCN are the first cells to migrate from the rhombic lip, followed by CGNPs and UBCs. In the adult brain, DCN are located in the white matter, where they receive excitatory inputs from mossy fibres [69], climbing fibres from the inferior olive [70] and inhibitory inputs from the Purkinjie cells in the PCL. DCN provide cerebellar outputs to the premotor areas as well as to the inferior olive (IO), establishing a feedback loop. In common with other cells of RL origin, glutamatergic DCN express PAX6, TBR1 and TBR2 sequentially during embryonic development [27].

1.5.3 Cerebellar Granule Neurons

Cerebellar Granule Neurons (CGN) are the most numerous neurons in the cerebellum and indeed the brain, and arise from a pool of precursors (CGNPs) that undergo clonal expansion in the RL [71, 72]. Between ~E12.5 and E16, CGNPs from the RL begin to migrate, spreading across the cerebellar anlage to form the external granule cell layer (EGL). CGNPs in the RL strongly express a number key transcription factors including MATH1[50, 61], the zinc finger proteins ZIC1 and ZIC2[73] and the master regulator of development PAX6[74]. Expression of MATH1 is associated with CGP identity and is induced by BMP/SMAD signalling from cells in the choroid plexus and the roof plate of the developing cerebellum (for a review of BMP signalling in the cerebellum, see [75]).
After rostro-medial migration from the RL, CGNPs in the EGL rapidly proliferate, driven mainly by the expression of the protein Sonic Hedgehog (SHH) from nearby Purkinjie Neurons [13].

Signalling through the Notch pathway also plays a role in encouraging expansion of CGNPs in the EGL. Activation of NOTCH2 and JAG1 stimulate proliferation, which peaks between days 7 and 10 postnatal [76, 77]. As proliferation starts to decrease, so does the expression of MATH1 in EGL cells, whilst the expression of the adhesion molecule TAG1 increases, indicating parallel fibre extension of now post-mitotic CGNs and further tangential migration. Working concurrently with this, WNT3 expression starts to inhibit CGNP proliferation by down-regulating expression of SHH and MATH1 target genes. Furthermore, BMP2 and BMP4 mediated SMAD expression supresses and overcomes the effects of SHH, allowing the switch from proliferation to differentiation in maturing granule cells [78, 79]. Once in their final position in the EGL, Semaphorin 6A (SEMA6A) helps facilitate the switch from tangential to radial migration [80], and post-mitotic granule cells extend a solitary vertical process and migrate along Bergmann glia, through the molecular layer (ML) and Purkinjie cell layer (PCL) and into their final positions in the internal granule layer (IGL) [17, 19]. Upon migration to the IGL, mossy fibres extend afferent axons to form excitatory synapses with granule cells. Receiving stimulation from mossy fibres, granule cells generate synchronous charges that travel up their ascending axons to synapses with Golgi cells [37] or Purkinjie neurons, which also receive inputs via synapses with CGN parallel fibres [81].

1.6 Cerebellar stem cells and NFI transcription factors.

It has been well established that both cerebellar neurons and glia originate from pools of neural stem and progenitor cells. At a cellular level, the cerebellum is a heterogeneous mixture of different cell types, that originate from the same stem cell pool. Thus, there is great merit in investigating what causes these stem cells to become lineage specific and lose their 'stem-ness' as it not only provides insights into the mechanisms controlling brain development, but may also as to what happens when development goes wrong. Neural stem cells are self-renewing and multipotent. They either undergo symmetric division or asymmetric division, the former giving rise to two daughter stem cells and the latter giving rise to one stem cell and one intermediate or specialised progenitor cell. The change in division, and the eventual differentiation of stem and progenitor cells is driven in part by the action of transcription factors (TF), often activating or being activated in turn by signalling pathways, such as Shh, Wnt and Notch. Transcription factors play a crucial role in regulating gene expression throughout neural development and in the adult brain. Previously, NFI family members have been shown to be highly expressed in neural stem cell and progenitor populations[82-87].

1.6.1 The NFI Family

In mammals, the NFI family of TFs consists of four members, *Nfia, Nfib, Nfic* and *Nfix*, originally isolated from HeLa cells and identified as being essential for in vitro replication of adenovirus DNA [88]. NFI proteins bind as both hetero- and homo-dimers to the nucleotide motif **TTGCC(N5)GGCAA** and have been shown to be expressed in multiple vertebrate species with very high levels of sequence conservation [89]. Additionally, one NFI protein homologue is also found in *C. elegans, Xenopus and Drosophila spp.* Interestingly, no orthologues have been found in prokaryotes. NFIs are constitutively expressed throughout the developing CNS, including in the spinal cord, hippocampus, sub-ventricular zones and the cerebellum [86, 90-92]. During development, mRNA species of all four NFIs have been identified in the brain [93]. Despite similarities in binding domains and overlapping expression of NFIs in the neo-cortex during development, no evidence of compensatory function has been found [82, 93, 94]. This may be due to differences is the C-terminal domain of the different NFI family members. Furthermore, alternatively spliced variants of all four NFIs have been discovered, with each variant having different promoter binding and thus, gene expression profiles [95].Crucially, NFIs have been shown to regulate the differentiation and proliferation of neural progenitor cells, with loss of function mutants displaying delayed glial differentiation and malformations in the structure of the hippocampus and forebrain [94, 96-98]. Furthermore, complete *Nfi* knockout models have shown similar phenotypes in the cerebellum.

NFIs have been shown to act upstream of *Tag-1* to regulate parallel fibre axon extension in CGNs indicating they might play a crucial role in progenitor maturation [99, 100].This is supported by data investigating cerebellar phenotypes in *Nfix*$^{-/-}$ mice, which display delayed differentiation and migration of progenitor cells of both neuronal and glial lineages. [91].Interestingly, *Nfi* genes have been implicated in the regulation of multiple 'late' genes governing processes including CGN maturation, parallel fibre extension and dendrite formation. These include, but are not limited to: *Tag-1*, *Wnt7a*, *Cdh2* and *Gabra6* [99-101]. The interaction with *Gabra6* is of particular interest as it selectively expressed over other $GABA_A$ receptor subunits in CGNs, and is crucial in driving granule cell dendritogenesis [102, 103]. NFIs have been found to directly bind to a consensus site in the proximal promoter of *Gabra6*, with lentiviral repression of NFIs resulting in up to a fourfold reduction in *Gabra6* expression in maturing CGNs [101].

1.6.2 NFIA

Somatic deletion of *Nfia* results in severe developmental defects in mice. On a Swiss-black background, homozygous deletion of *Nfia* results in lethality within the first day of birth for a majority of mice, with ~95% dying within the first two postnatal weeks. A similar phenotype was seen in *Nfia*$^{-/-}$ mice backcrossed onto an inbred C57BL/6 background, with loss of over 90% of mice [104]. Of the mice that survive to adulthood, all have agenesis of the corpus callosum (CC), severe hydrocephalus as well as sterility in males and low fertility in females [104]. NFIA (and NFIB) have recently been identified to play a major role in the control of the onset of gliogenesis. In *Nfia*$^{-/-}$ mice, there is a dysgenesis of the corpus callosum, related to a severe delay in the development of midline glia and their projections [105]. Previously, NFIA expression has been determined to be non-essential for cell viability and DNA replication but essential for proper neural development [104]. Recent studies in *Nfia* knockout mice elucidated possible causes of delayed brain development, including elevated doublecortin (DCX, a marker of migratory neurons) mRNA at P16, decreased levels of GABRA6 (expressed in differentiated neurons), decreased levels of differentiated astrocytes (as determined by expression of GFAP, a glial marker), increased expression of precursor oligodendrocyte markers such as SOX2, decreased size and aberrant foliation of the cerebellum and a general delay cerebellar granule neuron (CGN) migration to the internal granule cell layer (IGL) at P17 [106, 107].

1.6.3 NFIB

In the developing brain, *Nfib* has a very similar role to *Nfia* and thus, deletion results in a similar, albeit more severe, phenotype. For example, whilst both *Nfia*$^{-/-}$ and *Nfib*$^{-/-}$ mice display defects of the corpus callosum and forebrain, defects from *Nfib* knockout extend to aberrant formation of the hippocampus and basilar pons, as well as enlarged lateral ventricles and failure of glial maturation at the cortical midline[108]. Furthermore, these mice also exhibit major lung defects and subsequently die at birth[108-110]. Interestingly, *Nfib*-null mice also exhibit altered foliation of the cerebellum late in embryogenesis[108]. *Nfib* has been shown to play a role in regulating expression of cellular adhesion molecules during cerebellar development. Specifically, in *Nfib*-null mice, expression of transient axonal glycoprotein 1 (TAG1), is markedly reduced at E18 [99]. TAG1 is normally expressed in the cell body and elongating parallel fibres of late stage cerebellar granule neuron progenitors (CGNPs) and is required for path-finding of neuronal axons [111]. Thus, NFIB is proposed to affect CGNP maturation at this age [103].

1.6.4 NFIC

NFIC is expressed in the brain and is also expressed in the liver, spleen and heart [112]. Unlike other NFIs, *Nfic*$^{-/-}$ mutants do not display serious neurological or physical defects. *Nfic* is, however, essential for tooth development, with deletion resulting in major molar and tooth deformities [108, 113]. Deletion also results in the failure of odontoblasts to differentiate in the developing mouse [114]. *Nfic* has a regulatory role in modulating TGF-β1 signalling in stem cells from the apical papilla. TGF-β1 signalling is in turn, required for NFIC expression in the cranial neural crest derived dental mesenchyme (SMAD4-SHH-NFIC) [115, 116]. Interestingly, NFIC has recently been found to supress migration and invasion of breast cancer cells by modulating expression of the zinc finger transcription factor KLF4, upregulating E-cadherin expression by binding to the *E-cadherin* promoter [117].

1.6.5 NFIX

Nfix has been suggested to play a critical role in neural development, however less is known of its role compared to that of *Nfia* or *Nfib*. However, *Nfix* deficiency is linked to a number of developmental disorders. Indeed, Heterozygosity or loss of function of one allele of *NFIX* in humans results in Malan Syndrome (Sotos syndrome 2), characterised by macrocephaly, intellectual impairment, developmental delay and other CNS abnormalities[118-125]. NFIX is highly expressed in different stem cell niches in the CNS and is a mediator of quiescence in neural stem cells [83-87, 126]. NFIX has been identified as a key transcription factor involved in promoting expression of astrocyte-specific genes during development, as well as regulating the timing of progenitor cell differentiation in the hippocampus and cerebellum [91, 98]. *Nfix*$^{-/-}$ mutants display delayed eye and ear opening, slow weight gain and postnatal mortality at around ~P21 [96]. They also develop severe hydrocephalus, have partial agenesis of the CC as well as kyphosis of the spine and other bone and muscle deformities. Significantly, *Nfix*$^{-/-}$ mice have significant abnormalities of the cerebellum at both a gross morphological level and at a cellular level [91]. The *Nfix*-null cerebellum is hypoplastic in the first week postnatally and displays overgrowth and misshapen lobules in the third postnatal week. In addition to this, development of both Bergmann glia and Purkinje neurons are delayed [91]. Whilst NFIX expression has been identified in the EGL and IGL of the postnatal cerebellum, analysis has been largely limited to single-antibody immunohistochemistry without any cell-type specific co-expression analysis [91]. NFI transcription factors are ubiquitously expressed in a number of tissues throughout the body and CNS, so expression in cerebellar cells of different developmental origins in not unexpected. Indeed, extrapolating on the role of *Nfix* in neural stem cells and the brain, it is plausible that *Nfix* has a key role in the development of granule neuron progenitors in the developing cerebellum.

1.7 Identifying the role of *Nfix* in the cerebellum

Proper spatial organisation of CGNs and their progenitors, and the establishment of synaptic connections is crucial for proper morphology of the overall cerebellum. For example, in the *Nfix*$^{-/-}$ mutant the size of the cerebellum is greatly reduced [91, 96]. Furthermore, CGN, astrocyte and Purkinje cell development is also significantly delayed, with the latter showing aberrant dendritic branching at P5 [91]. Whether the changes in Purkinje neuron, granule neuron and glial development is due to cell autonomous or endogenous effects, or indeed a combination of both is yet to be determined.

It is already known that SHH expression from PNs has a major role in the proliferation and eventual maturation of CGNPs. A potential role of NFIX in this process, if any, is yet to be determined. SHH is secreted continuously from PCs from approximately E17.5 onwards [127] and binds to the Patched 1 (PTCH1) cell surface receptor. This relieves PTCH1-mediated inhibition of Smoothened (SMO), which in turn activates translocation of GLI transcription factors to the cell nucleus [128]. Interestingly, the Notch pathway protein HES1 has been shown to be a SHH-mediated direct transcriptional target of GLI2 in proliferative cells of the retina[129]. Although NFIA has recently been shown to suppress HES1 in the cerebellum[130], a relationship between HES1 and NFIX is yet to be described. Recent evidence suggests that activated Notch interferes with the transcriptional activity of NFIX in myogenic stem cells[131], so further investigation may reveal a common interaction found between NFI and Notch in multiple stem and progenitor cell types. Notch and SHH are by no means the only two pathways implicated in CGN development. Canonical and non-canonical WNT as well as BMP/SMAD signalling have been flagged to facilitate a number of processes in these cells [75, 78]. Additionally, as each pathway has dozens of cross-regulatory and independent protein interactions, it is highly possible that *Nfix* is regulating aspects of these pathways during CGNP maturation.

Determining the role of NFIX during cerebellar development needs to be approached in a stepwise manner. First, cell-type specific expression of NFIX in all major neuronal and glial lineages of the cerebellum need to be undertaken to determine where in the cerebellar architecture NFIX is potentially playing a cell autonomous role during development. Expression of NFIX for examples has not been investigated in stellate or basket interneurons. Their interaction with CGNs in the ML raises the possibility that *Nfix* deletion may have an effect on their function, maturation or morphology, whether through direct or indirect means. Compared to interneurons, we know more about the potential role of *Nfix* in cerebellar astrocytes and glia, as research has determined that

NFIX drives the expression of several astrocyte-specific genes during development [132]. Additionally *Nfix*$^{-/-}$ mutants display delayed differentiation of mature glia in the cerebellum [91]. Despite this phenotype, NFIX expression has not been characterised in these cells or in their progenitors with cell-type specific markers. Thus, the first aim of this project is to thoroughly analyse the cell-type specific role of *Nfix* in the developing mouse cerebellum. Expression of NFIX in granule neurons and their precursors needs to be established throughout cerebellar development, to determine whether NFIX plays a temporal role or continual role throughout the granule neuron life cycle. Ubiquitous expression in cerebellar germinal zones, or temporally and spatially restricted expression would provide us with a picture of the role of NFIX in the genesis of both neuronal and glial cell lineages in the cerebellum. Further, expression in multiple mature lineages of neurons and glia will clarify cell autonomous or non-autonomous roles of *Nfix,* in addition to providing a clearer picture of where NFIs fit into the developmental picture of the cerebellum, especially due to the breadth of literature demonstrating interactions between BG, interneurons and granule neurons.

Whilst co-expression analysis provides a general picture of the role of *Nfix in* germinal zones, transcriptomic profiling is needed to provide analysis at a molecular level. Indeed, the next aim of this project is to utilise both RNA-seq and ChIP-seq technologies to identify direct targets of NFIX in CGNPs. Previous research suggests a delay in CGNP differentiation in *Nfix*$^{-/-}$ mice, potentially related to an arrest of precursor cell differentiation. Therefore, comparison of both wild-type and *Nfix*-null CGNPs should provide us with a discrete list of genes involved in the proliferation-differentiation switch in these progenitors. As previously discussed, there is already a wealth of literature identifying regulators of CGNP proliferation. This experimental design presents an unbiased way to identify novel regulators of this process and validate their role in the development of granule neuron precursors.

Due to potentially overlapping expression patterns of NFIs in the cerebellum, the question arises as to whether these transcription factors have functional redundancies or complementing roles during development. We aim to address this by again conducting further transcriptomic analysis, this time utilising both an *Nfix*$^{-/-}$ mouse line and an *Nfia*$^{fl/fl}$; *Math1*-cre conditional deletion mutant, to selectively ablate NFIA expression in CGNPs. This will shed insight into whether or not these transcription factors work co-ordinately or in tandem to drive CGN development and differentiation.

Overall, this work will provide a comprehensive picture of NFI-mediated transcriptional regulation of the developing mouse cerebellum. NFIs have an irreplaceable role in the development of the CNS, with manipulation of their expression resulting in drastic disorder and developmental disease [96,

104-106, 108, 118-124, 133-136]. If we can better understand the role of these TFs during neurogenesis, we may better be able to conceptualise new treatment strategies and gene targets for a number of CNS tumours such as glioma and medulloblastoma, of which NFIs are suggested to play a role [133, 137, 138].

The work in the following chapter is published and the relevant citation can be found below:

Fraser J.M., Essebier A., Gronstajski R.M., Boden M., Wainwright B.J., Harvey T.J., Piper M. Cell-type specific expression of NFIX in the developing and adult cerebellum. *Brain Structure and Function 2017 Jul;222(5):2251-2270, Online Nov 2016*

Contributor	Contribution to publication
James Fraser (Candidate)	Conceptualisation and design (50%) Experimentation (75%) Analysis and interpretation (60%) Drafting and writing (45%)

For this chapter, I conducted a majority of the experimentation as well as the analysis and interpretation of the results. qPCR and transcript analysis was conducted by co-authors. Additionally, I was involved heavily in the background and design of this paper and contributed to writing and proofreading all sections of the manuscript, which were collaborative processes.

Chapter 2 - **Cell type specific expression of NFIX in the developing and adult cerebellum**

2.1 Aim and overview of Chapter 2

Chapter 2, the first data chapter of this thesis, aims to examine the expression of NFIX in the developing cerebellum to shed light on potential roles in neural development. Initially, this chapter uses IHC to examine the expression of NFIX in the embryonic cerebellum, as well as the postnatal cerebellum at from P5-adulthood. Next, it uses co-immunofluorescence staining to examine the cell-type specific expression of NFIX in a number of different neuronal and non-neuronal cell types, focusing on the postnatal cerebellum. Lastly, it examines the expression of alternate NFIX transcripts in postnatal CGNPs.

2.2 Abstract

Transcription factors from the Nuclear Factor One (NFI) family have been shown to play a central role in regulating neural progenitor cell differentiation within the embryonic and postnatal brain. NFIA and NFIB, for instance, promote the differentiation and functional maturation of granule neurons within the cerebellum. Mice lacking *Nfix* exhibit delays in the development of neuronal and glial lineages within the cerebellum, but the cell type-specific expression of this transcription factor remains undefined. Here we examined the expression of NFIX, together with various cell type-specific markers, within the developing and adult cerebellum using co-immunofluorescence labelling and confocal microscopy. In embryos, NFIX was expressed by progenitor cells within the rhombic lip and ventricular zone. After birth, progenitor cells within the external granule layer, as well as migrating and mature granule neurons, expressed NFIX. Within the adult cerebellum, NFIX displayed a broad expression profile, and was evident within granule cells, Bergmann glia and interneurons, but not within Purkinje neurons. Furthermore, transcriptomic profiling of cerebellar granule neuron progenitor cells showed that multiple splice variants of *Nfix* are expressed within this germinal zone of the postnatal brain. Collectively, these data suggest that NFIX plays a role in regulating progenitor cell biology within the embryonic and postnatal cerebellum, as well as an ongoing role within multiple neuronal and glial populations within the adult cerebellum

2.3 Introduction

The cerebellum is a hindbrain-derived structure that plays a central role in the regulation of motor control, co-ordination, and the timing and precision of movement. Consequently, disorders involving the abnormal development of the cerebellum can be severely debilitating. Furthermore, the cerebellum is prone to the development of a number of different types of paediatric and adult cancers [139, 140], highlighting the need to clearly map the expression of key genes involved in the regulation of cerebellar development, especially those genes governing cellular differentiation, identity and proliferation.

The mature cerebellum consists of multiple developmentally distinct cell types including cerebellar granule neurons, Purkinje cells, unipolar brush cells, deep cerebellar neurons and various interneurons and glial cells [21, 41, 68, 71, 72]. CGNPs are the most populous cerebellar neuron; indeed there are more of these than any other neuronal cell type within the central nervous system [141]. Developmentally, these cells arise from a highly proliferative region of the neuroepithelium known as the rhombic lip. In mice, $MATH1^{+}$ CGNPs form at the rhombic lip from approximately embryonic day (E) 12 onwards [61]. Here, they rapidly proliferate and then migrate tangentially to populate the external surface of the cerebellar anlage, forming a transient germinal zone called the external granule layer (EGL) [71]. Postnatally, CGNPs continue to proliferate, before differentiating into immature neurons, which migrate radially through the molecular layer to become mature granule cells within the internal granule layer [142]. In rodents, the differentiation of CGNPs ensures that the EGL is fully depleted approximately two weeks after birth, with the cerebellum being functionally mature around the third week after birth, [76, 143]. Granule cells are not the only cells produced in the rhombic lip, with glutamatergic deep cerebellar neurons produced between E9.5 and E12 and unipolar brush cells after E12 [61, 66].

GABAergic inhibitory interneurons, Purkinje cells and glia on the other hand, are derived from a pool of precursor cells in the ventricular zone adjacent to the rhombic lip between E10.5 and E13.5 in mice [144]. Progenitor cells from the ventricular zone follow a developmental trajectory distinct to those found within the rhombic lip. For example, Purkinje cells are generated between E11-E13 from progenitor cells within the ventricular zone, and they subsequently migrate through the cerebellar anlage to form the Purkinje cell layer underneath the EGL. Purkinje cells play a crucial role in the expansion of CGNPs within the EGL, through the secretion of Sonic hedgehog (SHH) and Jagged-1, both of which promote CGNP proliferation [13, 77]. Furthermore, recent studies

suggest that the SHH pathway is both active and required for development of interneuron progenitors in the developing cerebellum [144, 145].

Cerebellar development is largely dependent on the coordinated activity of transcription factors. For example, the sequential expression of PAX6, TBR2, and TBR1 is essential for the differentiation of radial glia within the rhombic lip into deep cerebellar neurons [27, 146]. Unipolar brush cells express PAX6 and TBR2 *en route* to the internal granule layer and cerebellar granule neurons express PAX6 throughout all stages of their development, although these cells express TBR2 only transiently during their migration from the EGL to the internal granule layer [147]. The transcription factor MATH1 is another key protein that regulates cerebellar development; indeed, all progenitor cells within the rhombic lip express MATH1 [61, 148]. *Math1* is also intimately associated with the regulation of CGNP proliferation within the postnatal cerebellum and is essential for morphological formation of this structure [62]. Indeed, *Math1*$^{-/-}$ mice, which die shortly after birth, display cerebellar defects such as the absence of the EGL [63, 149]. The importance of MATH1 in regulating CGNP proliferation is also highlighted by the fact that the overexpression of this transcription factor has been identified as a hallmark in the SHH-subgroup of medulloblastoma [150], a cerebellar cancer that is the most frequent paediatric malignancy of the brain.

Another group of transcription factors that have recently been shown to play a prominent role in postnatal cerebellar development are the Nuclear Factor One (NFI) family, which consists of four members in vertebrates: NFIA, NFIB, NFIC and NFIX [107]. These transcription factors are expressed in neural stem cell populations throughout the developing central nervous system [83, 84, 104, 151]. Critically, knockout mouse models have highlighted the role of this family in contributing to neural progenitor cell differentiation during development. Indeed, mice lacking *Nfi* genes display deficits in neural stem cell differentiation within the neocortex, hippocampus and spinal cord [104, 108]. Within the cerebellum, NFIA and NFIB are expressed in CGNPs and mature granule neurons, and at a mechanistic level, have been shown to promote migration, maturation and synaptogenesis within nascent granule neurons [99, 100]. NFIX is also expressed by CGNPs within the postnatal cerebellum, and a preliminary report revealed that mice lacking *Nfix* exhibit delayed cerebellar development [91]. However, a comprehensive analysis of NFIX expression at a cell-type specific level within the embryonic, postnatal and adult cerebellum has yet to be performed. Such an analysis is critical if we are to understand the different roles NFIX plays during development and in the adult, and to enable the interpretation of cerebellar phenotype of *Nfix*$^{-/-}$ mice. Here we address this issue using co-immunofluorescence labelling and confocal microscopy, coupled with RNA-sequencing of isolated postnatal day (P) 7 CGNPs. We reveal a broad and dynamic pattern of NFIX

expression within multiple cell types, indicative of a key role for this transcription factor in the development and ongoing function of the cerebellum.

2.4 Methods

2.4.1 Animals

C57Bl/6J mice were used in this study with approval from the University of Queensland Animal Ethics Committee (AEC approval number: QBI/353/13/NHMRC). All experiments were performed according to the Australian Code of Practice for the Care and Use of Animals for Scientific Purposes.

2.4.2 Immunohistochemistry

Mice were anesthetised and perfused transcardially with phosphate-buffered saline (PBS), followed by 4% paraformaldehyde (PFA), then post-fixed for 48-72 h before long term storage in PBS at 4°C. Whole brains (E15.5 and E18) and dissected cerebella (post-natal ages) were embedded in 3% Noble agar and sectioned in a sagittal plane at 50 μm intervals using a vibratome. Sections were mounted on slides before heat-mediated antigen retrieval was performed in 10 mM sodium-citrate solution at 95°C for 15 min. Chromogenic immunohistochemistry (IHC) using 3,3'-diaminobenzidine (DAB) or fluorescence immunohistochemistry (IF) was then performed as previously described [130]. A table of antibodies can be found in Table 1.

Table 1 Antibodies used in this chapter

Antibody	Source species	Company	Catalogue number	Dilution used	Purpose
NFIX	Mouse	SIGMA	SAB1401263	1/200; 1/1000	IF/IHC
NFIX	Rabbit	ABCAM	AB101341	1/100	IF
Ki67 (conjugated)	Rat	eBioscience	11-5698-82	1/400	IF
PAX6	Rabbit	Millipore	AB2237	1/200	IF
NEUN	Rabbit	Millipore	MAB377	1/200	IF
Calbindin	Rabbit	SWANT	CB38	1/400	IF
Parvalbumin	Mouse	SIGMA	P3088	1/200	IF
GFAP	Rabbit	DAKO	Z0334	1/1000	IF
OLIG2	Rabbit	Millipore	AB9610	1/400	IF
IBA1	Rabbit	Wako	019-19741	1/400	IF
Calretinin	Rabbit	SWANT	7699/3	1/200	IF

2.4.3 Cerebellar Imaging

IHC sections were imaged with both a 5x and 20x objective, using bright-field microscopy. For IHC, a Zeiss Axio Imager fluorescent microscope was used, with Zeiss Zen 2009 (Zeiss, Germany) software. Fluorescent sections were imaged using a 20x objective on a Zeiss LSM 510 META Inverted Confocal Microscope, using Zeiss Zen 2009 software (Zeiss, Germany). In all cases high magnification images were taken of the same lobule of the cerebellum (VI) due to its distinctive shape, and sections close to the midline were selected for analysis. In all cases we analysed expression using at least three biological replicates at each of the ages assessed. For quantification of NFIX co-expression with cellular markers in the cerebellum, approximately 200 cells (from 3 biological replicates) were counted from 1 μm-thick optical sections of the cerebellum using the cell counter plugin in FIJI (NIH, USA).

2.4.4 Granule cell isolation

CGNPs from P7 adolescent mice were isolated using the method outlined by [141] and a Papain Dissociation Kit (Worthington Biochemical, USA). Briefly, the cerebellum was dissected from three wild-type and three *Nfix*$^{-/-}$ mice and the tissue was dissociated using a 20 units/ml papain solution at 37°C for 15 mins. A single cell suspension was obtained by trituration with a serum-coated P1000 pipette tip and nuclear membranes were removed using an albumin-ovomucoid inhibitor gradient. CGNPs were separated from large non-neuronal cells using a 35%-60% percoll gradient. Purified CGNP cells were then lysed in Trizol (Ambion, USA) and RNA isolated using an RNeasy miniprep kit (Qiagen, USA). RNA-sequencing was then performed on these samples using the Illumina NextSeq High Output system (Illumina; 150 base pair read length, paired-end reads).

2.4.5 RNA-seq analysis

TopHat2 (v2.0.9) and Cufflinks (v2.1.1) were used to identify known *Nfix* transcripts (NM_001081981, NM_001297601, NM_001081982 and NM_010906) present in the RNA-sequencing results for wild type (WT) samples of P7 CGNPs [152]. TopHat2 was used to align each WT sample to the *Mus musculus,* UCSC, mm10 reference transcriptome and FASTA annotation downloaded from the TopHat Index and annotations page (https://ccb.jhu.edu/software/tophat/igenomes.shtml). Cufflinks was then used to assemble the transcripts based on the alignment files generated by TopHat for each WT sample. Cuffmerge was used to create a single assembly containing transcripts across all WT samples. All transcripts annotated with "*Nfix*", based on the label in the reference transcriptome, were extracted from the

merged.gtf result file for further analysis. Three of the four known *Nfix* transcript variants were identified from this analysis. The nucleotide sequence for all four variants was aligned using the Clustal Omega website and unique regions for each were used to quantify the level of expression by qPCR.

2.4.6 qPCR analysis

cDNA was prepared from the original RNA samples used for RNA-seq using the Superscript III Reverse Transcription kit (Invitrogen) and qPCR performed with the Quantifast SYBR kit (Qiagen, USA). Primers used for qPCR are shown in Table 2. The level of expression was calculated as the fold change compared to the housekeeping gene, *glyceraldehyde-3-phosphatedehydrogenase* (*Gapdh)*.

Table 2 qPCR primers used in this chapter

	Forward Primer	**Reverse Primer**	**Product length**
***Nfix* variant 1**	AGTCAGACCAGGGAGCCC	TCGTTGTGAATGCTGTCCG	199 base pairs
***Nfix* variant 2**	CTTCCACCAGCAGCACCAA	GGGCTCCCTGCATCCAC	154 base pairs
***Nfix* variant 3**	GCCCAACGGTAGCGGCCAGG	AAGGTGATGGAGGAGTCAAG	149 base pairs
***Nfix* variant 4**	CTTCCACCAGCACCAAGC	GGGCTCCCTGCATCCAC	151 base pairs

2.5 Results

2.5.1 Expression of NFIX within the embryonic cerebellum.

NFIX expression has been reported to be present at low levels within the EGL of E17 mice [91], but whether it is present within cells of the rhombic lip or ventricular zone that give rise to the mature cells of the cerebellum is unclear. To address this, we first investigated the expression of NFIX within the E15.5 hindbrain and cerebellum (Figure 2-1). Co-immunofluorescence labelling using antibodies specific for NFIX and the proliferative marker Ki67 revealed that NFIX was strongly expressed by proliferating cells within the rhombic lip (Figure 2-1D-D''). Expression of NFIX was also evident, albeit at a reduced level, within cells of the adjacent ventricular zone (Figure 2-1B). Expression of NFIX by cells within the developing cerebellar anlage was also detected (Figure 2-1A) these cells likely represent neurons derived from the cerebellar ventricular zone. However, despite the presence of proliferating precursor cells with the EGL, ((Figure 2-1C'), we did not detect any appreciable expression of NFIX by CGNPs at this age (Figure 2-1C). By E18, chromogenic immunohistochemistry revealed that NFIX was expressed by CGNPs within the EGL (Figure 2-2 A-C). NFIX expression was stronger in regions of the EGL closest to the rhombic lip (Figure 2-2 C'). Collectively these data reveal that NFIX is expressed in both the rhombic lip and the cerebellar ventricular zone, indicative of this transcription factor playing a role during the early stages of cerebellar specification and development.

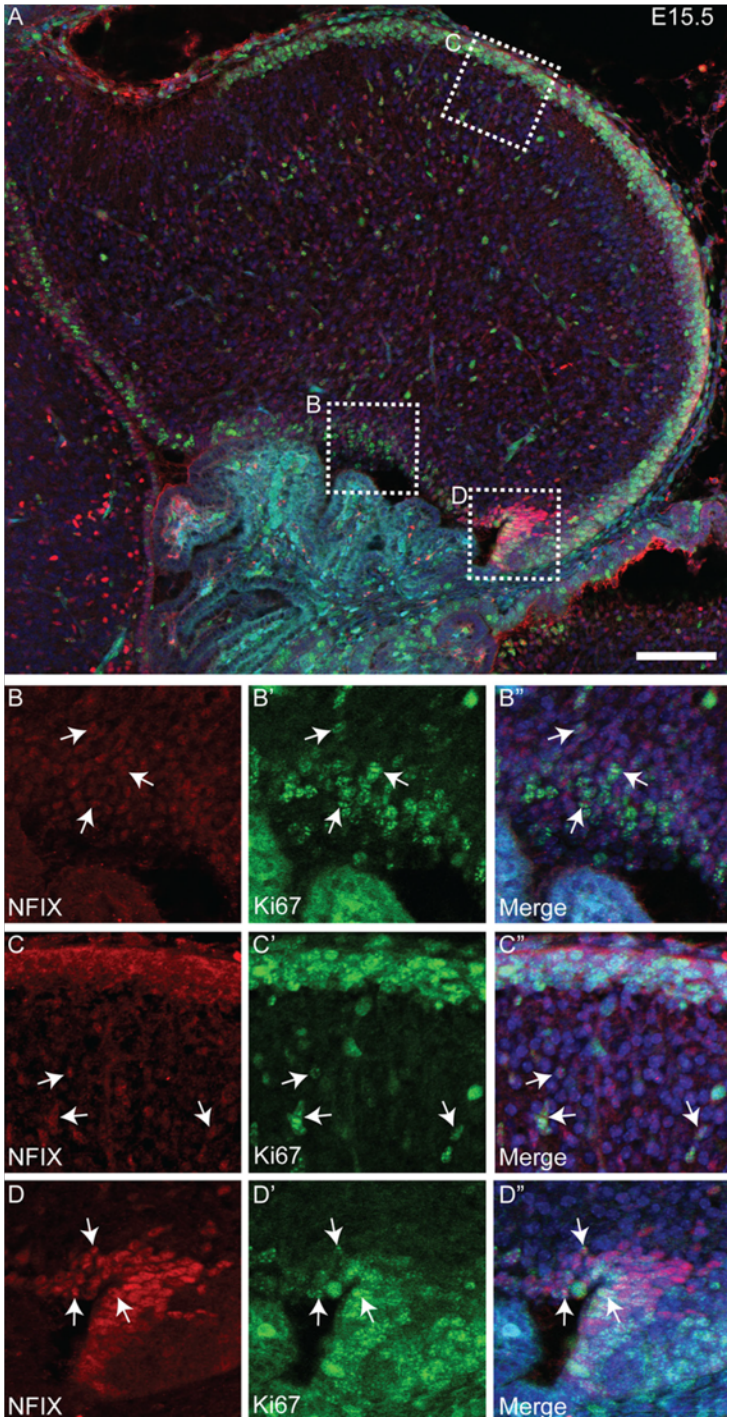

Figure 2-1: NFIX expression within the embryonic cerebellum.

(A) Mid-sagittal section of an E15.5 cerebellum stained with antibodies against NFIX red), the proliferative marker Ki67 (green) and the nuclear marker DAPI (blue). (B-B'') Cells within the ventricular zone adjacent to the rhombic lip expressed both NFIX and Ki67 (arrows). (C-C'') Within the nascent EGL, NFIX expression was not detected within the nuclei of proliferating cells at this age. Some NFIX-expressing cells were, however, observed within the cerebellar anlage (arrows). (D'-D'') NFIX was highly expressed by cells within the rhombic lip (arrows). Scale bar (in A) A =100 μm, B-D'' = 50 μm.

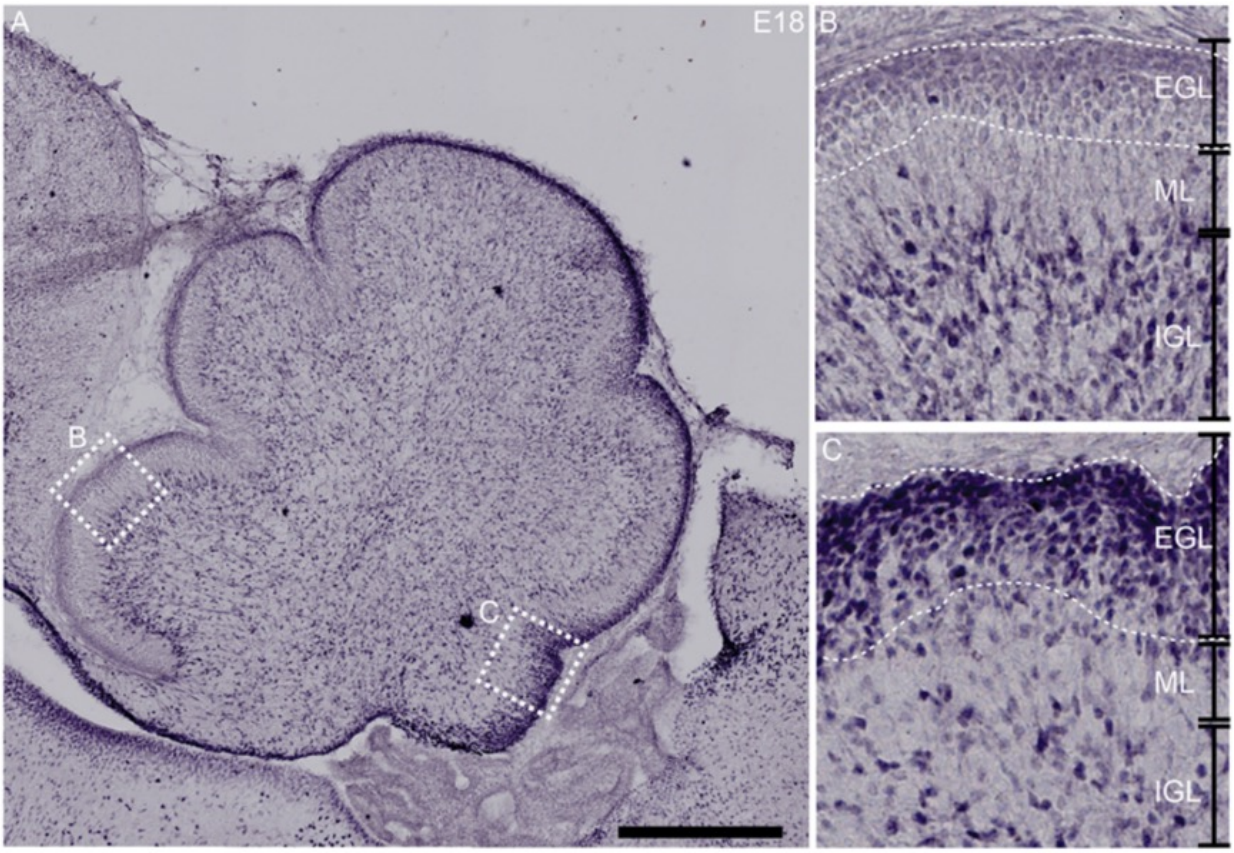

Figure 2-2 Expression of NFIX within the late-embryonic cerebellum.

(A-C) Chromogenic immunohistochemistry revealing the expression of NFIX within a mid-sagittal section of an E18 cerebellum. NFIX expression was evident within cells of the external granule layer (EGL) at this age (B, C), with EGL cells closer to the rhombic lip expressing NFIX at a higher level (C) than those more distant from the rhombic lip (B). NFIX expression was also evident within cells located in the internal granule layer (IGL) at this age. ML – molecular layer. Scale bar (in A) A = 200 μm, B-C = 75 μm.

2.5.2 Expression of NFIX within the postnatal and adult cerebellum.

NFIX is expressed by CGNPs and CGNs postnatally, and by granule neurons in the adult cerebellum [91]. Is NFIX expression confined to these cellular populations? To address this question, we first performed chromogenic immunohistochemistry within the postnatal (Figure 2-3) and adult cerebellum (Figure 2-4). This analysis confirmed the expression of NFIX by CGNPs within the EGL postnatally (Figure 2-3) and by mature CGNs at all postnatal ages including in adults Figure 2-4). Interestingly, we also observed expression of NFIX by cells within the molecular layer at all of the ages examined. Postnatally, these cells likely represent postmitotic granule neurons migrating radially into the internal granule layer. Within the adult, these NFIX-expressing cells are potentially basket or stellate cells, as these interneurons have their cell bodies within the molecular layer of the mature cerebellum [29]. In the adult cerebellum, NFIX expression was also prominent within cells located in the white matter, suggesting that NFIX may also be expressed by both glia and deep cerebellar neurons (Figure 2-4 C, D).

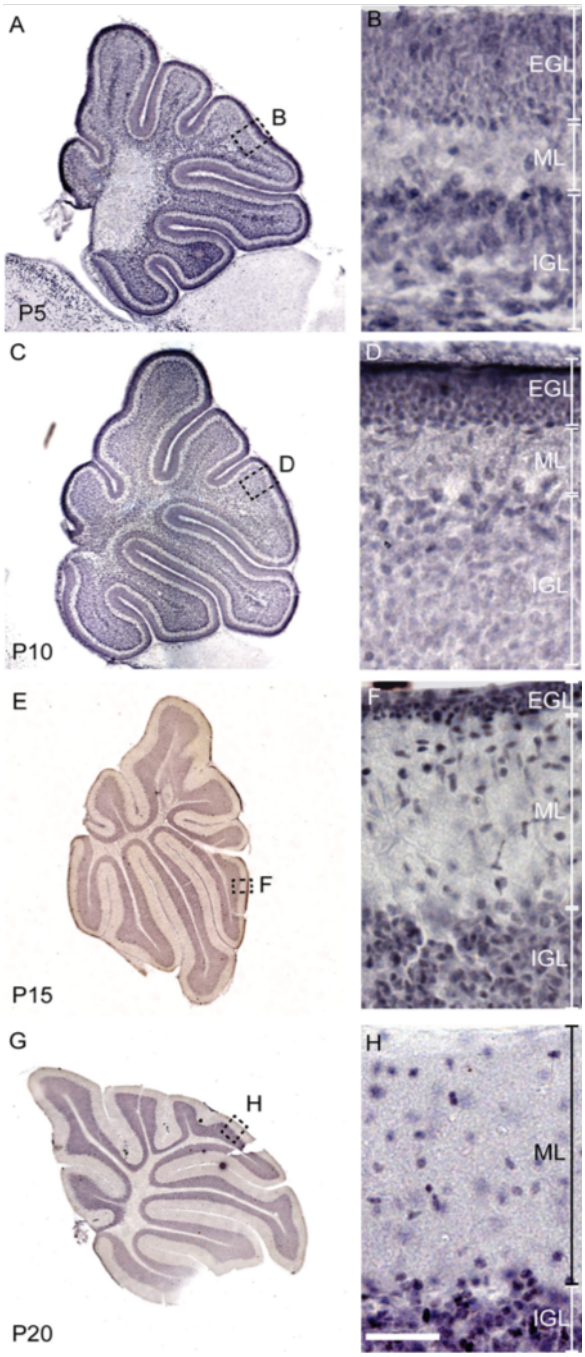

Figure 2-3: Dynamic expression of NFIX within the postnatal cerebellum. Chromogenic immunohistochemistry revealing the expression of NFIX within mid-sagittal sections of P5 (A, B), P10 (C, D), P15 (E, F) and P20 (G, H) cerebellum. At P5, NFIX expression was evident within the external granule layer (EGL) and the internal granule layer (IGL; A, B), a pattern that was replicated at both P10 and P15 (C-F). EGL cells also express NFIX at P20 (G, H). Scattered cells within the molecular layer (ML) also expressed NFIX at each of these postnatal ages. Scale bar (in H) A, C = 250 μm, E, G = 400 μm; B, D = 50 μm; F, H = 75 μm.

2.5.3 Proliferative cells within the postnatal EGL and post-mitotic cells within the IGL express NFIX.

We next analysed NFIX expression at a cell type-specific level using co-immunofluorescence labelling and confocal microscopy. Firstly, to verify the expression of NFIX by cells within the EGL of the postnatal brain we performed co-labelling with markers expressed by CGNPs, including PAX6 (Figure 2-5) and Ki67 (Figure 2-6). Between P5 and P15, NFIX expression was co-incident with both PAX6 and Ki67 within the EGL. Indeed, within the EGL of P5 mice, ~97% of PAX6-positive cells expressed NFIX, a number that was even higher at P15 (~99%). Moreover, within the internal granule layer, PAX6-positive cells were nearly all immunopositive for NFIX (99% at P5; 98% at P15). Furthermore, NFIX was co-expressed with PAX6 by immature granule neurons migrating radially through the ML into the IGL (Figure 2-5). However, not all of the NFIX-positive cells within the molecular layer were immunopositive for PAX6 or Ki67. This indicates that a different population of cells within the molecular layer of the postnatal cerebellum expresses NFIX. These are likely to be basket and stellate cells, as these interneuron populations reside within the molecular layer of the cerebellum [153].PAX6 expression is maintained by granule neurons within the internal granule layer of the adult cerebellum [154] and NFIX expression was observed in the majority of these cells within the adult cerebellum (99% of PAX6-expressing cells were immunopositive for NFIX). PAX6 and NFIX were also co-expressed by a small number of cells with in the molecular layer of the adult cerebellum (Figure 2-5). These cells are likely to be ectopic granule neurons, as previous reports indicate that stellate and basket cells express PAX2 and not PAX6 [155].

Next, we used the expression of NeuN to label post-mitotic neurons within the postnatal and adult cerebellum (Figure 2-7). NFIX was co-expressed by NeuN-positive cells localised to the inner EGL, at P5 (99%) and P15 (99%) and by mature granule neurons within the internal granule layer of the adult cerebellum (98%). We also observed a small population of cells immunopositive for both NeuN and NFIX in the molecular layer of the adult cerebellum, again likely representing ectopic granule cells , as basket and stellate cells do not express NeuN [156]. Collectively, these findings demonstrate a broad pattern of NFIX expression within both CGNPs and mature CGNs within the developing and mature mouse cerebellum.

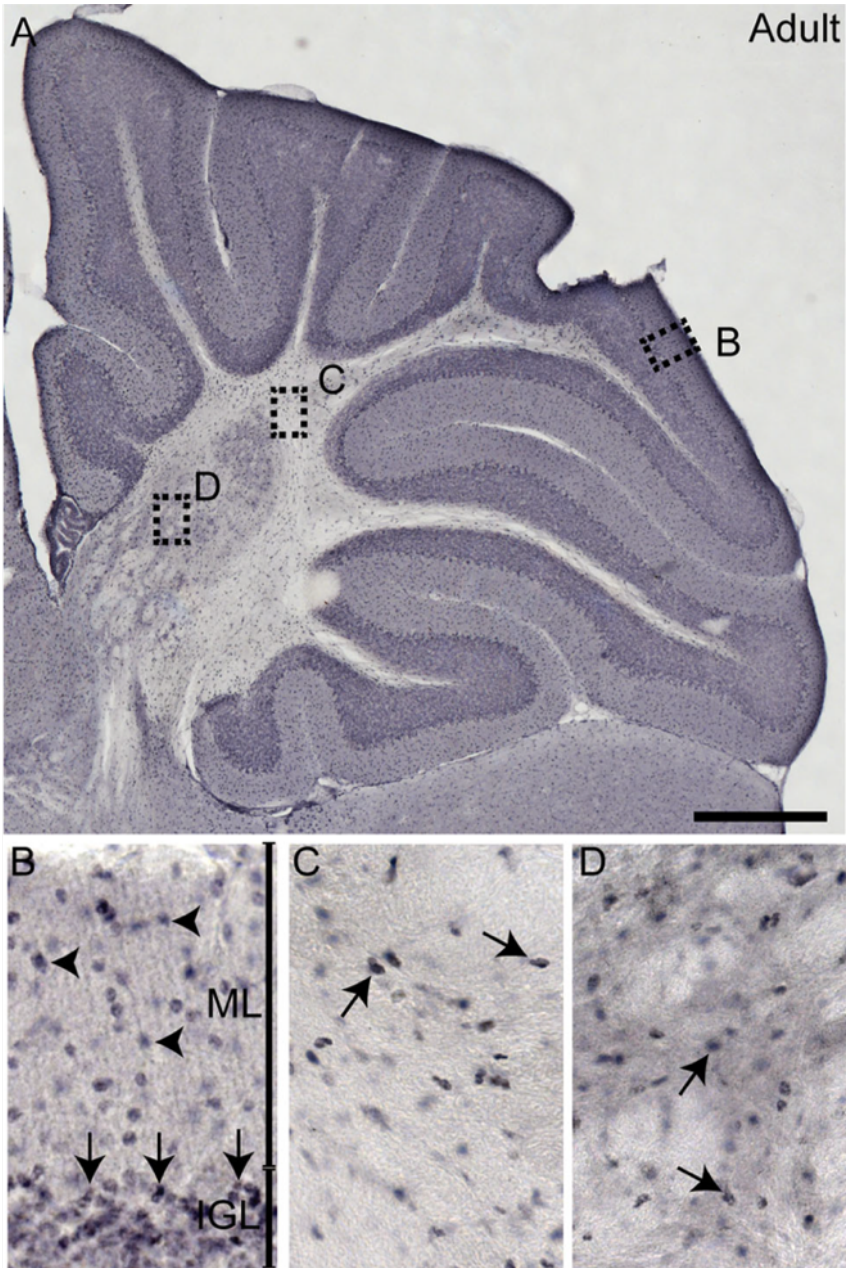

Figure 2-4: Robust expression of NFIX by granule neurons of the mature cerebellum.

(A) Mid-sagittal section of an adult cerebellum stained with antibodies against NFIX. NFIX expression was clearly evident within the granule cells in the internal granule layer (IGL; A, arrows in B). There were also many scattered cells within the molecular layer that express NFIX (arrowheads, B). Within the white matter (C, D), there were also cells that were immuno-positive for NFIX within the adult cerebellum (arrows). ML – molecular layer. Scale bar (in A) = 250 μm, B-D = 50 μm.

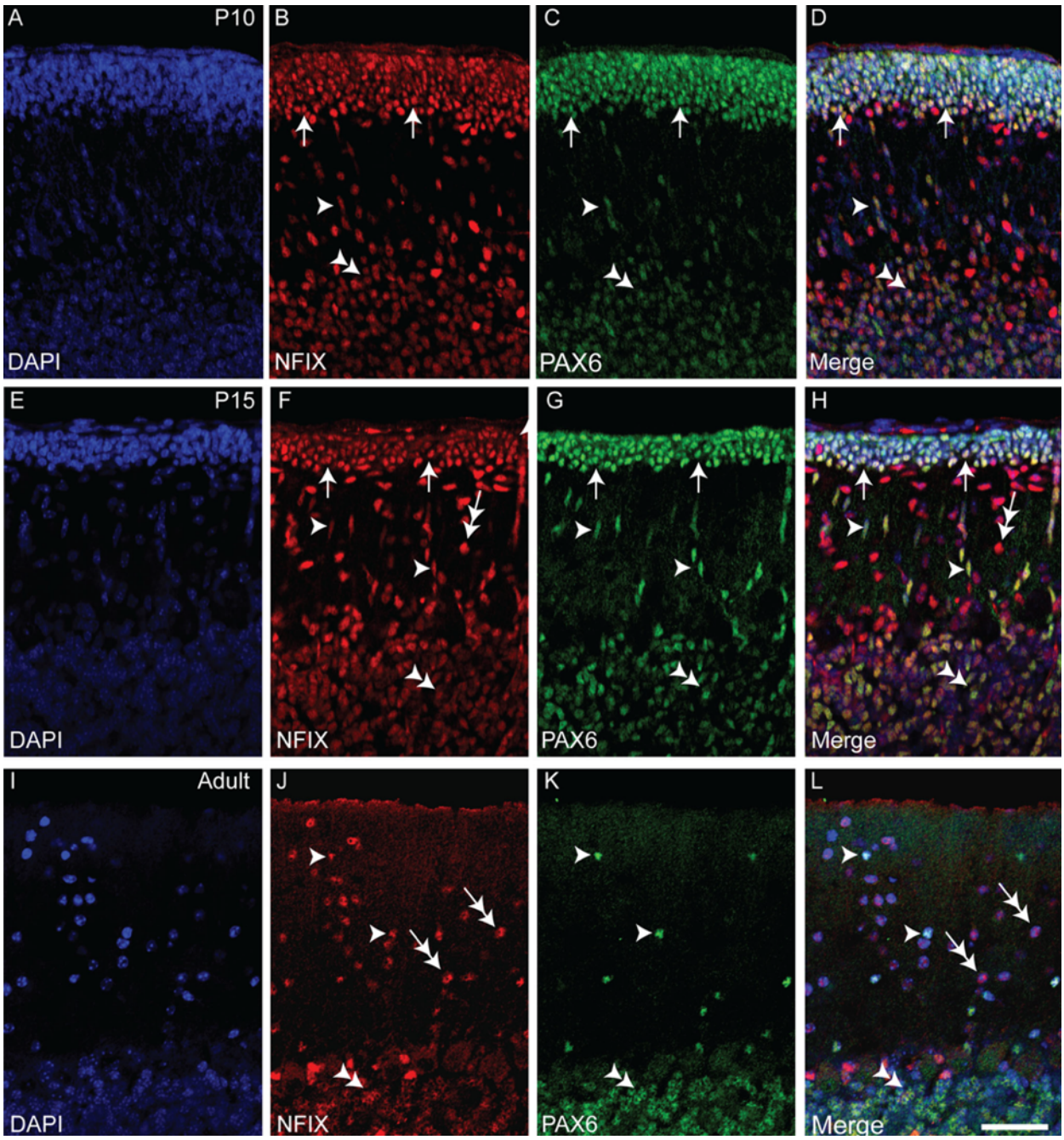

Figure 2-5: Granule neuron progenitors within the postnatal EGL express NFIX.
Expression of DAPI (A, E, I), NFIX (B, F, J) and PAX6 (C, G, K) in the cerebellum of P10 (A-D), P15 (E-H) and adult (I-L) mice. Merged panels are shown in D, H and L. PAX6 was expressed by proliferative cells within the external granule layer (EGL; arrows), cells within the molecular layer (arrowheads) and granule neurons within the internal granule layer (double arrowheads). NFIX expression was also evident within these cellular populations. Within the molecular layer however, there were also cells exhibiting NFIX expression that were not immunopositive for PAX6 (double headed arrows). Scale bar (in L) = 50 μm.

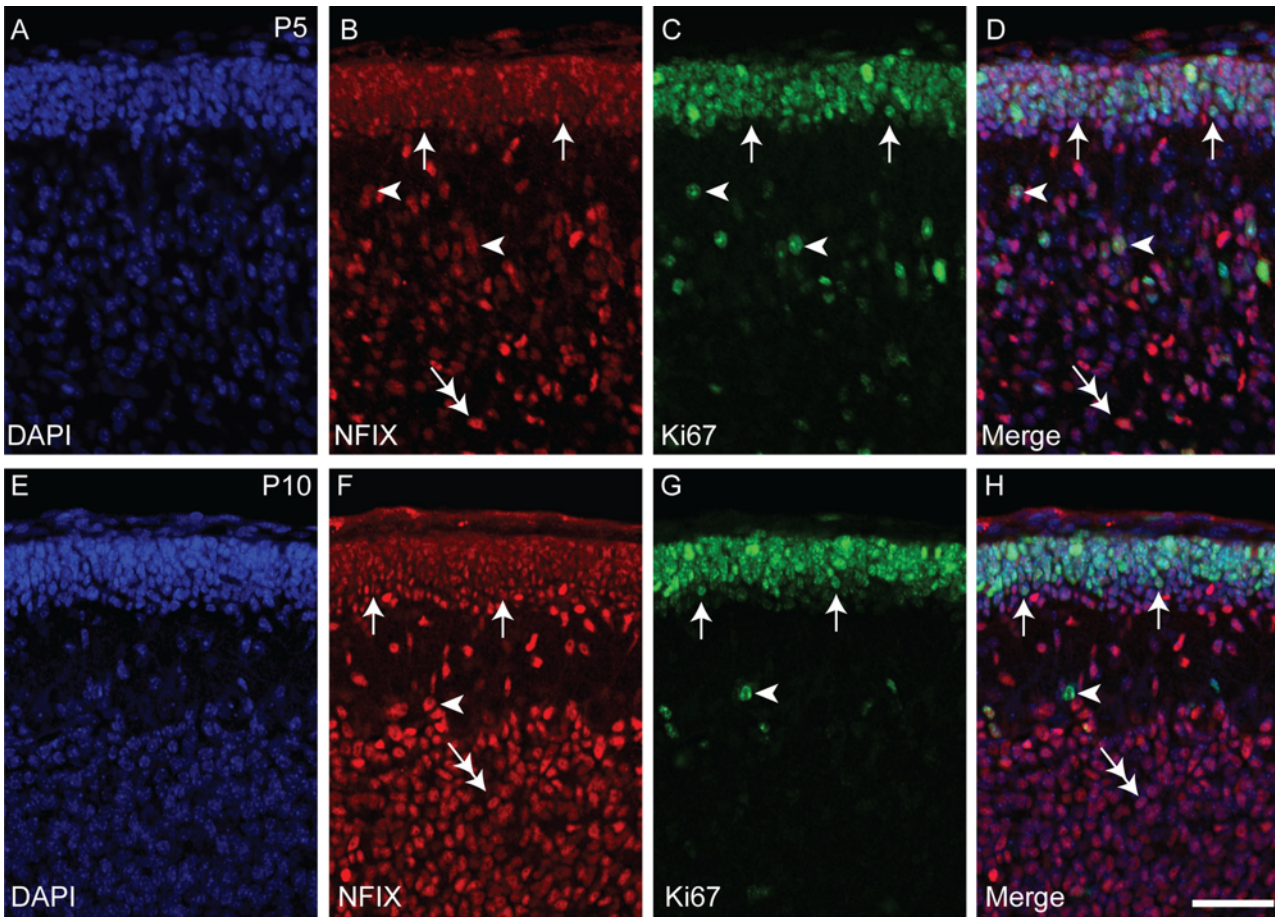

Figure 2-6 Proliferating cells within the postnatal EGL express NFIX

Expression of DAPI (A, E), NFIX (B, F) and Ki67 (C, G) in the cerebellum of P5 (A-D) and P10 (E-H) mice. Merged panels are shown in D and H. Proliferating Ki67-potitive cells within the EGL of postnatal mice co-express NFIX (arrows), as do proliferative cells within the molecular layer at these ages (arrowheads). Within the molecular layer and internal granule layer of the postnatal cerebellum there are numerous post-mitotic cells that express NFIX (double headed arrows). Scale bar (in H) = 50 μm.

2.5.4 Astrocytes and cerebellar interneurons express NFIX within the adult cerebellum.

Having established that CGNPs and their progeny express NFIX, we next sought to investigate its expression by other cell-types within the cerebellum, including GFAP-expressing astrocytes, Purkinje cells and interneurons. The cerebellum is known to contain multiple types of astrocytes. For example, Bergmann Glia play a crucial role during development in that they help guide astrotactin-expressing immature granule neurons towards the internal granule layer [19]. These cells also persist in the adult cerebellum. Immunolabelling with antibodies against NFIX and glial fibrillary acidic protein (GFAP) revealed that GFAP-expressing Bergmann glia (which have their cell bodies within the Purkinje cell layer), likely co-express NFIX within the postnatal and adult cerebellum (Figure 2-8). Similarly, protoplasmic astrocytes within both the internal granule layer and white matter of the adult cerebellum were immunopositive for NFIX. One caveat to this interpretation is that NFIX is found in the nucleus, whereas GFAP immunoreactivity is confined to the cytoplasm. As such, it can be difficult to unequivocally determine co-expression with these two markers. However, given that our analysis was performed using confocal microscopy, and that GFAP-expressing fibres were in many cases seen to envelop NFIX-expressing nuclei, we are confident that cerebellar astrocytes do indeed express NFIX. These data suggest a role for NFIX in astrocyte development and biology, a finding supported by studies *in vitro* [82], as well as the delayed cerebellar astrocyte development evident within postnatal *Nfix*$^{-/-}$ mice [91].

The presence of cells within the molecular layer that were immunoreactive for NFIX, but not for NeuN or PAX6 (Figures 4 and 6) led us to speculate as to whether interneurons also express this transcription factor. We first investigated the expression of NFIX by Purkinje cells in the developing and postnatal cerebellum. Using the expression of the calcium binding protein calbindin [156] to identify Purkinje cells, we discovered that these cells do not express NFIX either during the postnatal period, or within the adult cerebellum (Figure 2-9). Similarly, when we used a second Purkinje cell marker, parvalbumin, we did not observe any NFIX expression by Purkinje cells (Figure 2-10). However, we did observe many instances of parvalbumin-expressing cells what were also immunoreactive for NFIX within the molecular layer of the postnatal and adult cerebellum (Figure 2-10and data not shown), confirming that basket and stellate cells express NFIX within the developing and mature cerebellum.

Finally, we used the expression of calretinin to identify unipolar brush cell, and IBA1 and OLIG2 to label microglia and oligodendroglia, respectively. Analysis of cerebella from developing (P5 and P10) and adult mice revealed that NFIX was expressed by a small proportion of unipolar brush cells (6/45 cells at P5, 1/41 cells at P15, and 2/53 cells in the adult; Figure 2-11), microglia (10/37 cells at P5, 8/40 cells at P15, and 1/38 cells in the adult; Figure 2-12) and oligodendroglia (20/172 cells at P5, 14/120 cells at P15, and 30/165 cells in the adult; Figure 2-13) within the cerebellum.

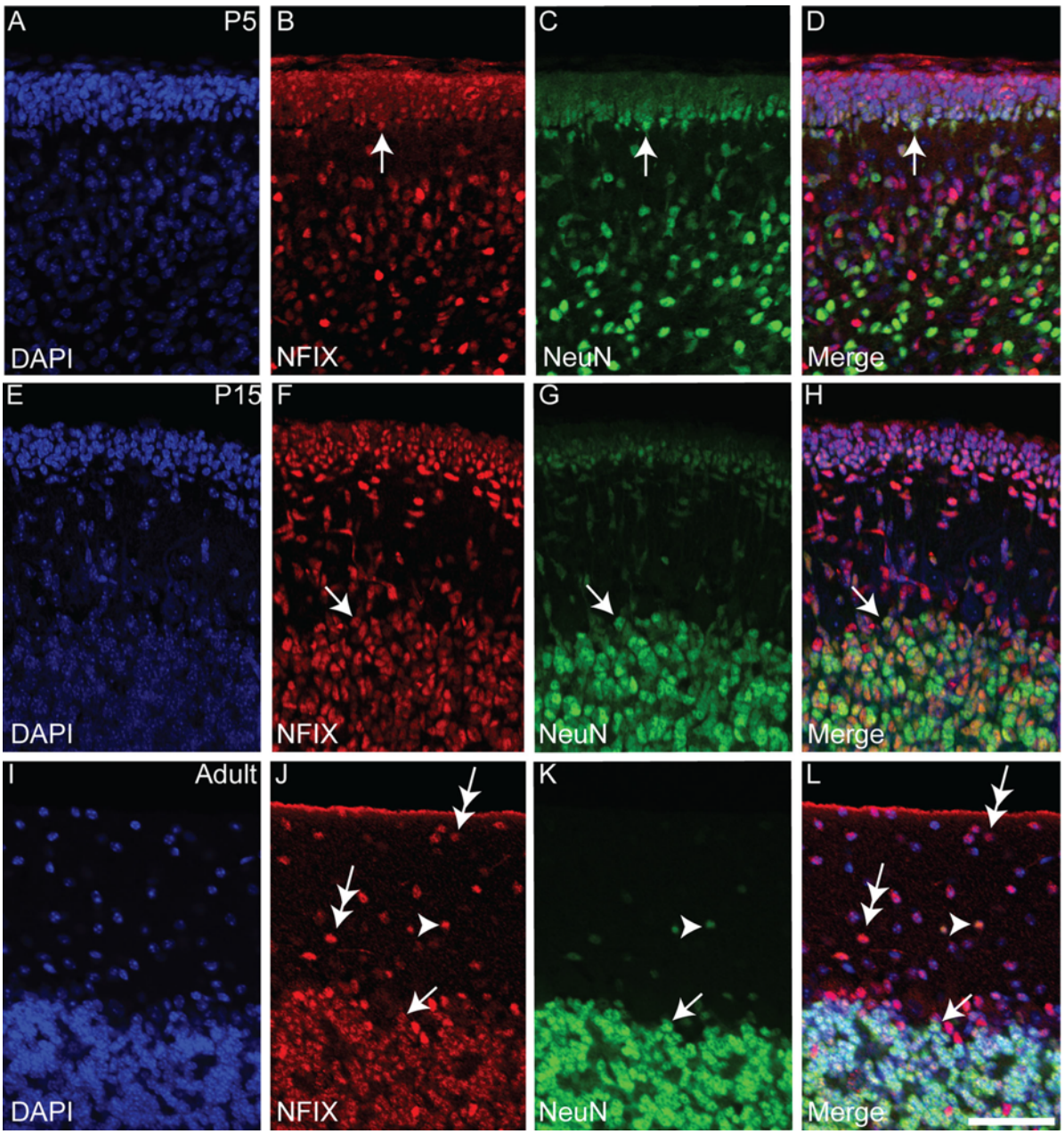

Figure 2-7 NeuN expressing neurons co-express NFIX within the developing and adult cerebellum.

Expression of DAPI (A, E, I), NFIX (B, F, J) and NeuN (C, G, K) in the cerebellum of P5 (A-D), P15 (E-H) and adult (I-L) mice. Merged panels are shown in D, H and L. At P5 and P15, NeuN-expressing cells are seen within the inner EGL, as well as the molecular layer and internal granule cell layer. These cells also express NFIX (arrows). Within the adult cerebellum (I-L) NFIX and NeuN are co-expressed by granule neurons within the internal granule layer (arrows), as well as by a small population of cells within the molecular layer (arrowheads). Interestingly, there were also cells within the molecular layer of the adult cerebellum that were immunopositive for NFIX, but not for NeuN (double headed arrows). Scale bar (in L) = 50 μm.

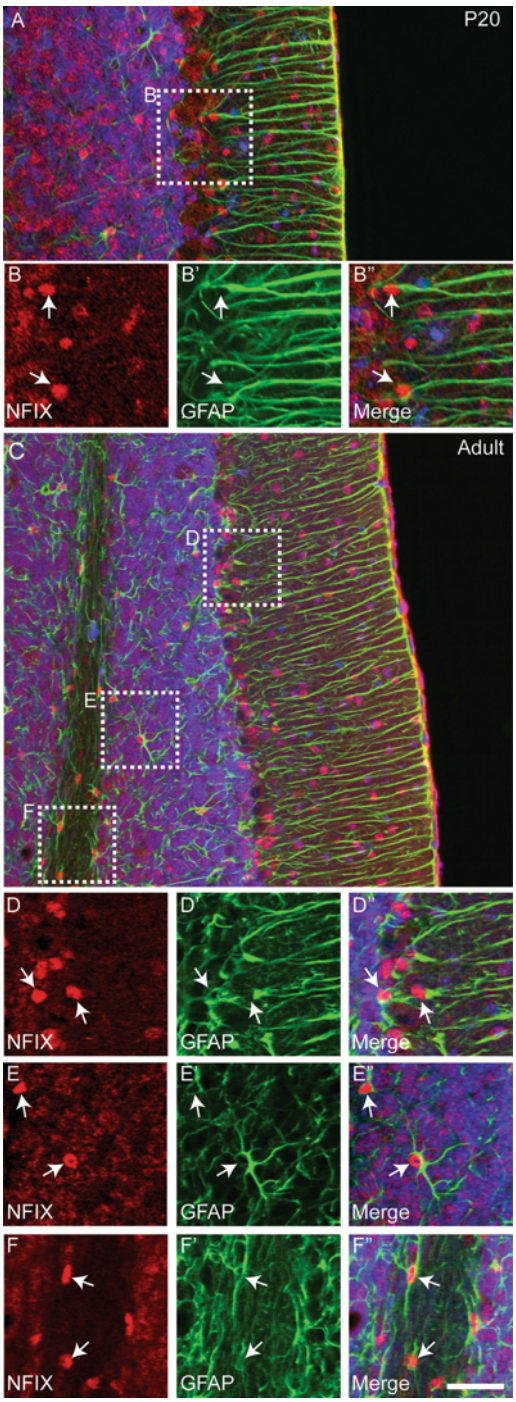

Figure 2-8 Expression of NFIX by mature astrocytes within the cerebellum.

Expression of DAPI (blue), NFIX (red) and GFAP (green) in mid-sagittal sections of P20 (A, B) and adult (C-F'') cerebellar tissue. At P20, expression of GFAP delineates the processes of Bergman glia (A, arrows in B', B''). Many of these GFAP-positive processes envelop NFIX-expressing nuclei, suggesting that these glia express NFIX. Similarly, within the adult cerebellum (C), the processes of GFAP-positive Bergmann glia encircle NFIX-expressing nuclei (arrows in D-D''), as do those in the internal granule layer (arrows in E-E'') and white matter (arrows in F-F''), indicating that many cerebellar astrocytes likely express NFIX. Scale bar (in F'') = 50 μm.

2.5.5 Multiple *Nfix* isoforms are expressed by CGNPs within the postnatal cerebellum.

Nfix, like other *Nfi* genes, undergoes alternative splicing [95, 157], but almost nothing is known about the relative expression of these transcripts within the developing brain. Given the expression of NFIX by cells within the postnatal EGL, we used a percoll-based centrifugation technique [141] to isolate a highly purified population of these cells from the cerebellum of P7 wild-type mice, in order to determine which *Nfix* isoforms were expressed at this age of development. This was achieved by isolating RNA from these cells and performing RNA-seq. Analysis of the RNA-seq data revealed that three of the four characterised *Nfix* transcripts (NM_001081981, NM_001081982 and NM_010906, respectively) were expressed by CGNPs at this stage of development (Figure 2-14 A). Although RNA-seq produces robust results, lowly expressed transcript variants can often fail to be detected during analysis. Thus, to further validate the expression of all four known transcripts, we performed qPCR on mRNA isolated from the original RNA samples used for RNA-seq (Figure 2-14 B). The data were normalised to the housekeeping gene *Gapdh*, and confirmed that the *Nfix* variant 1 (NM_001081982) was the most abundantly expressed transcript found in P7 CGNPs. Variant 2 (NM_010906) and 3 (NM_001081981) were less abundant at 2.6-fold and 28-fold lower expression levels compared to variant 1. In contrast to the data generated by the RNA-seq analysis, *Nfix* variant 4 (NM_001297601) transcript was detected, albeit at low levels, (65-fold less expression compared to variant 1). These data indicate that all of the four known *Nfix* variants are expressed within postnatal CGNPs. Similarly, we identified that multiple isoforms of other *Nfi* family members were expressed within these cells (data not shown). Collectively, these data reveal a dynamic pattern of *Nfi* isoform expression within the postnatal germinal zone of the EGL, indicative of NFIs potentially regulating different transcriptional targets via the production of different splice variants.

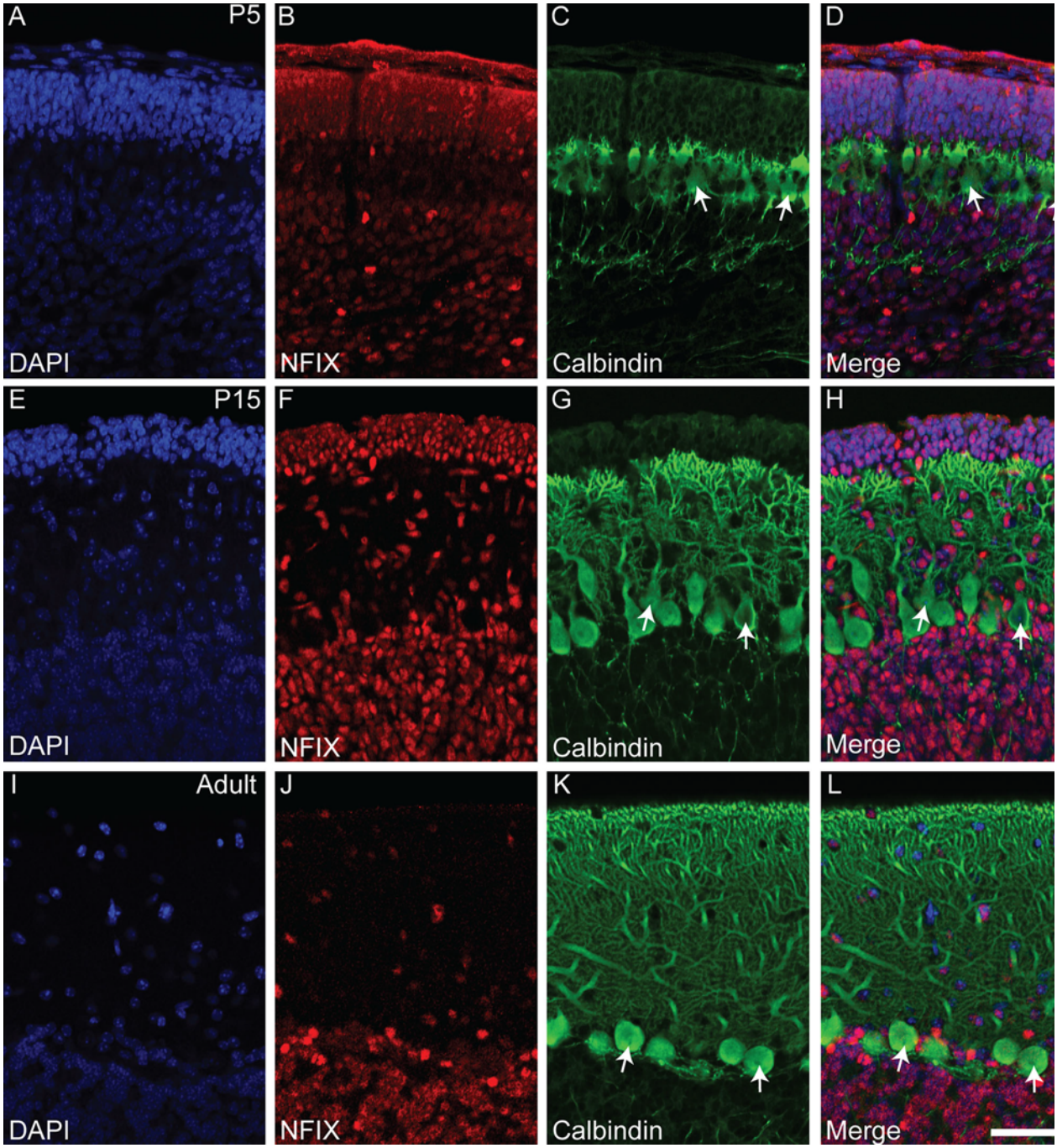

Figure 2-9 Cerebellar Purkinje neurons do not express NFIX.

Expression of DAPI (A, E, I), NFIX (B, F, J) and calbindin (C, G, K) in the cerebellum of P5 (A-D), P15 (E-H) and adult (I-L) mice. Merged panels are shown in D, H and L. Calbindin labels Purkinje neuronal cell bodies and their projections (arrows). The expression of NFIX was not detected within Purkinje neurons at either postnatal (A-H) or adult (I-L) ages. Scale bar (in L) = 50 μm.

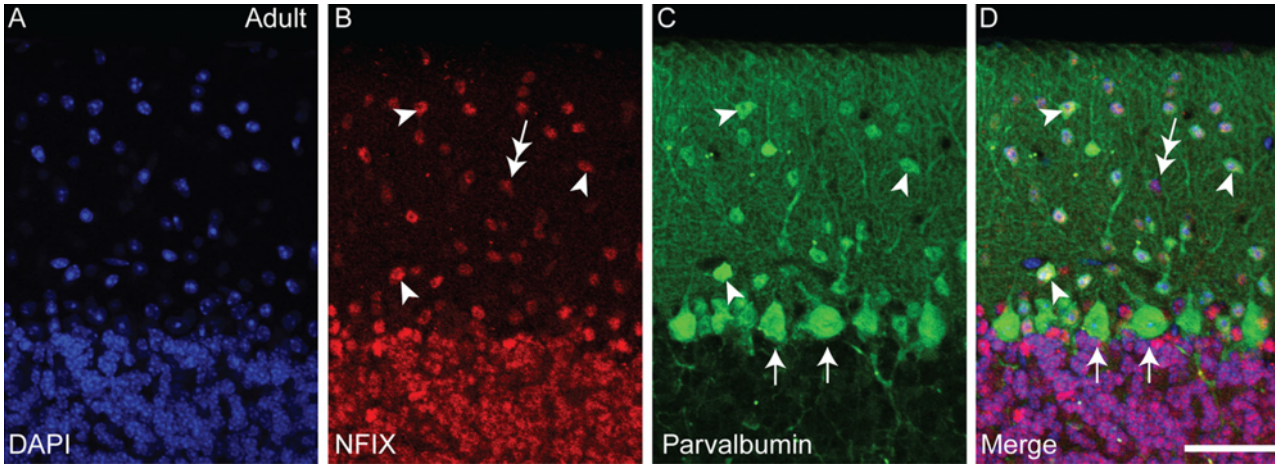

Figure 2-10 Stellate and basket neurons express NFIX within the adult cerebellum.
Expression of DAPI (A), NFIX (B) and parvalbumin (C) in the cerebellum of adult mouse. The merged panel is shown in D. Parvalbumin-expressing Purkinjie neurons were not immunopositive for NFIX (arrows). Within the molecular layer there were a population of parvalbumin-expressing cells that co-expressed NFIX (arrowheads in B-D); these are likely basket and stellate interneurons. There was also a population of NFIX-expressing cells within the molecular layer that did not express parvalbumin (double headed arrows). Scale bar (in D) = 50 μm.

2.7 Discussion:

Transcriptional regulation of gene expression plays a crucial role in many facets of development. Recent work has highlighted that the NFI family of transcription factors play a pivotal role in regulating the development of many diverse physiological systems, including the lungs [108, 109], kidneys [158], skeletal system [159], musculature [160] and the central nervous system (for a review of NFIs in nervous system development, see [90]). NFIs are intimately involved in the development of the nervous system, as evidenced by malformations in development of key structures such as the hippocampus, spinal cord and pons [108] in the absence of individual *Nfi* family members (Mason et al 2009). Interestingly, whereas the role of NFIs in promoting neuronal progenitor cell differentiation has been well studied, the role of NFIs in other cell types is less well understood. For instance, NFIA and B are widely expressed within the mature forebrain and cerebellum, but our understanding of which cells actually express NFIs, let alone what role NFIs are playing in these cells, is very limited. Here we use the developing and mature cerebellum as a model to probe the cell-type expression of NFIX. We reveal that NFIX is expressed by progenitor cells within the embryonic rhombic lip and ventricular zone, as well as by CGNPs in the postnatal cerebellum. Moreover, we demonstrate that NFIX is expressed by multiple cell types within the mature cerebellum, including granule cells, astrocytes and basket and stellate cells. These findings reveal an unexpected breadth of cellular expression that implicates NFIX in many different roles within the developing and adult cerebellum.

A key finding from this current study is that NFIX expression is evident in multiple different cell populations throughout development and in the adult cerebellum. This broad pattern of expression makes the phenotypic interpretation of full *Nfi* knockout mice difficult. Indeed, most of the studies on the role of NFIs in cerebellar development have been performed in full knockout models. Mice lacking *Nfix,* for instance, display delays in differentiation of CGNPs and subsequent granule neuron migration, but whether this arises from deficits within NFIX-expressing EGL progenitor cells themselves, or because of delays in the production of CGNPs from the rhombic lip, is unknown. How can the differing roles of *Nfi* genes be parsed in different cellular populations? This is now feasible as conditional alleles for *Nfi* genes, including *Nfix*, have been generated. This has enabled the role of *Nfix* in muscular development, for example, to be analysed in a cell-type-specific manner [161]. Looking forward, a similar approach would be a very powerful way to address the role NFIX plays in discrete cellular populations within the cerebellum. For instance, crossing the $Nfix^{fl/fl}$ line to a *Math1-Cre* line [50] would enable the role of *Nfix* within progenitor cells within the rhombic lip to be assessed. Similarly, a tamoxifen-inducible *Math1* line (*Math1 Cre-ER*) would

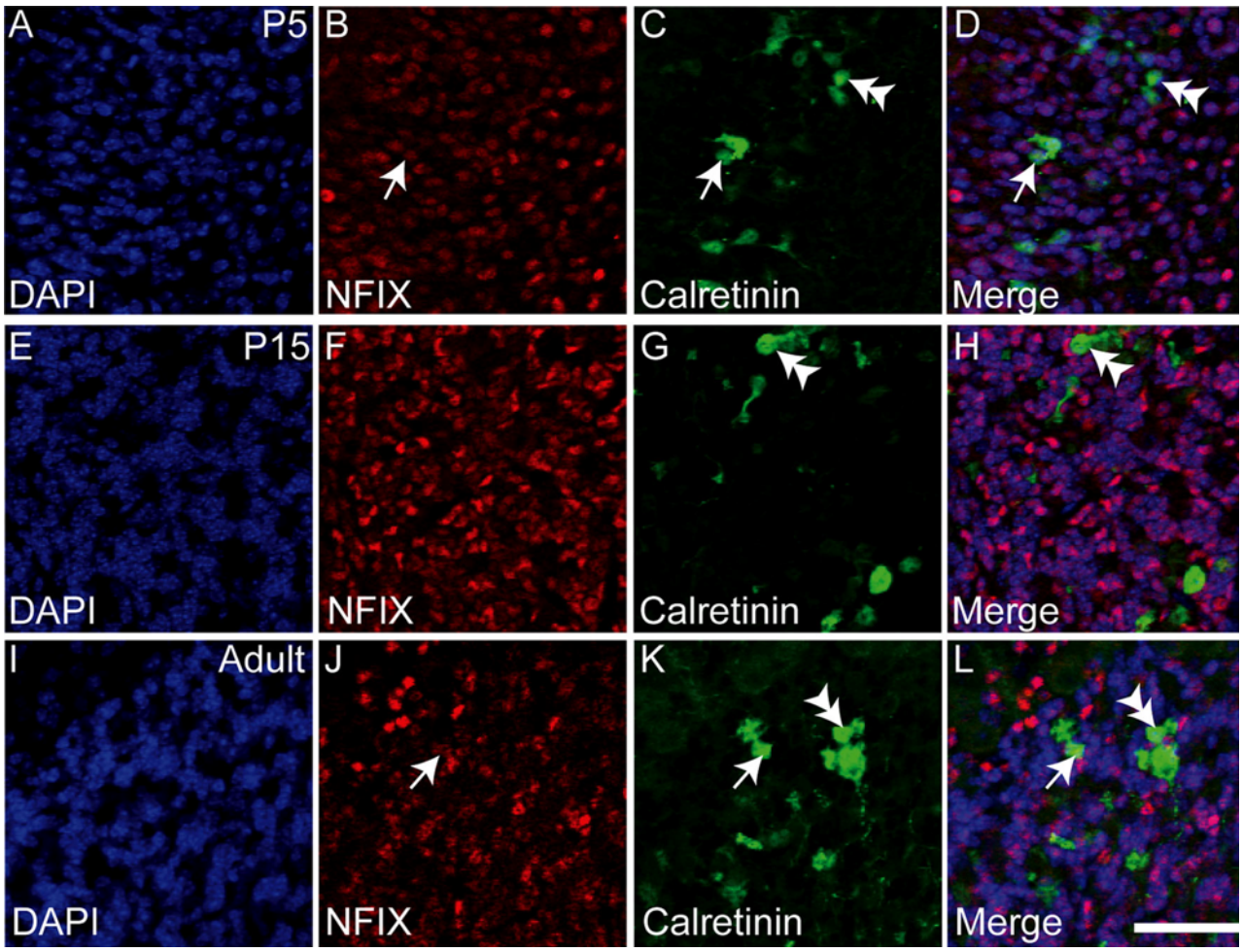

Figure 2-11 Expression of NFIX by a subpopulation of unipolar brush cells within the cerebellum.

Expression of DAPI (blue), NFIX (red) and calretinin (green) in mid-sagittal sections of P5 (a–d), P15 (e–h), and adult (i–l) cerebellar tissue. At each of these ages, expression of calretinin was coincident with NFIX in some unipolar brush cells (arrows), but not in all of these cells (double arrowheads). Scale bar (in L) 50 μm

enable ablation of *Nfix* from MATH1-expressing CGNPs in the EGL at different times during cerebellar development. This approach could also be valuable in the mature cerebellum to study the role of *Nfix* in astrocytes using the recently characterised GFAP-CreER line; the Cre-recombinase under control of a GFAP promoter [162]. Recent studies have also described inducible Cre-ER knocking lines that target GABAergic interneurons, which may allow the investigation of *Nfix* deletion in interneurons of the cerebellum, although a specific driver to target stellate and basket interneurons has not been clearly defined [163]. These experiments are critical if we are to pursue a comprehensive understanding of the role this transcription factor plays during formation and functioning of the cerebellum.

Similar to the other NFI family members, *Nfix* undergoes alternative splicing during transcription to generate distinct variants with unique gene activation and repression profiles [157]. Here we have identified and quantified the expression of four known *Nfix* variants in CGNPs isolated from the early postnatal mouse cerebellum. Previous studies have identified alternatively spliced variants of *Nfix* in many different tissues in multiple species. For example, novel *Nfix* isoforms have been identified in both dairy goats [164] and cattle [165], with varied expression levels in different tissues, suggesting *Nfix* isoform function may be relative to tissue type. Multiple *Nfix* isoforms have also been reported in human neural tissue. For instance, the human *NFI-X3* isoform is upregulated during the differentiation of astrocytic progenitors, and drives the expression of the astrocytic genes *GFAP* and *SPARCL1* in glioma cells [166]. Interestingly, the *NFI-X3* variant is also highly conserved across mammalian species [166]. We reveal here that the four known *Nfix* variants are present in cerebellar CGNPs at detectable levels via qPCR, with variants 1 and 3 showing significantly higher levels of expression. To ascertain the role of each transcript in cerebellar development, overexpression of individual variants *in vitro*, followed by RNA-seq analysis, would help to identify the relative transcriptomic changes observed when each transcript is overexpressed. In addition to this, lentiviral overexpression of individual variants could be used to determine the spatial and temporal roles of individual variants *in vivo*.

Since NFIs play a key role in regulating the differentiation of neuronal and glial progenitors [90], they may also play a role in the failure of cells to differentiate - a hallmark trait of many cancer stem cells. Indeed, NFIs have been implicated in a variety of different cancers; *Nfib* has been identified as an oncogene in small cell lung cancer, [167] and *Nfib* variants have also been linked to metastasis in osteosarcoma [168]. *Nfic* has been shown to be involved in regulation of breast cancer [117] and downregulation of *Nfia* represses tumour cell growth in oesophageal carcinoma carcinoma [169] and medulloblastoma [136, 170]. Medulloblastoma is the most common paediatric

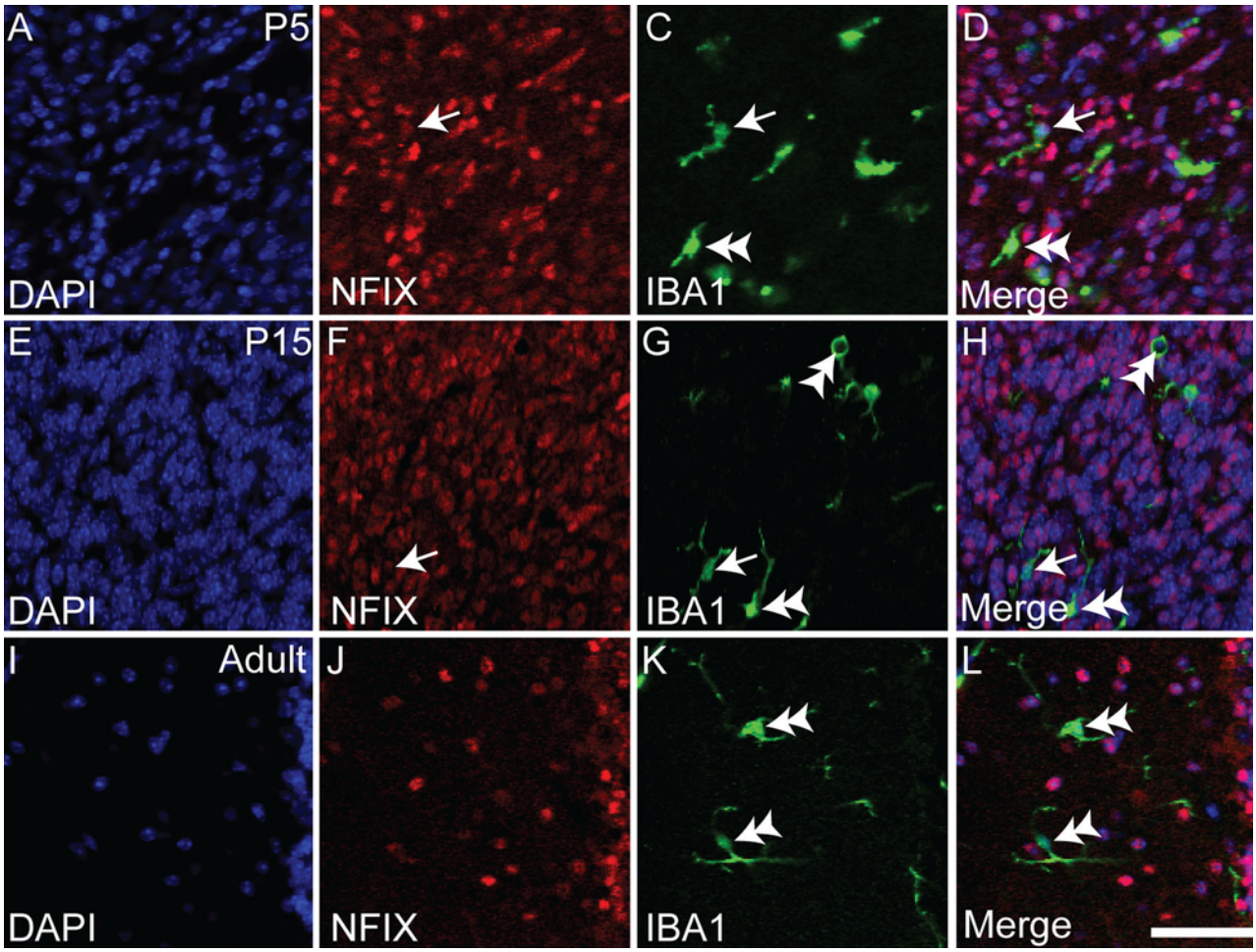

Figure 2-12 Expression of IBA1 and NFIX within the developing and adult cerebellum. Expression of DAPI (blue), NFIX (red), and IBA1 (green) in mid-sagittal sections of P5 (a–d), P15 (e–h), and adult (i–l) cerebellar tissue. Although we observed some co-expression of IBA1 and NFIX within the cerebellum (arrows), the majority ofIBA1-expressing microglia were not immunopositive for NFIX (double arrowheads). Scale bar (in l) 50 μm

malignant brain cancer in humans, with four distinct subtypes based on variable gene expression and morphological profiles [171]. In the mouse cerebellum, conditional deletion of one *Nfia* allele has been demonstrated to result in decreased tumour latency and poorer prognosis in a SHH model of medulloblastoma [136]. The overlapping expression patterns of *Nfia* and *Nfix* in the cerebellum, coupled with the delay in differentiation of CGNPs lacking *Nfix* [91] suggests that aberrant *NFIX* expression may also be a feature in some medulloblastoma patients. Future work aimed at investigating the role of NFIX in medulloblastoma biology is needed to address whether or not this factor plays a role in the formation of this malignant cancer. Both conditional deletion and overexpression of the gene *in vivo* and *in vitro* will allow us to determine the role of *Nfix* in driving tumour formation, and identify *Nfix* as a suitable marker for tumour prognosis.

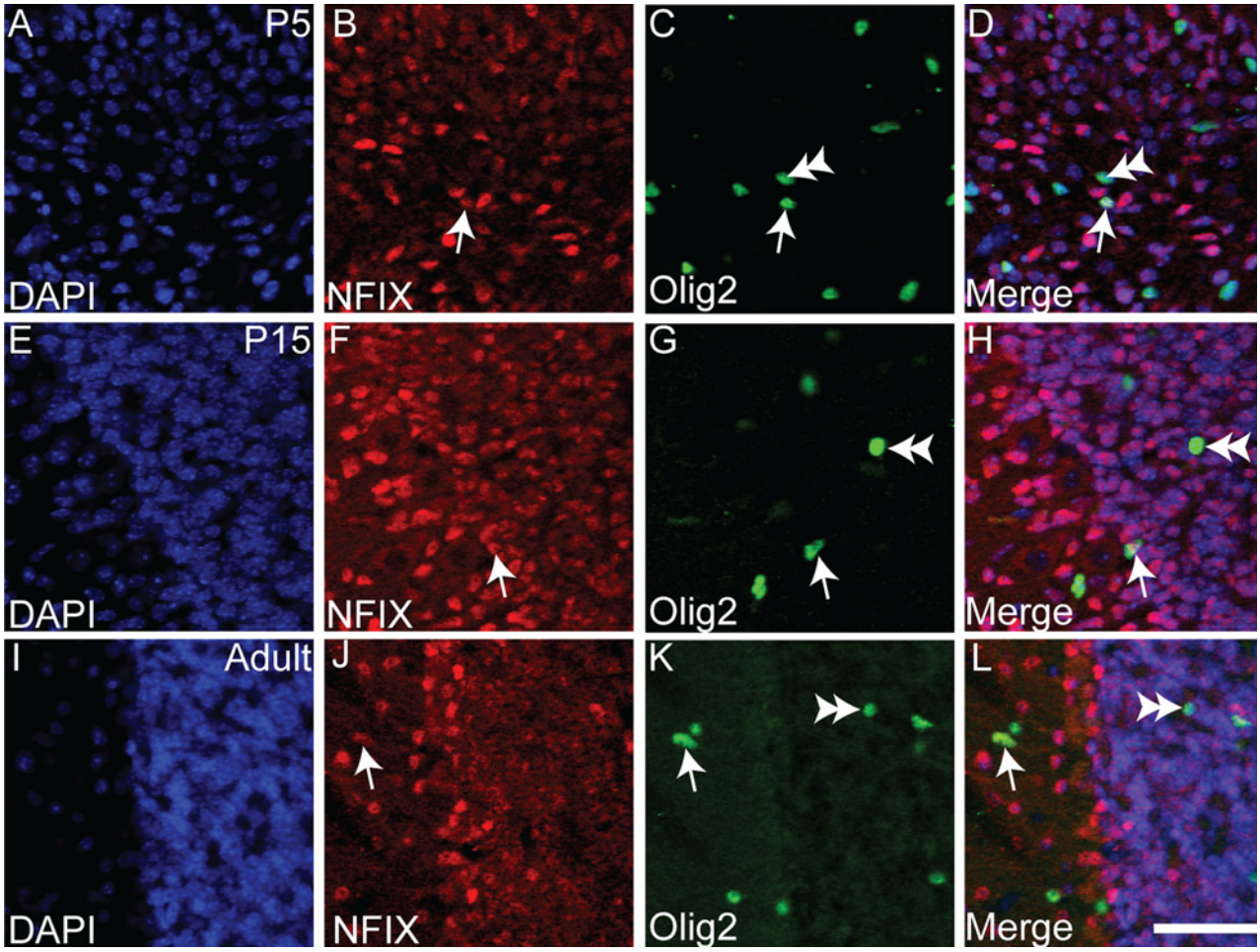

Figure 2-13 Expression of NFIX by oligodendroglial cells within the cerebellum.

Expression of DAPI (*blue*), NFIX (*red*), and OLIG2 (*green*) in mid-sagittal sections of P5 (**a**–**d**), P15 (**e**–**h**), and adult (**i**–**l**) cerebellar tissue. At each age, we observed OLIG2-expressing oligodendroglial cells that were immunopositive for NFIX (*arrows*), as well as oligodendroglial cells that were not (*double arrowheads*). *Scale bar* (in **l**) 50 μm.

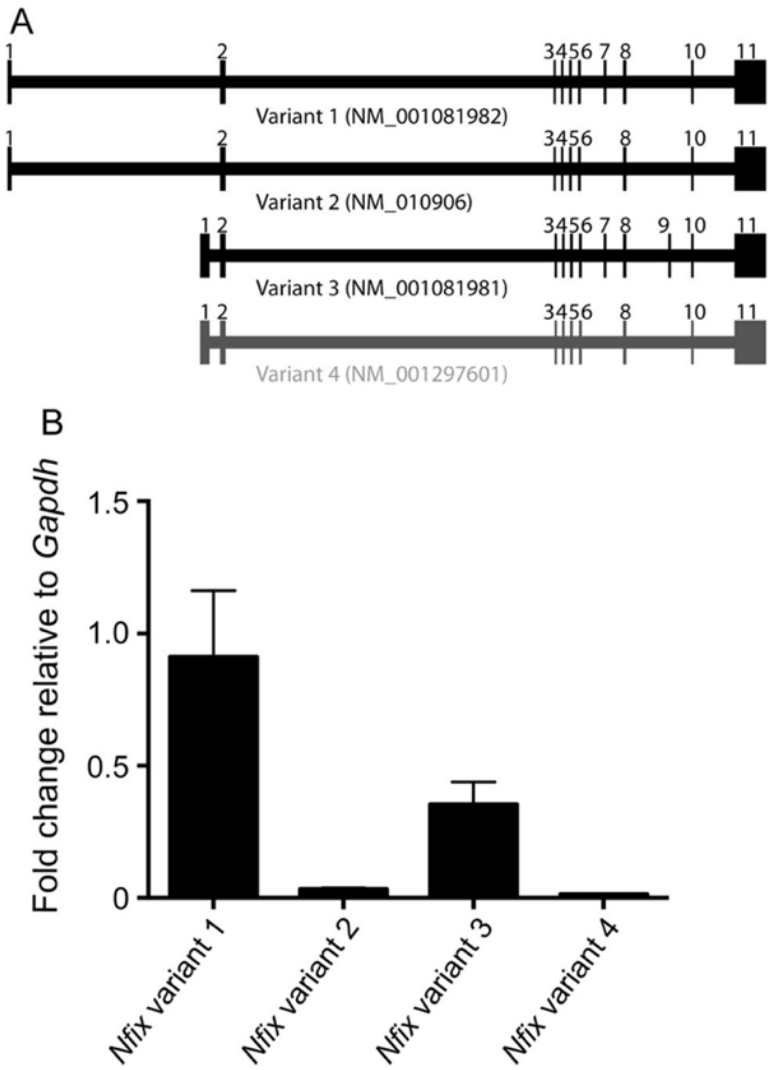

Figure 2-14 Four *Nfix* isoform variants are expressed by granule neuron progenitor cells in the postnatal cerebellum.

(A) Structure of the four characterized *Nfix* isoforms. Isoforms 1-3 were identified in the RNA-seq analysis. Variant four (shown in grey) was not sufficiently abundant to be identified in this analysis. (B) qPCR analysis performed on cDNA generated from isolated P7 CGNPs revealed that all four *Nfix* isoforms were expressed as this age, albeit with variants 2 and 4 at very low levels. Fold enrichment of mRNA expression was measured against the internal control, *Gapdh*. Error bars indicate SEM. Fold increase for each variant: Variant 1= 0.912 (± 0.251), Variant 2= 0.033 (±0.005), Variant 3= 0.354 (± 0.085) and Variant 4= 0.014 (±0.003).

2.8 Conclusions and Chapter Summary

In conclusion, the research in this chapter shows that NFIX expression is extensive throughout the development of the postnatal cerebellum. Expression is present in cell-types of unique developmental origins and persists in both progenitor and post-mitotic populations. Additionally, we show that presence of four novel isoforms of NFIX are expressed in granule neuron progenitors. Taken together, this shows that NFIX plays a diverse role in cerebellar development and raises the question; what molecular mechanisms are being manipulated by the action of this transcription factor?

The text in chapter 3was published in the journal '*Brain Structure and Function'* in March 2019. The citation is as follows:

Fraser J.M.*, Essebier A.*, Brown A., Davila R.A., Sengar A., Tu A., Ensbey K., Day B., Scott M., Gronostajski R., Wainwright B.M, Boden M, Harvey T., Piper M. 2018. Granule neuron precursor cell proliferation is regulated by NFIX and intersectin 1 during postnatal cerebellar development. *Brain Structure and Function. March 2019, Volume 224, Issue 2, pp 811–827, Online Dec 2018*

Contributor	**Statement of Contribution**
James Fraser	Conceptualisation and design (50%) Experimentation (55%) Analysis and interpretation (45%) Drafting and writing (30%)

For this chapter, I conducted a majority of the biological experimentation as well as the analysis and interpretation of these relevant results. Additionally, I was involved heavily in the background and design of this paper and contributed to writing and proofreading the manuscript. Co-authors contributed to all sections, especially RNA-seq and ChIP-seq analysis and the interpretation of these results.

Chapter 3 - **Granule neuron precursor cell proliferation is regulated by NFIX and Intersectin 1 during postnatal cerebellar development**

3.1 Chapter overview and aims

Chapter 3, is the second data chapter of this thesis. Whilst Chapter 2 explored NFIX expression patterns in wild-type mice, chapter 3 utilises the *Nfix*$^{-/-}$ mouse line, and aims to determine a) what phenotypic changes occur upon global loss of NFIX and b) how loss of NFIX affects the transcriptomic network of the developing cerebellum. This work expanded on data in Chapter 2 that showed broad NFIX expression in postnatal CGNPs. Using RNA-sequencing and Chromatin Immunoprecipitation -sequencing (RNA-seq and ChIP-seq respectively), our data show that NFIX regulates the expression of an extensive network of developmentally significant genes, a number of which are crucial for timely differentiation of CGNPs.

3.2 Chapter abstract

Cerebellar granule neurons are the most numerous neuronal subtypes in the central nervous system. Within the developing cerebellum, these neurons are derived from a population of progenitor cells found within the external granule layer of the cerebellar anlage, namely the cerebellar granule neuron precursors. The timely proliferation and differentiation of these precursor cells, which, in rodents occurs predominantly in the postnatal period, is tightly controlled to ensure the normal morphogenesis of the cerebellum. Despite this, our understanding of the factors mediating how CGNP differentiation is controlled remains limited. Here, we reveal that the transcription factor nuclear factor I X (NFIX) plays an important role in this process. Mice lacking *Nfix* exhibit reduced numbers of CGNPs during early postnatal development, but elevated numbers of these cells at postnatal day 15. Moreover, *Nfix*$^{-/-}$ CGNPs exhibit increased proliferation when cultured *in vitro*, suggestive of a role for NFIX in promoting CGNP differentiation. At a mechanistic level, profiling analyses using both ChIP-seq and RNA-seq identified the actin-associated factor *intersectin 1* as a downstream target of NFIX during cerebellar development. In support of this, mice lacking *intersectin 1* also displayed delayed CGNP differentiation. Collectively, these findings highlight a key role for NFIX and intersectin 1 in the regulation of cerebellar development.

3.3 Introduction

During nervous system development, transcription factors play a variety of key roles, including the regulation of the genes that control proliferation and self-renewal, differentiation, migration and maturation. The cerebellum provides a salient example of how different transcription factors mediate the development of neural stem cells and their progeny [91, 103, 107]. The cerebellum coordinates the timing and execution of motor commands in response to sensory feedback from the peripheral nervous system [7, 44]. In the developing rodent brain, the cerebellum is ultimately derived at approximately embryonic day (E) 12 from precursor cells in the rhombic lip, a rapidly dividing group of neuroepithelial cells located within the emerging hindbrain [143]. The specification and proliferation of these cells is driven in large part by transcription factors including OTX2, PAX6 and MATH1 [50, 172, 173]. These progenitor cells then migrate to populate the outer surface of the cerebellar anlage [174], forming a secondary, transient proliferative zone known as the external granule cell layer (EGL) [143]. The proliferation of these cells continues well into the postnatal period, a process regulated by transcription factors including PAX6, ZIC1 and ZIC3 [73, 74]. During the first 2 weeks postnatally, progenitor cells within the EGL differentiate into immature granule neurons, which subsequently migrate radially into the emerging cerebellum to the inner granule layer (IGL), where they fully mature. Again, transcription factors such as NEUROD1, MBH1, MBH2, ZIC1 and ZIC2 contribute to these processes [175-177].

Another suite of transcription factors that have been shown to regulate development of the hindbrain and cerebellum are the nuclear factor I (NFI) family [103, 107]. These transcription factors are expressed in a variety of progenitor cell populations within the developing [93, 130, 178] and adult nervous system [86, 179], as well as by progenitor cells in other regions of the body [97, 180, 181]. NFIs have been implicated in a variety of facets of brainstem development [103]. NFIB, for example, has been shown to mediate basilar pontine development, as precerebellar neurons and pontine neurons exhibit delayed differentiation in the absence of this gene [182]. NFIA and NFIB are also expressed by CGNPs within the postnatal EGL, and by the progeny of these cells as they migrate to, and differentiate within, the postnatal IGL [100]. Importantly, many aspects of granule neuron migration and maturation are abnormal in *Nfia*$^{-/-}$ mice, including migration, axonal formation and arborisation of dendritic processes [100, 101]. NFIs have further been shown to control these processes via the regulation of genes that mediate granule neuron maturation, including *Tag1, Wnt7a* and *Gabra6* [99-101]. These findings highlight the critical role played by NFI transcription factors in cerebellar development.

We have recently shown that another NFI family member, NFIX, is highly expressed by CGNPs within the postnatal EGL [Chapter 2]. Moreover, *Nfix*-deficient mice exhibit delayed cerebellar development [91]. These findings are suggestive of NFIX mediating progenitor cell differentiation within the postnatal cerebellum. Our previous work within the forebrain supports this concept, as we have shown NFIX to be a pivotal factor in promoting neural stem cell differentiation within the neocortex [86, 96] and hippocampus [84, 183], via the transcriptional regulation of genes such as *Sox9, Gfap, Insc* and *Bbx* [84, 183, 184]. Here we sought to define the mechanism by which NFIX regulates CGNP biology. We reveal that *Nfix*$^{-/-}$ mice exhibit delayed CGNP differentiation *in vivo*, and that *Nfix*-deficient CGNPs proliferate more extensively than control CGNPs *in vitro*. Moreover, we used both chromatin immunoprecipitation and sequencing (ChIP-seq) and RNA sequencing (RNA-seq) to identify potential NFI targets within postnatal CGNPs, and identified *intersectin 1* as a target for NFIX-mediated transcriptional activation. Crucially, analysis of *intersectin 1* mutant mice revealed phenotypically similar cerebellar defects. These findings thus provide novel insights into the transcriptional regulation of CGNP differentiation, revealing that NFIX-mediated regulation of *intersectin 1* plays a central role in ensuring the timely differentiation of this postnatal neural progenitor cell pool.

3.4 Methods

3.4.1 Animals and ethics approvals

This research involved the use of animals. *Nfix*$^{+/+}$ and *Nfix*$^{-/-}$ mice were used in this study with approval from the University of Queensland Animal Ethics Committee (AEC approval numbers: QBI/143/16/NHMRC/ARC and QBI/149/16/ARC). *Itsn1*-deficient animals were also used in accordance with the recommendations of the Canadian Council on Animal Care and animal care regulations and policies of the Hospital for Sick Children, Toronto. Animals were genotyped as previously described [96, 185]. Primer sequences are available on request. All experiments were performed according to the Australian Code of Practice for the Care and Use of Animals for Scientific Purposes. Pregnant females were produced by placing male and female mice together overnight. The next day, females were inspected for the presence of a vaginal plug and, if present, this day was designated as E0. The day of birth was designated as postnatal day (P) 0. Mice were housed in Optimice IVC caging, with double HEPA filters and built in ventilation. Food and water were available *ad libitum*.

3.4.2 Immunohistochemistry

Chromogenic immunohistochemistry and immunofluorescence labelling were performed as described in Chapter 2. Briefly, mice were anesthetised and perfused transcardially with phosphate-buffered saline (PBS), followed by 4% paraformaldehyde (PFA), then post-fixed for 48-72 hours before long term storage in PBS at 4°C. Cerebella were isolated and embedded in 3% Noble agar and sectioned in a sagittal plane at 50 μm intervals using a vibratome. Sections were placed sequentially across the wells of a 6-well plate to ensure appropriate sampling from different medio-lateral regions of the cerebellum. There were between 6-8 cerebellar sections per well. Thus, for all analyses we had >6 sections per animal to image and analyse. Sections were mounted on slides before heat-mediated antigen retrieval was performed in 10 mM sodium-citrate solution at 95°C for 15 min. For chromogenic immunohistochemistry, sections were incubated overnight in primary antibodies at room temperature. A list of antibodies used in this study is given in Table 1. The following day, sections were rinsed in PBS, then incubated in a solution containing a biotinylated secondary antibody (Vector Laboratories) for 1 hour at room temperature, followed by processing with a VECTASTAIN ABC kit for 1 hour at room temperature (A used at 1/500, B used at 1/500, Vector Laboratories). Sections were rinsed again in PBS, then were processed for colour reaction using a nickel- 3,3'-diaminobenzidine (DAB, Sigma) solution (2.5% nickel sulfate and 0.02% DAB in 0.175 M sodium acetate) activated with 0.01% (v/ v) hydrogen peroxide. The colour reaction was stopped by rinsing

multiple times with PBS, and sections were then coverslipped with DPX mounting medium (Thermo Fisher Scientific). For IF labeling, sections were incubated at 4°C overnight with primary antibodies against the target proteins (see Table 1). The following day sections were rinsed in PBS, then incubated with the relevant secondary antibodies (Table 1) for 1 hour in the dark at room temperature. Sections were rinsed in PBS, then were counterstained with 4',6-diamidino-2-phenylindole (DAPI), and mounted in fluorescent mounting media (DAKO). For all experiments, at least three animals at each age were analysed.

Table 3 Antibodies used in this chapter

Antibody	*Source species*	*Company*	*Catalogue number*	*Dilution used*	*Purpose*
NFIX	Mouse	SIGMA	SAB1401263	1/200;1/1000	IF/IHC
PAX6	Rabbit	Millipore	AB2237	1/400	IF
NEUN	Rabbit	Millipore	MAB377	1/200	IF
GFAP	Rabbit	DAKO	Z0334	1/1000	IF
PHH3	Rabbit	Millipore	06-570	1/400	IF
Ki67	Mouse	BD Pharmigen	550609	1/400	IF

3.4.3 Cerebellar imaging

All brightfield images were captured using an Aperio XT Slide scanner and visualized using Aperio ImageScope (Leica Biosystems). For fluorescence images a Diskovery inverted spinning disk confocal microscope using a 20 X objective and a 70 μm pinhole (Nikon TiE; Nikon) was used. We took 10 consecutive 1 μm-thick optical sections to generate a 10 μm-thick z-stack. In all cases the 10 μm z-stack was taken from the middle of the section to minimize potential artefacts arising from the sectioning process such as damage to the tissue. Image acquisition was performed using NIS-elements Advanced Research software (Nikon). For comparative analysis of *Nfix*$^{-/-}$ and *Nfix*$^{+/+}$ mice, high magnification images were taken of the same lobe of the cerebellum, using at least five biological replicates at each of the ages assessed. For *Itsn1*$^{-/-}$ and *Itsn1*$^{+/+}$ mice, at least three biological replicates were used. For quantification of granule neuron and proliferative markers (PAX6 and Ki67, respectively), three 200 μm regions of the EGL were quantified for each section. This ensured more representative count of the EGL thickness. 1 μm-thick optical sections were viewed in Fiji, and the 'cell counter' plugin used to mark and quantify cells expressing respective markers in each fluorescent channel. Cells co-expressing markers (for example PAX6 and Ki67) were also quantified this way, and DAPI was used to visualize the cell nucleus, to ensure accuracy, especially in areas of high cell density.

3.4.4 Granule cell isolation

CGNPs from P7 *Nfix*$^{+/+}$ and *Nfix*$^{-/-}$ mice were isolated using the method outlined by Lee and colleagues [141] and a papain dissociation kit (Worthington Biochemical Corporation). Briefly, the cerebellum was dissected from three wild-type and three knockout mice and the tissue was dissociated using a 20 units/mL papain solution at 37°C for 15 mins. A single cell suspension was obtained by trituration with a serum-coated P1000 pipette tip and nuclear membranes were removed using an albumin-ovomucoid inhibitor gradient. CGNPs were separated from other cells using a 30%-60% percoll gradient. Purified CGNPs were then lysed in Trizol (Ambion) and RNA isolated using an RNeasy miniprep kit (Qiagen). RNA-sequencing was then performed on the samples using the Illumina NextSeq High Output system (Illumina; 150 base pair read length, paired-end reads).

3.4.5 RNA-seq analysis

Three RNA-seq replicates each from P7 wild type CGNPs and *Nfix*$^{-/-}$ mice were aligned by TopHat2 (v2.0.9) [152] to the *Mus musculus*, UCSC, mm10 reference transcriptome and FASTA annotation downloaded from the TopHat index and annotations page (https://ccb.jhu.edu/software/tophat/igenomes.shtml). Cufflinks (v2.1.1) [152] was used to assemble each replicate's transcripts from the alignment file generated by TopHat. Cuffmerge was used to create a single assembly containing transcripts across all samples and replicates. Cuffdiff was run using the merged set of transcripts and the three replicate TopHat2 bam files from each sample. *Math1* differential expression data was obtained from Klisch and colleagues [186], comparing RNA-seq expression of E18.5 wild-type and *Math1*$^{-/-}$ cerebellar tissue.

3.4.6 NFIX ChIP-seq

For chromatin immunoprecipitation, litters of P7 pups were pooled for CGNP isolation. Isolated CGNPs were crosslinked with 1% formaldehyde for 10 minutes, then were quenched with glycine. Cells were lysed in RIPA buffer supplemented with protease and phosphatase inhibitors (Roche) and sonicated with a Bioruptor (Diagenonde) for six 15 minute intervals of 30 seconds on, 30 seconds rest. Chromatin immunoprecipitation was performed as described previously [187], using a mouse anti-NFIX antibody (Sigma Aldrich). We have previously shown the specificity of this antibody using tissue from *Nfix*$^{-/-}$ mice [179]. Briefly, immunocomplexes were isolated with protein G-agarose beads (Roche), washed once for 5 minutes with buffers 1 through 4. Crosslinking was reversed by incubation with proteinase K (Roche) at 60 degrees overnight. DNA was isolated by phenol-chloroform extraction then incubated with RNAse A (Roche) for 30 minutes before final cleanup with PCR columns (Qiagen). Sequencing libraries were constructed using the standard protocol for

the NEBNext Ultra II DNA Library Prep Kit for Illumina (New England BioLabs). Pooled libraries were sequenced on an Illumina HiSeq2000 (Illumina; 30 base pair single end read).

3.4.7 ChIP-seq analysis

Alignment was performed on both the NFIX ChIP-seq data and MATH1 ChIP-seq data set (GSE22111) by bowtie2 [188] to mm10. Unaligned reads and reads which aligned to multiple locations were removed leaving only uniquely mapped reads. MACS2 [189] was used to call narrow peaks with default parameters for both datasets. Both experiments contained two biological replicates and if both biological replicates shared a peak, it was recorded using the maximum boundaries of the supporting peaks to generate a merged set of peaks for each experiment. Uniform 500 base pair peaks from the NFIX ChIP-seq data were created using a ± 250 base pair window around peak centres. This uniform set of peaks was input to MEME Suite to perform *de novo* motif discovery using MEME-ChIP version 5.0.1 [190, 191].

3.4.8 Annotation of ChIP-seq peaks

A set of target genes was identified for both NFIX and MATH1 by the following method. A promoter region was defined as ± 2000 base pairs around a transcription start site. ChIP-seq binding sites located in a promoter region were annotated as *proximal*, while sites outside the promoter region but overlapping gene boundaries (transcription start to stop) were labelled as *genic*. All remaining binding sites were labelled as *distal*. A binding site annotated as proximal was assigned the nearest gene as a target while genic binding sites were assigned the overlapping gene as a target. Distal binding sites are difficult to assign target genes to, as they are not necessarily regulating the nearest gene (by genomic distance). CisMapper was used to annotate distal binding sites and provide a secondary annotation to proximal and genic sites, with resulting links filtered to a threshold of 0.05 [192].

After identifying a gene target for each NFIX binding site; the associated *p*-value from both the *Nfix* and *Math1* RNA-seq differential expression analyses was recorded. Genes targeted by both *Nfix* and *Math1* with a significant ($p < 0.05$) change in expression in both experiments were extracted. Genes showing coordinated positive or negative log fold change values across both experiments were selected to generate a putative set of genes under the control of *Nfix* and *Math1*. Functional annotation was performed using DAVID (6.8) on target genes identified for *Nfix* [193, 194].

3.4.9 DNase I hypersensitivity analysis

DNase I hypersensitivity (DHS) called peaks from whole cerebellum at P7 across three replicates were retrieved from Frank et al. 2015 (GEO: GSE60731). UCSC liftover was used to convert the mm9 files to mm10. If at least two replicates shared a peak, it was recorded using the maximum boundaries of the supporting peaks to generate a merged DHS peak file. Transcription factors are known to bind preferentially in regions of accessible chromatin [195, 196] and DHS was therefore used to extract NFIX ChIP-seq peaks occurring in accessible regions.

3.4.10 Neurosphere assays

CGNPs were isolated from P7 wild-type and *Nfix*$^{-/-}$ mice and were seeded into a T25 flask in neurobasal stem cell medium containing 20 ng/mL of epidermal growth factor (EGF), 10 ng/mL of basic fibroblast growth factor (bFGF) and 3.5 µg/mL of heparin. After 7 days, neurospheres were dissociated using trypsin to form a single cell suspension. Cells were counted and seeded at a density of 2.5 x 10^5 cells per T25 flask. Cells were passaged until passage three. Neurospheres were counted and sphere diameter was measured at each passage.

3.4.11 Medulloblastoma cell lines

The medulloblastoma cell lines DAOY, D283, and UW228 were maintained in RPMI medium containing 10% foetal bovine serum. The MB4 primary cell line was maintained in StemPro NSC SFM media (Thermo Fisher). 2.5 x 10^5 cells were seeded into a 6 well plate and cells were lysed in Trizol (Ambion) after 48 hours. RNA was extracted using the RNAeasy miniprep kit (Qiagen). cDNA was prepared from RNA isolated from the medulloblastoma cell lines using a Superscript III Reverse Transcription kit (Invitrogen). cDNA was transcribed from human cerebellum RNA (Clontech) and used as a control for comparison of gene expression levels. qPCR was performed with the Quantifast SYBR kit (Qiagen). Gene expression was calculated using $2^{-\Delta\Delta Ct}$ method relative to the housekeeping gene *glyceraldehyde 3-phosphate dehydrogenase* (*GAPDH*).

3.4.12 qPCR analysis of target genes

RNA isolated from CGNPs of wild-type and *Nfix*$^{-/-}$ mice at P7 was used to prepare cDNA as described previously [178]. qPCR was performed with Quantifast SYBR Green (Qiagen) to detect gene expression levels of the genes identified in the RNA-seq analysis. Gene expression was calculated using $2^{-\Delta\Delta Ct}$ method relative to the housekeeping gene *glyceraldehyde 3-phosphate dehydrogenase* (*Gapdh*). All the samples were tested in triplicate within each experiment, and each experiment was repeated three times.

Table 4 qPCR primers used in this chapter

Gene	*Forward*	*Rev*
Itsn1	TCAGTTTCCCACACCTTTCG	TCAGGCTAAGGAACTGCTGG
Kit	CACATACACGTGCAGCAACA	GAAGGCCAACCAGGAAAAGT
Serpine2	ACGGCAAGACAAAGAAGCAG	AGCCTTGTTGATCTTCTTCAGC
Dab1	AACCAGCGCCAAGAAAGAC	ATCAGCTTGGCTTTGTACCG
Hes1	TCTGAGCACAGAAAGTCATCA	AGCTATCTTTCTTAAGTGCATC
Dll1	TTCTCTGGCTTCAACTGTGAG	CATTGTCCTCGCAGTACCTC
Notch3	AGTGCCGATCTGGTACAACTT	CACTACGGGGTTCTCACACA
Neurod1	ATGACCAAATCATACAGCGAGAG	TCTGCCTCGTGTTCCTCGT
Rbfox3	GGCAAATGTTCGGGCAATTCG	TCAATTTTCCGTCCCTCTACGAT
Gapdh	GCACAGTCAAGGCCGAGAAT	GCCTTCTCCATGGTGGTGAA
Nfix	AGGACTGTTTTGTGACTTCCG	GGTTGATGTTGTAGTAGCTGGG
Gapdh	CCCTTCATTGACCTCAACTACAT	TCCTGGAAGATGGTGATGG
Itsn1	GGGCCATAACTGTAGAGGAAAGA	ACAGGTTGAGGTAACCCAGAT

3.5 Results

3.5.1 Delayed EGL differentiation in the cerebellum of postnatal *Nfix*$^{-/-}$ mice.

In our preliminary description of the cerebellar phenotype of *Nfix*$^{-/-}$ mice, we demonstrated that these mice have reduced numbers of PAX6-positive CGNPs in the EGL at P5 in comparison to wild-type controls [91]. Within the embryonic forebrain of these mutant mice, radial glial progenitor cells exhibit delayed differentiation [183, 184]. We hypothesised that CGNPs within the EGL would exhibit a similar delay in differentiation within *Nfix*$^{-/-}$ mice. To test this hypothesis, we used PAX6-immunocytochemistry to visualise CGNPs within the EGL of P5, P10 and P15 wild-type and *Nfix*$^{-/-}$ mice. At P5, there were fewer CGNPs in the EGL of mutant mice in comparison to controls, whereas at P10, the number of these cells in both genotypes was comparable (Figure 3-1 A-D). Interestingly, at P15 there were more PAX6-positive cells in the EGL of the mutant in comparison to the control (Figure 3-1 E, F), indicative of delayed CGNP differentiation.

To quantify this phenotype, we performed co-immunofluorescence labelling against PAX6 and the proliferation marker, Ki67, followed by confocal microscopy. We performed cell counts within the EGL on confocal optical sections of the emerging cerebellum. At P5, there were significantly more cells expressing PAX6 and Ki67 in the wild-type EGL compared to the mutant (Figure 3-2 A-J). At P10, however, the numbers of PAX6-positive cells and proliferating cells within the EGL was not significantly different between genotypes (Figure 3-2 K-T). In contrast, there were significantly more CGNPs within the EGL of P15 *Nfix*$^{-/-}$ mice compared to the control, as the majority of these cells had differentiated in wild-type mice by this age (Figure 3-2 U-DD). A similar trajectory of CGNP differentiation was observed when we used a second marker for proliferation, the mitotic marker phosphohistone H3 (PHH3; Figure 3-3).

3.5.2 *Nfix*$^{-/-}$ CGNPs exhibit increased proliferation *in vitro.*

These findings led us to posit that NFIX mediates CGNP differentiation, and that the absence of this gene could lead to elevated CGNP proliferation, as has been previously reported in the embryonic hippocampus of *Nfix*$^{-/-}$ mice [183]. To test this hypothesis, we isolated CGNPs from the EGL of P7 wild-type and *Nfix*$^{-/-}$ mice using papain dissociation and a percoll gradient [141], [Chapter 2]. We performed qPCR on cDNA generated from this tissue, and revealed that the expression of the stem cell markers *Hes1* and *Notch 3* was significantly elevated in CGNPs isolated from P7 *Nfix*$^{-/-}$ mice in comparison to controls (*Hes1:* control 0.0051 ± 0.0001, *Nfix*$^{-/-}$ 0.0079 ± 0.0003; *Notch 3:* control 0.0023 ± 0.0001, *Nfix*$^{-/-}$ 0.0038 ± 0.0002; $p < 0.01$, *t*-test). Moreover, the analysis of two markers for neuronal differentiation, *Neurod1* and *NeuN* (*Rbfox3*) revealed significantly reduced expression of these factors in CGNPs isolated from P7 *Nfix*$^{-/-}$ mice in comparison to controls (*Neurod1:* control 0.53 ± 0.01, *Nfix*$^{-/-}$ 0.37 ± 0.002; *Rbfox3:* control 0.13 ± 0.003, *Nfix*$^{-/-}$ 0.005 ± 0.004; $p < 0.01$, *t*-test).

Next, we used the percoll gradient protocol to again isolate CGNPs from the EGL of P7 wild-type and *Nfix*$^{-/-}$ mice and cultured these cells in a neurosphere assay. We cultured cells for three passages, and quantified both the number of spheres, as well as sphere diameter. At each passage, there were significantly more spheres in cultures derived from *Nfix*$^{-/-}$ EGL progenitors in comparison to controls (Figure 3-4 A-C). Furthermore, whereas the majority of wild-type spheres were less than 50 μm in diameter, in the mutant, the majority of spheres were over 70 μm in diameter (Figure 3-4 D). Interestingly, the expression of GFAP by developing Bergmann glia was also delayed in the absence of *Nfix* [Figure 3-5; [91]], suggesting that a delay in glial differentiation could also potentially underlie the accumulation of PAX6-positive cells within the EGL of *Nfix*$^{-/-}$ mice. However, our neurosphere data clearly indicate elevated levels of proliferation in CGNPs isolated from *Nfix*$^{-/-}$ cerebella, indicating that NFIX plays a central role in mediating the differentiation of cerebellar CGNPs.

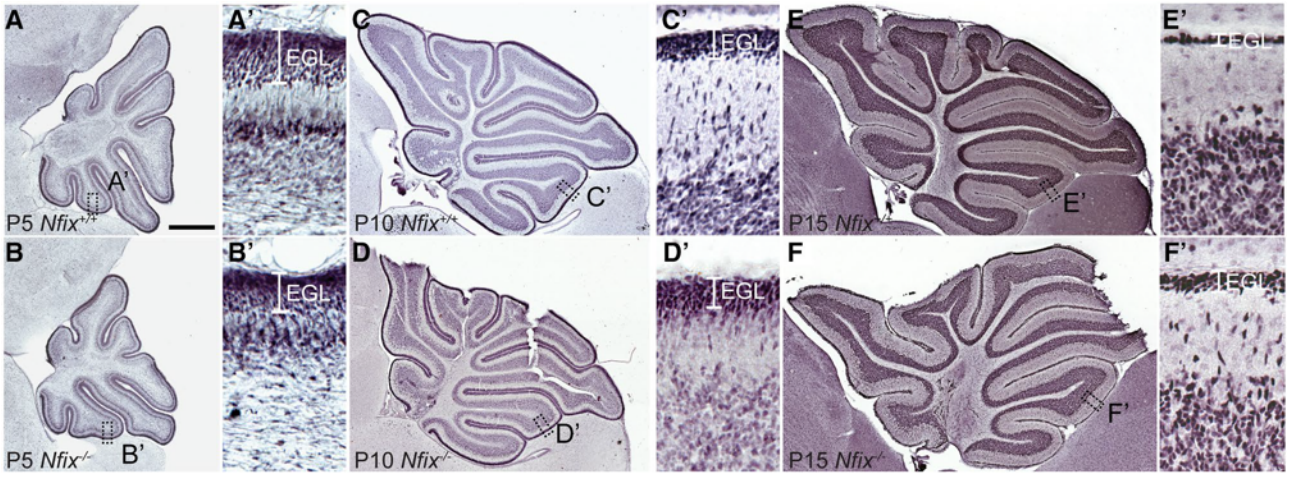

Figure 3-1 Delayed differentiation of CGNPs in the cerebellum of Nfix deficient mice.

Mid-sagittal sections of P5 (a–b'), P10 (c–d') and P15 (e–f') wild-type (a, c, e) and *Nfix*$^{-/-}$ (b, d, f) mice stained with antibodies against PAX6. The boxed regions in A-F are shown at higher magnification in a'–f' respectively. The morphology of the cerebellum appeared grossly normal in mice lacking *Nfix*. However, higher magnification views of the external granule layer (EGL) revealed that this germinal zone was thinner at P5 in mutant mice. At P10 the EGL of the mutant was comparable to the control. At P15, whereas the EGL was almost completely depleted in the wild-type, there were still numerous PAX6-positive cells in this cellular layer of *Nfix*$^{-/-}$ mice. Scale bar (in a) a–f = 250 μm, a'–f' = 25 μm

Mutations in another NFI family member, *Nfia*, have previously been implicated in medulloblastoma, a paediatric cancer of the cerebellum [136]. Using a Sleeping Beauty transposon screen, Genovesi and colleagues [136] revealed that mutations to *Nfia* led to reduced latency of medulloblastoma formation in a *Ptch1*$^{+/-}$ background. Transposon insertions were also identified within the *Nfix* locus in this screen, but the role of *NFIX* in medulloblastoma is poorly defined. In light of our data in the developing cerebellum, we analysed *NFIX* expression in three medulloblastoma cell lines (DAOY, UW228 and D238), and a primary medulloblastoma cell line (MB4). *NFIX* mRNA was significantly reduced in comparison to control mRNA isolated from the adult cerebellum (Figure 3-4 E). A similar reduction in expression was also obtained when we analysed the expression of the other NFI family members, *NFIA, NFIB* and *NFIC* (data not shown). Collectively, these data are consistent with the *in vivo* cerebellar phenotype of *Nfix*$^{-/-}$ mice, and suggest that NFIX acts to drive the differentiation of cerebellar CGNPs.

3.5.3 Transcriptomic profiling reveals a broad suite of potential targets of NFIX within GNPs.

To define transcriptional targets for NFIX during CGNP differentiation, we undertook a range of bioinformatic approaches using both published, and newly generated, transcriptomic data, aimed at defining a small list of high-confidence targets that we could experimentally validate. To determine the transcriptomic landscape in CGNPs lacking *Nfix*, we first isolated CGNPs from both wild-type and *Nfix*$^{-/-}$ cerebella at P7, and performed transcriptomic profiling (RNA-seq) on the RNA isolated from these cells. Analysis revealed 1,402 genes as being significantly misregulated in *Nfix*$^{-/-}$ CGNPs in comparison to controls (Figure 3-6 A) Gene Ontology and Pathway analyses of these genes using DAVID [193, 194] identified a diverse range of processes potentially controlled by NFIX within CGNPs, including cell adhesion, extracellular matrix organisation and axon guidance (Figure 3-6 B).

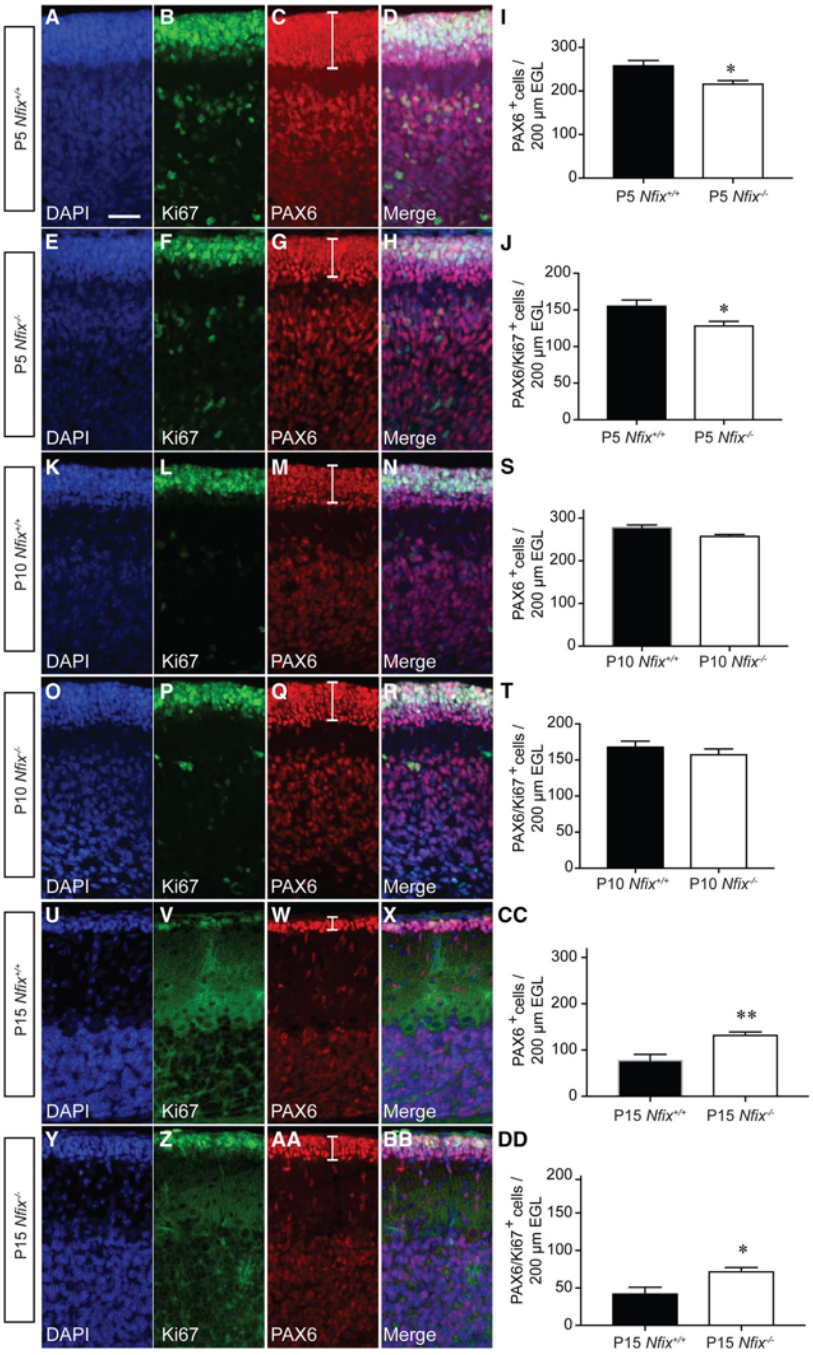

Figure 3-2 Retention of CGNPs in late postnatal Nfix−/− mice.

Expression of the nuclear marker DAPI (blue), the proliferative marker Ki67 (green), and PAX6 (red), a marker of CGNPs and their progeny, in P5 (a–h), P10 (k–r) and P15 (u–bb) mice. The EGL in delineated by brackets in panels c, g, m, q, w and aa. At P5 there were significantly more PAX6-positive cells (i) and PAX6/Ki67 double-positive cells (j) in the wild-type EGL in comparison to the mutant. At P10, there were no significant differences in either PAX6- (s) or PAX6/Ki67-expressing (t) cells between groups. At P15, however, there were significantly more PAX6-positive cells (cc) and PAX6/Ki67 double-positive cells (dd) in the EGL of Nfix−/− mice in comparison to the control. *$p < 0.05$, t test. Scale bar (in a) = 25 µm

To determine direct targets of NFIX in CGNP differentiation, we next performed ChIP-seq on DNA derived from isolated P7 CGNP preparations using an anti-NFIX antibody whose specificity has been previously demonstrated [179, 197]. This experiment identified 6,910 specific NFIX binding peaks (Figure 3-6 C). Interestingly, a recent publication used DNase 1 hypersensitivity analysis on whole cerebellar tissue to investigate chromatin accessibility within these cells at different stages in development [198]. We posited that NFIX ChIP-seq peaks identified within regions of open chromatin would be more likely to regulate gene transcription directly. As such, we filtered our NFIX ChIP-seq data using the DNase 1 hypersensitivity data from P7 [198], an analysis that revealed that 5,843 of the NFIX ChIP-seq peaks were found in regions of accessible chromatin at this age (Figure 3-6 C). Finally, the intersection of the differentially expressed genes identified via RNA-seq (Figure 3-6 A) with those genes identified as having an NFIX ChIP-seq peak in an accessible region of chromatin (Figure 3-6 C) identified 578 genes as being potential targets for direct NFIX-mediated regulation within P7 CGNPs (Figure 3-6 D, Table A10). This analysis revealed a number of genes previously implicated in cerebellar development, such as *Otx2* and *Dab1*, as well as a range of genes whose role in cerebellar development has not been previously studied (e.g. *Heg1, Tiam2*). Interestingly, *Nfix* was also identified via this filtering analysis, suggesting that NFIX autoregulates its own expression within the context of CGNP development.

To search for further ways in which we could refine our list of potential NFIX target genes, we performed motif discovery and enrichment analyses (Bailey et al. 2009, Machanick et al. 2011) on the NFIX binding peaks isolated in our ChIP-seq experiment. As expected, the conserved motif bound by NFI transcription factors [107] was identified as being enriched in our ChIP-seq peaks. Interestingly, we also observed enrichment of the MATH1 binding motif within NFIX ChIP-seq peaks (Figure 3-7 A). MATH1 is strongly and specifically expressed by CGNPs, and has previously been shown to regulate the proliferation of these cells, as well as concomitantly priming them for differentiation [186]. This finding indicates that NFIX and MATH1 could potentially regulate a common suite of genes developmentally. Given this, we postulated that we could use the analysis of MATH1 target genes to further refine our list of potential NFIX targets. To do this, we used a recent analysis of the MATH1 targetome in cerebellar tissue [186]. This study mapped differential gene expression in E18.5 cerebellar tissue isolated from *Math1*-deficient mice, as well as identifying potential direct targets of

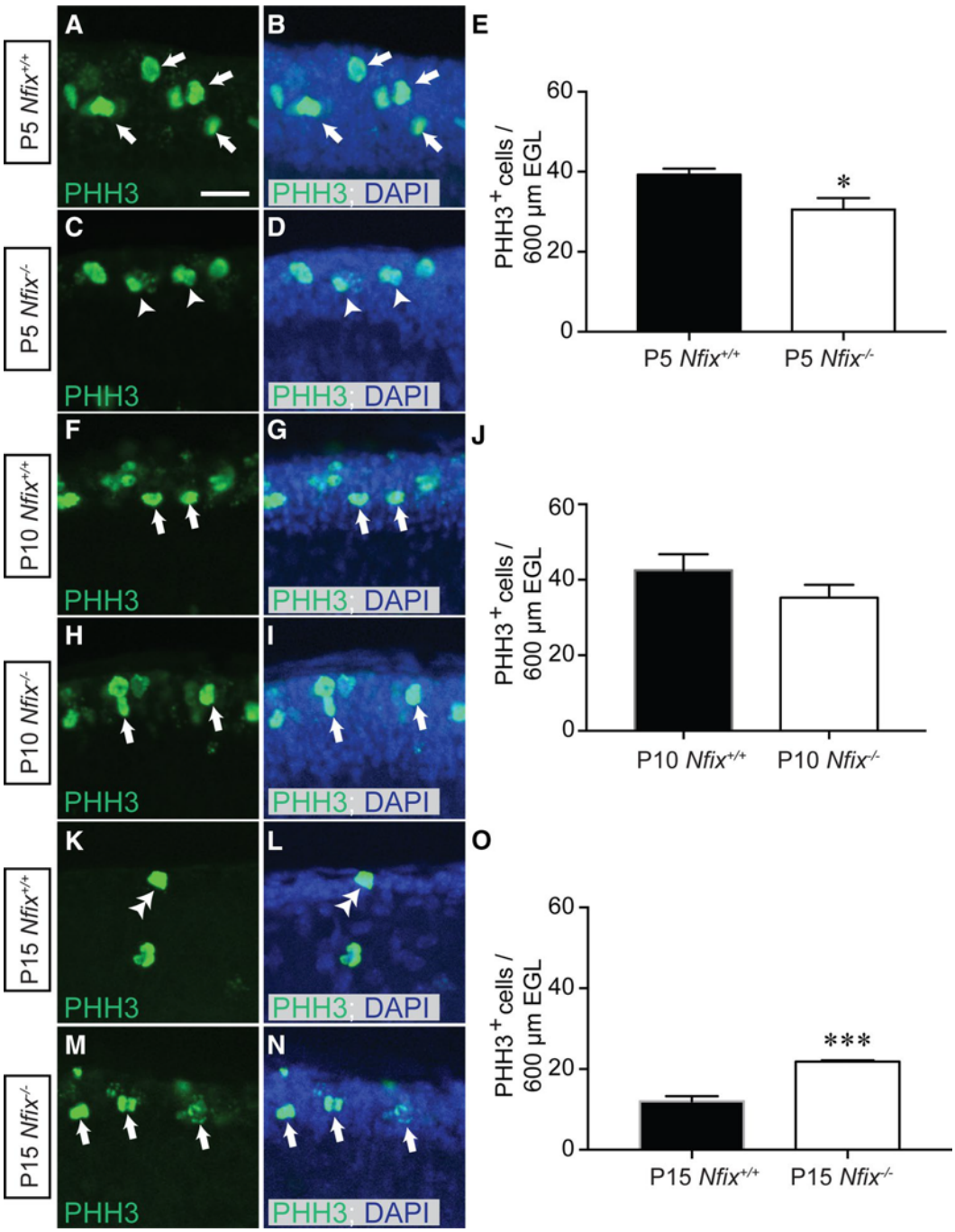

Figure 3-3 Delayed proliferation profile of CGNPs in the absence of Nfix.

Transverse sections of P5 (a–d), P10 (f–i) and P15 (k–n) wild-type and mutant cerebella labelled with DAPI (blue) and antibodies against the proliferative marker phosphohistone H3 (PHH3). At P5, there were significantly more proliferating cells in the EGL of the wild-type (arrows in a, b) in comparison the control (arrowheads in c, d; quantified in e). At P10, however, the rate of proliferation within the EGL was comparable between sample wild-types and mutants (arrows in f–i; quantified in j). At P15, the situation was reversed, with there being significantly fewer proliferating cells within the EGL of wildtype mice (double arrowheads in k, l) in comparison to mutant mice (arrows in m, n; quantified in o). *$p < 0.05$, ***$p < 0.001$ t test. Scale bar (in a) = 25 µm

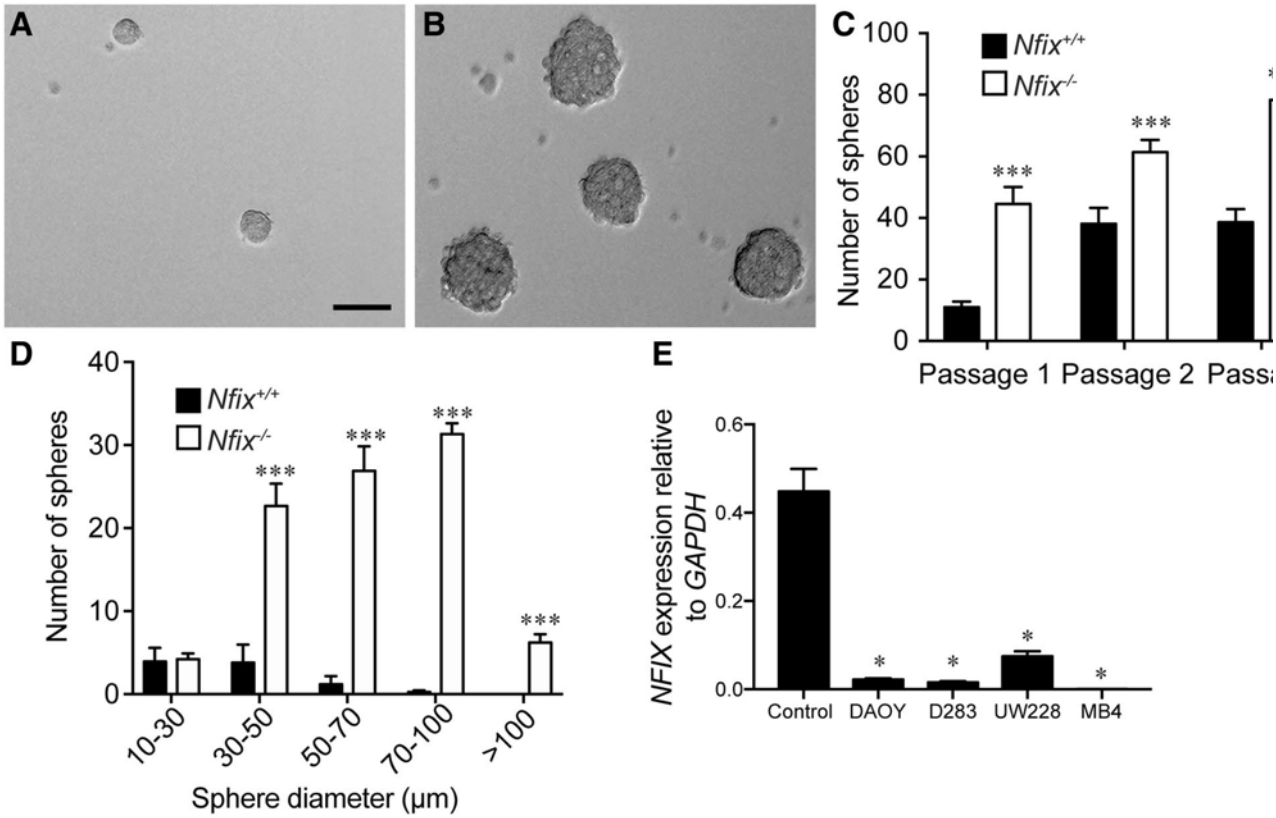

Figure 3-4 Fig. 4 *Nfix*$^{-/-}$ CGNPs exhibit elevated proliferation in vitro.

CGNPs were isolated from P7 wild-type and *Nfix*$^{-/-}$ cerebella and were cultured in a neurosphere assay for multiple passages. At passage 3, wild-type spheres (a) were smaller and fewer in number than those derived from *Nfix*$^{-/-}$ CGNPs (b). Indeed, there were significantly more spheres derived from *Nfix*$^{-/-}$ GNPs at each passage in comparison to the control (c). Moreover, at passage 3, spheres derived from *Nfix*$^{-/-}$ CGNPs were on average larger than controls (d). e qPCR revealed that different medulloblastoma cell lines had significantly lower NFIX expression in comparison to normal cerebellar tissue. *p < 0.05, ***p < 0.001 ANOVA. Scale bar (in a) = 30 μm

MATH1 by performing ChIP-seq on P5 cerebellar tissue [186]. Analysis of these two sequencing datasets identified 1551 genes as potential MATH1 targets (i.e. the target gene contained at least one MATH1 ChIP-seq peak, and was significantly differentially expressed in E18.5 *Math1*$^{-/-}$ cerebellar tissue; Figure 3-7 B) [186]. The comparison of these potential MATH1 target genes with those 578 NFIX target genes identified in our RNA-seq and ChIP-seq analyses (Figure 3-7 D) revealed 177 genes as potential targets of both MATH1 and NFIX in cerebellar development. Critically, 90 of these genes were co-ordinately misregulated in both *Nfix*$^{-/-}$ CGNPs and *Math1*$^{-/-}$ cerebellar tissue (Figure 3-7 B, C). This list of putative NFIX targets included *Nfix* itself, as well as other factors previously implicated in cerebellar development, including *Otx2, Robo1* and *Dab1* [173, 199, 200]. Interestingly, this analysis also revealed a range of genes that have not previously been implicated in cerebellar development, including *Coro2b,* and *intersectin 1* (*Itsn1*; Figure 3-7D).

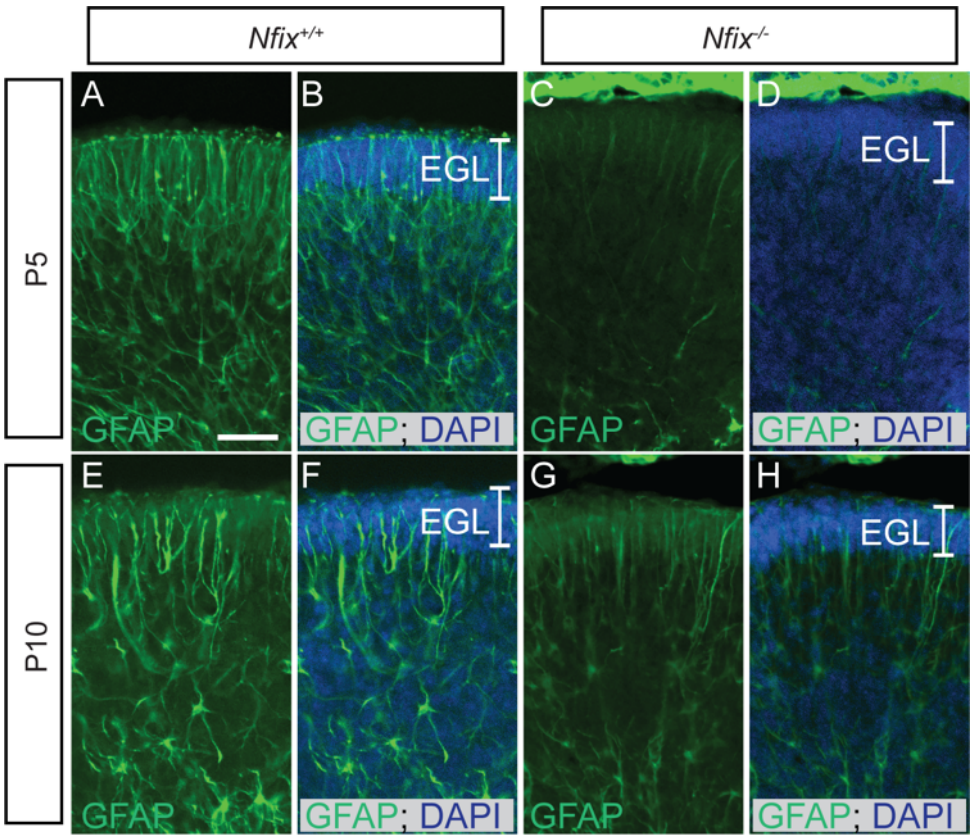

Figure 3-5 GFAP expression is reduced in early postnatal *Nfix*$^{-/-}$ mice.

Expression of the nuclear marker DAPI (blue) and the glial marker, GFAP (green), in P5 (A-D) and P10 (E-H) wild-type (A, B, E, F) and *Nfix*$^{-/-}$ (C, D, G, H) mice. The EGL in delineated by brackets in panels B, D, F and H. At both P5 and P10 the expression of GFAP was reduced in the absence of *Nfix*. Scale bar (in A) = 25 μm

3.5.4 *Intersectin 1* is a target for transcriptional activation by NFIX during CGNP differentiation.

Of those novel factors identified in our transcriptomic screens, *Itsn1* was of particular interest to us. This gene encodes a multi-domain scaffold protein that has been implicated in regulating numerous cellular signalling pathways [201]. With relation to neuronal development, *Itsn1* has been implicated in connectivity at the cortical midline of the dorsal telencephalon, with deficiencies to this gene correlated with aberrant higher order cognition [185]. Mechanistically, *Itsn1* has recently been implicated in neuronal migration within the hippocampus as part of the reelin signalling pathway, via its interaction with the reelin receptor VLDLR, and with *Dab1*, a signalling molecule downstream of VLDLR [202]. Given the importance of reelin signalling for cerebellar development [203], and the identification of *Dab1* in our transcriptomic screen, we focussed on *Itsn1* as a target for NFIX in CGNP differentiation. We first validated our RNA-seq dataset by performing qPCR on CGNPs isolated from independent P7 *Nfix*$^{-/-}$ and control cerebella (Figure 3-8 A). In line with our sequencing results, *Itsn1* mRNA was significantly reduced in *Nfix*$^{-/-}$ samples in comparison to controls, whereas the mRNA levels of *Kit, serpine 2* and *Dab1* were significantly increased in the mutant. These data suggest that NFIX acts to promote the expression of *Itsn1* during CGNP differentiation. If this were the case, we would hypothesise that mice lacking *Itsn1* would potentially phenocopy those lacking *Nfix* with regards to cerebellar development. To test this hypothesis, we analysed the cerebellum of *Itsn1*$^{-/-}$ mice at P15. Hematoxylin staining revealed that foliation of the cerebellum was grossly normal in these mice in comparison to controls (Figure 3-8 B, C). However, closer analysis of the EGL of mutant mice revealed that the EGL of *Itsn1*$^{-/-}$ mice at P15 was markedly thicker when compared to control mice (Figure 3-8 B', C'). Indeed, immunofluorescence labelling with PAX6, followed by confocal microscopy, revealed significantly more CGNPs within the EGL of *Itsn1*$^{-/-}$ mice at this age than controls (Figure 3-8 D - J). Similarly, there were significantly more Ki67-expressing cells in the EGL of mutant mice at this age in comparison to wild-type controls (Figure 3-8 K). The expression of GFAP by Bergmann glia was comparable between wild-type and *Itsn1*$^{-/-}$ mice at this age (Figure 3-9), although it is possible that GFAP expression was reduced at earlier time points akin to what we observed with the *Nfix* mutant, and that this may also have contributed to the enlarged EGL at P15 in the absence of *Itsn1*. Finally, like *NFIX,* the expression of *ITSN1* was also significantly reduced in medulloblastoma cell lines (Figure 3-8 L). Collectively, these data, in association with our RNA-seq and ChIP-seq analyses, suggest that NFIX-mediated regulation of *Itsn1* plays an important role in CGNP differentiation during cerebellar development.

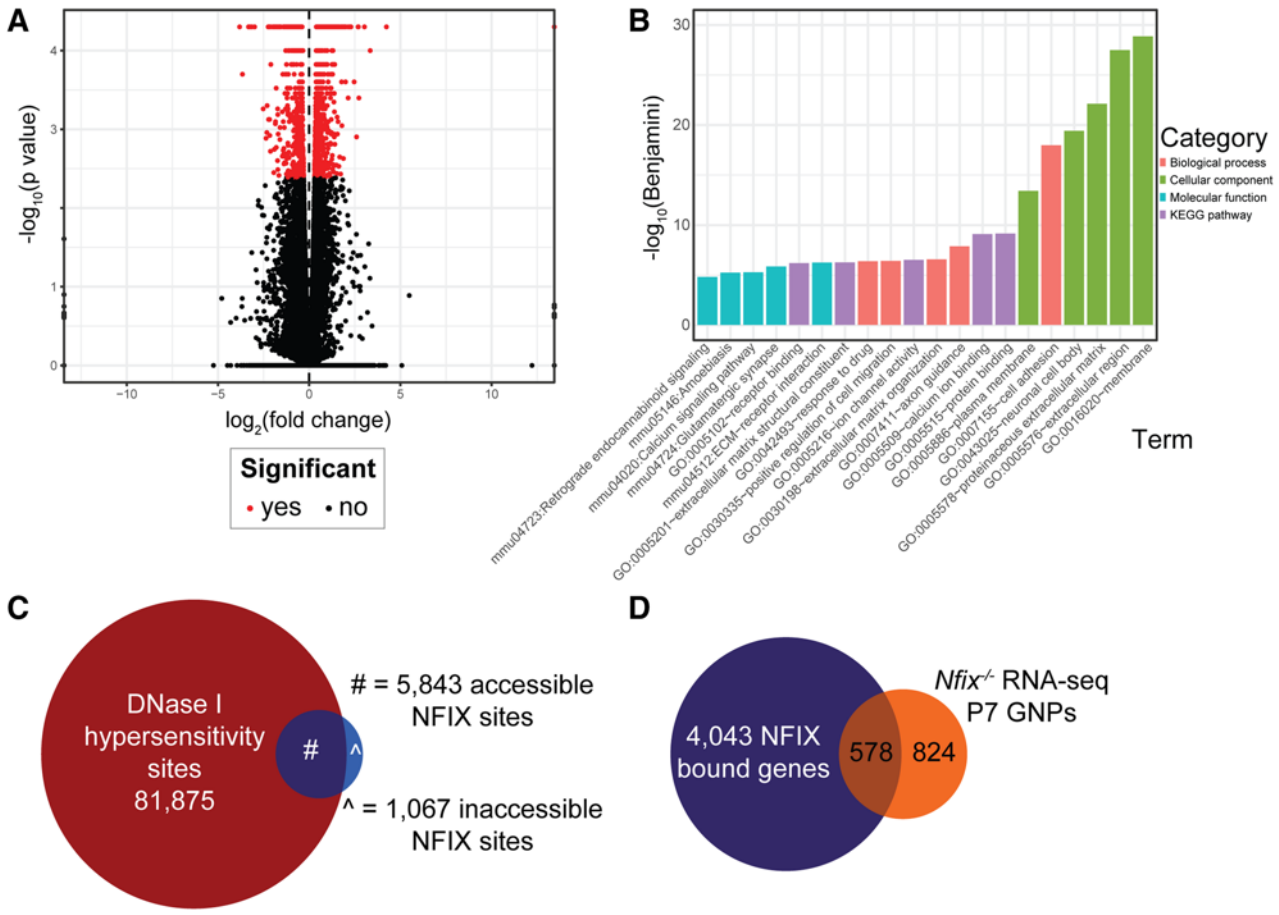

Figure 3-6 Transcriptomic profiling of *Nfix*$^{-/-}$ CGNPs.

(A) Volcano plot representing the transcriptional profile of P7 *Nfix*$^{-/-}$ CGNPs in comparison to controls. Red dots represent the 1,402 significantly misregulated genes in P7 *Nfix*$^{-/-}$ CGNPs as identified by RNA-seq. (B) Gene Ontology (DAVID 6.8) analysis, showing those biological processes, cellular components and molecular functions misregulated in P7 *Nfix*$^{-/-}$ CGNPs, as well as KEGG pathways identified as being abnormal in these cells. (C) To narrow the list of potential NFIX target genes, we performed ChIP-seq on wild-type P7 CGNPs with an anti-NFIX antibody. This revealed 6,910 NFIX binding peaks. We compared this with a published DNase I hypersensitivity analysis of P7 cerebellar tissue (Frank et al. 2015). Of the 6,910 ChIP peaks, 5,843 were in regions of accessible chromatin. We then compared the 4,621 genes associated with these 5,843 NFIX peaks with our RNA-seq data (A). This analysis identified 578 potential NFIX target genes (D).

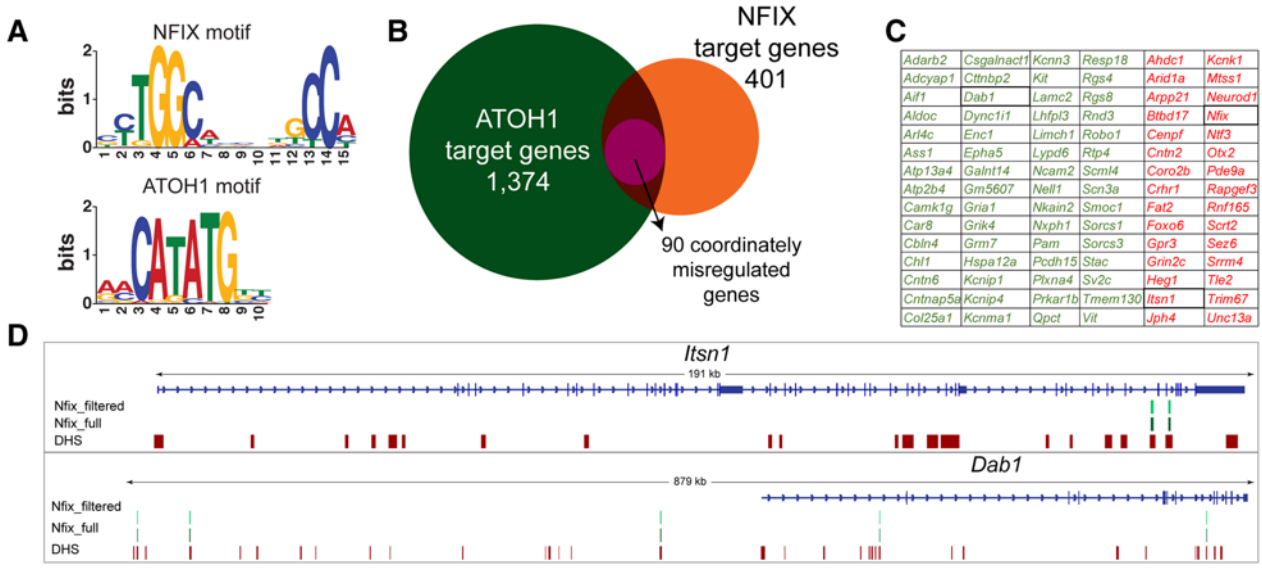

Figure 3-7 Combined analysis of *Nfix*$^{-/-}$ CGNPs and *Math1*$^{-/-}$ cerebellar tissue

(A) MEME-suite *de novo* motif discovery run on NFIX ChIP-seq peaks revealed both the NFI motif, and the MATH1 motif, suggesting the two transcription factors potentially regulate a common suite of target genes. (B) Comparison of 1,551 genes bound by MATH1 and misregulated in *Math1*$^{-/-}$ cerebellar tissue [186] and 578 genes bound by NFIX and misregulated in *Nfix*$^{-/-}$ CGNPs identified 177 shared target genes. Of the 177 shared target genes, 90 were coordinately misregulated (i.e. up in both datasets, or down in both datasets) in both *Math1*$^{-/-}$ cerebellar tissue [186] and *Nfix*$^{-/-}$ CGNPs. These 90 genes are listed in panel C, with those genes in red being downregulated in *Nfix*$^{-/-}$ CGNPs, and those genes in green being upregulated in *Nfix*$^{-/-}$ CGNPs. The remaining 87 genes were not coordinately misregulated in the two datasets (i.e. expression was up in one dataset and down in the other, or *vice versa*). (D) Panel D shows genome browser tracks for the regions around the *Itsn1* and *Dab1* genes. The tracks reveal NFIX binding sites from our ChIP-seq dataset (NFIX_full, dark green), NFIX binding sites that appear in regions of accessible chromatin (NFIX_filtered, light green) and regions of open chromatin from published DNase 1 hypersensitivity analysis (DHS, red). *Itsn1* has binding events occurring intronically and *Dab1* has binding events occurring distally and intronically.

3.6 Discussion

Studies into the role of the NFI family in cerebellar development have highlighted a key role for these transcription factors in mediating neuronal migration and synaptic maturation [103]. Here, we extend these findings, revealing that NFIX regulates CGNP biology within the postnatal cerebellum. Indeed, the delayed differentiation of CGNPs *in vivo* in *Nfix*-deficient mice, coupled with the elevated proliferation of *Nfix*$^{-/-}$ CGNPs *in vitro*, are supportive of a role for NFIX in promoting timely CGNP differentiation within the postnatal cerebellum. This is in accordance with studies into the role of the NFI family during nervous system development [97, 204], with impairments in neural stem cell differentiation observed in the absence of NFIs from diverse regions of the brain, including the neocortex [205], hippocampus [84, 178] and spinal cord [206]. Collectively, these data implicate the NFI family, including NFIX, as key drivers of neural development via the promotion of neural stem cell differentiation.

How do NFIs drive this process at a mechanistic level? A number of studies have investigated the roles these factors play during nervous system development. Early studies using *Nfi*-deficient mice revealed severe delays in astrocyte differentiation, suggesting a central role for this family in gliogenesis within the cerebral cortex and spinal cord [105, 207]. More recently, transcriptional profiling experiments such as microarrays, coupled with molecular analyses and bioinformatics, have identified a range of target genes in the developing and adult nervous system that act to either repress stem cell identity or to promote cellular differentiation [87, 183]. These include *Apcdd1, Mmd2* and *Zcchc24* (spinal cord) [208], *Insc, Sox9* and *Ezh2* and (hippocampus) [84, 178, 183], as well as *Bbx* and *Hes1* (cerebral cortex) [130, 184]. The advent of genome-wide profiling using techniques such as RNA-seq and ChIP-seq now means that the direct targets of transcription factors like NFIX can be investigated globally in a more rigorous manner. To the best of our knowledge, this is the first study that has investigated downstream targets of a specific NFI family member within the nervous system by using these techniques co-operatively. Moreover, when coupled with available data relating to chromatin accessibility [198] and the MATH1 targetome [186], this study provides a significant conceptual advance in our understanding of the transcriptional landscape regulated by NFIX within the postnatal cerebellum.

One of the novel targets identified as a potential regulator of CGNP biology downstream of NFIX using these techniques was the scaffold protein Intersectin 1. The gene coding for this factor contained NFIX ChIP-seq peaks near its 3' UTR, and was significantly downregulated in the absence of *Nfix*. Moreover, mice lacking *Itsn1* phenocopied *Nfix*$^{-/-}$ mice with regards to delayed differentiation of

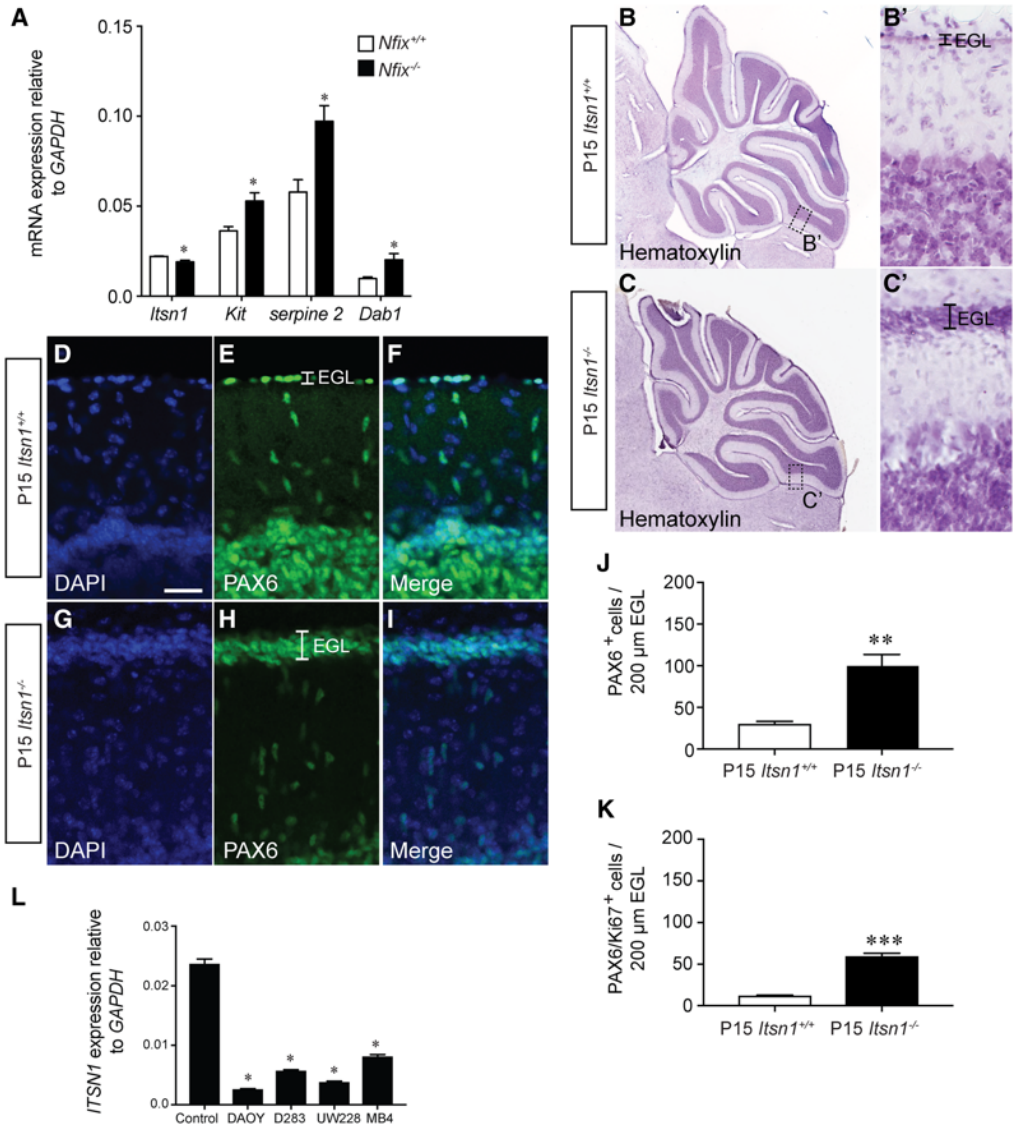

Figure 3-8 *Intersectin 1* is a downstream target for NFIX in CGNP development.

(A) qPCR performed on P7 CGNPs from wild-type and *Nfix*$^{-/-}$ mice revealed significantly reduced levels of *Itsn1*. Levels of *Kit, serpine 2* and *Dab1* were, conversely, significantly elevated in the mutant in comparison to the controls. (B, C) Mid-sagittal sections of P15 wild-type (B) and *Itsn1*$^{-/-}$ (C) mice stained with hematoxylin. Gross morphology of the cerebellum was not altered in the absence of *Itsn1*. The boxed regions in B and C are shown in B' and C' respectively. These reveal that the EGL is markedly larger in *Itsn1*$^{-/-}$ mice on comparison to the controls. (D-I) Immunofluorescence staining with PAX6 revealed that, whereas few PAX6-expressing cells remained in the EGL of wild-type mice (D-F) at this age, there were numerous PAX6-expressing CGNPs in in the EGL of *Itsn1*$^{-/-}$ mice (G-I). Quantitation of the EGL of P15 mice revealed significantly more PAX6-expressing (J) and PAX6/Ki67-expressing (K) cells in the EGL of the mutant in comparison to the control at P15. (L) qPCR revealed that different medulloblastoma cell lines had significantly lower *ITSN1* expression in comparison to normal cerebellar tissue. * $p < 0.05$, ** $p < 0.01$, *** $p < 0.001$ *t*-test

CGNPs within the postnatal EGL. These data suggest that *Itsn1* contributes to the differentiation of CGNPs. At this stage, it is unclear precisely how *Itsn1* regulates the differentiation of CGNPs. However, given the nature of this protein as a scaffold capable of binding and influencing many signalling pathways [201], there are many potential means by which *Itsn1* could mediate CGNP differentiation. For example, *Itsn1* has been shown to regulate *Ras* family GTPases, and is thought to promote *Ras* activation [209]. As Ras signalling has previously been shown to be required for the proliferation of CGNPs postnatally [210], abnormal activation of this factor, and the downstream ERK-MAPK pathway, may potentially contribute to the phenotype evident in these mice. *Itsn1* has also been shown to mediate caveolin-mediated endocytosis [211]. This may be particularly pertinent for CGNP biology, as the continued proliferation of these cells is controlled, at least in part, by SHH released by Purkinje cells [212]. Endocytosis of the *Shh* receptor, *Ptch1*, to the lysosome plays a key role in continued CGNP proliferation [213]. It is feasible that *Itsn1* may contribute to this process. Looking forward, proteomic studies performed on postnatal CGNPs will provide a framework in which to understand the molecular partners of ITSN1, and so the processes this scaffold protein may regulate *in vivo*.

Our findings also suggest a potential role for *Nfix* in medulloblastoma, a malignant childhood cancer of the cerebellum. Another NFI family member, *Nfia*, was recently linked to the formation of medulloblastoma using a Sleeping Beauty transposon screen to identify genetic modifiers of tumour formation in *Ptch1* heterozygous mice [136]. This study also identified *Nfix* as being significantly enriched as a tumour-suppressor. In humans, recent gene expression analyses of patient medulloblastoma samples revealed that *NFIX* expression is significantly lower in type 3α and type 3γ medulloblastomas, subtypes with poor prognosis and increased frequency of metastasis [214]. Although both of these studies identified NFIX, *Shh* and Type 3 medulloblastoma subgroups are characterised by different oncogenic drivers. However, preliminary data suggest that Hedgehog-dependent tumours, including medulloblastomas and basal cell carcinomas, are capable of switching oncogenic pathways, and hence becoming more metastatic [215, 216]. It remains to be tested whether NFI family members play a role in this transition, or appear as tumour suppressors solely due to their pro-differentiation roles. Furthermore, haploinsufficiency to *NFIX* in human patients culminates in Malan Syndrome, a disorder characterised by overgrowth of many organ systems, including the brain [121, 123]. This implies a pro-differentiation role for NFIX during development, and is consistent with our work on NFIX in the cerebellum.

A key advance we have made in this work is to use RNA-seq, ChIP-seq (this study) and chromatin accessibility [198] to define the potential targets of NFIX during development. This approach enabled

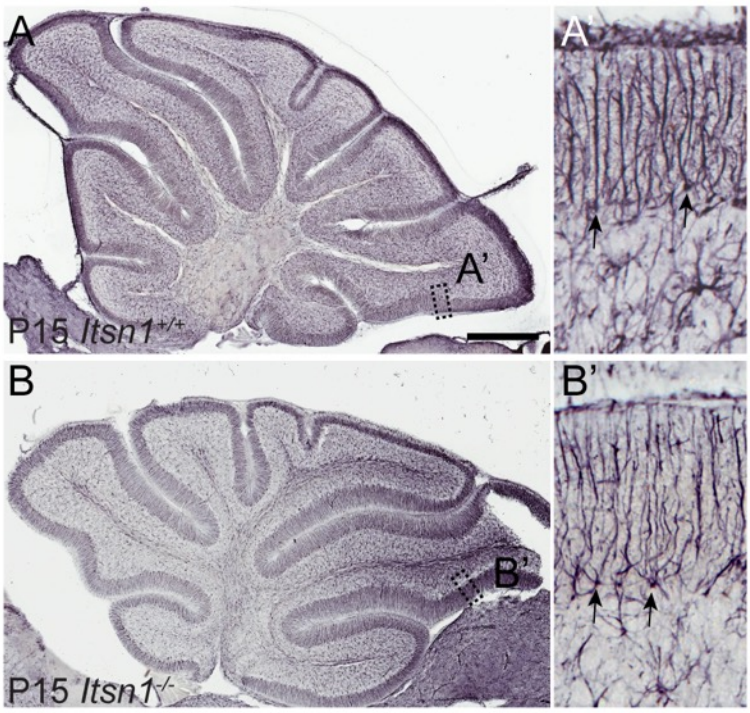

Figure 3-9 GFAP expression is comparable in late postnatal *Itsn1*$^{-/-}$ mice.

Expression of the glial marker, GFAP, in P15 wild-type (A, A') and *Istn1*$^{-/-}$ (B, B') mice. The boxed regions in A and B are shown at higher magnification in A' and B' respectively. The arrows in A' illustrate GFAP-expressing Bergmann glia. These cells were also present in the cerebellum of P15 *Itsn1*$^{-/-}$ mice (arrows in B'). Scale bar (in A) A, B =250 μm, A', B' = 25 μm.

us to identify 5,843 high-confidence NFIX ChIP-seq peaks. Through the combination of our RNA-seq analysis, these high-confidence peaks were subsequently linked to 578 target genes. Motif discovery further led us to identify MATH1 as a factor that may bind to similar genes as NFIX during CGNP development. Published data pertaining to the loss of *Math1* expression [186] revealed that *Nfix* is downregulated in *Math1*$^{-/-}$ cerebellar tissue, suggesting that MATH1 potentially regulates *Nfix* expression. Indeed, a number of genes were commonly misregulated in both RNA-seq perturbation data sets (Figure 3-7 B). Therefore, genes bound by NFIX and showing expression changes in both data sets where NFIX was perturbed, albeit using different approaches, were considered to be high-confidence target genes of NFIX.

Ultimately, this focussed, multifaceted approach led us to identify 90 potential NFIX target genes. While we focussed here on *Itsn1*, the role of NFIX in mediating other genes identified via this screen offers a number of interesting avenues of future research. For example, the factors mediating the transcriptional activation of the NFIs themselves is very poorly defined. Our findings suggest that NFIX may autoregulate itself, a finding consistent with a recent report identifying NFIB as a regulator of *Nfix* expression in the developing spinal cord [206]. Moreover, investigating the expression and role of other novel factors highlighted in this screen will enhance our understanding of CGNP biology. Another point to consider is the fact that we filtered our target gene list (RNA-seq and ChIP-seq; Figure 3-6 D) following our use of motif enrichment, which identified the MATH1 consensus binding site within our NFIX ChIP-seq peaks (Figure 3-7 A, B). We filtered our gene list based on those genes that were also potential targets of MATH1 [i.e. contained an MATH1 ChIP-seq peak, and were differentially regulated in *Math1*-deficient cerebellar tissue [186]] Many potential NFIX target genes (401 in total) were not identified in the MATH1 datasets, and as such, many more avenues remain to study novel targets of NFIX in CGNP differentiation (e.g. *Tiam2, Lingo3, Adamts1*). Finally, we also filtered our NFIX ChIP-seq peaks by only considering those peaks located within open chromatin [198]. An interesting finding of our ChIP-seq data was that many of the peaks were located in regions of closed chromatin. This suggests that NFIX may play roles in addition to regulating direct gene transcription. Indeed, NFIs have previously been shown to bind to histone H3, and to regulate nucleosomal architecture [204, 217, 218]. NFIB was also shown recently to regulate chromatin accessibility in small cell lung cancer in a manner that promoted tumour metastasis [219]. Looking forward, defining the functional significance of NFIX binding to closed regions of chromatin may provide new insights into how these factors regulate neural stem cell biology.

3.7 Conclusion

In conclusion, the research in this chapter shows that loss of NFIX disrupts the developmental program of CGNPs, resulting in a delay in progenitor cell differentiation. NFIX directly regulates a large network of developmentally significant genes, of which a subset are co-ordinately regulated by the bHLH transcription factor MATH1. This suggests that NFI and bHLH transcription factors may work in tandem to drive CNS development, through regulation of downstream signalling pathways such as Reelin. The novel gene targets identified from this analysis warrant further investigation, not just from a developmental biology perspective, but also in the context of CNS cancer biology. Lastly, to get a wholistic picture of the role of NFIs in cerebellar development, we need to expand this analysis to include the other members of this transcription factor family.

Research included in chapter 4 was published in the journal *The Cerebellum*, in December 2019: A typeset version of this publication is included in the appendix.

Fraser J*, Essebier A*, Brown AS, Davila RA, Harkins D, Zalucki O, Shapiro LP, Penzes P, Wainwright BJ, Scott MP, Gronostajski RM, Bodén M, Piper M, Harvey TJ.Common Regulatory Targets of NFIA, NFIX and NFIB during Postnatal Cerebellar Development. *The Cerebellum doi: 10.1007/s12311-019-01089-3 Online Dec 2019.*

Contributor	**Statement of contribution**
James Fraser	Conceptualisation and design (40%) Experimentation (52%) Analysis and interpretation (45%) Drafting and writing (40%)

For this chapter, I conducted a majority of the biological experimentation as well as the analysis and interpretation of these relevant results. Additionally, I was involved heavily in the background and design of this paper and contributed to writing and proofreading the manuscript. Co-authors contributed to all sections, especially RNA-seq and ChIP-seq analysis and the interpretation of these results. The senior author contributed heavily to writing the final manuscript.

Chapter 4 **Common regulatory targets of NFIA, NFIX and NFIB during postnatal cerebellar development**

4.1 Aims and chapter overview

Chapter 4, is the last data chapter of this thesis. Chapter 4 expands on the work of the previous chapter utilising a similar methodology of combining RNA-seq and ChIP-seq, but this time incorporating data generated in *Nfia*$^{fl/fl}$;*Math1*-cre conditional knockout mice with that from *Nfix*$^{-/-}$ mice. Our data show that NFI transcription factors regulate a discrete subset of genes in a co-ordinate manner, including a number of other transcription factors of which a large portion have not previously been investigated in the cerebellum.

4.2 Abstract:

In germinal niches, transcription factors play an overarching role in regulating the proliferation and differentiation of progenitor cells. Nuclear Factor One transcription factors regulate the differentiation of both neuronal and glial progenitors in the central nervous system and have an emerging role in neoplasms arising from these cells including medulloblastoma and glioma. Previous research has shown that loss of function or deletion mutations in *NFI family members* result in severe neural phenotypes in both humans and mice. These similar and often overlapping phenotypes suggest that this transcription factor family may co-ordinately regulate downstream gene targets. In the mouse cerebellum, we have shown that *Nfix* regulates the differentiation of cerebellar granule neuron progenitors by controlling the transcription of a large cohort of downstream gene targets. As of yet, a comprehensive functional profile of other NFI family members is lacking in these cells. Using co-immunofluorescence microscopy, we first found out that NFIA is expressed in CGNPs, CGNs and Glia in the postnatal cerebellum, in an expression pattern that closely overlaps that of NFIX in these cells. Next, we integrated transcriptomic sequencing and epigenetic profiling to reveal a specific subset of gene targets, co-ordinately regulated by *Nfia* and *Nfix* in postnatal CGNPs. Our results show that NFIs work both individually and co-ordinately, regulating a large number of developmentally significant genes and other transcription factors in these progenitors. Additionally, these data identify a large suite of novel target genes that may have roles in regulating neurogenesis in the cerebellum. Collectively, these results highlight convergent roles of NFI family members in regulating CGNP development and position these transcription factor family members as key promoters of neurogenesis.

4.3 Introduction

The development of the cerebellum is a complex process that relies on both directional and reciprocal interactions between transcription factors and gene targets, often in prominent signalling pathways. In germinal zones of the cerebellum, these interactions help demarcate progenitor populations and regulation their development and differentiation, often in a temporally dependent manner [28, 50, 149, 220, 221]. Many transcription factors in the cerebellum belong to families with multiple members similar binding motifs. Often these can work in tandem manner to drive developmental programs forward. Whilst expression analysis can be used to infer co-ordinated roles of TF family members in mediating development, a combination of both chromatin profiling and transcriptomic analysis is needed to provide functional insight into the role of individual family members in progenitor populations. For example, a combination of DNase-seq and RNA-seq recently identified a co-ordinated role of *Zic1* and *Zic2* in mediating CGNP maturation [198]. Indeed, if we are to fully understand the roles of other transcription factor families in the cerebellum, similar analysis is needed.

NFI transcription factors are highly expressed in the central nervous system [90]. Despite this, little functional analysis has been undertaken to determine the individual or combined roles of this family in cerebellar development. Previously, we have shown that NFIX is highly expressed in CGNPs during postnatal cerebellar development, and that loss of expression results in a delay in progenitor cell differentiation [Chapter 3], [91]. Interestingly, *Nfix* and *Math1* co-ordinately regulate a small subset of gene targets in CGNPs, suggesting transcription factors from these different families may have overlapping functions [Chapter 3]. Analysis of *Nfia* in the cerebellum has mainly focused on the *Nfia*$^{-/-}$ mouse strain, which alike with *Nfix*$^{-/-}$ mice display a delay in CGNP maturation, hinting at a shared role of with *Nfix* in governing progenitor development. Limited mechanistic or functional investigation of *Nfia* has been conducted in granule neurons. *Nfia* has been shown to promote GABRA6 expression [101], and loss of *Nfia* decreases expression of SYNAPSIN1 and WNT7A, both required for mossy-fibre-CGN synapse formation and axonal remodelling [99, 222, 223]. Interestingly, we have previously shown that loss of *Nfix* also leads to a reduction in both *Wnt7a* and *Gabra6* expression [Chapter 3]. This similarity in both downstream gene targets and progenitor development delay in the respective *null*-mutants suggest that *Nfia* and *Nfix* may work in a co-ordinate manner to regulate development of CGNPs. Additionally, both *Nfix* and *Nfia* have been both been implicated in the formation of medulloblastoma, of which CGNPs are the cell of origin in some subtypes. For example, in a mouse model of SHH-type medulloblastoma, which arises exclusively from CGNPs, loss of *Nfia* results in a poorer prognosis and accelerated tumorigenesis

[136, 170]. These findings suggest that *Nfia,* alike with *Nfix*, likely play a significant role in the CGN developmental program and progenitor differentiation in the cerebellum.

NFI transcription factors have been shown to interact with and regulate a number of other transcription factor families during neurogenesis. Interactions between NFI and bHLH transcription factors have been established previously in progenitor lineages in the developing cerebellum[130], [Chapter 3]. Additionally, we have shown that NFIX and MATH1 co-ordinately regulate a subset of genes important in CGNP differentiation in the previous chapter [Chapter 3]. Therefore, it is likely that if *Nfix* and *Nfia* are co-expressed in CGNPs, they could also work in tandem to co-ordinately regulate a number of key developmental genes, driving cerebellar development. Logically, it is also likely that several of these will be other transcription factors from different TF families. To answer this, in this chapter we set out to investigate 1) whether or not NFIA and NFIX expression overlaps in developing CGNPs, 2) whether co-ordinate regulation of gene targets by NFIA and NFIX exists in CGNPs and 3) and of these how many of these are transcription factors. We first looked at expression patterns of NFIA and NFIX in the postnatal mouse cerebellum using co-immunofluorescence microscopy. Next, we used RNA-seq in wild-type, *Nfia* and *Nfix*-deficient CGNPs to identify differentially expressed genes in these mutants. To find directly regulated targets from this list, we used ChIP-seq with α-NFIA and α-NFIX antibodies and used DNase I hypersensitive regions to find which of these directly regulated gene targets are in regions of accessible chromatin. Finally, we compared these genes to online transcription factor and expression databases. Our analysis revealed that NFIA and NFIX co-ordinately regulate a substantial number of developmental genes and transcription factors in postnatal granule neuron progenitors. Of these genes and transcription factors, a large proportion have no previously identified role in CGNPs, but several are known regulators of neurogenesis. Additionally, several of these gene targets have identified roles as oncogenes in CNS tumours such as medulloblastoma. Taken collectively, these analyses provide a detailed expansion on the previously known role of NFIs in the cerebellum, and provide new evidence that these transcription factors work together to drive forward cerebellar development.

4.4 Methods

4.4.1 Animal ethics details

Nfia null mice on this genetic background are embryonically lethal. As such, we used a conditional *Nfia* allele ($Nfia^{fl/fl}$) crossed to an *Math1* cre line [224]. This line enabled the ablation of *Nfia* from MATH1-expressing cells from embryonic day 9 [50, 61] including the cells of the rhombic lip that will ultimately give rise to CGNPs within the EGL of the postnatal cerebellum. Knockout animals were $Nfia^{fl/fl;}$ *Math1*-cre^{+}; controls were $Nfia^{fl/fl;}$ *Math*-cre^{-}. Animals were used with approval from the University of Queensland Animal Ethics Committee (AEC approval numbers: QBI/143/16/ NHMRC/ARC and QBI/149/16/ARC). All experiments were performed according to the Australian Code of Practice for the Care and Use of Animals for Scientific Purposes. For all animals, genotyping was done by PCR using genomic DNA, which was extracted using alkaline lysis, from mouse-tail and toe tissue. Pregnant females were acquired by placing male and female mice together overnight. The next day, females were inspected for the presence of a vaginal plug and, if present, this day was designated as E0. The day of birth was designated as P0. Mice were housed in Optimice IVC caging, with double HEPA filters and built-in ventilation. Food and water was available *ad libitum*, and materials were provided for nesting and enrichment.

4.4.2 Immunohistochemistry

Chromogenic immunohistochemistry and immunofluorescence labelling was performed as described previously [Chapter 2]. Briefly, mice were anesthetised and perfused transcardially with phosphate-buffered saline (PBS), followed by 4% paraformaldehyde (PFA), then post-fixed for 48-72 hours before long term storage in PBS at 4°C. Cerebella were isolated and embedded in 3% Noble agar and sectioned in a sagittal plane at 50 μm intervals using a vibratome. Sections were placed sequentially across the wells of a 6-well plate to ensure appropriate sampling from different medio-lateral regions of the cerebellum. For all analyses we had >6 sections per animal to image and analyze. Sections were mounted on slides before heat-mediated antigen retrieval was performed in 10 mM sodium-citrate solution at 95°C for 15 min. For chromogenic immunohistochemistry, sections were incubated overnight in primary antibodies at 4°C. A list of antibodies used in this study is given in Table 1. The following day, sections were rinsed in PBS, then incubated in a solution containing a biotinylated secondary antibody (Vector Laboratories) for 1 hour at room temperature, followed by processing with a VECTASTAIN ABC kit for 1 hour at room temperature (A used at 1/500, B used at 1/500, Vector Laboratories). Sections were rinsed again in PBS, then were processed for colour reaction using a nickel- 3,3'-diaminobenzidine (DAB, Sigma) solution (2.5% nickel sulfate and 0.02% DAB in 0.175 M sodium acetate) activated with 0.01% (v/ v) hydrogen peroxide. The colour reaction was stopped by rinsing multiple times with PBS, and

sections were then coverslipped with DPX mounting medium (Thermo Fisher Scientific). For IF labeling, sections were incubated at 4°C overnight with primary antibodies against the target proteins (see Table 1). The following day sections were rinsed in PBS, then incubated with the relevant secondary antibodies (Table 1) for 1 hour in the dark at room temperature. Sections were rinsed in PBS, then were counterstained with Hoechst 33342 (Thermo-Fisher Scientific) and mounted in fluorescent mounting media (DAKO). For all experiments, at least three animals at each age were analysed.

Table 5 Antibodies used in this chapter

Antibody	*Source species*	*Company*	*Catalogue number*	*Dilution used*	*Purpose*
NFIX	Mouse	SIGMA	SAB1401263	1/200;1/1000	IF/IHC
NFIA	Rabbit	ABCAM	HPA008884	1/200/1/1000	IF/IHC
S100β - Alexa 647	Rabbit	ABCAM	AB196175	1/400	IF
PAX6	Rabbit	DAKO	Z0334	1/400	IF
NFIB	Rabbit	SIGMA	HPA003956	1/400	IF
Ki67	Mouse	BD Pharmigen	550608	1/400	IF

4.4.3 Cerebellar imaging

Fluorescent immunolabelling was visualized using a Nikon 20x Air objective on a spinning disk confocal microscope (Diskovery; Andor Technology, UK) on a Nikon Ti-E body (Nikon Corporation, Japan), equipped with a Zyla 4.2 10-tap sCMOS camera (Andor Technologies). For comparative sections, identical imaging parameters were used including pinhole size (70 µm), laser power and exposure time. We took 10 consecutive 1-µm-thick optical sections to generate a 10-µmthick z-stack. In all cases, the 10-µm z-stack was taken from the middle of the section to minimize potential artefacts arising from the sectioning process such as damage to the tissue. Image acquisition, tiling and stitching were performed using NIS-Elements Advanced Research Imaging software (Nikon Corporation, Japan). All brightfield images were captured using an Aperio ScanScope XT Slide scanner (Leica Biosystems, Germany) with a doubled x20 objective (×40 magnification overall; Nikon Corporation, Japan) and visualized using Aperio ImageScope software. For analysis of wild-type, *Nfia*$^{fl/fl}$; *Math1* Cre^{+} and *Nfia*$^{fl/fl}$; *Math1* Cre^{-} mice, high-magnification images were taken of the same lobule of the cerebellum, using at least three biological replicates at each of the ages assessed. For quantification of granule neuron and proliferative markers (PAX6 and Ki67, respectively), three 200-µm regions of the EGL were quantified for each section. This ensured a more representative count of the EGL thickness across the whole lobule. One micrometer- thick optical sections were viewed in ImageJ/Fiji, and the 'cell counter' plugin was used to mark and quantify cells expressing respective markers in each

fluorescent channel. Cells co-expressing markers (for example, PAX6 and Ki67) were also quantified this way, and DAPI was used to visualize the cell nucleus, to ensure accuracy, especially in areas of high cell density.

4.4.4 Granule neuron progenitor isolation

CGNPs from P7 *Nfia*$^{fl/fl}$; *Math1* Cre^{+} and *Nfia*$^{fl/fl}$; *Math1* Cre^{-} mice were isolated using the method outlined by Lee and colleagues [141] and a papain dissociation kit (Worthington Biochemical Corporation). Briefly, the cerebellum was dissected from three wild-type and three knockout mice and carefully separated from choroid plexus and meningeal tissue. Remaining cerebellar tissue was dissociated using a 20 units/mL papain solution at 37°C for 15 mins. A single cell suspension was obtained by trituration with a serum-coated P1000 pipette tip and nuclear membranes were removed using an albumin-ovomucoid inhibitor gradient. CGNPs were separated from other cells using a 30%-60% percoll gradient. Purified CGNPs cells were then lysed in Trizol (Ambion) and RNA isolated using an RNeasy miniprep kit (Qiagen).

4.4.5 RNA-seq analysis

RNA sequencing was performed on the samples using the Illumina NextSeq High-Output system (Illumina; 150-bpread length, paired-end reads). We isolated cells from three P7 *Nfia*$^{fl/fl;}$ *Math1*-cre^{-} mice and three P7 *Nfia*$^{fl/fl}$; *Math1*-cre^{+} mice. RNA-seq analysis was performed on RNA isolated from P7 cerebella as described in previous chapters. Sequences were aligned using TopHat2 (v2.0.9) [152] to the *Mus musculus*, UCSC, mm10 reference transcriptome and FASTA annotation downloaded from the TopHat index and annotations page (https://ccb.jhu.edu/software/tophat/igenomes.shtml). Cufflinks (v2.1.1) [152] was used to assemble each replicate's transcripts from the alignment file generated by TopHat. Cuffmerge was used to create a single assembly containing transcripts across all samples and replicates. Cuffdiff was run using the merged set of transcripts and the three replicate TopHat2 .bam files from each sample.

4.4.6 DNase I hypersensitivity analysis

DNase I hypersensitivity (DHS) called peaks from whole cerebellum at P7 across three replicates were retrieved from Frank et al. 2015 (GEO: GSE60731). UCSC liftover was used to convert the mm9 files to mm10. If at least two replicates shared a peak, it was recorded using the maximum boundaries of the supporting peaks to generate a merged DHS peak file. Transcription factors are known to bind preferentially in regions of accessible chromatin [195, 196] and DHS was therefore used to extract NFIX and NFIA ChIP-seq peaks occurring in accessible regions.

4.4.7 ChIP-seq

ChIP-seq was performed on chromatin isolated from P7 wildtype C57Bl/6 CGNPs as described in Chapter 3. We used antibodies against NFIA, NFIB or NFIX, for which specificity has previously been demonstrated [179]. For chromatin immunoprecipitation, litters of P7 pups were pooled for CGNP isolation. Isolated CGNPs were crosslinked with 1% formaldehyde for 10 min then were quenched with glycine. Cells were lysed in RIPA buffer supplemented with protease and phosphatase inhibitors (Roche) and sonicated with a Bioruptor (Diagenode) for six x 15-min intervals of 30s on, 30s rest. Chromatin immunocomplexes were isolated with protein G agarose beads (Roche) and washed once for 5 min with buffers 1 through 4. Crosslinking was reversed by incubation with proteinase K (Roche) at 60° overnight. DNA was isolated by phenol-chloroform extraction then incubated with RNase A (Roche) for 30min before final clean-up with PCR columns (Qiagen). Sequencing libraries were constructed using the standard protocol for the NEB Next Ultra II DNA Library Prep Kit (New England BioLabs). Pooled libraries were sequenced on an Illumina HiSeq 2000 (Illumina; 30-bp single end read).

Previously we have published an NFIX ChIP-seq dataset in P7 CGNPs [Chapter 3]. Alignment was performed on an both NFIA and NFIX ChIP-seq data by bowtie2 [188] to mm10. Unaligned reads and reads which aligned to multiple locations were removed leaving only uniquely mapped reads. MACS2 [189] was used to call narrow peaks with default parameters for both datasets. Both experiments contained two biological replicates and if both biological replicates shared a peak, it was recorded using the maximum boundaries of the supporting peaks to generate a merged set of peaks for each experiment.

4.4.8 Annotation of ChIP-seq peaks

A set of target genes was identified for NFIA and NFIX by the following method; A promoter region was defined as ± 2000 base pairs around a transcription start site. ChIP-seq binding sites located in a promoter region were annotated as *proximal*, while sites outside the promoter region but overlapping gene boundaries (transcription start to stop) were labelled as *genic*. All remaining binding sites were labelled as *distal*. A binding site annotated as proximal was assigned the nearest gene as a target while genic binding sites were assigned the overlapping gene as a target. Distal binding sites are difficult to assign target genes to, as they are not necessarily regulating the nearest gene (by genomic distance). CisMapper was used to annotate distal binding sites and provide a secondary annotation to proximal and genic sites, with resulting links filtered to a threshold of 0.05 [192].

4.4.9 qPCR analysis.

cDNA was prepared from RNA isolated from P7 CGNPs using a Superscript III Reverse Transcription Kit (Invitrogen). qPCR was performed with the Quantifast SYBR kit (Qiagen). Gene expression was calculated using the $2^{-\Delta\Delta CT}$ method, relative to the housekeeping gene g*lyceraldegyde 3-phosphate dehydrogenase (Gapdh)*. All samples were tested in triplicate with each experiment and each was repeated three times. Mean values + SEM were entered into *Graphpad Prism 7* and multiple t-tests conducted, with a Hold-Sidak method to correct for multiple comparisons. qPCR was performed on the QuantStudio7 Flex Real-Time PCR System (Applied Biosystems, USA).

Table 6 qPCR primers used in this chapter

Gene	Forward	Reverse
Id3	CTGTCGGAACGTAGCCTGG	GTGGTTCATGTCGTCCAAGAG
Wnt5a	CAACTGGCAGGACTTTCTCAA	CCTTCTCCAATGTACTGCATGTG
Gas6	GACCCCGAGACGGAGTATTTC	TGCACTGGTCAGGCAAGTTC
Kalrn	AAGACCTACGGAAACTTGTGACG	CCCCGCATGTCGATGATGAC
Etv5	TCAGTCTGATAACTTGGTGCTTC	CTACAGGACGACAACTCGGAG
FoxO6	TCATGGACAGTGACGAAATGG	ACCCAGCTCTGGTTAGGGG
Gapdh	GCACAGTCAAGGCCGAGAAT	GCCTTCTCCATGGTGGTGAA

4.4.10 Gene annotation and ontology

After identifying a gene target for each NFIX binding site; the associated *p*-value from both the *Nfix* and *Nfia* RNA-seq differential expression analyses was recorded. Genes 'targeted' by *Nfix and Nfia* with a significant ($p < 0.05$) change in expression in both experiments were extracted. Genes showing coordinated positive or negative log fold change values across both experiments were selected to generate a putative set of genes under the control of both TFs. Functional annotation was performed using the PANTHER Gene Ontology system (Version 14.1, pantherdb.org)[225] through the Gene Ontology web portal (http://geneontology.org/), on target genes identified from our preceding transcriptomic and chromatin profiling analyses. Enriched GO-terms for Molecular function, Biological Process and KEGG Pathways were selected, based on corrected p-value and FDR of <0.05. To identify putative transcription factors from our gene lists, raw gene names were entered into TFCheckpoint, an online compendium of Human, mouse and rat transcription factors (www.tfcheckpoint.org)[226].

4.5 Results

4.5.1 NFIA and NFIX show overlapping expression patterns in the postnatal cerebellum.

To identify whether or not NFIA and NFIX co-regulate gene targets in the cerebellum, we first need to identify whether or not these transcription factors have overlapping expression patterns. NFIA and NFIX are both expressed in CGNPs (Chapter 2,3) [100, 101, 227] but co-expression is yet to be described. We used co-immunofluorescence staining (Co-IF) with anti-NFIX, anti-NFIA and anti-s100β antibodies to look for co-expression, first in CGNPs and then in cerebellar glia across postnatal cerebellar development. Our data show that both NFIA expression and NFIX show strong expression in the cerebellar EGL at P3, P7 and P15 (Figure 4-1). Interestingly, expression of NFIX was strongest in the most posterior lobules at P3 and weaker in lobules anterior. However, NFIX expression was strong in the EGL of all lobules by P7 consistent with our previous data (Chapter 2]. Migratory cells in the ML (identified by their stretched polar morphology) express NFIA and NFIX at all ages investigated, and do not express s100β, suggesting they are newly post-mitotic CGNs (Figure 4-1 G, H, J, single arrowhead). The expression of both transcription factors is strong at all ages cells in the IGL, a majority of which are post-mitotic CGNs. Interestingly, both NFIA and NFIX are strongly expressed in the cell body of Bergmann Glia at all ages examined. This co-expression also extends to astrocytes in the IGL at these ages (Figure 4-2). Indeed, both transcription factors are co-expressed in a majority of $s100\beta^{+}$ cells, before the glial scaffold is fully in place (P3) and after, when glial projections extend to interact with CGNPs in the EGL (P15). These data suggest that NFIA and NFIX have strongly overlapping expression patterns in both cerebellar granule neurons and glia during development of the postnatal cerebellum, indicating potentially overlapping roles.

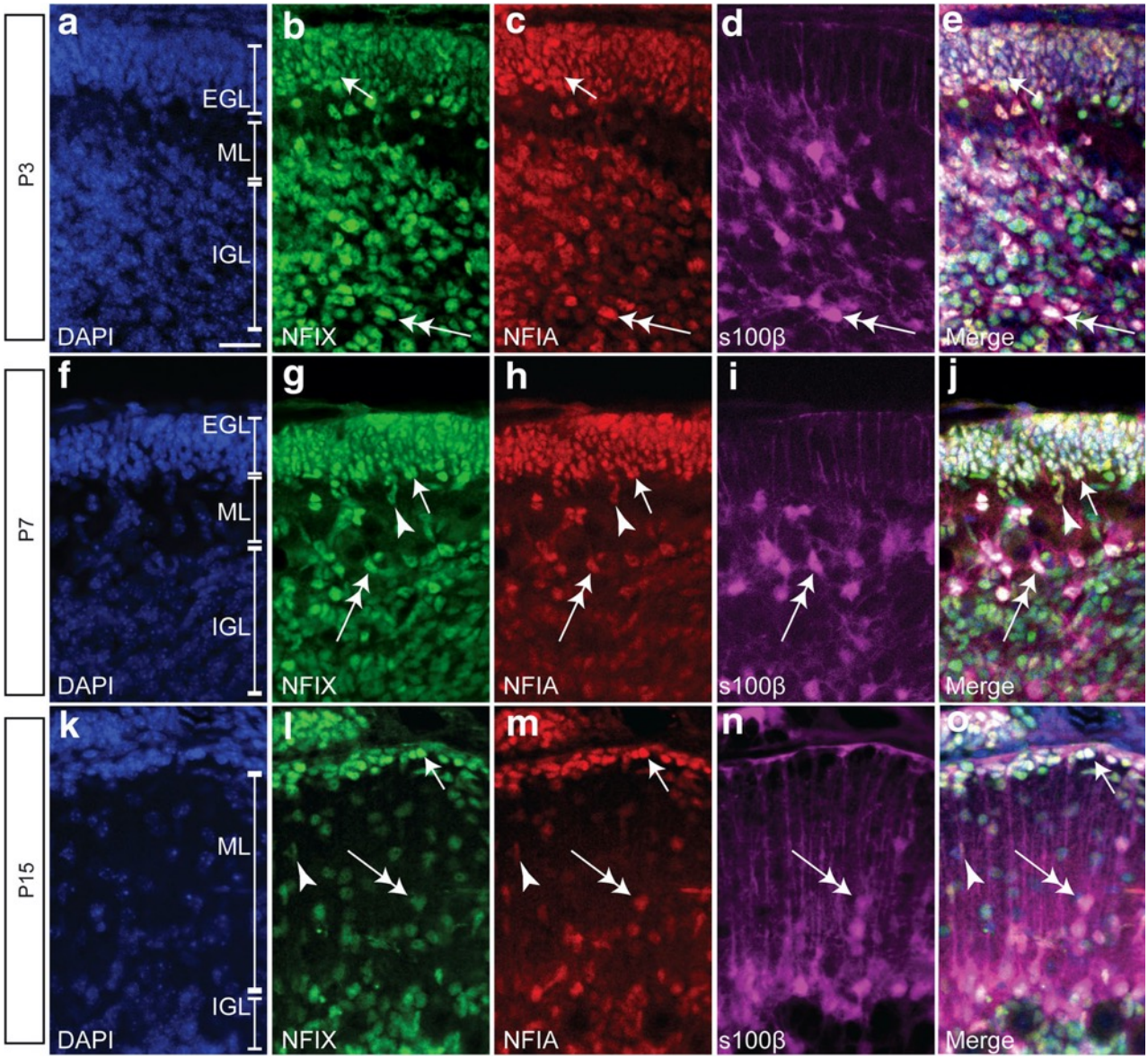

Figure 4-1 NFIX and NFIA are co-expressed in various cellular populations in the developing mouse cerebellum

Sagittal cerebellar sections showing the nuclear marker DAPI (blue), NFIX (green), NFIA (red) and s100β expression (magenta) in P3 (a–e), P7 (f–j) and P15 (k– o) wild-type mice. NFIX and NFIA are co-expressed by CGNPs within the external granule layer (EGL; arrows in b–e, g–j, l–o). NFIX and NFIA are also expressed by s100β-positive glial cells (double-headed arrows in b– e, g–j, l–o). These transcription factors are also expressed by cells leaving the EGL (arrowheads in g–j, l–o); these are likely immature neurons migrating to the internal granule layer (IGL). ML molecular layer. Scale bar (in A) = 20 μm

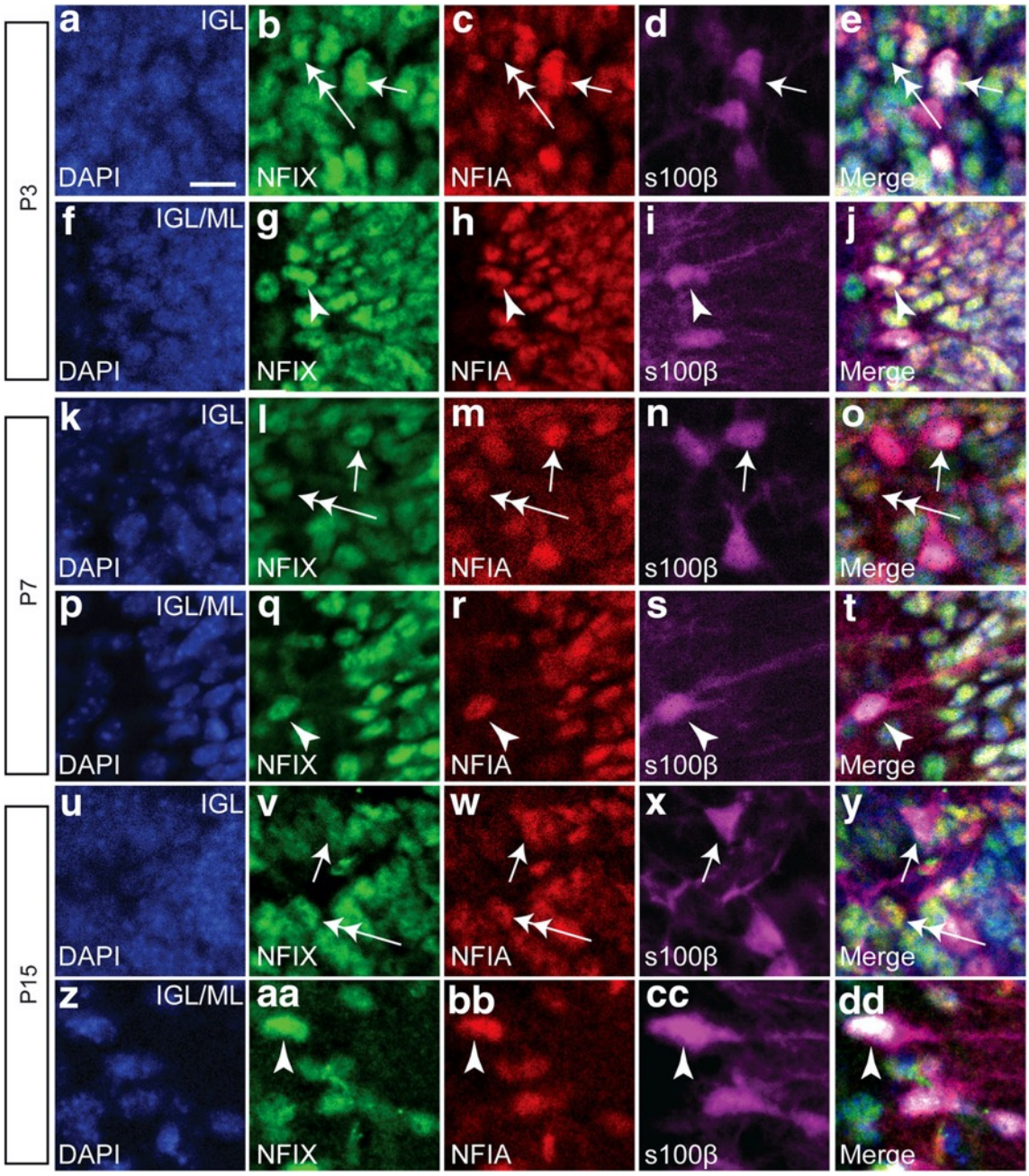

Figure 4-2 NFIX and NFIA are co-expressed in astrocytes and glia in the postnatal cerebellum.

High magnification sagittal cerebellar sections showing the nuclear marker DAPI (blue), NFIX (green), NFIA (red) and s100β expression (magenta) in P3 (A–J), P7 (K–T) and P15 (U–DD) wild-type mice. NFIX and NFIA are co-expressed in IGL white matter astrocytes at these ages (arrows in B–D, L–O, V–Y). NFIX and NFIA are also co-expressed in Bergmann glia at P3, P7 and P15 (arrowheads in G–J, Q–T, AA–DD). The NFI factors are also co-expressed in mature granule neurons within the IGL (double-headed arrows in B– D, L–O, V–Y). IGL inner granule layer, ML molecular layer. Scale bar (in A) = 10 μm

Previously, we have shown that NFIX plays a role in the differentiation of CGNPs in the EGL, with *Nfix*$^{-/-}$ mice displaying delays in progenitor differentiation and increased proliferation *in vitro* [Chapter 3]. To determine the function of *Nfia* in these cells, we first examined co-expression of NFIA with the granule neuron marker PAX6 (Figure 4-3 A-D). Next, to determine expression patterns in the progenitor fraction of these neurons, we co-stained cerebellar with NFIA and Ki67, and examined the EGL of postnatal mice (Figure 4-3 E-H). At P7, a vast majority of fluorescently labelled cells are PAX6^{+}/NFIA^{+} including cells in the EGL (single arrow), migratory CGNs in the ML (arrowhead) and adult granule neurons in the IGL (double arrow). Additionally, Ki67 staining revealed that a majority of PAX6^{+} progenitors in the EGL that are proliferative co-express NFIA. These expression patterns are almost identical to the previously identified expression patterns of NFIX in the cerebellum. This raises the hypothesis that these transcription factors have either complementary, inhibitory or fully independent roles in these cells stressing the need for further functional analysis.

4.5.2 Conditional deletion of *Nfia* in the mouse cerebellum causes cerebellar abnormalities

To investigate this hypothesis, we adopted a similar approach that was used in the previous chapter [Chapter 3], performing: RNA-seq and ChIP-seq on isolated CGNPs . Germline *Nfia*-null mutations are lethal on a C57/B6 background [105], so we utilised a conditional *Nfia* allele (*Nfia*$^{fl/fl}$) crossed onto an *Math1*-cre mouse line [224]. As MATH1 is expressed by progenitors in the rhombic lip from ~E9 onwards [50, 61], an effective *Math1*-cre driver should selectively delete NFIA from all CGNPs which in turn arise from the RL from ~E12.5 onwards. Thus, we used this resultant *Nfia*$^{fl/fl}$; *Math1*-cre mouse line to attempt to constitutively and selectively eliminate NFIA in CGNPs (Figure 4-4 A-D). Immunolabelling using NFIA, and PAX6 as a marker for granule neurons revealed that NFIA is poorly expressed in CGNPs in the EGL of *Nfia*$^{fl/fl}$; *Math1*-cre^{+} mice, with the most effective recombination in the more anterior lobules of the cerebellum (Figure 4-4 E-G). Of note, *Nfia* ablation was not completely penetrant in all lobes of the cerebellum, and deletion patterns seemed to mimic those previously seen in studies using this particular Cre driver [228, 229]. Interestingly, some NFIA expression is still found in the IGL. These cells are likely CGNs that arose from progenitors where *Nfia* was inefficiently deleted [single arrowhead Figure 4-4] or due to the presence of non-neuronal cells such as astrocytes, which we have shown express NFIA [Figure 4-2]. As loss of *Nfia* and *Nfix* both result in similar phenotypic changes in other parts of the CNS, we examined the phenotype of our *Nfia*$^{fl/fl}$; *Math1*-cre^{+} mouse. Haematoxylin staining at P15 revealed that *Nfia*$^{fl/fl}$; *Math1*-cre^{+} display increased lobulation compared to wild type controls [Figure 4-4 H, I] and an overall increase in PAX6^{+} cells in the EGL [Figure 4-4 L]. These data show that this mouse line is an effective way to study the phenotypes resulting from NFIA loss in CGNPs, without the lethality that occurs in *Nfia*$^{-/-}$ mice.

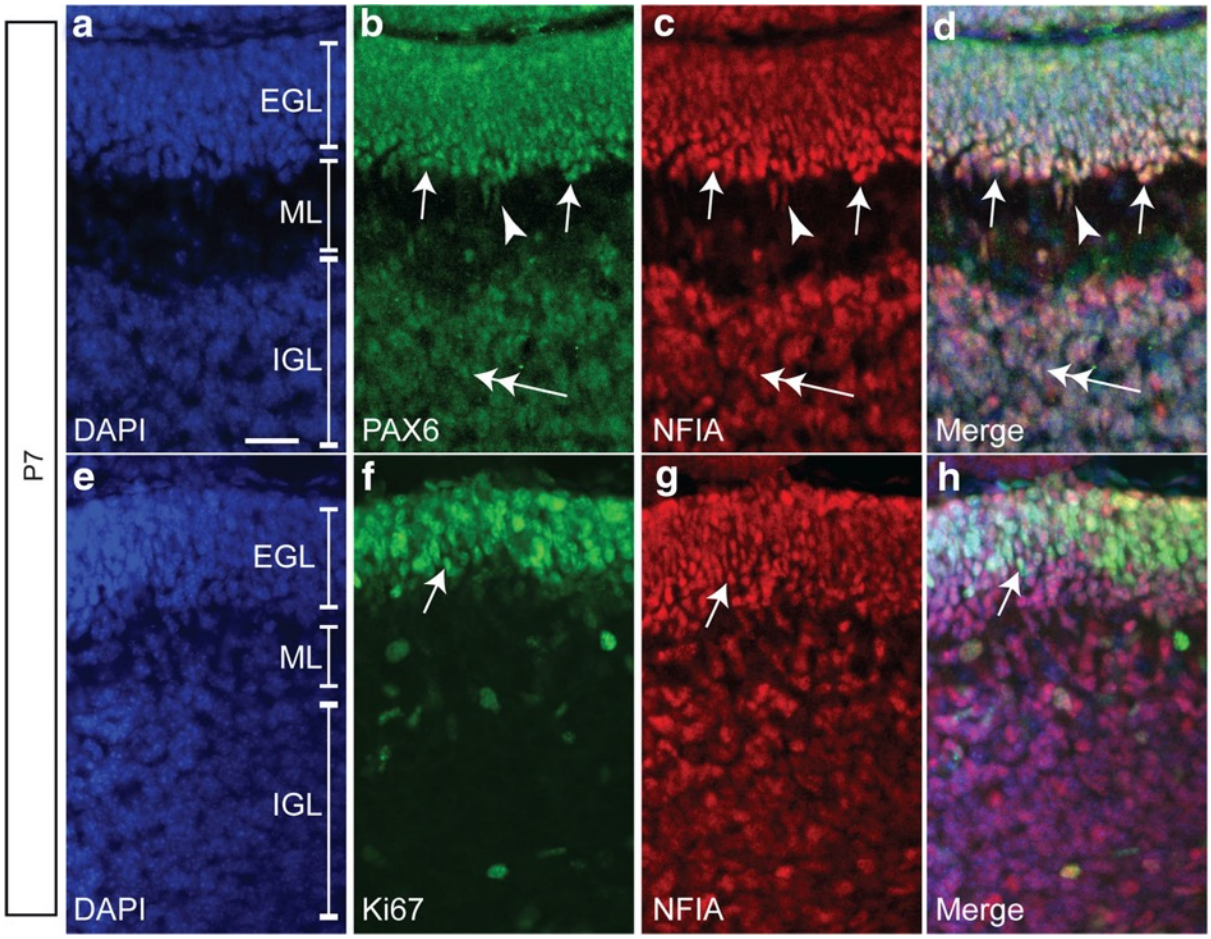

Figure 4-3 NFIA is ubiquitously expressed in granule neuron progenitors of the postnatal cerebellum.

a-d Expression of the nuclear marker DAPI (blue, a), PAX6 (green, b) and NFIA (red, c) reveals NFIA expression in PAX6-positive EGL progenitor cells (arrows in b–d). NFIA is also expressed in IGL granule neurons (double headed arrows in b–d) and migrating cells exiting the EGL (arrowheads in b–d). e–h Expression of the nuclear marker DAPI (blue, e), Ki67 (green, f) and NFIA (red, g) also shows NFIA expression in proliferating EGL progenitor cells (arrows in f–h). EGL external granule layer, ML molecular layer, IGL inner granule layer. Scale bar (in a) = 20 μm

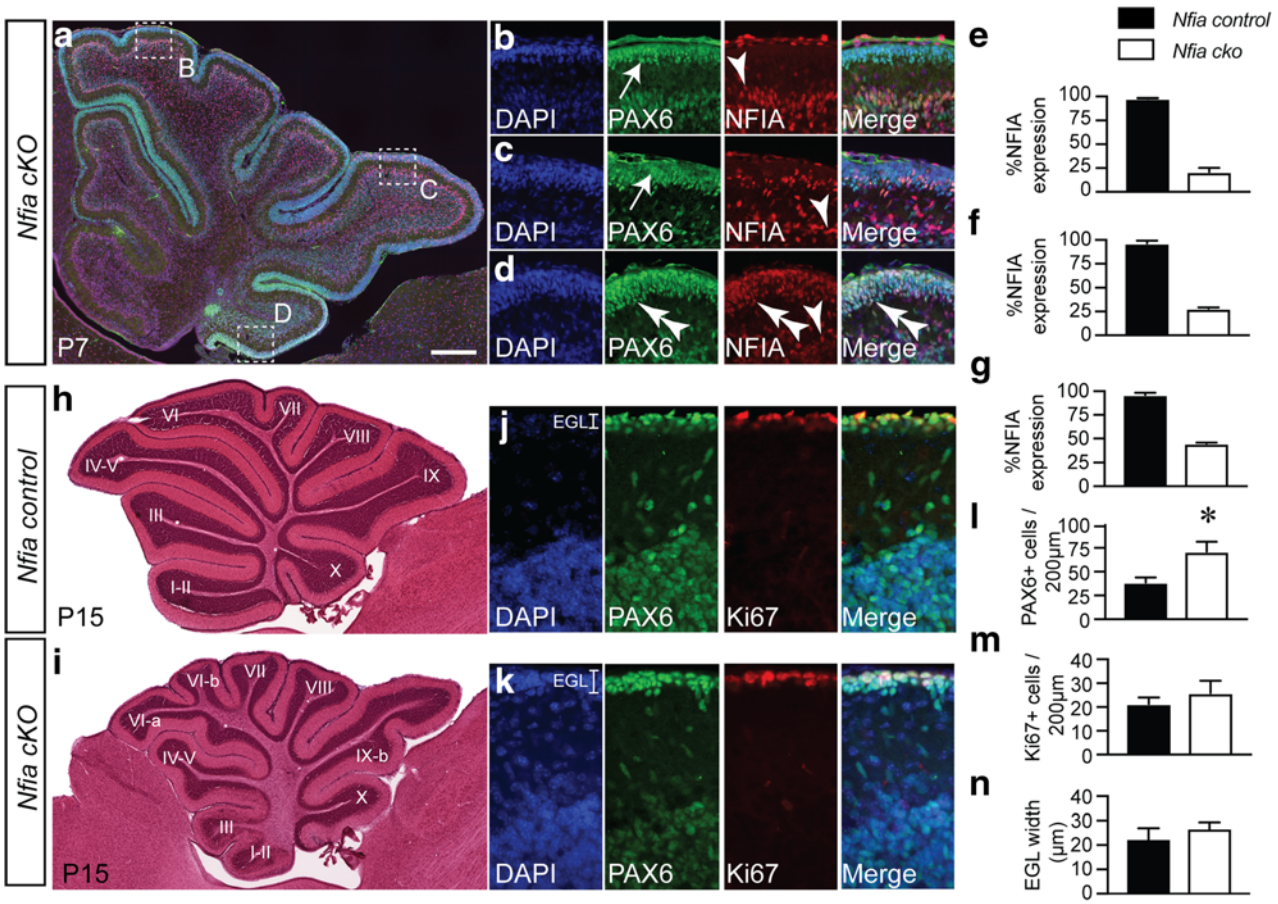

Figure 4-4 Conditional ablation of NFIA from EGL progenitors using *Math1*-cre.

(A) Sagittal cerebellar section in a P7 *Nfia*$^{fl/fl}$; *Math1*-cre^{+} mouse (*Nfia* cKO). (B-D) Co-expression of PAX6 and NFIA was examined in different cerebellar lobes and is shown in the respective high magnification panels, with DAPI (blue), PAX6 (green) and NFIA (red). Expression revealed that cells at the margin of the molecular layer and IGL expressed NFIA (arrowheads in B–D). Importantly, the majority of cells in the EGL of lobes VI and IX were immunopositive for PAX6 but did not express NFIA (arrows in B, C). Within lobe X, there were more cells within the EGL that had not undergone Cre-mediated ablation and hence retained NFIA expression (double arrowheads in D). (E–G) Quantification of the percentage of cells within the EGL of lobes VI (E), IX (F) and X (G) that expressed NFIA. (H, I) Hematoxylin staining of *Nfia* control and *Nfia* cKO cerebella at P15. The cerebellum of mice lacking *Nfia* was dysmorphic, with elevated foliation of the cerebellar lobes evident. Expression of DAPI, PAX6 and Ki67 in *Nfia* control (J) and *Nfia*$^{fl/fl}$; *Math1*-cre^{+} (K) cerebella at P15 revealed significantly more PAX6-positive cells within the EGL of the mutant (L), although the number of proliferating cells (M), and the width of the EGL(N), was not significantly different between sample groups. *$p < 0.05$, t test. Scale bar = 250 µm, in A; 400 µm, in H and I; 30 µm, in B–D; and 25 µm, in J and K.

4.5.3 Transcriptomic and chromatin profiling reveal a discrete set of co-ordinately regulated targets of NFIA and NFIX in postnatal CGNPs.

Whilst we have determined overlapping expression patterns of NFIA and NFIX in the cerebellum, co-expression does not necessarily indicate a conserved functional role. Functional insight into the role of transcription factors can be determined by a combination of chromatin profiling (to determine putative TF binding sites) and transcriptomic analysis (to determine changes in gene regulation under different conditions. In Chapter 3, we used this analysis to investigate the role of NFIX in CGNPs. Here, we have used this approach to examine how *Nfia* functions in these cells in these cells, and combined our two datasets to look for shared gene targets between these two transcription factors.

In Chapter 3, P7 CGNPs were isolated and purified from wild-type mice, before ChIP-seq was performed using an anti-NFIX antibody. This analysis revealed 6910 putative gene-associated NFIX binding sites. We then combined these data with a published dataset of global DNase I hypersensitivity at P7 [198]. DNase I hypersensitivity occurs in regions of accessible chromatin that are typically enriched for gene regulatory elements and transcription factor binding sites [230]. This analysis revealed 5843 accessible NFIX binding sites, associated with 4621 genes.

With this method as a template, we repeated a similar analysis, this time using an anti-NFIA antibody to identify putative NFIA binding sites. In total, 14025 NFIA binding peaks were found, with 12539 found in DNase I-hypersensitive regions associated with 7870 known genes [Figure 4-5 A, B]. A total of 1486 binding peaks were found in closed regions of chromatin. Next, we performed RNA-seq on CGNPs isolated from P7 control and *Nfia*$^{fl/fl}$; *Math1*-cre^{+} mice. This analysis identified 2267 genes as being significantly mis-regulated in the absence of *Nfia* [Figure 4-5 B]. We then took this gene list, and compared it with our cohort of 7870 known genes bound by NFIA in regions of accessible chromatin. This identified 1232 genes from the 2267 that were both significantly mis-regulated and contained an NFIA binding peak. We interpreted this as strong evidence that these genes were direct targets of NFIA in these cells during development.

We then combined both of these datasets (NFIX and NFIA) to determine whether or not these two TFs directly regulated a common suite of gene targets [Figure 4-5 C]. Of the 1232 NFIA gene targets, and 578 NFIX gene targets, 304 were shared by both TFs. Additionally, of these 304 common targets, 283 (~93%) were co-ordinately mis-regulated (i.e. the target gene was upregulated or downregulated in both the *Nfix*$^{-/-}$ and *Nfia*$^{fl/fl}$; *Math1*-cre^{+} datasets), [Table A12]. Whilst we did not have access to *Nfib*-null mice for RNA-seq, we were able to use ChIP-seq dataset with an anti-

NFIB antibody to look for potential binding sites in P7 CGNPs. This revealed 24950 NFIB-associated ChIP peaks, of which 21712 were in regions of accessible chromatin. Interestingly, of the 283 co-ordinately mis-regulated genes from our *Nfia/Nfix* data, 282 also contained NFIB-associated peaks.

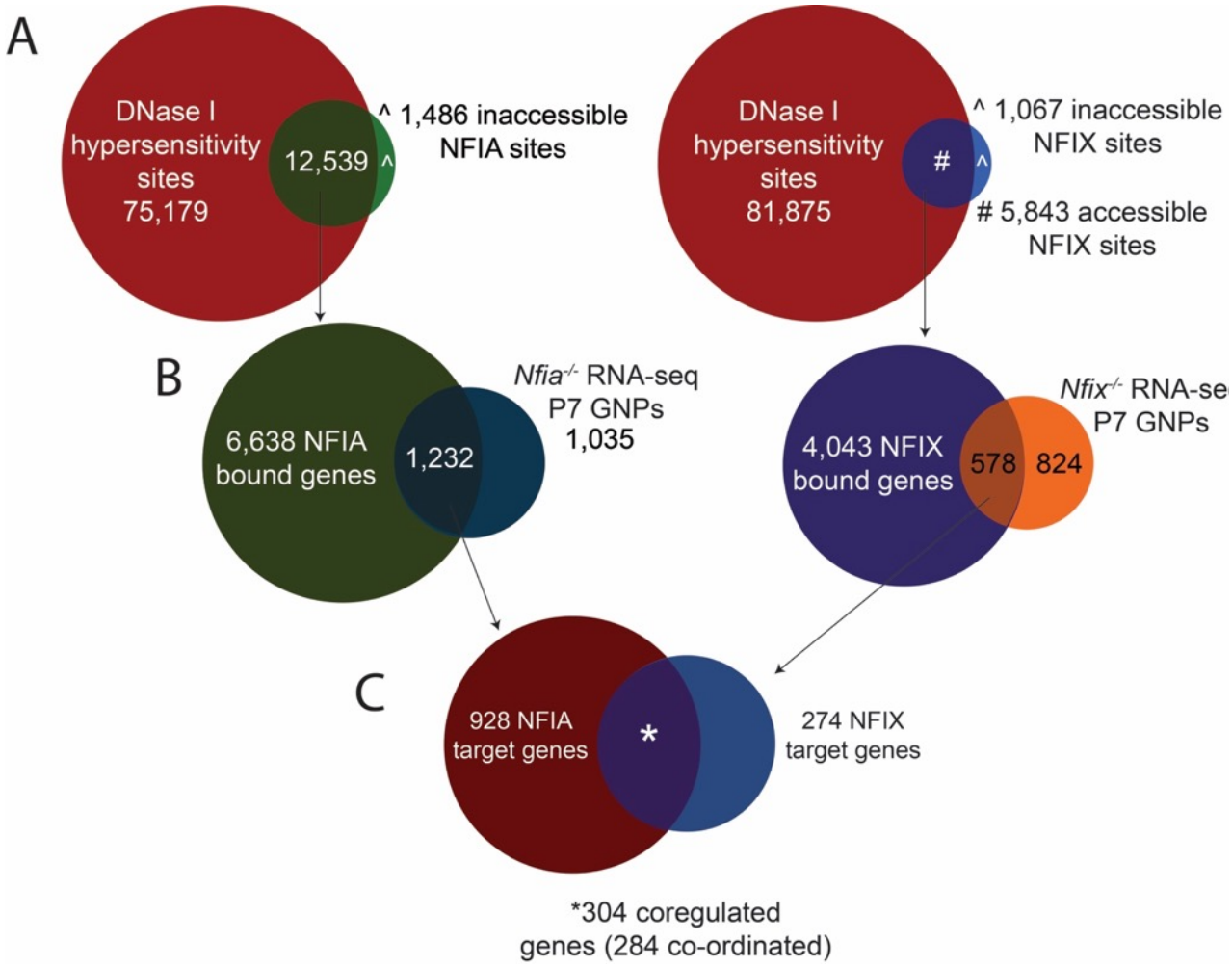

Figure 4-5 Transcriptomic and epigenetic profiling of NFIA and NFIX in postnatal CGNPs identifies co-ordinately regulated gene targets

(A, left-side) Combining ChIP-seq data using an anti-NFIA antibody with a dataset of DNase I hypersensitive sites [198], reveal putative binding sites for NFIA in regions of accessible chromatin. 14025 NFIA binding peaks were identified, with 12539 in accessible regions and 1486 in inaccessible sites. This is compared to equivalent data for NFIX from Chapter 3, (A-right-side) which identified 5843 accessible sites. B, left-side) of 12539 NFIA peaks in accessible regions, 7870 were associated with genes. RNA-seq in P7 *Nfia*$^{fl/fl}$*; Math1-*cre and control CGNPs revealed a total of 2267 mis-regulated genes, of which 1232 contained binding peaks for NFIA. These data suggest these are directly regulated targets of NFIA. A similar analysis for NFIX (B, right-side) was conducted in Chapter 3, and found 578 direct targets. C) To determine if direct-targets from B) were co-regulated by NFIA and NFIX, gene lists were compared. 304 genes were directly regulated by both transcription factors, of which 283 were regulated in a coordinated manner (i.e. either upregulated or downregulated in both NFIA and NFIX datasets).

Whilst a number of these co-ordinately regulated gene targets have well established roles in cerebellar development, with a large list of genes it is possible to use GO-term analysis to look collectively and in an unbiased manner for broad changes in both biological processes and molecular function. Thus, we used the PANTHER protein classification system (v.14.1 [225]) for gene ontology analysis, to determine the biological context of these mis-regulated genes. 280 of the co-ordinately mis-regulated genes were successfully mapped to the *Mus musculus* reference genome, as having unique gene identifiers. There, the tool was used to determine statistically significant over-representation of both GO-terms related to biological process [Table 7] and molecular function [Table 8].

As expected from the role that we and others have deduced for NFIs in the cerebellum, a number of key developmental GO-terms including 'nervous system development', 'neurogenesis' and 'cell differentiation' were ranked in the top 20, ranked based on p-value [Table 7]. Interestingly, a number of terms related to cell signalling ('regulation of signalling', 'regulation of cell communication', 'modulation of chemical synaptic transmission' and 'regulation of trans-synaptic signalling') were also highly ranked, suggesting that NFIs may play a broader role in establishing and regulating synaptic connections of developing granule neurons. This conclusion was further supported by examining the top 20 GO-terms related to molecular function. These almost exclusively related to ion/cation transmembrane transporter and channel activity [Table 8]. Combined, these data suggest that NFIs may drive the development of these cells by heavily regulating genes involved in synaptic connectivity and electrophysiological processes such as membrane potential.

In addition to GO-term analysis, we then used PANTHER pathways to search for significantly over-represented biological pathways in our co-ordinately mis-regulated gene list. 278 of 282 genes were mapped to 177 reference pathways in the PANTHER database. Of these, 11 were significantly overrepresented, including axon guidance mediated by *Robo*/*Slit* and *Cadherin*, *Notch* and *Wnt-signalling*, all of which have established roles in CGNP developmental programs [63, 77, 130, 222, 231-235]. Whilst these data identify a number of genes, processes and pathways with established roles in mediating CGN development (for example: *Otx2, NeuroD1, Robo1 and Rbfox3*), a significant proportion of those identified have little to no information or data available in the cerebellum or cerebellar granule neurons.

Lastly, we validated our dataset by performing qPCR on a selection of gene targets of both known (*Wnt5a)* and novel (*Foxo6, Kalrn, Etv5, ID3, Gas6*) roles in cerebellar development potential role

based on family members/associated genes. In both *Nfix*$^{-/-}$ and *Nfia*$^{fl/fl}$*; Math1*-cre^{+} CGNPs, expression was significantly higher than controls, replicating RNA-seq data [Figure 4-6].

4.5.4 NFIs regulate the expression of other transcription factors magnifying downstream effects.

Interestingly, a large number of genes identified in our RNA-seq analysis show differential expression despite no transcription factor binding site for either NFIA or NFIX. Since RNA-seq is a snapshot in time of RNA activity in a cell, it is hard to establish how directly regulated target genes may be influencing the expression of others downstream. However, this analysis does allow us to investigate our gene list and determine whether or not *Nfia* and *Nfix* are acting to co-ordinately regulate *other* transcription factors that may have functional roles in CGNP development, further broadening the role of NFIs in influencing the cerebellar transcriptome, albeit in an 'indirect' manner through effectors.

To investigate this, we compared our directly and differently expressed genes targets with a published database of transcription factors (TFcheckpoint [226]). This comparison revealed that NFIA directly regulates at least 78 known murine TFs in CGNPs, with NFIX regulating at least 46. Additionally, 26 of these are shared targets of both NFIs [Table 9]. Out of these shared 26 transcription factors targets, 25 of were co-ordinately regulated, with only one (*NeuroD6)* showing alternate regulation by NFIA and NFIX. This high proportionality of shared and co-ordinated targets further strengthens the hypothesis that NFIA and NFIX work synergistically to drive the developmental program of granule neurons in the cerebellum. This regulation of other transcription factors and their targets in turn are important to consider when determining the impact of gene deletions on the transcriptome.

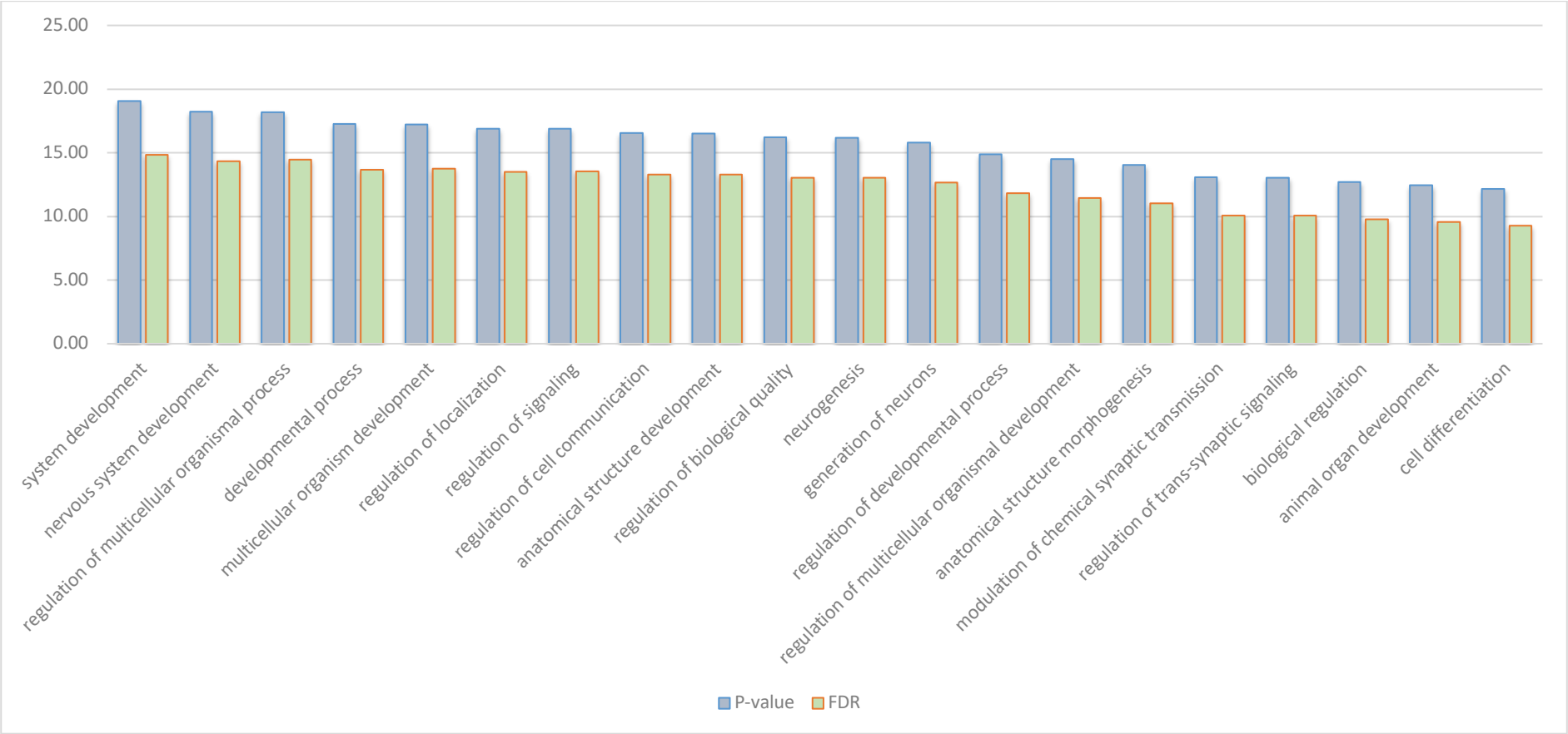

Table 7 Gene ontology analysis showing the biological processes enriched in the co-ordinately regulated gene targets of NFIs.

Raw gene targets names were used as input to search for GO-term over-representation, using the PANTHER Gene Ontology system (Version 14.1, pantherdb.org) through the Gene Ontology web portal (**http://geneontology.org/**). Of 282 coordinately upregulated gene targets identified in our analysis, 280 were uniquely mapped, against the PANTHER Mus Musculus reference gene list (22296 unique gene IDs). Biological process annotations were gained using the GO Biological Process tool. A Fisher's exact test with FDR correction was used, and significance set at $p < 0.05$. Shown here are the top 20 enriched terms based on corrected p-values. Values shown are -log of both p-value (blue) and FDR (green)

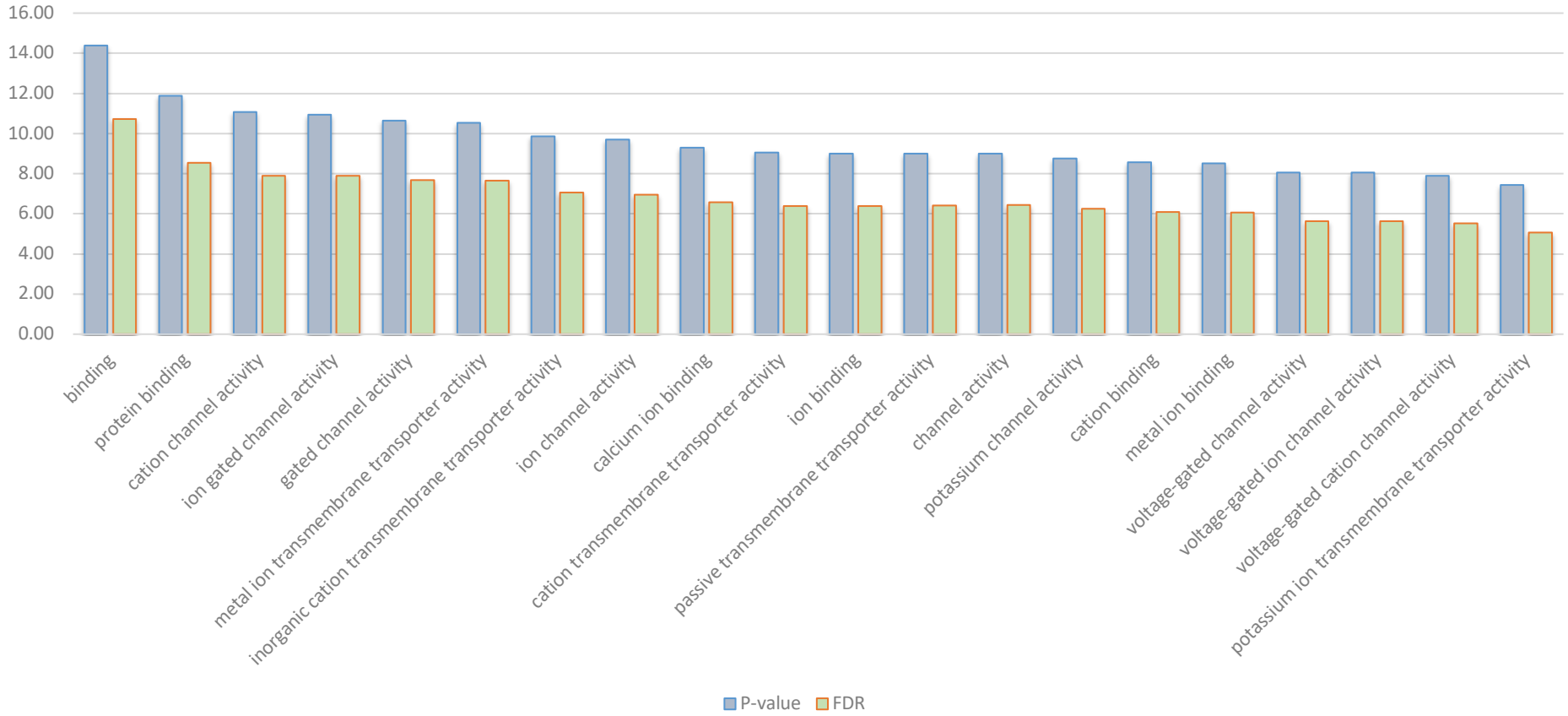

Table 8 Gene ontology analysis showing the molecular function terms enriched in the co-ordinately regulated gene targets of NFIs

Raw gene targets names were used as input to search for GO-term over-representation, using the PANTHER Gene Ontology system (Version 14.1, pantherdb.org) through the Gene Ontology web portal (**http://geneontology.org/**). Of 282 coordinately upregulated gene targets identified in our analysis, 280 were uniquely mapped, against the PANTHER *Mus Musculus* reference gene list (22296 unique gene IDs). Molecular function annotations were gained using the GO-molecular function tool. A Fisher's exact test with FDR correction was used, and significance set at $p < 0.05$. Shown here are the top 20 most enriched terms based on p-values. Values shown are -log of both p-value (blue) and FDR (green).

Of the 26 transcription factors identified, there are a mixture of both transcription factors with an identified role in cerebellar development and neurogenesis, and a number with no defined role in either process. To identify overlooked roles in the cerebellum, we performed literature searches in the NCBI PubMed library for publications using relevant key word combinations including "<TF name>" + "Neurogenesis", "<TF name>" + "Cerebellum", "<TF name>" and "Cerebellar granule neuron". Additionally, as novel genes with potential roles in development are often discovered through aberrant expression in diseased tissue compared to normal tissue, we included an addition al search for "<TF name>" + "medulloblastoma". This preliminary search method revealed a number of transcription factors with no currently described role in neurogenesis or the cerebellum (*Btbd11, Elk3, Hivep3, Mn1, Rfx4).* A majority of transcription factors identified from our gene list returned hits for the search term "Neurogenesis" (19/26), and "Cerebellum" (15/26). Less returned hits for "Cerebellar granule neuron" (8/26), indicating that the role of these transcription factors in this particular cell type has not been investigated to the same level. Currently, there are a number of publicly available expression databases examining RNA and protein expression databases including the GENSAT expression project (www.gensat.org) [236] and GenePaint (www.genepaint.org) [237]. Searching for TF names in these databases provided expression data for 23/26 transcription factors at ages e14.5 and/or P7 in the form either RNA-*in situ* hybridisation, eGFP, tdtomato or Cre-recombinase (*Rosa26* reporter) expression. Interestingly, at e14.5 very few of the transcription factors showed expression isolated to the RL or EGL, mimicking and expression pattern we noted for NFIX at e15.5 (Chapter 2). Whilst a particular TF's expression can vary dramatically at different embryonic and postnatal time-points, noting expression in RL progenitors does suggest that these transcription factors may co-ordinate with NFIs to regulate granule neuron progenitor development from the earliest stages. Furthermore, an additional eight of these TF's (*Ebf2, Elk3, Etv5, Irx1, NeuroD1, NeuroD4, NeuroD6* and *Otx2*) have data available at P7 showing expression in the EGL, with a select group of these shown in Figure 4-7. Taken together these data reveal that NFIs largely work in tandem to regulate a subset of genes with both novel and established roles in cerebellar granule neuron development. These include a number of transcription factors broadening the network of genes both directly and indirectly impacted by NFI expression in the developing cerebellum.

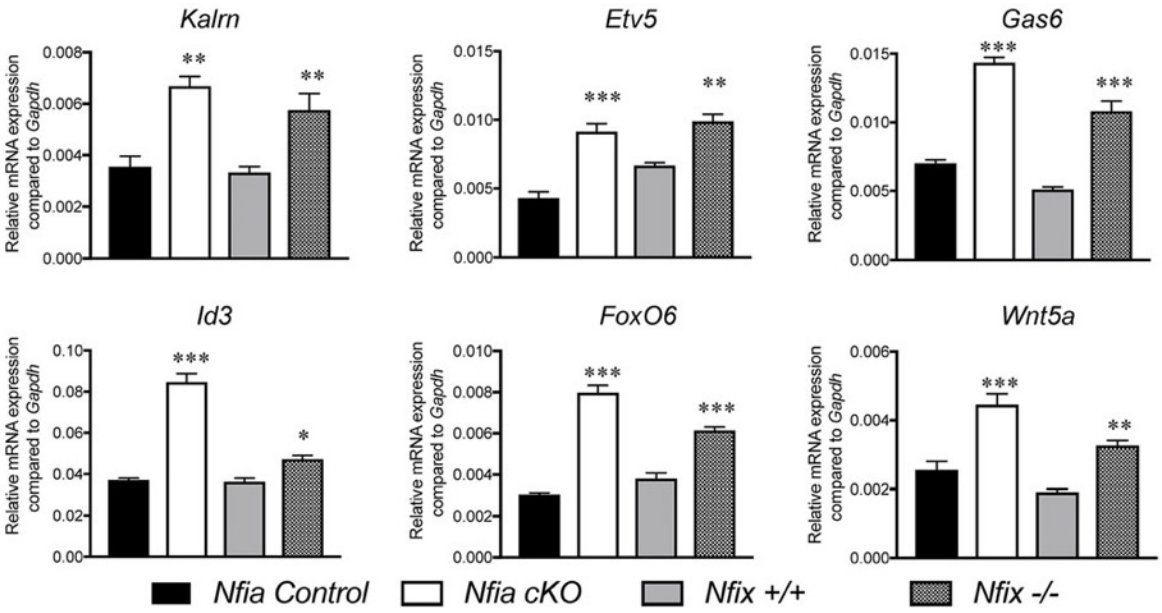

Figure 4-6 mRNA expression analysis of potential NFI targets by qPCR

qPCR was performed on P7 CGNPs isolated from control, *Nfia*$^{fl/fl}$*; Math1Cre*$^{+}$ and *Nfix*$^{-/-}$ mice. Analysis revealed that loss of *Nfia* and *Nfix* resulted in significantly increased expression of *Kalrn, Etv5, Gas6, Id3, FoxO6 and Wnt5a,* recapitulating RNA-seq data. Expression levels are shown relative to the housekeeping gene *Gapdh.* *p < 0.05; **p < 0.01; ***p < 0.001, t-test.

	"Neurogenesis"	"Cerebellum"	"Cerebellar granule neuron"	"Medulloblastoma"	GENSAT	GENSAT localisation	Genepaint exp
Akna	1	0	0	1	n/a	n/a	e14.5 EGL
Barhl2	2	2	1	0	n/a	n/a	e14.5 RL, VZ scattered
Btbd11	0	0	0	0	n/a	n/a	e14.5 EGL
Ebf2	12	9	0	0	Y	P7 EGL, IGL, Lobule specific	e14.5 widespread
Elk3	0	0	0	0	n/a	n/a	e14.5 scattered in the EGL, P7 weak EGL/IGL
Esrrg	0	2	0	2	n/a	n/a	n/a
Ets1	4	2	0	0	n/a	n/a	e14.5 scattered throughout, P7 scattered
Etv5	5	2	0	0	Y	P7 Scattered expression	e14.5 strong in VZ, weak EGL
Foxo6	0	2	1	0	n/a	n/a	n/a
Hivep3	0	0	0	1	n/a	n/a	e14.5 none
Irx1	3	1	0	0	n/a	n/a	e14.5 strong VZ/RL/EGL, P7 PCL and EGL,
Klf15	1	0	0	0	n/a	n/a	e14.5 weak VZ
Klf9	8	7	0	0	n/a	n/a	e14.5 strong, widespread
Mn1	0	0	0	0	n/a	n/a	e14.5 sparse VZ/RL
Neurod1	138	19	6	6	Y	P7 Strong EGL and IGL	e14.5 RL/EGL/NTZ, P7 strong EGL, IGL,
Neurod4	14	0	0	0	n/a	P7 Strong IGL, moderate EGL	e14.5 none
Neurod6	21	4	1	0	n/a	n/a	none at e14.5, P7 EGL, scattered IGL
Nfix	10	8	3	0	n/a	n/a	e14.5 RL/VZ, proximal EGL
Otx2	69	61	6	38	Y	P7 Strong, lobule specific	e14.5 RL, P7 Strong EGL/IGL, lobule specific
Pax3	51	8	1	5	n/a	n/a	e14.5 RL, proximal EGL, VZ strong
Prdm13	4	1	0	1	n/a	n/a	n/a
Rfx4	0	0	0	0	n/a	n/a	e14.5 weak RL/VZ
Sall1	5	0	0	0	n/a	n/a	e14.5 none
Scml4	1	0	0	0	n/a	n/a	e14.5 Prolific, widespread
Scrt2	1	0	0	0	n/a	n/a	e14.5 VZ
Smad3	24	8	1	2	n/a	n/a	e14.5 weak VZ/EGL

Table 9 : Investigation of downstream target transcription factors using online expression databases and text-searching

The respective gene name and the additional term ("Neurogenesis", "Cerebellum", "Cerebellar granule neuron" or "Medulloblastoma") was used to search for relevant publications, and the total retrieved number of publications included. GenePaint expression data was primarily in the form of in situ RNA-hybridisation, whilst GENSAT data was in the form of either eGFP, tdtomato or Cre-recombinase expression. "None" denotes no appreciable cerebellar expression, whilst "n/a" denotes no expression data for the particular gene was available in this database. RL= rhombic lip, VZ = Cerebellar ventricular zone, NTZ – Nuclear Transitionary Zone

4.6 Discussion

4.6.1 Co-ordinate gene regulation by NFIs drives the developmental program of cerebellar granule neuron progenitors.

NFI transcription factors are expressed in neural stem cells and progenitor populations of the developing CNS, where they play a multitude of roles such as mediating stem cell quiescence/self-renewal and progenitor differentiation [83-85, 87, 130]. Following on from Chapter 3 where we found that NFIX regulates the differentiation of CGNPs partly by co-ordinate regulation of gene targets with the bHLH transcription factor *Math1,* we went back to examine whether other NFI transcription factors themselves had common regulatory targets in CGNPs. We followed a similar approach, investigating first with immunohistochemistry and immunofluorescence, followed by analysis at both a transcriptomic, DNA-binding and functional level. We have shown that both NFIA and NFIX are highly expressed in both pre- and post-mitotic cerebellar granule neurons, Bergmann glia and other astrocytes in an overlapping manner. We identified that NFIs likely work co-ordinately to directly regulate a large subset of genes, driving forward the differentiation of CGNPs. Interestingly, a number of these genes have no previously described role in cerebellar development or indeed the CNS as a whole. This is an exciting prospect as these may potentially be new regulators of progenitor cell differentiation.

It is generally accepted that RNA-seq expression data show a high degree of concordance with qPCR expression data, despite generally being a noisier dataset [238]. To check that this was the case with the data from our RNA-seq analysis, we used qPCR to examine changes in expression levels of a number of gene targets (*Gas6, Wnt5a, Kalrn, Foxo6, ID3* and *Etv5),* in both *Nfia*$^{fl/fl}$*;Math1 Cre*$^{+}$*, Nfix*$^{-/-}$ and control CGNPs. Of these genes, only *Wnt5a* has been investigated specifically in the cerebellum, where it has been shown to regulate progenitor proliferation [235]. This presented us with an exciting prospect; it is possible that these genes (and others identified from our analysis that we did not examine with qPCR) could a) play a key role in established CGNP development processes or b) themselves present as novel regulators of CGNP development, in the similar manner to *Itsn1* in Chapter 3. Whilst examining these targets further was beyond the scope of this project, we can infer potential roles in the cerebellum from examining their roles in other parts of the CNS and progenitor populations where literature is available.

4.6.2 NFIs regulate *Gas6* a potent activator of TAM RPTKs in proliferative cells.

Growth arrest protein 6 (*Gas6*) binding activates the TAM (*Tyro-3*, *Axl* and *Mer*) group of receptor protein-tyrosine kinases (RPTKs). This binding axis has been shown to promote the proliferation of cancer cells and to regulate the self-renewal of cancer stem cells [239-242]. *Gas6*-TAM binding has been shown to prevent neuron death and encourage neurogenesis, depending on the particular receptor bound and the cellular context [243-247]. In the cerebellum, *Tyro-3* is the predominate *Gas6* binding partner, with expression noted in granule neurons and their parallel fibres, Bergmann glia and Purkinje neurons [248]. Normally, *Gas6* is expressed in low levels in CGNPs. Our data suggests that *NFIs* may play an important part in repressing GAS6 expression in CGNPs, thus potentially modulating Tyro-3 activation in these cells. Interestingly, *Tyro-3* has been found to be down-regulated in human childhood medulloblastoma samples compared to normal cerebellar tissue [249]. As *Gas6* has been shown to exist in both receptor bound and secreted forms [241], it is possible that the changes in GAS6 expression we identified in our *Nfi-null* CGNPs could affect the activation of TAM receptors in Bergmann glia and Purkinje neurons. This in turn could affect the differentiation and development of CGNPs, in both cell autonomous and non-autonomous manners. Future investigations on the cell-type specific expression of GAS6, its functional role in CGNPs, and how manipulation of the GAS6-TAM axis impacts the developmental program of these cells, will help to form a complete picture of how altering NFI expression can impact the development of the postnatal cerebellum.

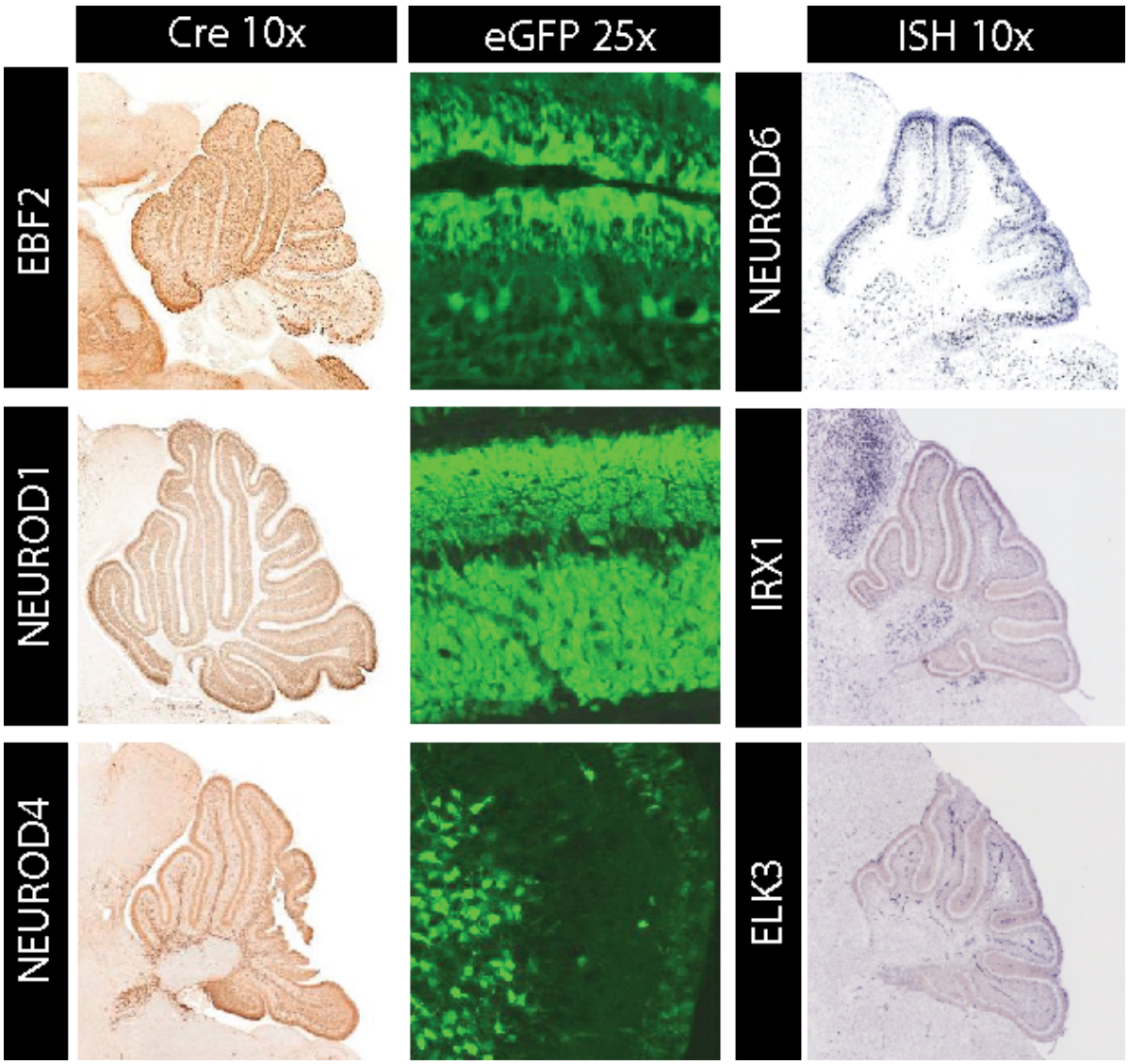

Figure 4-7 Selected transcription factor expression in the P7 mouse cerebellum.

Whole brain images at P7 were obtained from both GENSAT (Rosa26 Cre and eGFP) and GenePaint (ISH) databases, and cropped to focus on the cerebellum. Both Cre and ISH images were available at 10x resolution, whereas eGFP images were available at 25x. Whole cerebellum images were selected from as close to the midline as available.

4.6.3 NFIs repress the Rho-GEF *Kalirin*, perturbing GTPase action in CGNPs

Kalirin (*Kalrn)* is a multi-domain Rho-GEF essential for dendritic spine development and excitatory synapse formation [250-253]. Our data show enrichment for multiple *NFI* binding motifs in *Kalrn* genic, promoter and enhancer regions. This, combined with differential RNA expression of *Kalrn* in *Nfi*-null CGNPs, suggest that it is a directly regulated target of *NFIs* during cerebellar neurogenesis. Both alternate promoter usage and alternate splicing result in a number of *Kalrn* isoforms from a single gene with different functions, but largely overlapping expression in the CNS [254, 255]. Knockdown of *Kalrn in vitro* results in an arrest of BDNF-TrkB mediated neurite outgrowth in hippocampal neurons [256]. Additionally, $Kalrn^{-/-}$ mice have behavioural defects including deficiencies in cue and context-dependent fear conditioning [253, 257]. *Kalrn* has multiple GEF domains that activate GTPases including *Rac1* and *RhoA*, both of which are expressed in the developing cerebellum [258, 259]. It is possible that NFI-repression of *Kalrn* in turn modulates the activation of these GTPases. Targeted deletion of *RhoA* from CGNPs using a *Math1*; Cre^{ERT2} driver results in delayed migration, abnormal morphogenesis and ectopic localisation of post-mitotic neurons [259]. Additionally, *RhoA* loss results in foliation defects and abnormal fissure formation in the postnatal cerebellum. Interestingly, loss of *RhoA* also resulted in non-cell autonomous defects in both Purkinje neurons and glia, demonstrating again the important role of CGNPs in maintaining normal development of the cerebellum.

Our data shows that *Nfia* and *Nfix* act to upregulate another guanidine nucleotide exchange factor, *Spata13* (*Asef2)*. SPATA13 is strongly expressed in CGNs, where it is a target of thyroid hormone [260]. The function of this particular protein in CGNPs has not fully been determined; but alike with other GEFs it activates Rho GTPases *Rac1* and *Cdc42,* this time regulating cell adhesion, migration and dendritic spine development [261-264]. We have previously shown [Chapter 3] that NFIX also directly regulates *Itsn1*, a scaffolding protein that has been shown to interact with other small GTPases in the CNS such as Ras [209, 265]. These data raise the possibility that *NFIs* may have a previously overlooked role in regulating several developmentally significant GTPase families. Interestingly, RhoA/Rock expression has been found to inhibit ERK kinase activation in embryonic myoblasts, which in turn, results in the downregulation of *Nfix* expression [266]. This relationship continues postnatally, albeit independent of *RhoA/Rock*, with ERK activation in turn increasing NFIX expression. The interaction between *RhoA*, ERK and *Nfix* is yet to be explored in the cerebellum, but if this relationship is conserved it could insinuate that a feedback loop important for temporal control of NFI expression and this developmental progression is in place.

4.6.4 New relationships between *NFIs* and *Wnt*-signalling in cerebellar development

When it comes to signalling pathways involved in cerebellar development, few more are as prolific and extensive as the *Wnt*-signalling pathway. Our PANTHER pathway analysis revealed significant enrichment for the *Wnt*-signalling pathway in our co-ordinately regulated gene list, with 11 *Wnt*-associated genes unearthed. We investigated one of these genes, *Wnt5a,* using qPCR to support our RNA-seq findings. *Wnt5a* has been shown to act as a ligand for *Frizzled, Ror and Ryk* receptors, activating either canonical (*β*-catenin) *Wnt* signalling, or non-canonical (*β*-catenin independent) *Wnt* signalling [267]. In the cerebellum WNT5A expression peaks at P1, with expression slowly declining as postnatal development progresses. Despite this decline, expression is still found, albeit at a reduced level towards the end of cerebellar development (P21)[235]. Interestingly, conditional deletion of *Wnt5a* under a Nestin promoter (*Wnt5a*$^{fl/fl}$; NestinCre) results in a reduction in the number of CGNPs migrating from the RL at E14.5. Additionally, P1 EGL progenitors show a marked decrease in proliferation, with reduction in the expression of Ki67, PHH3 and Cyclin D1[235].

Depending on the receptor bound and the pathway activated, *Wnt* signalling can have a number of roles and outcomes in the cerebellum. For example, defective canonical *Wnt*-signalling has been suggested to play a causative role in cerebellar vermal hypoplasia, seen in patients with Joubert syndrome [268]. Conversely, receptor binding of the ligand *Wnt3* and subsequent activation of Non-canonical *Wnt* signalling, antagonises the proliferative effects of SHH on CGNPs, through downregulation of SHH downstream targets such as *Gli1*, *Gli2* and *Ptch1* and activation of MAPK/ERK pathways[234]. *Wnt5a* has been shown to inhibit Canonical-*Wnt* signalling in haemopoietic stem cells maintaining their quiescence, adding to the complexity of interactions between both canonical and non-canonical *Wnt*-signalling pathways in stem and progenitor cells [269]. These data suggest that *NFIs* may act to regulate the interplay between Canonical and non-canonical *Wnt* in the developing cerebellum, to help regulate the switch between proliferation and differentiation of progenitors. Moreover, our data suggest that *NFIs* regulate a number of other key *Wnt*-associated proteins, including two key pathway regulators *Dkk3* and *Sfrp1*, the canonical *Wnt* ligand *Wnt7b*, and another *Wnt*-activator *Amer3* (*Fam123c*) [270-273]. Interestingly, loss of *Nfix* and *Nfia* sees upregulation of *Ebf2*, which has been shown to act in synergy with β-catenin to regulate transcription, and downregulation of *Tle2,* a transcriptional co-repressor that inhibits this regulation [274-276]. The full effect of altered NFI expression on *Wnt* signalling in granule neurons is hard to determine without further experimentation, starting initially with examination of the role of each *Wnt*-related gene in the wild-type cerebellum. Examining the outputs and transcriptional activity of both canonical and non-canonical *Wnt* pathways in CGNPs would shed much needed

light on biases towards one pathway mediated by these transcription factors. Understanding transcriptional regulation of *Wnt*-signalling in the cerebellum is particularly important, as misregulation of *Wnt*-pathway is a hallmark of one of the four classical subtypes of medulloblastoma [277, 278].

4.6.5 *NFI*-regulation of other transcription factor families amplifies downstream effects

Transcription factors can amplify their effects on a target cell population by directly regulating other transcription factors. Whilst loss of non-transcription factor gene targets may explain (at least partially) the observed phenotypes (as shown in Chapter 3 with *Itsn1),* transcription factor-transcription factor regulation is important to investigate due to the amplified effect of developmental-gene regulation cascades. Our analysis revealed 26 transcription factors co-ordinately regulated by *Nfia* and *Nfix*. Several have well established roles in neural development, but a number have not been investigated in the cerebellum or CNS as a whole.

One of these transcription factors identified from our analysis and further investigated with qPCR is the forkhead box transcription factor *FoxO6*. FoxO proteins are transcription factors that function as part of a conserved PI3K-AKT-FoxO signalling pathway, and are required for NSC proliferation and renewal [279-281]. FOXO6 knockdown has been shown to inhibit the function of the PI3K/Akt/mTOR pathway and cell proliferation in colorectal cancer cells [282]. Similarly, overexpression of this TF is commonly found in breast cancer cells where it has been proposed activate proliferation [283]. High FOXO6 expression is correlated with poorer prognosis and increased aggressiveness of gastric cancer [284]. In the cerebellum FOXO6 is expressed in granule neurons, where it has been shown to be essential for the polarisation of developing progenitors [285]. Interestingly, knockdown of *FoxO6* in the embryonic forebrain neurons leads to a reduction in the expression of a number of key developmental genes, including *Nfia* and *Plxna4* [286]. Our data suggest that in postnatal CGNPs, *Plxna4* is in turn directly and co-ordinately downregulated by *Nfia* and *Nfix*. This suggests that there may be a conserved interaction between *NFIs*, *FoxO6* and plexins in both cerebellar neurons and neurons of the cortex. Plexins are crucial proteins in axon guidance processes, where they act as receptors for Semaphorins (for a thorough review, see [287], which are essential in regulating axon guidance in developing neurons. Our data show that *Nfia* and *Nfix* also co-ordinately upregulate the semaphorin *Sema3d* in CGNPs. Knockdown of *Sema3d* has been shown to reduce both cell migration and proliferation in neural crest cells in zebrafish embryos [288]. Further investigation is needed to see whether this phenotype is conserved in the mouse hindbrain. Our data show that individually *Nfix* and *Nfia* directly regulate a number of other semaphorins in CGNPs, raising the possibility that a point of divergent function of NFIs in the cerebellum might be due to their interactions with this particular protein family.

Our analysis unearthed direct regulation of members of the NeuroD family of bHLH transcription factors, which have established roles in neurogenesis and cerebellar development. *NeuroD1* is essential for the differentiation of granule neurons; *NeuroD1-null* cerebella have a clear loss of CGNPs and thinning of the EGL early in postnatal development, particularly pronounced in the

posterior lobules of the cerebellum [289]. Additionally, *NeuroD2* has been associated with survival of CNS neurons, including granule neurons in the postnatal cerebellum [290]. We have shown that the expression of two other NeuroD family members, *NeuroD4 and NeuroD6* is up-regulated by *Nfia* and *Nfix* expression in postnatal CGNPs. Both *NeuroD4* and *NeuroD6* have no described role in cerebellar granule neurons, but GENSAT expression data suggests and overlap of expression localisation between these family members. Whether or not these bHLH family members display functional redundancy in these cells is currently unknown.

Interestingly, *NeuroD6 is* regulated in a discordant manner by *Nfia* and *Nfix,* the only transcription factor from our dataset to be so. Depending on the magnitude of the role of *NeuroD6,* and whether functional redundancy with other NeuroD TFs exists, this discordance suggests a possible point of divergent function of *Nfia* and *Nfix* in CGNPs. This could in turn explain part of the varied cerebellar phenotype in *Nfia-null* and *Nfix-null* mice. Online expression databases show strong NEUROD6 expression in the forebrain of mice, where *Nfia* and *Nfix* regulate neurogenesis [96]. Further investigation into whether this discordant regulation pattern occurs in other regions of the brain where NFIs have been shown to regulate neurogenesis are warranted.

Our data show that *Nfia* and *Nfix* directly co-ordinately upregulate the expression of the BarH-like homeobox transcription factor *Barhl2*. Additionally, *Nfia* also directly regulates expression of *Barhl2* paralog *Barhl1*. The role of *Barhl2* has not been extensively investigated in the cerebellum, although expression in the EGL and upper rhombic lip is evident at P1[291]. Both *Barhl1* and *Barhl2* can transactivate the *Barhl1* promoter, indicating some redundancy between the two transcription factors [292]. *Barhl1* has been shown to regulate the migration and survival of CGNs though regulation of Neurotrophin-3, and loss of this transcription factor results in lobulation defects of the cerebellum [293]. This is of interest as our *Nfia$^{fl/fl}$;Math1-Cre* mutant also displayed altered lobule morphology. Investigation of *Barhl2* loss of function mutations are yet to be conducted in the cerebellum or CGNPs. Interesting however, is the interplay between BarH and other bHLH transcription factors. *Barhl2* has also been shown to regulate multiple neural bHLH genes [294]. Additionally, *Barhl2* is itself activated by MATH1 in the spinal cord through MATH1 binding to a downstream *Barhl2* enhancer [295]. If this relationship extends to the cerebellum, it would thus confine *Barhl2* expression to CGNPs. Adding to the this, loss of *Barhl1* has been associated with poorer prognosis and survival rates in human medulloblastoma, with tumours expressing low levels of differentiation markers such as NEUN [296]. *Barhl2* has been found to act upstream of the SHH-signalling pathway, playing a role in regulating patterning of progenitors in the diencephalon [297]. Our transcriptomic data combined with evidence from literature and

available expression databases suggest that NFI-regulation of BarH transcription factors in the EGL could indeed be another axis through which CGNP differentiation is mediated.

The developmental program of CGNPs in the EGL starts early in embryonic development and persists until the third postnatal week, when this layer disintegrates. Whilst expression of some transcription factors appears temporally constrained, expression of others persists throughout this period of development (such as PAX6 for example). Examining where expression varies, and what key developmental events occur at that time, could provide functional insight into the role of certain transcription factors at that time. Likewise, consistent expression could dictate a role in housekeeping processes, or that a protein relies on significant post-translational modification to alter its function. Recently, an interesting study used laser micro-dissection (LCM) to isolate embryonic CGNPs and identify differential transcription factor expression patterns in these cells between E13 and E18 [298]. This study identified a significant number of novel transcription factors, of which a significant proportion displayed differential expression between these embryonic time points. Interestingly a number of targets identified as differentially expressed (*Barhl2, Irx1, Neurod6, Pax3* and *Ets1)* in this dataset, are co-ordinately regulated targets of *NFIs* identified in our dataset at postnatal day seven. Additionally, a further six (*Math1, Ebf1, Hes6, Insm1, Lhx1* and *Zic1)* transcription factors from this LCM analysis are directly regulated by *Nfia* at P7 and another four *(Foxq1, Kcnip3, Klf4* and *Sox7)* are directly regulated by *Nfix.* For some transcription factors, these data suggest that their regulatory relationship with NFIs is initiated in the embryonic EGL and persists through postnatal development. However, for a substantial proportion of others, this suggests that the regulatory relationship may be forged during postnatal development. This is further evidence that the postnatal EGL is a dynamic regulatory environment.

An interesting point of contrast with the co-ordinate action of NFI transcription factors is to investigate directly regulated targets of NFIA that are not regulated by NFIX, and vice versa. Our analysis showed 50 transcription factor targets unique to *Nfia*, and 20 unique to *Nfix.* NFIA regulates a number of genes with known roles in defining cell linages of embryonic cerebellar progenitors, such as *Math1, Barhl1, NeuroD2, Insm1, Hes6* and *Zic1*, which are heavily involved in specialisation towards the granule neuron identity [61, 299]. NFIX on the other hand uniquely regulates few genes associated with this early granule neuron lineage specification. This raises the question as to whether *Nfia* plays a more dominant role than *Nfix* in regulating early CGNP development. Future work on lineage specification of progenitors in both our respective *NFI-null* mutants, potentially using laser microdissection and analysis of the rhombic lip, could provide key insights into these questions.

4.6.6 NFI's may modulate CGNP response to neurotrophins, though the ETS transcription factors *Etv5*

Another transcription factors, *Etv5* was selected for further examination via qPCR. *Etv5* is a member of the ETS-domain family of transcription factors, a number of which are expressed in the cerebellum and cerebellar granule neurons [300-302]. ETS-Family member *Etv1* has been show to interact with NFIs in post-mitotic CGNs, acting as a positive regulator of NFI-binding to/activation of genes involved in neuron dendritogenesis [303]. Interestingly, our data show that *Evt1* is a directly regulated target of *Nfix* in pre-mitotic progenitors (but not *Nfia*), with reduced expression of ETV1 upon *Nfix* loss. Very little is known about the role of *Etv5* in the CGNPs (or indeed the cerebellum), but some function may be inferred from the actions of other ETV family members, who share a conserved binding sequence and often conserved biological functions [304]. For example, BDNF stimulated ERK1/2 expression has been shown to activate ETV4 and ETV5 expression in Dorsal Root Ganglion neurons, initiating neurite outgrowth [305]. Additionally, ETV4 and ETV5 are required for proper dendrite development in hippocampal neurons [306]. BDNF is essential for proper cerebellar development, and preferentially activates the TrkB receptor in CGNPs and Purkinje neurons. Loss of BDNF results in extensive foliation defects in the developing cerebellum, as well as increased apoptosis and a reduction in the overall number of CGNPs in the postnatal IGL [307]. Additionally, the EGL persists for longer than normal, phenocopying the developmental delay we have previously identified in *Nfix*$^{-/-}$ mice [91], [Chapter 3].

Our data also show that that the low affinity neurotrophin receptor *Ngfr* (p75NTR) is also natively repressed by *NFIs* in CGNPs. This receptor is prolifically expressed in the EGL but not the IGL and binds neurotrophic factors such as BDNF and NGF [308, 309]. Activation of *Ngfr* has recently been shown to regulate timely cell-cycle withdrawal in the cerebellum, with loss of the receptor leading to extended proliferation of granule neuron progenitors [309]. Interestingly, this result seems to complement the phenotype we have witnessed in *Nfix*$^{-/-}$ mice; yet these mice should by extension have increased *Ngfr* expression, due to the lack of *Nfix*-mediated repression. It is possible that, since the receptor is co-ordinately regulated by both NFI transcription factors, *Nfia* may be acting to compensate for *Nfix* loss, through direct regulation or through other effectors. Indeed, much further investigation is needed to determine the specifics of this transcription factor-growth factor relationship. Taken holistically however, these data show that NFI expression may play a crucial role in modulating the developmental response to neurotrophins in CGNPs, potentially at both a receptor and effector level.

4.7 Conclusion

Cerebellar development is an incredibly complex process, requiring signalling from a multitude of pathways, influenced by a number of cell autonomous and non-autonomous factors. Here we have shown that two transcription factors, *Nfia* and *Nfix,* are expressed in broadly overlapping populations in the developing cerebellum, and co-ordinately regulate a subset of genes involved in cerebellar development. Additionally, we have shown that both NFIs exert further influence in regulating cerebellar development, by controlling the expression of other developmentally significant transcription factors, both individually and in a co-ordinated manner. Further investigation to the level of regulation and role of these gene targets may shed light on previously unknown developmental processes governing cerebellar development. Additionally, this may unearth new gene targets useful in the prognosis and treatment of malignant neoplasms of the cerebellum.

Chapter 5 : **General Discussion**

5.1 Aims of Chapter 5

The research presented in this thesis comprehensively profiles the role of the Nuclear Factor One transcription factors in cerebellar development, focusing on progenitors in the EGL. First, we investigated the expression of NFIX in the embryonic and postnatal cerebellum, finding broad expression in a number of different cell lineages, including CGNS and their embryonic and postnatal progenitors. Next, focusing on CGNPs, we identified key downstream gene targets directly regulated by NFIX. From these, a number involved in regulating progenitor differentiation were identified including *Itsn1*, which encodes a scaffold protein in the Reelin signalling pathway. Lastly, we expanded on this analysis to determine which of these gene targets are also directly and co-ordinately regulated by NFIA. The evidence from these findings suggest that a NFIs co-ordinately regulate an impressive number of developmentally significant genes, including other transcription factors. This chapter aims to contextualise the new findings from this research, and the broader implications that can be extrapolated from it, in understanding cerebellar development and the NFI family. It also aims to discuss the limitations of this thesis in terms of conclusions that can be drawn without further analysis. Lastly, it sets forward future avenues of investigation to help answer outstanding questions raised in this thesis to further understand the mechanics of cerebellar development.

5.1.1 Expanding on the roles of NFI transcription factors in the granule neurons

The importance of studying the cell-type specific expression of proteins is especially pertinent in regions of the brain such as the cerebellum, as it consists of a largely heterogeneous population of cells. This thesis has shown that NFI TFs have overlapping roles in cerebellar progenitors within the EGL. NFI expression is also ubiquitous in the many cell types in the cerebellum. For instance, NFIA and NFIX are expressed in both neurons and glia, which have notably distinct developmental origins. We have shown that loss of *Nfix* affects the normal developmental program of CGNPs, complementing other research, showing NFIs have important roles in stem and progenitor cell populations in the CNS [84, 85, 130, 151, 183]. Additionally, we have shown that NFIA and NFIX are expressed in these progenitor cells, with transcriptomic analysis showing both co-ordinated and distinct targeting of downstream gene effectors. This work further highlights NFIs as key regulators of CGNP development from embryogenesis to adulthood. Despite our analysis, there are still a number of avenues to be explored in future work, notably a more extensive look at the role of *Nfib* in CGNP development.

The work in this thesis predominately focused on NFIX and NFIA, but did not expand to examine the role of NFIB with the same depth. This is due partly to the lethality of $Nfib^{-/-}$ mutants and the absence of an available conditional deletion mutant line. Online expression data show that NFIA, B and X are all expressed in the embryonic rhombic lip, and expression is evident in postnatal CGNPs at P6 [100]. Previous studies have shown that $Nfib^{-/-}$ mice have similar, but more severe, neural defects in comparison to $Nfia^{-/-}$ mice, suggesting at least a partial overlap in function [100, 108]. At E18, $Nfib^{-/-}$ mice have a largely unfoliated cerebellum, a phenotype often found in cerebellar mutants with abnormal CGNPs, or where BG or Purkinje neurons development is disrupted [108]. No cell-type specific analysis of NFIB has been conducted in the normal cerebellum, despite strong evidence of expression postnatally [100]. Our data show a high overlap of NFIB binding peaks with that of NFIA and NFIX, supporting a conserved function in CGNPs. Following a similar protocol to that that was used in Chapter 3 and 4, a combination of cell-type specific analysis and transcriptomic data in *Nfib-null* CGNPs would help round out the picture as to what gene targets are shared amongst NFIs in these cells. Generating an $Nfib^{fl/fl}$; *Math1*Cre mouse would allow investigation of the loss of *Nfib* specifically in embryonic and postnatal CGNPs and likely avoid the embryonic lethality seen in $Nfib^{-/-}$ mice. From there, co-ordinated regulation, misregulation or individual regulation of gene targets by each NFI could be ascertained.

The postnatal cerebellum is an incredibly dynamic environment, and different developmental programs have a distinctly temporal basis. We used P7 primarily as a starting point to examine CGNPs, as this correlates approximately with the peak number of progenitor cells in the EGL. It is highly likely that both the number of individually and co-ordinately regulated genes, by each NFI, may have a temporal basis in CGNPs. Further expanding our transcriptomic analysis to include other ages would provide a picture of how NFI-mediated gene regulation changes throughout postnatal cerebellar development. Another interesting finding from these studies is that a large proportion of NFI binding sites are found in regions of closed chromatin at P7. It is possible that NFIs may either rely on other factors to modulate chromatin accessibility, or indeed may promote accessibility themselves. Broadening ChIP-seq and DNase I hypersensitivity analysis to examine changes in NFI binding patterns in CGNPs at different time points may provide some answers here.

The lack of double (*Nfia/x, Nfia/b, Nfib/x)* and triple (*Nfia/b/x)* knockout or knockdown mouse mutants limits our ability to make conclusions on how these family members natively interact in cerebellar granule neurons. With the single knockouts we used, it is possible that a compensatory function of other NFIs could obscure the roles of individual family members, considering our evidence of overlapping expression patterns and co-ordinated downstream gene targets. Phenotypic and transcriptomic profiling in a double or triple knockout line would further elucidate how these factors work together and provide insight into differences in function. Similar approaches using heterozygotes have been taken to investigate other transcription factors with prominent roles in CGNP development, such as the ZIC family[310]. However, as both *Nfia*$^{-/-}$ and *Nfib*$^{-/-}$ knockouts are perinatal lethal and *Nfix*-null mice die during postnatal development, it is possible that double and triple knockout mutants would not be viable for postnatal studies. Interestingly, *Nfi*-heterozygous mutants display intermediate neural phenotypes compared to full knockout counterparts and are viable postnatally [311]. Recently, *Nfia*$^{+/-}$; *Nfib*$^{+/-}$ double heterozygous mutants were shown to largely re-capitulate embryonic cortex defects seen in both *Nfia*$^{-/-}$ and *Nfib*$^{-/-}$ mice, but a cerebellar phenotype (if present) was not examined [312]. Complete allelic loss of both *Nfia* and *Nfib* resulted in a more severe cortical phenotype at E16 [312]. Indeed, authors reported low embryonic viability of these mutants, in addition to perinatal lethality. Utilising double heterozygotes or crossing these double and triple mutants onto the aforementioned *Math1;Cre* or inducible *Math1;*CreERT2 [313] genetic background could be another way of investigating con-current loss of NFIs within the postnatal cerebellum. Additionally, a comparison to how heterozygosity of NFIs compares phenotypically and transcriptomically to the induced loss of these TFs in CGNPs would be of great interest.

NFI proteins form functional homo and heterodimers *in vitro*, yet how exactly these combinations work to drive different developmental programs is yet to be fully resolved *in vivo* [89, 312, 314]. Knocking out one (or multiple NFIs) would theoretically change the ratio of binding partners available to act as heterodimers versus homodimers. Indeed, natural fluctuations in expression of these and other TFs is likely a mechanism in which particular developmental programs are regulated. This may explain the more extreme cortical phenotypes witnessed in full homozygous-null mutants, versus NFI-heterozygous mutants that can still function as heterodimers. Additionally, it is entirely possible that loss of one NFI family member can be partially compensated for in a functional manner by formation of heterodimers from remaining NFI TFs. This may explain the variations in severity of cerebellar and cortical phenotypes on NFI loss, especially if different NFIs have preferential binding partners. The similarity in cortical phenotype, strongly overlapping expression in the cerebellum at all timepoints and evidence of binding as cofactors for other transcription factors [312, 315], raises the possibility that NFIA and NFIB might form heterodimers together, in a preferential manner than forming them with NFIX. Further investigation here is needed if we are to fully understand how NFIs regulate gene expression in the developing cerebellum. Proximity based fluorescent assays such as FRET have previously been used to investigate dimerization of transcription factors *in vitro* [316, 317]. With the right constructs, this technique could be adapted to quantify both the levels of homo/heterodimerisation of NFIs, and changes in these ratios upon knockdown or loss of a family member. Additionally, this approach could be used to investigate the dimerization ability of the different NFI transcript variants found in CGNPs.

5.1.2 Targeting NFI expression outside of neurons would provide a more representative view of global NFI loss.

From a cell extrinsic viewpoint, by isolating pure populations of cells for analysis, we struggle to fully recapitulate the native environment these cells reside in. This is especially pertinent for CGNPs as proper development relies on inputs and outputs of BG, interneurons, oligodendrocytes and Purkinje neurons. For example, loss of oligodendrocytes in the cerebellum alters the morphology of PNs and CGN, and reduces the expression of key signalling molecules SHH, BDNF and RELN [318]. Whether or not loss of NFIX or NFIA results in increased cell death of oligodendrocytes has not been investigated thoroughly throughout cerebellar development, however NFI expression is present in a proportion of these cells.

Whilst this work predominately focused on CGNs, cell-type specific expression of NFIX and NFIA was shown in other cell types, including Bergmann glia. This is important to consider due to the dependent relationship between these cells and the migration of post-mitotic CGNPs [19]. Global loss of NFIX might therefore result in a double hit affecting CGNP migration- affecting cell-intrinsic pro-differentiation mechanisms whilst simultaneously interfering with the essential scaffold required for migration of these differentiated cells. Loss of NFIX results in a reduction in GFAP expression at P7 [91] (Chapter 3), with significantly fewer $GFAP^{+}$ glial fibres extending through the EGL to the pial surface. What role NFIX plays in the maturation of these particular glia is yet to be determined, however the work in chapter 3 has shown that loss of NFIX does delay glial maturation. Our data show strong NFIX expression in the embryonic cerebellar ventricular zone at e15.5, the site of genesis of cerebellar glial progenitors. Additionally, both NFIX and NFIA are expressed in $s100\beta^{+}$ Bergmann glia as early as P3 in the postnatal cerebellum, and this expression persists until at least P15 (Chapter 4).

In the cerebellum, conditional deletion mouse lines driven by either GFAP and GLAST promoters are used to selectively delete genes from glia and glial progenitors. Crossing both $Nfix^{fl/fl}$, $Nfia^{fl/fl}$ *and* $Nfib^{fl/fl}$ mouse lines onto either *(h)GFAP;* Cre or *GLAST;* Cre genetic backgrounds, would be a logical next step to investigate how these NFI TFs directly affect Bergman glia development through cell intrinsic processes and could provide insight into how they indirectly (cell-extrinsically) affect CGNP development. Additionally, generating a $Nfix^{fl/fl}$, $Nfia^{fl/fl}$, $Nfib^{fl/fl}$ double and triple mutants and crossing these strains onto *hGFAP;* Cre and *GLAST;*Cre genetic backgrounds could provide needed contrast to individual knockout mutants phenotypes. This would provide functional insight into independent or redundant roles of NFIs in these cells. One caveat of these experiments is that as of yet, no cerebellar-glia specific mouse line currently exists. Both

GFAP and GLAST, as well as newer glial specific promoters (such as *Aldh1l1*-CreERT2) all target astrocytes and glia prolifically throughout multiple regions the brain [319, 320]. One way to get around these off-target effects, would be to use glia-specific viral RNAi constructs injected proximally to the cerebellum, to knockdown NFIs in cerebellar BG and astrocytes with limited forebrain diffusion.

5.1.3 Manipulation of NFI expression; knockdown and rescue

Germline and conditional knockout mouse models emulate complete and cell-type specific loss of NFI expression respectively. These models are useful in understanding global roles of NFI proteins, but do not always recapitulate the phenotype of spontaneous mutants, where a loss of function mutation can occur, often in clonally expanding progenitors such as CGNPs. These types of mutations are interesting as they can result in a mixed population of post-mitotic cells, both mutant and normal phenotypes in the same environment. Replicating these types of mutations can be achieved using virally delivered shRNA and RNAi constructs, and cell-type specificity can be achieved using specific promoters. Lentiviral knockdown of NFIs has previously been performed in CGNs *in vitro* [101]. These could likely be extended to target cerebellar neurons and glia, using precise, transcranial injection of viral constructs. In humans, allelic *Nfix* mutations result Malan-Sotos syndrome, which has a variance severity of symptoms depending on the location and type of point mutation and/or deletion [118-122, 125, 321]. It is possible that viral delivery of CRISPR-CAS9 constructs could be used to introduce patient specific point mutations into mice, to further examine how this disorder affects the development of the brain and potentially new avenues for treatment.

Experiments using both adenoviral and lentiviral constructs *in vivo* have successfully transfected Purkinje neurons, Bergmann glia, granule neurons, cells in the molecular layer and in the white matter of the cerebellum with varying levels of specificity [322-324]. Virally-infected transgenic cells have been detected several weeks after injection in the cerebellum [324] suggesting that technique could be used to modulate NFI expression over the whole time-course of postnatal cerebellar development. As simultaneous co-injection of two adenoviruses and subsequent transgene expression has been successfully achieved in Purkinje Neurons [324], it is possible that this technique could be expanded to knockdown the expression of different combinations of NFIs at once. This might provide an alternate model to examine redundancy in NFI expression and function in these cells. Viral constructs could also be used in our germline and conditional mutants to knockdown the expression of additional NFIs, as well as other genes of interest. This approach may prove more time efficient than generating double and triple germline or conditional knockout mutants, with less potential side-effects such as perinatal lethality. It could also provide a useful intermediary between cell-type restricted NFI loss and global NFI-loss models.

Viral overexpression/gene transfer on the other hand can act as useful control, to restore NFI expression in mutant cells and rescue the mutant phenotype. This approach is a way to show that the phenotypes witnessed are indeed a result of the loss of a particular protein (in this case NFIA or

NFIX). Future experiments could examine whether or not rescue of NFIA or NFIX expression is enough to reverse both cell-specific and morphological abnormalities in our mutant mice. Additionally, rescue of NFI expression at specific postnatal timepoints (for example P3, P7 or P15) and examination of the level of phenotype rescue would provide insight as to where each NFI is most active in exerting developmental control.

5.1.4 Does NFI loss alter neural circuitry in the cerebellum?

The cerebellum is unique in the CNS in that it operates in a feed-forward manner, relying on a complex, interconnected signalling network of different cell types. Previous research left a gap as to what role NFIs played in the cerebellum, with some preliminary studies focusing predominately on CGNs and not expansively investigating these other cell types. The work in this thesis set out to investigate both the molecular mechanisms dictated by NFIs in CGNPs, and help fill in the gaps left by previous work. For example, we have shown for the first time that NFIX is expressed in basket and stellate interneurons in the molecular layer of the cerebellum [Chapter 2]. These inhibitory interneurons are crucial regulators of both feed-forward and feedback loops in this layer and form inhibitory synapses with Purkinje Neurons [325, 326]. It is possible that loss of NFIX expression in these interneurons causes cell intrinsic changes, as well as extrinsic effects that could exacerbate and contribute to the delay phenotypes we have identified in *Nfix*$^{-/-}$ mice. In CGNPs at least, we have shown that NFIs regulate the expression of a number of key axon growth and synaptic signalling proteins [Chapter 4]. Considering we have shown that NFIX is expressed in all cerebellar regions that contain interneuron progenitors during postnatal development including the embryonic VZ, and postal ML, IGL and WM (Chapter 2), it is possible that this TF regulates a similar suite of genes essential for interneuron synapse formation, like it does in CGNPs. Using Golgi-cox staining combined with high magnification stereomicroscopy would provide key details into any morphological deficits in axon, spine and synapse formation in these cells *in vivo*. Purification of interneuron subpopulations and downstream mRNA analysis has recently been achieved in the rat cortex using FACS [327]. FACS followed by qPCR or RNA-sequencing would allow investigation of changes in the expression of key axonal growth and signalling related genes, in pure populations of interneurons isolated from mutant cerebella.

One unexplored avenue in this thesis is how changes in NFI expression alter the electrophysiology of neurons and interneurons in the cerebellum. A number of different methods have been used to effectively measure the electrical activity of ML interneurons, PNs, Golgi cells and CGNs [328-334]. Examining induced and spontaneous firing activity in our mutants and comparing that with activity in our controls would provide novel insight into just how NFI loss alters the signalling pathways of the cerebellum. Combining this analysis with cell-type specific conditional deletion mutants with, would allow examination of cell intrinsic changes in mutant cells, as well as the subsequent extrinsic affects these mutations cause other cells in the cerebellar signalling network. A hallmark consequence of NFI loss or disruption is developmental delay and behavioural deficits, with associated ASD-like features [315, 335-339]. Unravelling how NFI loss impacts signalling

networks and synapse activity in the cerebellum would provide new information as to the biological changes that underpin these phenotypes.

From our DAVID and PANTHER analysis, it was noted that a number of GO-terms related to both signalling, ion and electrical activity were strongly enriched from our co-ordinately regulated gene lists [Chapter 3, 4]. Membrane depolarisation is a crucial component of CGNP development, encourages Ca^{2+} entry and activates kinase CaMK and phosphatase CaN. This signalling cascade upregulates factors involved in proliferation, differentiation and neuron migration, such as BDNF [340-342]. Potassium channels and K^+ levels control resting membrane potential and the duration of action potentials in neurons. K^+ can also induce apoptosis in granule neurons [343, 344]. Our data showing NFI regulation of multiple voltage gated potassium channels subunit genes suggest that these transcription factors could influence membrane potential, affecting downstream developmental signalling cascades. Determining how *NFI*-null CGNPs respond to manipulated K^+ levels *in vitro* would be a logical first step to see if mis-regulation of these potassium channel genes affects both neuron survival and action potential excitability.

5.1.5 Targeting NFIs in tumour therapy

Due to their prevalence in many tissues and in pools of proliferative progenitors, it is not unexpected that NFI mutations are associated with many different types of tumours. Indeed, the role of NFIs in developmental tumours was recently extensively reviewed, demonstrating a degree of convergence between family members [345]. In the cerebellum, NFIA, B and X expression have all been shown to have a potential role as a tumour suppressor in medulloblastoma [136, 170]. In human medulloblastoma cell lines, we have shown that NFIX is downregulated [Chapter 3]. Our analysis has shown that both NFIs directly regulate WNT and Notch signalling pathway members previously implicated in MB formation, as well as a number of pro-oncogenes and pro-differentiation factors [234, 346-355]. Further investigation is needed as to through which particular target pathways and effectors NFI-regulation mediates anti-tumour effects. Poorer outcomes from NFI loss in the *Ptch*$^{+/-}$ SHH-MB mouse model suggest that manipulation of this pathway may also be a mechanism in which NFIs exert a purported tumour-suppressive effect [136].

This exposes the inherent complexity in transcription factor mutations in cancer; the downstream affects are often incredibly varied and extensive. Drug therapies targeting transcription factors often focus on their degradation through proteolysis, functional inhibition or downregulation [356]. This strategy is less compatible with pro-differentiation transcription factors such as NFIA and NFIX, as their inhibition could potentially encourage tumour cell proliferation. Thus, analysis similar to what is presented in this thesis is essential in understanding normal TF-gene target relationships in native cells in the normal microenvironment. This provides essential understanding as to what genes and pathways are likely disrupted in neoplasms developing from these cells, offering a suite of targets potentially more druggable than TFs themselves.

NFI expression in glia has an important disease context. Gliomas arise from glia and are the most common malignancies in the CNS. In glioblastoma, NFIB has can act as a tumour suppressor (depending on the particular tumour subtype) and can suppress tumour cell migration [357, 358]. This is in contrast to NFIA which has been shown to promote glioblastoma tumour cell migration and survival [359, 360]. This presents a number of difficulties from a therapeutic perspective; a) the risk of cross reactivity between NFIs in targeted immunotherapies b) resistance to therapy due to autoregulation or redundancy between NFIs. Focusing instead on the downstream cascades and key oncogenic targets of NFIs is likely a more fruitful endeavour, but the importance of genetic profiling of these tumours cannot be understated even if for purely prognostic rather than treatment purposes.

5.1.6 Moving beyond transcriptomic analysis

Whilst this thesis has provided strong evidence and support for the conclusions within there are limitations in the methodology employed. A large proportion of our analysis focused on RNA-expression changes in cells isolated from the developing cerebellum. These changes can provide a good indication of global activity when using grouped analysis methods, such as GO-terms to look at broad changes in pathway activity, biological activity and molecular function. Correlation between mRNA and protein levels can be tenuous at best, and shows levels of tissue and context dependency[361-364]. RNA-analysis does not fully capture the myriad of post-translational modifications and factors that can affect both protein production, function and resultant expression in tissue. Indeed, the known cross and self-regulatory nature of the signalling pathways and transcription factors pulled out in our analysis beg the question; what protein:protein interactions are influencing the mutant phenotypes witnessed? Incorporating immunoassays such as ELISAs could be useful here to quantify protein expression of our identified co-ordinately regulated/mis-regulated targets in NFI-deficient granule neurons. These assays can be adapted using a number of commercial multiplexing systems to investigate multiple targets at once, which is invaluable considering the sheer number of downstream targets identified using our ChIP-seq + RNA-seq combined approach. Like other immunoassays however, these assays rely on the availability of specific antibodies, minimising its application in investigating novel targets proteins from our datasets. This hurdle can be surpassed however, by using approaches such as Label-free HPLC-tandem mass spectrometry, which was recently used to identify differentially expressed proteins in human cerebellar tissue [326, 365]. The high throughput nature of this technique provides an additional added advantage to immunoassay-based approaches. A recent study generated a workflow that combined RNA-seq, MS proteomics and a global post-translational modification database to help surpass the aforementioned shortcomings [366]. Adapting our analysis to incorporate similar workflows would provide greater confidence in our conclusions and comprehensive insights into how exactly NFI transcription factors regulate cerebellar development.

5.2 Conclusion:

This thesis set out to examine the Nuclear Factor One family of transcription factors and how they drive the development of the cerebellum. It showed that NFIs are expressed in a number of different cell types in the cerebellum and are notably highly expressed in cerebellar granule neurons and their progenitors. It investigated the changes in gene expression that occur when NFIs are deleted from these cells and though this, generated a dataset of gene targets directly regulated by each NFI. Our findings place *Nfia*, *Nfib* and *Nfix* as key drivers of the differentiation of cerebellar granule neuron progenitors in the postnatal brain. These findings have broad implications in better understanding the neurobiology of development, but also in understanding how mis-regulation of transcription factor expression can lead to disorder and disease. This thesis acts as the foundation for future research; investigating the biological significance of the key gene targets we have identified, incorporating proteomics into the analysis pipeline to improve coverage to protein expression, and is the first step in identifying new therapeutic targets for cerebellar tumours such as medulloblastoma.

Reference list

1. Koziol, L.F., et al., *Consensus paper: the cerebellum's role in movement and cognition.* Cerebellum, 2014. **13**(1): p. 151-77.
2. Pisotta, I. and M. Molinari, *Cerebellar contribution to feedforward control of locomotion.* Front Hum Neurosci, 2014. **8**: p. 475.
3. Ten Donkelaar, H.J. and M. Lammens, *Development of the human cerebellum and its disorders.* Clin Perinatol, 2009. **36**(3): p. 513-30.
4. Schuller, U., et al., *Acquisition of granule neuron precursor identity is a critical determinant of progenitor cell competence to form Shh-induced medulloblastoma.* Cancer Cell, 2008. **14**(2): p. 123-34.
5. Gibson, P., et al., *Subtypes of medulloblastoma have distinct developmental origins.* Nature, 2010. **468**(7327): p. 1095-9.
6. Martinez, S. and L. Puelles, *Neurogenetic compartments of the mouse diencephalon and some characteristic gene expression patterns.* Results Probl Cell Differ, 2000. **30**: p. 91-106.
7. Leto, K., et al., *Consensus Paper: Cerebellar Development.* Cerebellum, 2015.
8. Millet, S., et al., *The caudal limit of Otx2 gene expression as a marker of the midbrain/hindbrain boundary: a study using in situ hybridisation and chick/quail homotopic grafts.* Development, 1996. **122**(12): p. 3785-97.
9. Li, J.Y. and A.L. Joyner, *Otx2 and Gbx2 are required for refinement and not induction of mid-hindbrain gene expression.* Development, 2001. **128**(24): p. 4979-91.
10. Acampora, D., et al., *Otx genes in brain morphogenesis.* Prog Neurobiol, 2001. **64**(1): p. 69-95.
11. Goldowitz, D. and K. Hamre, *The cells and molecules that make a cerebellum.* Trends Neurosci, 1998. **21**(9): p. 375-82.
12. Hatten, M.E. and N. Heintz, *Mechanisms of neural patterning and specification in the developing cerebellum.* Annu Rev Neurosci, 1995. **18**: p. 385-408.
13. Corrales, J.D., et al., *The level of sonic hedgehog signaling regulates the complexity of cerebellar foliation.* Development, 2006. **133**(9): p. 1811-21.
14. Sudarov, A. and A.L. Joyner, *Cerebellum morphogenesis: the foliation pattern is orchestrated by multi-cellular anchoring centers.* Neural Dev, 2007. **2**: p. 26.
15. Wahlsten, D. and M. Andison, *Patterns of cerebellar foliation in recombinant inbred mice.* Brain Res, 1991. **557**(1-2): p. 184-9.
16. Cooper, P.A., et al., *Genetic analysis of cerebellar foliation patterns in mice (Mus musculus).* Behav Genet, 1991. **21**(4): p. 405-19.
17. Altman, J., *Postnatal development of the cerebellar cortex in the rat. II. Phases in the maturation of Purkinje cells and of the molecular layer.* J Comp Neurol, 1972. **145**(4): p. 399-463.
18. Rakic, P., *Extrinsic cytological determinants of basket and stellate cell dendritic pattern in the cerebellar molecular layer.* J Comp Neurol, 1972. **146**(3): p. 335-54.
19. Xu, H., et al., *Bergmann glia function in granule cell migration during cerebellum development.* Mol Neurobiol, 2013. **47**(2): p. 833-44.
20. Yamada, K. and M. Watanabe, *Cytodifferentiation of Bergmann glia and its relationship with Purkinje cells.* Anat Sci Int, 2002. **77**(2): p. 94-108.
21. Buffo, A. and F. Rossi, *Origin, lineage and function of cerebellar glia.* Prog Neurobiol, 2013. **109**: p. 42-63.
22. Laine, J. and H. Axelrad, *The candelabrum cell: a new interneuron in the cerebellar cortex.* J Comp Neurol, 1994. **339**(2): p. 159-73.
23. Miyata, T., et al., *Regulation of Purkinje cell alignment by reelin as revealed with CR-50 antibody.* J Neurosci, 1997. **17**(10): p. 3599-609.
24. Galliano, E., et al., *Anatomical investigation of potential contacts between climbing fibers and cerebellar Golgi cells in the mouse.* Front Neural Circuits, 2013. **7**: p. 59.

25. Geurts, F.J., et al., *Morphological and neurochemical differentiation of large granular layer interneurons in the adult rat cerebellum.* Neuroscience, 2001. **104**(2): p. 499-512.
26. Kalinichenko, S.G. and V.E. Okhotin, *Unipolar brush cells--a new type of excitatory interneuron in the cerebellar cortex and cochlear nuclei of the brainstem.* Neurosci Behav Physiol, 2005. **35**(1): p. 21-36.
27. Fink, A.J., et al., *Development of the deep cerebellar nuclei: transcription factors and cell migration from the rhombic lip.* J Neurosci, 2006. **26**(11): p. 3066-76.
28. Hoshino, M., et al., *Ptf1a, a bHLH transcriptional gene, defines GABAergic neuronal fates in cerebellum.* Neuron, 2005. **47**(2): p. 201-13.
29. Leto, K., et al., *Different types of cerebellar GABAergic interneurons originate from a common pool of multipotent progenitor cells.* J Neurosci, 2006. **26**(45): p. 11682-94.
30. Carletti, B. and F. Rossi, *Neurogenesis in the cerebellum.* Neuroscientist, 2008. **14**(1): p. 91-100.
31. Grimaldi, P., et al., *Origins and control of the differentiation of inhibitory interneurons and glia in the cerebellum.* Dev Biol, 2009. **328**(2): p. 422-33.
32. Hoshino, M., *Molecular machinery governing GABAergic neuron specification in the cerebellum.* Cerebellum, 2006. **5**(3): p. 193-8.
33. Maricich, S.M. and K. Herrup, *Pax-2 expression defines a subset of GABAergic interneurons and their precursors in the developing murine cerebellum.* J Neurobiol, 1999. **41**(2): p. 281-94.
34. Mizuhara, E., et al., *Purkinje cells originate from cerebellar ventricular zone progenitors positive for Neph3 and E-cadherin.* Dev Biol, 2010. **338**(2): p. 202-14.
35. Zhang, L. and J.E. Goldman, *Generation of cerebellar interneurons from dividing progenitors in white matter.* Neuron, 1996. **16**(1): p. 47-54.
36. Kanichay, R.T. and R.A. Silver, *Synaptic and cellular properties of the feedforward inhibitory circuit within the input layer of the cerebellar cortex.* J Neurosci, 2008. **28**(36): p. 8955-67.
37. Cesana, E., et al., *Granule cell ascending axon excitatory synapses onto Golgi cells implement a potent feedback circuit in the cerebellar granular layer.* J Neurosci, 2013. **33**(30): p. 12430-46.
38. Duguid, I., et al., *Control of cerebellar granule cell output by sensory-evoked Golgi cell inhibition.* Proc Natl Acad Sci U S A, 2015. **112**(42): p. 13099-104.
39. Braak, H., *On the intermediate cells of lugaro within the cerebellar cortex of man. A pigmentarchitectonic study.* Cell Tissue Res, 1974. **149**(3): p. 399-411.
40. Fox, C.A., *The intermediate cells of Lugaro in the cerebellar cortex of the monkey.* J Comp Neurol, 1959. **112**: p. 39-53.
41. Laine, J. and H. Axelrad, *Lugaro cells target basket and stellate cells in the cerebellar cortex.* Neuroreport, 1998. **9**(10): p. 2399-403.
42. Ambrosi, G., et al., *Non-traditional large neurons in the granular layer of the cerebellar cortex.* Eur J Histochem, 2007. **51 Suppl 1**: p. 59-64.
43. Sotelo, C., *Molecular layer interneurons of the cerebellum: developmental and morphological aspects.* Cerebellum, 2015. **14**(5): p. 534-56.
44. Martinez, S., et al., *Cellular and molecular basis of cerebellar development.* Front Neuroanat, 2013. **7**: p. 18.
45. Rancillac, A. and F. Crepel, *Synapses between parallel fibres and stellate cells express long-term changes in synaptic efficacy in rat cerebellum.* J Physiol, 2004. **554**(Pt 3): p. 707-20.
46. Mori, T., et al., *Inducible gene deletion in astroglia and radial glia--a valuable tool for functional and lineage analysis.* Glia, 2006. **54**(1): p. 21-34.
47. Kim, E.J., et al., *Ascl1 (Mash1) lineage cells contribute to discrete cell populations in CNS architecture.* Mol Cell Neurosci, 2008. **38**(4): p. 595-606.
48. Sudarov, A., et al., *Ascl1 genetics reveals insights into cerebellum local circuit assembly.* J Neurosci, 2011. **31**(30): p. 11055-69.

49. Kita, Y., et al., *Development of cerebellar neurons and glias revealed by in utero electroporation: Golgi-like labeling of cerebellar neurons and glias.* PLoS One, 2013. **8**(7): p. e70091.
50. Machold, R. and G. Fishell, *Math1 is expressed in temporally discrete pools of cerebellar rhombic-lip neural progenitors.* Neuron, 2005. **48**(1): p. 17-24.
51. Machold, R.P., D.J. Kittell, and G.J. Fishell, *Antagonism between Notch and bone morphogenetic protein receptor signaling regulates neurogenesis in the cerebellar rhombic lip.* Neural Dev, 2007. **2**: p. 5.
52. Silbereis, J., et al., *Astroglial cells in the external granular layer are precursors of cerebellar granule neurons in neonates.* Mol Cell Neurosci, 2010. **44**(4): p. 362-73.
53. Hoogland, T.M. and B. Kuhn, *Recent developments in the understanding of astrocyte function in the cerebellum in vivo.* Cerebellum, 2010. **9**(3): p. 264-71.
54. Hoogland, T.M., et al., *Radially expanding transglial calcium waves in the intact cerebellum.* Proc Natl Acad Sci U S A, 2009. **106**(9): p. 3496-501.
55. Sotelo, C., *Cellular and genetic regulation of the development of the cerebellar system.* Prog Neurobiol, 2004. **72**(5): p. 295-339.
56. Rice, D.S. and T. Curran, *Role of the reelin signaling pathway in central nervous system development.* Annu Rev Neurosci, 2001. **24**: p. 1005-39.
57. Miyata, T., et al., *Migration, early axonogenesis, and Reelin-dependent layer-forming behavior of early/posterior-born Purkinje cells in the developing mouse lateral cerebellum.* Neural Dev, 2010. **5**: p. 23.
58. Larouche, M., et al., *The Reelin receptors Apoer2 and Vldlr coordinate the patterning of Purkinje cell topography in the developing mouse cerebellum.* PLoS One, 2008. **3**(2): p. e1653.
59. Kawamura, Y., et al., *Spike timing-dependent selective strengthening of single climbing fibre inputs to Purkinje cells during cerebellar development.* Nat Commun, 2013. **4**: p. 2732.
60. Uesaka, N., et al., *Retrograde signaling for climbing fiber synapse elimination.* Cerebellum, 2015. **14**(1): p. 4-7.
61. Machold, R., C. Klein, and G. Fishell, *Genes expressed in Atoh1 neuronal lineages arising from the r1/isthmus rhombic lip.* Gene Expr Patterns, 2011. **11**(5-6): p. 349-59.
62. Wang, V.Y., M.F. Rose, and H.Y. Zoghbi, *Math1 expression redefines the rhombic lip derivatives and reveals novel lineages within the brainstem and cerebellum.* Neuron, 2005. **48**(1): p. 31-43.
63. Gazit, R., V. Krizhanovsky, and N. Ben-Arie, *Math1 controls cerebellar granule cell differentiation by regulating multiple components of the Notch signaling pathway.* Development, 2004. **131**(4): p. 903-13.
64. Mugnaini, E., G. Sekerkova, and M. Martina, *The unipolar brush cell: a remarkable neuron finally receiving deserved attention.* Brain Res Rev, 2011. **66**(1-2): p. 220-45.
65. Nunzi, M.G., R. Shigemoto, and E. Mugnaini, *Differential expression of calretinin and metabotropic glutamate receptor mGluR1alpha defines subsets of unipolar brush cells in mouse cerebellum.* J Comp Neurol, 2002. **451**(2): p. 189-99.
66. Englund, C., et al., *Unipolar brush cells of the cerebellum are produced in the rhombic lip and migrate through developing white matter.* J Neurosci, 2006. **26**(36): p. 9184-95.
67. Morin, F., M.R. Dino, and E. Mugnaini, *Postnatal differentiation of unipolar brush cells and mossy fiber-unipolar brush cell synapses in rat cerebellum.* Neuroscience, 2001. **104**(4): p. 1127-39.
68. Mugnaini, E. and A. Floris, *The unipolar brush cell: a neglected neuron of the mammalian cerebellar cortex.* J Comp Neurol, 1994. **339**(2): p. 174-80.
69. Gruart, A., et al., *Very short-term potentiation of climbing fiber effects on deep cerebellar nuclei neurons by conditioning stimulation of mossy fiber afferents.* Exp Brain Res, 1994. **101**(1): p. 173-7.

70. Van der Want, J.J., et al., *Anterograde tracing of the rat olivocerebellar system with Phaseolus vulgaris leucoagglutinin (PHA-L). Demonstration of climbing fiber collateral innervation of the cerebellar nuclei.* J Comp Neurol, 1989. **288**(1): p. 1-18.
71. Alder, J., N.K. Cho, and M.E. Hatten, *Embryonic precursor cells from the rhombic lip are specified to a cerebellar granule neuron identity.* Neuron, 1996. **17**(3): p. 389-99.
72. Alder, J., et al., *Generation of cerebellar granule neurons in vivo by transplantation of BMP-treated neural progenitor cells.* Nat Neurosci, 1999. **2**(6): p. 535-40.
73. Aruga, J., *The role of Zic genes in neural development.* Mol Cell Neurosci, 2004. **26**(2): p. 205-21.
74. Engelkamp, D., et al., *Role of Pax6 in development of the cerebellar system.* Development, 1999. **126**(16): p. 3585-96.
75. Tong, K.K., T.C. Ma, and K.M. Kwan, *BMP/Smad signaling and embryonic cerebellum development: stem cell specification and heterogeneity of anterior rhombic lip.* Dev Growth Differ, 2015. **57**(2): p. 121-34.
76. Fujita, S., M. Shimada, and T. Nakamura, *H3-thymidine autoradiographic studies on the cell proliferation and differentiation in the external and the internal granular layers of the mouse cerebellum.* J Comp Neurol, 1966. **128**(2): p. 191-208.
77. Solecki, D.J., et al., *Activated Notch2 signaling inhibits differentiation of cerebellar granule neuron precursors by maintaining proliferation.* Neuron, 2001. **31**(4): p. 557-68.
78. Rios, I., et al., *Bmp2 antagonizes sonic hedgehog-mediated proliferation of cerebellar granule neurones through Smad5 signalling.* Development, 2004. **131**(13): p. 3159-68.
79. Zhao, H., et al., *Post-transcriptional down-regulation of Atoh1/Math1 by bone morphogenic proteins suppresses medulloblastoma development.* Genes Dev, 2008. **22**(6): p. 722-7.
80. Renaud, J., et al., *Plexin-A2 and its ligand, Sema6A, control nucleus-centrosome coupling in migrating granule cells.* Nat Neurosci, 2008. **11**(4): p. 440-9.
81. Gundappa-Sulur, G., E. De Schutter, and J.M. Bower, *Ascending granule cell axon: an important component of cerebellar cortical circuitry.* J Comp Neurol, 1999. **408**(4): p. 580-96.
82. Wilczynska, K.M., et al., *Nuclear factor I isoforms regulate gene expression during the differentiation of human neural progenitors to astrocytes.* Stem Cells, 2009. **27**(5): p. 1173-81.
83. Martynoga, B., et al., *Epigenomic enhancer annotation reveals a key role for NFIX in neural stem cell quiescence.* Genes Dev, 2013. **27**(16): p. 1769-86.
84. Heng, Y.H., et al., *NFIX regulates neural progenitor cell differentiation during hippocampal morphogenesis.* Cereb Cortex, 2014. **24**(1): p. 261-79.
85. Zhou, B., et al., *Loss of NFIX Transcription Factor Biases Postnatal Neural Stem/Progenitor Cells Toward Oligodendrogenesis.* Stem Cells Dev, 2015. **24**(18): p. 2114-26.
86. Heng, Y.H., et al., *NFIX Regulates Proliferation and Migration Within the Murine SVZ Neurogenic Niche.* Cereb Cortex, 2015. **25**(10): p. 3758-78.
87. Harris, L., et al., *Neurogenic differentiation by hippocampal neural stem and progenitor cells is biased by NFIX expression.* Development, 2018. **145**(3).
88. Gronostajski, R.M., K. Nagata, and J. Hurwitz, *Isolation of human DNA sequences that bind to nuclear factor I, a host protein involved in adenovirus DNA replication.* Proc Natl Acad Sci U S A, 1984. **81**(13): p. 4013-7.
89. Kruse, U. and A.E. Sippel, *Transcription factor nuclear factor I proteins form stable homo- and heterodimers.* FEBS Lett, 1994. **348**(1): p. 46-50.
90. Mason, S., et al., *Nuclear factor one transcription factors in CNS development.* Mol Neurobiol, 2009. **39**(1): p. 10-23.
91. Piper, M., et al., *Nuclear factor one X regulates the development of multiple cellular populations in the postnatal cerebellum.* J Comp Neurol, 2011. **519**(17): p. 3532-48.

92. Vidovic, D., et al., *Expansion of the lateral ventricles and ependymal deficits underlie the hydrocephalus evident in mice lacking the transcription factor NFIX.* Brain Res, 2015. **1616**: p. 71-87.
93. Chaudhry, A.Z., G.E. Lyons, and R.M. Gronostajski, *Expression patterns of the four nuclear factor I genes during mouse embryogenesis indicate a potential role in development.* Dev Dyn, 1997. **208**(3): p. 313-25.
94. Plachez, C., et al., *Nuclear factor I gene expression in the developing forebrain.* J Comp Neurol, 2008. **508**(3): p. 385-401.
95. Kruse, U. and A.E. Sippel, *The genes for transcription factor nuclear factor I give rise to corresponding splice variants between vertebrate species.* J Mol Biol, 1994. **238**(5): p. 860-5.
96. Campbell, C.E., et al., *The transcription factor Nfix is essential for normal brain development.* BMC Dev Biol, 2008. **8**: p. 52.
97. Harris, L., et al., *Nuclear factor one transcription factors: Divergent functions in developmental versus adult stem cell populations.* Dev Dyn, 2015. **244**(3): p. 227-38.
98. Heng, Y.H., et al., *NFIX Regulates Proliferation and Migration Within the Murine SVZ Neurogenic Niche.* Cereb Cortex, 2014.
99. Wang, W., et al., *Targets of the nuclear factor I regulon involved in early and late development of postmitotic cerebellar granule neurons.* J Neurosci Res, 2010. **88**(2): p. 258-65.
100. Wang, W., et al., *Nuclear factor I coordinates multiple phases of cerebellar granule cell development via regulation of cell adhesion molecules.* J Neurosci, 2007. **27**(23): p. 6115-27.
101. Wang, W., et al., *A role for nuclear factor I in the intrinsic control of cerebellar granule neuron gene expression.* J Biol Chem, 2004. **279**(51): p. 53491-7.
102. Kato, K., *Novel GABAA receptor alpha subunit is expressed only in cerebellar granule cells.* J Mol Biol, 1990. **214**(3): p. 619-24.
103. Kilpatrick, D.L., et al., *Nuclear factor I and cerebellar granule neuron development: an intrinsic-extrinsic interplay.* Cerebellum, 2012. **11**(1): p. 41-9.
104. das Neves, L., et al., *Disruption of the murine nuclear factor I-A gene (Nfia) results in perinatal lethality, hydrocephalus, and agenesis of the corpus callosum.* Proc Natl Acad Sci U S A, 1999. **96**(21): p. 11946-51.
105. Shu, T., et al., *Abnormal development of forebrain midline glia and commissural projections in Nfia knock-out mice.* J Neurosci, 2003. **23**(1): p. 203-12.
106. Wong, Y.W., et al., *Gene expression analysis of nuclear factor I-A deficient mice indicates delayed brain maturation.* Genome Biol, 2007. **8**(5): p. R72.
107. Heng, Y.H., et al., *Nuclear factor I genes regulate neuronal migration.* Neurosignals, 2012. **20**(3): p. 159-67.
108. Steele-Perkins, G., et al., *The transcription factor gene Nfib is essential for both lung maturation and brain development.* Mol Cell Biol, 2005. **25**(2): p. 685-98.
109. Grunder, A., et al., *Nuclear factor I-B (Nfib) deficient mice have severe lung hypoplasia.* Mech Dev, 2002. **112**(1-2): p. 69-77.
110. Piper, M., et al., *Multiple non-cell-autonomous defects underlie neocortical callosal dysgenesis in Nfib-deficient mice.* Neural Dev, 2009. **4**: p. 43.
111. Baeriswyl, T. and E.T. Stoeckli, *Axonin-1/TAG-1 is required for pathfinding of granule cell axons in the developing cerebellum.* Neural Dev, 2008. **3**: p. 7.
112. Lamani, E., et al., *Tissue- and cell-specific alternative splicing of NFIC.* Cells Tissues Organs, 2009. **189**(1-4): p. 105-10.
113. Kim, M.Y., et al., *Role of the transcription factor NFIC in odontoblast gene expression.* J Calif Dent Assoc, 2009. **37**(12): p. 875-81.

114. Park, J.C., et al., *Nfic gene disruption inhibits differentiation of odontoblasts responsible for root formation and results in formation of short and abnormal roots in mice.* J Periodontol, 2007. **78**(9): p. 1795-802.
115. Huang, X., et al., *Smad4-Shh-Nfic signaling cascade-mediated epithelial-mesenchymal interaction is crucial in regulating tooth root development.* J Bone Miner Res, 2010. **25**(5): p. 1167-78.
116. He, W., et al., *Regulatory interplay between NFIC and TGF-beta1 in apical papilla-derived stem cells.* J Dent Res, 2014. **93**(5): p. 496-501.
117. Lee, H.K., D.S. Lee, and J.C. Park, *Nuclear factor I-C regulates E-cadherin via control of KLF4 in breast cancer.* BMC Cancer, 2015. **15**: p. 113.
118. Dong, H.Y., et al., *19p13.2 Microdeletion including NFIX associated with overgrowth and intellectual disability suggestive of Malan syndrome.* Mol Cytogenet, 2016. **9**: p. 71.
119. Gurrieri, F., et al., *NFIX mutations affecting the DNA-binding domain cause a peculiar overgrowth syndrome (Malan syndrome): a new patients series.* Eur J Med Genet, 2015. **58**(9): p. 488-91.
120. Jezela-Stanek, A., et al., *Malan syndrome (Sotos syndrome 2) in two patients with 19p13.2 deletion encompassing NFIX gene and novel NFIX sequence variant.* Biomed Pap Med Fac Univ Palacky Olomouc Czech Repub, 2016. **160**(1): p. 161-7.
121. Klaassens, M., et al., *Malan syndrome: Sotos-like overgrowth with de novo NFIX sequence variants and deletions in six new patients and a review of the literature.* Eur J Hum Genet, 2015. **23**(5): p. 610-5.
122. Lu, Y., et al., *Mutations in NSD1 and NFIX in Three Patients with Clinical Features of Sotos Syndrome and Malan Syndrome.* J Pediatr Genet, 2017. **6**(4): p. 234-237.
123. Malan, V., et al., *Distinct effects of allelic NFIX mutations on nonsense-mediated mRNA decay engender either a Sotos-like or a Marshall-Smith syndrome.* Am J Hum Genet, 2010. **87**(2): p. 189-98.
124. Oshima, T., et al., *A novel mutation of NFIX causes Sotos-like syndrome (Malan syndrome) complicated with thoracic aortic aneurysm and dissection.* Hum Genome Var, 2017. **4**: p. 17022.
125. Trimouille, A., et al., *19p13 microduplications encompassing NFIX are responsible for intellectual disability, short stature and small head circumference.* Eur J Hum Genet, 2018. **26**(1): p. 85-93.
126. Zalucki, O., et al., *Analysis of hippocampal-dependent learning and memory behaviour in mice lacking Nfix from adult neural stem cells.* BMC Res Notes, 2018. **11**(1): p. 564.
127. Dahmane, N. and A. Ruiz i Altaba, *Sonic hedgehog regulates the growth and patterning of the cerebellum.* Development, 1999. **126**(14): p. 3089-100.
128. Vaillant, C. and D. Monard, *SHH pathway and cerebellar development.* Cerebellum, 2009. **8**(3): p. 291-301.
129. Wall, D.S., et al., *Progenitor cell proliferation in the retina is dependent on Notch-independent Sonic hedgehog/Hes1 activity.* J Cell Biol, 2009. **184**(1): p. 101-12.
130. Piper, M., et al., *NFIA controls telencephalic progenitor cell differentiation through repression of the Notch effector Hes1.* J Neurosci, 2010. **30**(27): p. 9127-39.
131. Mourikis, P., et al., *Cell-autonomous Notch activity maintains the temporal specification potential of skeletal muscle stem cells.* Development, 2012. **139**(24): p. 4536-48.
132. Gopalan, S.M., et al., *Nuclear factor-1-X regulates astrocyte-specific expression of the alpha1-antichymotrypsin and glial fibrillary acidic protein genes.* J Biol Chem, 2006. **281**(19): p. 13126-33.
133. Glasgow, S.M., et al., *Glia-specific enhancers and chromatin structure regulate NFIA expression and glioma tumorigenesis.* Nat Neurosci, 2017. **20**(11): p. 1520-1528.
134. Glasgow, S.M., et al., *The miR-223/nuclear factor I-A axis regulates glial precursor proliferation and tumorigenesis in the CNS.* J Neurosci, 2013. **33**(33): p. 13560-8.

135. Song, H.R., et al., *Nuclear factor IA is expressed in astrocytomas and is associated with improved survival.* Neuro Oncol, 2010. **12**(2): p. 122-32.
136. Genovesi, L.A., et al., *Sleeping Beauty mutagenesis in a mouse medulloblastoma model defines networks that discriminate between human molecular subgroups.* Proc Natl Acad Sci U S A, 2013. **110**(46): p. E4325-34.
137. Brun, M., et al., *Nuclear factor I regulates brain fatty acid-binding protein and glial fibrillary acidic protein gene expression in malignant glioma cell lines.* J Mol Biol, 2009. **391**(2): p. 282-300.
138. Glasgow, S.M., et al., *Mutual antagonism between Sox10 and NFIA regulates diversification of glial lineages and glioma subtypes.* Nat Neurosci, 2014. **17**(10): p. 1322-9.
139. Packer, R.J., et al., *Medulloblastoma: clinical and biologic aspects.* Neuro Oncol, 1999. **1**(3): p. 232-50.
140. Dohrmann, G.J. and R.H. Dunsmore, *Gliobastoma multiforme of the cerebellum.* Surg Neurol, 1975. **3**(4): p. 219-23.
141. Lee, H.Y., et al., *Isolation and culture of post-natal mouse cerebellar granule neuron progenitor cells and neurons.* J Vis Exp, 2009(23).
142. Kerjan, G., et al., *The transmembrane semaphorin Sema6A controls cerebellar granule cell migration.* Nat Neurosci, 2005. **8**(11): p. 1516-24.
143. Chizhikov, V. and K.J. Millen, *Development and malformations of the cerebellum in mice.* Mol Genet Metab, 2003. **80**(1-2): p. 54-65.
144. De Luca, A., et al., *Exogenous Sonic hedgehog modulates the pool of GABAergic interneurons during cerebellar development.* Cerebellum, 2015. **14**(2): p. 72-85.
145. Fleming, J.T., et al., *The Purkinje neuron acts as a central regulator of spatially and functionally distinct cerebellar precursors.* Dev Cell, 2013. **27**(3): p. 278-92.
146. Englund, C., et al., *Pax6, Tbr2, and Tbr1 are expressed sequentially by radial glia, intermediate progenitor cells, and postmitotic neurons in developing neocortex.* J Neurosci, 2005. **25**(1): p. 247-51.
147. Hevner, R.F., et al., *Transcription factors in glutamatergic neurogenesis: conserved programs in neocortex, cerebellum, and adult hippocampus.* Neurosci Res, 2006. **55**(3): p. 223-33.
148. Akazawa, C., et al., *A mammalian helix-loop-helix factor structurally related to the product of Drosophila proneural gene atonal is a positive transcriptional regulator expressed in the developing nervous system.* J Biol Chem, 1995. **270**(15): p. 8730-8.
149. Ben-Arie, N., et al., *Math1 is essential for genesis of cerebellar granule neurons.* Nature, 1997. **390**(6656): p. 169-72.
150. Lee, Y., et al., *A molecular fingerprint for medulloblastoma.* Cancer Res, 2003. **63**(17): p. 5428-37.
151. Betancourt, J., S. Katzman, and B. Chen, *Nuclear factor one B regulates neural stem cell differentiation and axonal projection of corticofugal neurons.* J Comp Neurol, 2014. **522**(1): p. 6-35.
152. Trapnell, C., et al., *Differential gene and transcript expression analysis of RNA-seq experiments with TopHat and Cufflinks.* Nat Protoc, 2012. **7**(3): p. 562-78.
153. Pouzat, C. and S. Hestrin, *Developmental regulation of basket/stellate cell-->Purkinje cell synapses in the cerebellum.* J Neurosci, 1997. **17**(23): p. 9104-12.
154. Yamasaki, T., et al., *Pax6 regulates granule cell polarization during parallel fiber formation in the developing cerebellum.* Development, 2001. **128**(16): p. 3133-44.
155. Chung, S.H., et al., *Early cerebellar granule cell migration in the mouse embryonic development.* Anat Cell Biol, 2010. **43**(1): p. 86-95.
156. Weyer, A. and K. Schilling, *Developmental and cell type-specific expression of the neuronal marker NeuN in the murine cerebellum.* J Neurosci Res, 2003. **73**(3): p. 400-9.

157. Grunder, A., et al., *Genomic organization, splice products and mouse chromosomal localization of genes for transcription factor Nuclear Factor One.* Gene, 2003. **304**: p. 171-81.
158. Lu, W., et al., *NFIA haploinsufficiency is associated with a CNS malformation syndrome and urinary tract defects.* PLoS Genet, 2007. **3**(5): p. e80.
159. Driller, K., et al., *Nuclear factor I X deficiency causes brain malformation and severe skeletal defects.* Mol Cell Biol, 2007. **27**(10): p. 3855-3867.
160. Pistocchi, A., et al., *Conserved and divergent functions of Nfix in skeletal muscle development during vertebrate evolution.* Development, 2013. **140**(7): p. 1528-36.
161. Rossi, G., et al., *Nfix Regulates Temporal Progression of Muscle Regeneration through Modulation of Myostatin Expression.* Cell Rep, 2016. **14**(9): p. 2238-49.
162. Chow, L.M., J. Zhang, and S.J. Baker, *Inducible Cre recombinase activity in mouse mature astrocytes and adult neural precursor cells.* Transgenic Res, 2008. **17**(5): p. 919-28.
163. Taniguchi, H., et al., *A resource of Cre driver lines for genetic targeting of GABAergic neurons in cerebral cortex.* Neuron, 2011. **71**(6): p. 995-1013.
164. Zhang, X., et al., *Novel alternative splice variants of NFIX and their diverse mRNA expression patterns in dairy goat.* Gene, 2015. **569**(2): p. 250-8.
165. Zhou, Y., et al., *Novel isoforms of the bovine Nuclear factor I/X (CCAAT-binding transcription factor) transcript products and their diverse expression profiles.* Anim Genet, 2014. **45**(4): p. 581-4.
166. Singh, S.K., et al., *The unique transcriptional activation domain of nuclear factor-I-X3 is critical to specifically induce marker gene expression in astrocytes.* J Biol Chem, 2011. **286**(9): p. 7315-26.
167. Dooley, A.L., et al., *Nuclear factor I/B is an oncogene in small cell lung cancer.* Genes Dev, 2011. **25**(14): p. 1470-5.
168. Mirabello, L., et al., *A Genome-Wide Scan Identifies Variants in NFIB Associated with Metastasis in Patients with Osteosarcoma.* Cancer Discov, 2015. **5**(9): p. 920-31.
169. Liu, C., et al., *miR-29a activates Hes1 by targeting Nfia in esophageal carcinoma cell line TE-1.* Oncol Lett, 2015. **9**(1): p. 96-102.
170. Lastowska, M., et al., *Identification of a neuronal transcription factor network involved in medulloblastoma development.* Acta Neuropathol Commun, 2013. **1**: p. 35.
171. Northcott, P.A., et al., *The clinical implications of medulloblastoma subgroups.* Nat Rev Neurol, 2012. **8**(6): p. 340-51.
172. Landsberg, R.L., et al., *Hindbrain rhombic lip is comprised of discrete progenitor cell populations allocated by Pax6.* Neuron, 2005. **48**(6): p. 933-47.
173. Vernay, B., et al., *Otx2 regulates subtype specification and neurogenesis in the midbrain.* J Neurosci, 2005. **25**(19): p. 4856-67.
174. Miale, I.L. and R.L. Sidman, *An autoradiographic analysis of histogenesis in the mouse cerebellum.* Exp Neurol, 1961. **4**: p. 277-96.
175. Aruga, J., et al., *Zic2 controls cerebellar development in cooperation with Zic1.* J Neurosci, 2002. **22**(1): p. 218-25.
176. Kawauchi, D. and T. Saito, *Transcriptional cascade from Math1 to Mbh1 and Mbh2 is required for cerebellar granule cell differentiation.* Dev Biol, 2008. **322**(2): p. 345-54.
177. Pan, N., et al., *Defects in the cerebella of conditional Neurod1 null mice correlate with effective Tg(Atoh1-cre) recombination and granule cell requirements for Neurod1 for differentiation.* Cell Tissue Res, 2009. **337**(3): p. 407-28.
178. Piper, M., et al., *NFIB-mediated repression of the epigenetic factor Ezh2 regulates cortical development.* J Neurosci, 2014. **34**(8): p. 2921-30.
179. Chen, K.S., et al., *Differential neuronal and glial expression of nuclear factor I proteins in the cerebral cortex of adult mice.* J Comp Neurol, 2017. **525**(11): p. 2465-2483.
180. Chang, C.Y., et al., *NFIB is a governor of epithelial-melanocyte stem cell behaviour in a shared niche.* Nature, 2013. **495**(7439): p. 98-102.

181. Messina, G., et al., *Nfix regulates fetal-specific transcription in developing skeletal muscle.* Cell, 2010. **140**(4): p. 554-66.
182. Kumbasar, A., et al., *Absence of the transcription factor Nfib delays the formation of the basilar pontine and other mossy fiber nuclei.* J Comp Neurol, 2009. **513**(1): p. 98-112.
183. Harris, L., et al., *Transcriptional regulation of intermediate progenitor cell generation during hippocampal development.* Development, 2016. **143**(24): p. 4620-4630.
184. Dixon, C., et al., *Nuclear Factor One X Regulates Bobby Sox During Development of the Mouse Forebrain.* Cell Mol Neurobiol, 2013.
185. Sengar, A.S., et al., *Vertebrate intersectin1 is repurposed to facilitate cortical midline connectivity and higher order cognition.* J Neurosci, 2013. **33**(9): p. 4055-65.
186. Klisch, T.J., et al., *In vivo Atoh1 targetome reveals how a proneural transcription factor regulates cerebellar development.* Proc Natl Acad Sci U S A, 2011. **108**(8): p. 3288-93.
187. Blythe, S.A., et al., *Chromatin immunoprecipitation in early Xenopus laevis embryos.* Dev Dyn, 2009. **238**(6): p. 1422-32.
188. Langmead, B. and S.L. Salzberg, *Fast gapped-read alignment with Bowtie 2.* Nat Methods, 2012. **9**(4): p. 357-9.
189. Feng, J., et al., *Identifying ChIP-seq enrichment using MACS.* Nat Protoc, 2012. **7**(9): p. 1728-40.
190. Bailey, T.L., et al., *MEME SUITE: tools for motif discovery and searching.* Nucleic Acids Res, 2009. **37**(Web Server issue): p. W202-8.
191. Machanick, P. and T.L. Bailey, *MEME-ChIP: motif analysis of large DNA datasets.* Bioinformatics, 2011. **27**(12): p. 1696-7.
192. O'Connor, T., M. Boden, and T.L. Bailey, *CisMapper: predicting regulatory interactions from transcription factor ChIP-seq data.* Nucleic Acids Res, 2017. **45**(4): p. e19.
193. Huang da, W., B.T. Sherman, and R.A. Lempicki, *Bioinformatics enrichment tools: paths toward the comprehensive functional analysis of large gene lists.* Nucleic Acids Res, 2009. **37**(1): p. 1-13.
194. Huang da, W., B.T. Sherman, and R.A. Lempicki, *Systematic and integrative analysis of large gene lists using DAVID bioinformatics resources.* Nat Protoc, 2009. **4**(1): p. 44-57.
195. Guertin, M.J. and J.T. Lis, *Mechanisms by which transcription factors gain access to target sequence elements in chromatin.* Curr Opin Genet Dev, 2013. **23**(2): p. 116-23.
196. Hughes, T.R., *Introduction to "a handbook of transcription factors".* Subcell Biochem, 2011. **52**: p. 1-6.
197. Vidovic, D., et al., *Transcriptional regulation of ependymal cell maturation within the postnatal brain.* Neural Dev, 2018. **13**(1): p. 2.
198. Frank, C.L., et al., *Regulation of chromatin accessibility and Zic binding at enhancers in the developing cerebellum.* Nat Neurosci, 2015. **18**(5): p. 647-56.
199. Gallagher, E., et al., *Cerebellar abnormalities in the disabled (mdab1-1) mouse.* J Comp Neurol, 1998. **402**(2): p. 238-51.
200. Tamada, A., et al., *Crucial roles of Robo proteins in midline crossing of cerebellofugal axons and lack of their up-regulation after midline crossing.* Neural Dev, 2008. **3**: p. 29.
201. Herrero-Garcia, E. and J.P. O'Bryan, *Intersectin scaffold proteins and their role in cell signaling and endocytosis.* Biochim Biophys Acta, 2017. **1864**(1): p. 23-30.
202. Jakob, B., et al., *Intersectin 1 is a component of the Reelin pathway to regulate neuronal migration and synaptic plasticity in the hippocampus.* Proc Natl Acad Sci U S A, 2017. **114**(21): p. 5533-5538.
203. Vaswani, A.R. and S. Blaess, *Reelin Signaling in the Migration of Ventral Brain Stem and Spinal Cord Neurons.* Front Cell Neurosci, 2016. **10**: p. 62.
204. Fane, M., et al., *Nuclear factor one transcription factors as epigenetic regulators in cancer.* Int J Cancer, 2017. **140**(12): p. 2634-2641.
205. Piper, M., et al., *Multiple non-cell-autonomous defects underlie neocortical callosal dysgenesis in Nfib-deficient mice.* Neural Dev, 2009. **4**(1): p. 43.

206. Matuzelski, E., et al., *Transcriptional regulation of Nfix by NFIB drives astrocytic maturation within the developing spinal cord.* Dev Biol, 2017. **432**(2): p. 286-297.
207. Deneen, B., et al., *The transcription factor NFIA controls the onset of gliogenesis in the developing spinal cord.* Neuron, 2006. **52**(6): p. 953-68.
208. Kang, P., et al., *Sox9 and NFIA coordinate a transcriptional regulatory cascade during the initiation of gliogenesis.* Neuron, 2012. **74**(1): p. 79-94.
209. Adams, A., et al., *Intersectin, an adaptor protein involved in clathrin-mediated endocytosis, activates mitogenic signaling pathways.* J Biol Chem, 2000. **275**(35): p. 27414-20.
210. Sanchez-Ortiz, E., et al., *NF1 regulation of RAS/ERK signaling is required for appropriate granule neuron progenitor expansion and migration in cerebellar development.* Genes Dev, 2014. **28**(21): p. 2407-20.
211. Gubar, O., et al., *Intersectin: The Crossroad between Vesicle Exocytosis and Endocytosis.* Front Endocrinol (Lausanne), 2013. **4**: p. 109.
212. Roussel, M.F. and M.E. Hatten, *Cerebellum development and medulloblastoma.* Curr Top Dev Biol, 2011. **94**: p. 235-82.
213. Yue, S., et al., *Requirement of Smurf-mediated endocytosis of Patched1 in sonic hedgehog signal reception.* Elife, 2014. **3**.
214. Cavalli, F.M.G., et al., *Intertumoral Heterogeneity within Medulloblastoma Subgroups.* Cancer Cell, 2017. **31**(6): p. 737-754 e6.
215. Ransohoff, K.J., J.Y. Tang, and K.Y. Sarin, *Squamous Change in Basal-Cell Carcinoma with Drug Resistance.* N Engl J Med, 2015. **373**(11): p. 1079-82.
216. Zhao, X., et al., *RAS/MAPK Activation Drives Resistance to Smo Inhibition, Metastasis, and Tumor Evolution in Shh Pathway-Dependent Tumors.* Cancer Res, 2015. **75**(17): p. 3623-35.
217. Esnault, G., et al., *Transcription factor CTF1 acts as a chromatin domain boundary that shields human telomeric genes from silencing.* Mol Cell Biol, 2009. **29**(9): p. 2409-18.
218. Muller, K. and N. Mermod, *The histone-interacting domain of nuclear factor I activates simian virus 40 DNA replication in vivo.* J Biol Chem, 2000. **275**(3): p. 1645-50.
219. Denny, S.K., et al., *Nfib Promotes Metastasis through a Widespread Increase in Chromatin Accessibility.* Cell, 2016. **166**(2): p. 328-342.
220. Pascual, M., et al., *Cerebellar GABAergic progenitors adopt an external granule cell-like phenotype in the absence of Ptf1a transcription factor expression.* Proc Natl Acad Sci U S A, 2007. **104**(12): p. 5193-8.
221. Hori, K., et al., *A nonclassical bHLH Rbpj transcription factor complex is required for specification of GABAergic neurons independent of Notch signaling.* Genes Dev, 2008. **22**(2): p. 166-78.
222. Lucas, F.R. and P.C. Salinas, *WNT-7a induces axonal remodeling and increases synapsin I levels in cerebellar neurons.* Dev Biol, 1997. **192**(1): p. 31-44.
223. Hall, A.C., F.R. Lucas, and P.C. Salinas, *Axonal remodeling and synaptic differentiation in the cerebellum is regulated by WNT-7a signaling.* Cell, 2000. **100**(5): p. 525-35.
224. Schuller, U., et al., *Forkhead transcription factor FoxM1 regulates mitotic entry and prevents spindle defects in cerebellar granule neuron precursors.* Mol Cell Biol, 2007. **27**(23): p. 8259-70.
225. Mi, H., et al., *PANTHER version 14: more genomes, a new PANTHER GO-slim and improvements in enrichment analysis tools.* Nucleic Acids Res, 2019. **47**(D1): p. D419-D426.
226. Chawla, K., et al., *TFcheckpoint: a curated compendium of specific DNA-binding RNA polymerase II transcription factors.* Bioinformatics, 2013. **29**(19): p. 2519-20.
227. Wang, W., et al., *Temporal control of a dendritogenesis-linked gene via REST-dependent regulation of nuclear factor I occupancy.* Mol Biol Cell, 2011. **22**(6): p. 868-79.
228. Yang, H., et al., *Generation and characterization of Atoh1-Cre knock-in mouse line.* Genesis, 2010. **48**(6): p. 407-13.

229. Constantin, L. and B.J. Wainwright, *MicroRNAs Promote Granule Cell Expansion in the Cerebellum Through Gli2.* Cerebellum, 2015. **14**(6): p. 688-98.
230. Thurman, R.E., et al., *The accessible chromatin landscape of the human genome.* Nature, 2012. **489**(7414): p. 75-82.
231. Lorenz, A., et al., *Severe alterations of cerebellar cortical development after constitutive activation of Wnt signaling in granule neuron precursors.* Mol Cell Biol, 2011. **31**(16): p. 3326-38.
232. Horn, Z., H. Behesti, and M.E. Hatten, *N-cadherin provides a cis and trans ligand for astrotactin that functions in glial-guided neuronal migration.* Proc Natl Acad Sci U S A, 2018. **115**(42): p. 10556-10563.
233. Selvadurai, H.J. and J.O. Mason, *Wnt/beta-catenin signalling is active in a highly dynamic pattern during development of the mouse cerebellum.* PLoS One, 2011. **6**(8): p. e23012.
234. Anne, S.L., et al., *WNT3 inhibits cerebellar granule neuron progenitor proliferation and medulloblastoma formation via MAPK activation.* PLoS One, 2013. **8**(11): p. e81769.
235. Subashini, C., et al., *Wnt5a is a crucial regulator of neurogenesis during cerebellum development.* Sci Rep, 2017. **7**: p. 42523.
236. Schmidt, E.F., et al., *BAC transgenic mice and the GENSAT database of engineered mouse strains.* Cold Spring Harb Protoc, 2013. **2013**(3).
237. Visel, A., C. Thaller, and G. Eichele, *GenePaint.org: an atlas of gene expression patterns in the mouse embryo.* Nucleic Acids Res, 2004. **32**(Database issue): p. D552-6.
238. Consortium, S.M.-I., *A comprehensive assessment of RNA-seq accuracy, reproducibility and information content by the Sequencing Quality Control Consortium.* Nat Biotechnol, 2014. **32**(9): p. 903-14.
239. Jin, Y., et al., *Gas6/AXL Signaling Regulates Self-Renewal of Chronic Myelogenous Leukemia Stem Cells by Stabilizing beta-Catenin.* Clin Cancer Res, 2017. **23**(11): p. 2842-2855.
240. Sainaghi, P.P., et al., *Gas6 induces proliferation in prostate carcinoma cell lines expressing the Axl receptor.* J Cell Physiol, 2005. **204**(1): p. 36-44.
241. Wu, G., et al., *Molecular insights of Gas6/TAM in cancer development and therapy.* Cell Death Dis, 2017. **8**(3): p. e2700.
242. Shiozawa, Y., et al., *GAS6/AXL axis regulates prostate cancer invasion, proliferation, and survival in the bone marrow niche.* Neoplasia, 2010. **12**(2): p. 116-27.
243. Yagami, T., et al., *Gas6 rescues cortical neurons from amyloid beta protein-induced apoptosis.* Neuropharmacology, 2002. **43**(8): p. 1289-96.
244. Pierce, A., et al., *Axl and Tyro3 modulate female reproduction by influencing gonadotropin-releasing hormone neuron survival and migration.* Mol Endocrinol, 2008. **22**(11): p. 2481-95.
245. Zheng, Y., et al., *NGF-induced Tyro3 and Axl function as survival factors for differentiating PC12 cells.* Biochem Biophys Res Commun, 2009. **378**(3): p. 371-5.
246. Ray, A.K., et al., *Loss of Gas6 and Axl signaling results in extensive axonal damage, motor deficits, prolonged neuroinflammation, and less remyelination following cuprizone exposure.* Glia, 2017. **65**(12): p. 2051-2069.
247. Ji, R., et al., *TAM receptor deficiency affects adult hippocampal neurogenesis.* Metab Brain Dis, 2015. **30**(3): p. 633-44.
248. Prieto, A.L., J.L. Weber, and C. Lai, *Expression of the receptor protein-tyrosine kinases Tyro-3, Axl, and mer in the developing rat central nervous system.* J Comp Neurol, 2000. **425**(2): p. 295-314.
249. Park, P.C., et al., *Transcriptional profiling of medulloblastoma in children.* J Neurosurg, 2003. **99**(3): p. 534-41.
250. Penzes, P., et al., *The neuronal Rho-GEF Kalirin-7 interacts with PDZ domain-containing proteins and regulates dendritic morphogenesis.* Neuron, 2001. **29**(1): p. 229-42.

251. Ma, X.M., et al., *Kalirin-7 is required for synaptic structure and function.* J Neurosci, 2008. **28**(47): p. 12368-82.
252. Ma, X.M., et al., *Kalirin, a multifunctional Rho guanine nucleotide exchange factor, is necessary for maintenance of hippocampal pyramidal neuron dendrites and dendritic spines.* J Neurosci, 2003. **23**(33): p. 10593-603.
253. Cahill, M.E., et al., *Kalirin regulates cortical spine morphogenesis and disease-related behavioral phenotypes.* Proc Natl Acad Sci U S A, 2009. **106**(31): p. 13058-63.
254. Miller, M.B., et al., *Alternate promoter usage generates two subpopulations of the neuronal RhoGEF Kalirin-7.* J Neurochem, 2017. **140**(6): p. 889-902.
255. Miller, M.B., et al., *Neuronal Rho GEFs in synaptic physiology and behavior.* Neuroscientist, 2013. **19**(3): p. 255-73.
256. Yan, Y., B.A. Eipper, and R.E. Mains, *Kalirin is required for BDNF-TrkB stimulated neurite outgrowth and branching.* Neuropharmacology, 2016. **107**: p. 227-238.
257. Mandela, P., et al., *Elimination of Kalrn expression in POMC cells reduces anxiety-like behavior and contextual fear learning.* Horm Behav, 2014. **66**(2): p. 430-8.
258. Richard, V., D. Dulon, and A. Hafidi, *Expression of Rho GTPases Rho-A and Rac1 in the adult and developing gerbil cerebellum.* Int J Dev Neurosci, 2008. **26**(7): p. 723-32.
259. Mulherkar, S., et al., *The small GTPases RhoA and Rac1 regulate cerebellar development by controlling cell morphogenesis, migration and foliation.* Dev Biol, 2014. **394**(1): p. 39-53.
260. Chatonnet, F., et al., *Genome-wide search reveals the existence of a limited number of thyroid hormone receptor alpha target genes in cerebellar neurons.* PLoS One, 2012. **7**(5): p. e30703.
261. Kawasaki, Y., et al., *Identification and characterization of Asef2, a guanine-nucleotide exchange factor specific for Rac1 and Cdc42.* Oncogene, 2007. **26**(55): p. 7620-267.
262. Jean, L., et al., *Activation of Rac by Asef2 promotes myosin II-dependent contractility to inhibit cell migration on type I collagen.* J Cell Sci, 2013. **126**(Pt 24): p. 5585-97.
263. Evans, J.C., et al., *The guanine nucleotide exchange factor (GEF) Asef2 promotes dendritic spine formation via Rac activation and spinophilin-dependent targeting.* J Biol Chem, 2015. **290**(16): p. 10295-308.
264. Bristow, J.M., et al., *The Rho-family GEF Asef2 activates Rac to modulate adhesion and actin dynamics and thereby regulate cell migration.* J Cell Sci, 2009. **122**(Pt 24): p. 4535-46.
265. Tong, X.K., et al., *Intersectin can regulate the Ras/MAP kinase pathway independent of its role in endocytosis.* J Biol Chem, 2000. **275**(38): p. 29894-9.
266. Taglietti, V., et al., *RhoA and ERK signalling regulate the expression of the transcription factor Nfix in myogenic cells.* Development, 2018. **145**(21).
267. He, X., et al., *A member of the Frizzled protein family mediating axis induction by Wnt-5A.* Science, 1997. **275**(5306): p. 1652-4.
268. Lancaster, M.A., et al., *Defective Wnt-dependent cerebellar midline fusion in a mouse model of Joubert syndrome.* Nat Med, 2011. **17**(6): p. 726-31.
269. Nemeth, M.J., et al., *Wnt5a inhibits canonical Wnt signaling in hematopoietic stem cells and enhances repopulation.* Proc Natl Acad Sci U S A, 2007. **104**(39): p. 15436-41.
270. Nakamura, R.E. and A.S. Hackam, *Analysis of Dickkopf3 interactions with Wnt signaling receptors.* Growth Factors, 2010. **28**(4): p. 232-42.
271. Kawano, Y. and R. Kypta, *Secreted antagonists of the Wnt signalling pathway.* J Cell Sci, 2003. **116**(Pt 13): p. 2627-34.
272. Alok, A., et al., *Wnt proteins synergize to activate beta-catenin signaling.* J Cell Sci, 2017. **130**(9): p. 1532-1544.
273. Brauburger, K., et al., *Adenomatous polyposis coli (APC) membrane recruitment 3, a member of the APC membrane recruitment family of APC-binding proteins, is a positive regulator of Wnt-beta-catenin signalling.* FEBS J, 2014. **281**(3): p. 787-801.

274. Kieslinger, M., et al., *EBF2 regulates osteoblast-dependent differentiation of osteoclasts.* Dev Cell, 2005. **9**(6): p. 757-67.
275. Cavallo, R.A., et al., *Drosophila Tcf and Groucho interact to repress Wingless signalling activity.* Nature, 1998. **395**(6702): p. 604-8.
276. Brantjes, H., et al., *All Tcf HMG box transcription factors interact with Groucho-related co-repressors.* Nucleic Acids Res, 2001. **29**(7): p. 1410-9.
277. Kool, M., et al., *Molecular subgroups of medulloblastoma: an international meta-analysis of transcriptome, genetic aberrations, and clinical data of WNT, SHH, Group 3, and Group 4 medulloblastomas.* Acta Neuropathol, 2012. **123**(4): p. 473-84.
278. Northcott, P.A., et al., *Subgroup-specific structural variation across 1,000 medulloblastoma genomes.* Nature, 2012. **488**(7409): p. 49-56.
279. Tzivion, G., M. Dobson, and G. Ramakrishnan, *FoxO transcription factors; Regulation by AKT and 14-3-3 proteins.* Biochim Biophys Acta, 2011. **1813**(11): p. 1938-45.
280. Paik, J.H., et al., *FoxOs cooperatively regulate diverse pathways governing neural stem cell homeostasis.* Cell Stem Cell, 2009. **5**(5): p. 540-53.
281. Santo, E.E. and J. Paik, *FOXO in Neural Cells and Diseases of the Nervous System.* Curr Top Dev Biol, 2018. **127**: p. 105-118.
282. Li, Q., et al., *Silencing of FOXO6 inhibits the proliferation, invasion, and glycolysis in colorectal cancer cells.* J Cell Biochem, 2018.
283. Lallemand, F., et al., *Involvement of the FOXO6 transcriptional factor in breast carcinogenesis.* Oncotarget, 2018. **9**(7): p. 7464-7475.
284. Wang, J.H., et al., *Elevated FOXO6 expression correlates with progression and prognosis in gastric cancer.* Oncotarget, 2017. **8**(19): p. 31682-31691.
285. de la Torre-Ubieta, L., et al., *A FOXO-Pak1 transcriptional pathway controls neuronal polarity.* Genes Dev, 2010. **24**(8): p. 799-813.
286. Paap, R.H., et al., *FoxO6 affects Plxna4-mediated neuronal migration during mouse cortical development.* Proc Natl Acad Sci U S A, 2016. **113**(45): p. E7087-E7096.
287. Alto, L.T. and J.R. Terman, *Semaphorins and their Signaling Mechanisms.* Methods Mol Biol, 2017. **1493**: p. 1-25.
288. Berndt, J.D. and M.C. Halloran, *Semaphorin 3d promotes cell proliferation and neural crest cell development downstream of TCF in the zebrafish hindbrain.* Development, 2006. **133**(20): p. 3983-92.
289. Miyata, T., T. Maeda, and J.E. Lee, *NeuroD is required for differentiation of the granule cells in the cerebellum and hippocampus.* Genes Dev, 1999. **13**(13): p. 1647-52.
290. Olson, J.M., et al., *NeuroD2 is necessary for development and survival of central nervous system neurons.* Dev Biol, 2001. **234**(1): p. 174-87.
291. Mo, Z., et al., *Role of the Barhl2 homeobox gene in the specification of glycinergic amacrine cells.* Development, 2004. **131**(7): p. 1607-18.
292. Chellappa, R., et al., *Barhl1 regulatory sequences required for cell-specific gene expression and autoregulation in the inner ear and central nervous system.* Mol Cell Biol, 2008. **28**(6): p. 1905-14.
293. Li, S., et al., *Barhl1 regulates migration and survival of cerebellar granule cells by controlling expression of the neurotrophin-3 gene.* J Neurosci, 2004. **24**(12): p. 3104-14.
294. Saito, T., et al., *Mammalian BarH homologue is a potential regulator of neural bHLH genes.* Dev Biol, 1998. **199**(2): p. 216-25.
295. Saba, R., J.E. Johnson, and T. Saito, *Commissural neuron identity is specified by a homeodomain protein, Mbh1, that is directly downstream of Math1.* Development, 2005. **132**(9): p. 2147-55.
296. Poschl, J., et al., *Expression of BARHL1 in medulloblastoma is associated with prolonged survival in mice and humans.* Oncogene, 2011. **30**(47): p. 4721-30.
297. Ding, Q., et al., *Barhl2 Determines the Early Patterning of the Diencephalon by Regulating Shh.* Mol Neurobiol, 2017. **54**(6): p. 4414-4420.

298. Zhang, P.G.Y., et al., *Discovery of Transcription Factors Novel to Mouse Cerebellar Granule Cell Development Through Laser-Capture Microdissection.* Cerebellum, 2018. **17**(3): p. 308-325.
299. Wizeman, J.W., et al., *Specification of diverse cell types during early neurogenesis of the mouse cerebellum.* Elife, 2019. **8**.
300. Zhu, Y. and S. Guthrie, *Expression of the ETS transcription factor ER81 in the developing chick and mouse hindbrain.* Dev Dyn, 2002. **225**(3): p. 365-8.
301. Abe, H., M. Okazawa, and S. Nakanishi, *The Etv1/Er81 transcription factor orchestrates activity-dependent gene regulation in the terminal maturation program of cerebellar granule cells.* Proc Natl Acad Sci U S A, 2011. **108**(30): p. 12497-502.
302. Scoles, D.R., et al., *ETS1 regulates the expression of ATXN2.* Hum Mol Genet, 2012. **21**(23): p. 5048-65.
303. Ding, B., et al., *Reciprocal autoregulation by NFI occupancy and ETV1 promotes the developmental expression of dendrite-synapse genes in cerebellar granule neurons.* Mol Biol Cell, 2016. **27**(9): p. 1488-99.
304. Cooper, C.D., et al., *Structures of the Ets Protein DNA-binding Domains of Transcription Factors Etv1, Etv4, Etv5, and Fev: DETERMINANTS OF DNA BINDING AND REDOX REGULATION BY DISULFIDE BOND FORMATION.* J Biol Chem, 2015. **290**(22): p. 13692-709.
305. Liu, D., et al., *Brain-derived neurotrophic factor promotes vesicular glutamate transporter 3 expression and neurite outgrowth of dorsal root ganglion neurons through the activation of the transcription factors Etv4 and Etv5.* Brain Res Bull, 2016. **121**: p. 215-26.
306. Fontanet, P.A., et al., *Pea3 Transcription Factors, Etv4 and Etv5, Are Required for Proper Hippocampal Dendrite Development and Plasticity.* Cereb Cortex, 2018. **28**(1): p. 236-249.
307. Schwartz, P.M., et al., *Abnormal cerebellar development and foliation in BDNF-/- mice reveals a role for neurotrophins in CNS patterning.* Neuron, 1997. **19**(2): p. 269-81.
308. Rahimi Balaei, M., et al., *Cerebellar Expression of the Neurotrophin Receptor p75 in Naked-Ataxia Mutant Mouse.* Int J Mol Sci, 2016. **17**(1).
309. Zanin, J.P., E. Abercrombie, and W.J. Friedman, *Proneurotrophin-3 promotes cell cycle withdrawal of developing cerebellar granule cell progenitors via the p75 neurotrophin receptor.* Elife, 2016. **5**.
310. Blank, M.C., et al., *Multiple developmental programs are altered by loss of Zic1 and Zic4 to cause Dandy-Walker malformation cerebellar pathogenesis.* Development, 2011. **138**(6): p. 1207-16.
311. Harris, L., et al., *Heterozygosity for nuclear factor one x affects hippocampal-dependent behaviour in mice.* PLoS One, 2013. **8**(6): p. e65478.
312. Bunt, J., et al., *Combined allelic dosage of Nfia and Nfib regulates cortical development.* Brain and Neuroscience Advances, 2017. **1**: p. 2398212817739433.
313. Forget, A., et al., *Shh signaling protects Atoh1 from degradation mediated by the E3 ubiquitin ligase Huwe1 in neural precursors.* Dev Cell, 2014. **29**(6): p. 649-61.
314. Chaudhry, A.Z., A.D. Vitullo, and R.M. Gronostajski, *Nuclear factor I (NFI) isoforms differentially activate simple versus complex NFI-responsive promoters.* J Biol Chem, 1998. **273**(29): p. 18538-46.
315. Hickey, S.L., S. Berto, and G. Konopka, *Chromatin Decondensation by FOXP2 Promotes Human Neuron Maturation and Expression of Neurodevelopmental Disease Genes.* Cell Rep, 2019. **27**(6): p. 1699-1711 e9.
316. Centonze, V.E., B.A. Firulli, and A.B. Firulli, *Fluorescence Resonance Energy Transfer (FRET) as a method to calculate the dimerization strength of basic Helix-Loop-Helix (bHLH) proteins.* Biol Proced Online, 2004. **6**: p. 78-82.
317. Wang, C., et al., *Visualization of bHLH transcription factor interactions in living mammalian cell nuclei and developing chicken neural tube by FRET.* Cell Res, 2006. **16**(6): p. 585-98.

318. Collin, L., et al., *Oligodendrocyte ablation affects the coordinated interaction between granule and Purkinje neurons during cerebellum development.* Exp Cell Res, 2007. **313**(13): p. 2946-57.
319. Srinivasan, R., et al., *New Transgenic Mouse Lines for Selectively Targeting Astrocytes and Studying Calcium Signals in Astrocyte Processes In Situ and In Vivo.* Neuron, 2016. **92**(6): p. 1181-1195.
320. Winchenbach, J., et al., *Inducible targeting of CNS astrocytes in Aldh1l1-CreERT2 BAC transgenic mice.* F1000Res, 2016. **5**: p. 2934.
321. Shimojima, K., et al., *An association of 19p13.2 microdeletions with Malan syndrome and Chiari malformation.* Am J Med Genet A, 2015. **167A**(4): p. 724-30.
322. Kim, Y., et al., *Selective transgene expression in cerebellar Purkinje cells and granule cells using adeno-associated viruses together with specific promoters.* Brain Res, 2015. **1620**: p. 1-16.
323. Croci, C., et al., *Cerebellar neurons and glial cells are transducible by lentiviral vectors without decrease of cerebellar functions.* Dev Neurosci, 2006. **28**(3): p. 216-21.
324. Bosch, M.K., J.M. Nerbonne, and D.M. Ornitz, *Dual transgene expression in murine cerebellar Purkinje neurons by viral transduction in vivo.* PLoS One, 2014. **9**(8): p. e104062.
325. Consalez, G.G. and R. Hawkes, *The compartmental restriction of cerebellar interneurons.* Front Neural Circuits, 2012. **6**: p. 123.
326. Blot, A., et al., *Time-invariant feed-forward inhibition of Purkinje cells in the cerebellar cortex in vivo.* J Physiol, 2016. **594**(10): p. 2729-49.
327. Martin, D., et al., *Neurocytometry: Flow Cytometric Sorting of Specific Neuronal Populations from Human and Rodent Brain.* ACS Chem Neurosci, 2017. **8**(2): p. 356-367.
328. Delvendahl, I., I. Straub, and S. Hallermann, *Dendritic patch-clamp recordings from cerebellar granule cells demonstrate electrotonic compactness.* Front Cell Neurosci, 2015. **9**: p. 93.
329. Eshra, A., P. Hirrlinger, and S. Hallermann, *Enriched Environment Shortens the Duration of Action Potentials in Cerebellar Granule Cells.* Front Cell Neurosci, 2019. **13**: p. 289.
330. Eyre, M.D. and Z. Nusser, *Only a Minority of the Inhibitory Inputs to Cerebellar Golgi Cells Originates from Local GABAergic Cells.* eNeuro, 2016. **3**(2).
331. Nguyen-Minh, V.T., et al., *Electrophysiological Excitability and Parallel Fiber Synaptic Properties of Zebrin-Positive and -Negative Purkinje Cells in Lobule VIII of the Mouse Cerebellar Slice.* Front Cell Neurosci, 2018. **12**: p. 513.
332. Person, A.L. and I.M. Raman, *Purkinje neuron synchrony elicits time-locked spiking in the cerebellar nuclei.* Nature, 2011. **481**(7382): p. 502-5.
333. Witter, L., et al., *Purkinje Cell Collaterals Enable Output Signals from the Cerebellar Cortex to Feed Back to Purkinje Cells and Interneurons.* Neuron, 2016. **91**(2): p. 312-9.
334. Zhang, B. and T.C. Sudhof, *Neuroligins Are Selectively Essential for NMDAR Signaling in Cerebellar Stellate Interneurons.* J Neurosci, 2016. **36**(35): p. 9070-83.
335. Mikhail, F.M., et al., *Clinically relevant single gene or intragenic deletions encompassing critical neurodevelopmental genes in patients with developmental delay, mental retardation, and/or autism spectrum disorders.* Am J Med Genet A, 2011. **155A**(10): p. 2386-96.
336. Choi, J., et al., *Cut-like homeobox 1 and nuclear factor I/B mediate ENGRAILED2 autism spectrum disorder-associated haplotype function.* Hum Mol Genet, 2012. **21**(7): p. 1566-80.
337. Priolo, M., et al., *Further delineation of Malan syndrome.* Hum Mutat, 2018. **39**(9): p. 1226-1237.
338. Tsang, K.M., et al., *A genome-wide survey of transgenerational genetic effects in autism.* PLoS One, 2013. **8**(10): p. e76978.
339. Schanze, I., et al., *NFIB Haploinsufficiency Is Associated with Intellectual Disability and Macrocephaly.* Am J Hum Genet, 2018. **103**(5): p. 752-768.

340. Nakanishi, S. and M. Okazawa, *Membrane potential-regulated Ca2+ signalling in development and maturation of mammalian cerebellar granule cells.* J Physiol, 2006. **575**(Pt 2): p. 389-95.
341. Kokubo, M., et al., *BDNF-mediated cerebellar granule cell development is impaired in mice null for CaMKK2 or CaMKIV.* J Neurosci, 2009. **29**(28): p. 8901-13.
342. Kramer, D., et al., *Calcineurin controls the expression of numerous genes in cerebellar granule cells.* Mol Cell Neurosci, 2003. **23**(2): p. 325-30.
343. Lauritzen, I., et al., *K+-dependent cerebellar granule neuron apoptosis. Role of task leak K+ channels.* J Biol Chem, 2003. **278**(34): p. 32068-76.
344. Martin-Romero, F.J., et al., *Potassium-induced apoptosis in rat cerebellar granule cells involves cell-cycle blockade at the G1/S transition.* J Mol Neurosci, 2000. **15**(3): p. 155-65.
345. Chen, K.S., et al., *The convergent roles of the nuclear factor I transcription factors in development and cancer.* Cancer Lett, 2017. **410**: p. 124-138.
346. Bai, R.Y., et al., *OTX2 represses myogenic and neuronal differentiation in medulloblastoma cells.* Cancer Res, 2012. **72**(22): p. 5988-6001.
347. Cordeiro, B.M., et al., *SHH, WNT, and NOTCH pathways in medulloblastoma: when cancer stem cells maintain self-renewal and differentiation properties.* Childs Nerv Syst, 2014. **30**(7): p. 1165-72.
348. Garzia, L., et al., *MicroRNA-199b-5p impairs cancer stem cells through negative regulation of HES1 in medulloblastoma.* PLoS One, 2009. **4**(3): p. e4998.
349. Huang, P., Y.D. Guo, and H.W. Zhang, *Identification of Hub Genes in Pediatric Medulloblastoma by Multiple-Microarray Analysis.* J Mol Neurosci, 2020. **70**(4): p. 522-531.
350. Lee, S.E., et al., *Prognostic significance of Ror2 and Wnt5a expression in medulloblastoma.* Brain Pathol, 2013. **23**(4): p. 445-53.
351. Michiels, E.M., et al., *Genes differentially expressed in medulloblastoma and fetal brain.* Physiol Genomics, 1999. **1**(2): p. 83-91.
352. Schreck, K.C., et al., *The Notch target Hes1 directly modulates Gli1 expression and Hedgehog signaling: a potential mechanism of therapeutic resistance.* Clin Cancer Res, 2010. **16**(24): p. 6060-70.
353. Yokota, N., et al., *Identification of differentially expressed and developmentally regulated genes in medulloblastoma using suppression subtraction hybridization.* Oncogene, 2004. **23**(19): p. 3444-53.
354. Xu, P., et al., *Differential expression of Notch family members in astrocytomas and medulloblastomas.* Pathol Oncol Res, 2009. **15**(4): p. 703-10.
355. Kongkham, P.N., et al., *The SFRP family of WNT inhibitors function as novel tumor suppressor genes epigenetically silenced in medulloblastoma.* Oncogene, 2010. **29**(20): p. 3017-24.
356. Bushweller, J.H., *Targeting transcription factors in cancer - from undruggable to reality.* Nat Rev Cancer, 2019. **19**(11): p. 611-624.
357. Stringer, B.W., et al., *Nuclear factor one B (NFIB) encodes a subtype-specific tumour suppressor in glioblastoma.* Oncotarget, 2016. **7**(20): p. 29306-20.
358. Vo, T.M., et al., *A positive feedback loop involving nuclear factor IB and calpain 1 suppresses glioblastoma cell migration.* J Biol Chem, 2019. **294**(34): p. 12638-12654.
359. Lee, J., E. Hoxha, and H.R. Song, *A novel NFIA-NFkappaB feed-forward loop contributes to glioblastoma cell survival.* Neuro Oncol, 2017. **19**(4): p. 524-534.
360. Lee, J.S., et al., *A novel tumor-promoting role for nuclear factor IA in glioblastomas is mediated through negative regulation of p53, p21, and PAI1.* Neuro Oncol, 2014. **16**(2): p. 191-203.
361. Payne, S.H., *The utility of protein and mRNA correlation.* Trends Biochem Sci, 2015. **40**(1): p. 1-3.

362. Edfors, F., et al., *Gene-specific correlation of RNA and protein levels in human cells and tissues.* Mol Syst Biol, 2016. **12**(10): p. 883.
363. Liu, Y., A. Beyer, and R. Aebersold, *On the Dependency of Cellular Protein Levels on mRNA Abundance.* Cell, 2016. **165**(3): p. 535-50.
364. Parkes, G.M. and M. Niranjan, *Uncovering extensive post-translation regulation during human cell cycle progression by integrative multi-'omics analysis.* BMC Bioinformatics, 2019. **20**(1): p. 536.
365. Meierhofer, D., et al., *Ataxin-2 (Atxn2)-Knock-Out Mice Show Branched Chain Amino Acids and Fatty Acids Pathway Alterations.* Mol Cell Proteomics, 2016. **15**(5): p. 1728-39.
366. Cesnik, A.J., et al., *Human Proteomic Variation Revealed by Combining RNA-Seq Proteogenomics and Global Post-Translational Modification (G-PTM) Search Strategy.* J Proteome Res, 2016. **15**(3): p. 800-8.

Appendix

Chapter 3

Downregulated NFIX genes			Upregulated NFIX target genes					
1700048O20Rik	Il16	Snap25	Arl4a	Cyth4	Gsg1l	Msrb3	Resp18	Tmem179
A730043L09Rik	Impg2	Soga1	Arl4c	Dab1	Gstm6	Mxra7	Rfx4	Tmem196
Abca2	Iqcj	Sorbs1	Asap1	Dact2	Gusb	Myrip	Rgs3	Tmem200a
Abcc8	Itsn1	Sostdc1	Ass1	Dennd3	Hdac11	Ncam2	Rgs4	Tnc
Adam11	Jph4	Sowahb	Atp13a4	Dhrs3	Hhip	Nckap5	Rgs8	Tnf
Adamts18	Kcna1	Spata13	Atp2b4	Dkk3	Hmga2	Ndufc2	Rhbdl3	Triqk
Adcy1	Kcnip3	Sphkap	B3gat1	Dlc1	Hpca	Nek7	Rhoj	Trpc7
Ahdc1	Kcnj11	Sptbn4	Barx2	Dlgap2	Hspa12a	Nell1	Rimbp2	Tsc22d4
Amer3	Kcnj9	Srcin1	Bcan	Dnm3	Htr7	Neurod6	Rnd3	Tspan11
Ano5	Kcnk1	Srrm4	Bcas1	Dock2	Icmt	Nfam1	Robo1	Tspan9
Ap3b2	Kcnk3	Stxbp5l	Begain	Dpp6	Ier5	Nfkbiz	Rtn4rl1	Txlnb
Arid1a	Kcnq5	Syne1	Blnk	Dpysl4	Igf2bp2	Ngfr	Rtp4	Txnrd3
Arpp21	Kcns2	Syt9	Bmp5	Dtx4	Igfbp2	Nhlrc4	Rxra	Vim
Atp2b1	Kl	Tenm1	Bmper	Dusp2	Igfbp3	Ninj1	Ryr3	Vit
Atp2b3	Klf9	Tgfb2	Btbd11	Dusp6	Igsf11	Nkain2	Sall1	Vstm2b
Barhl2	Ksr2	Tle2	C1qtnf4	Dync1i1	Il17rd	Notch3	Samsn1	Vwf
Brinp2	Ky	Tmem63c	Cacna1h	Ebf2	Ildr2	Nptx1	Scml4	Wnt5a
Btbd17	Lipc	Tmprss13	Cacna2d2	Ecscr	Inpp5a	Ntng2	Scn1a	Wnt7b
Cacna1c	Lrrtm3	Trim67	Cacng4	Efnb1	Insc	Nuak2	Scn3a	Zfp618
Cacna2d3	Lyst	Trpc4ap	Calb1	Egln3	Iqsec1	Nwd2	Scube2	Zfp804a
Cadps	Marchf3	Tspan4	Calcrl	Elfn2	Iqsec3	Nxph1	Serinc5	
Camk4	Map3k5	Unc13a	Camk1d	Elk3	Irx1	Ogdhl	Serpine2	
Car10	Megf10	Unc5b	Camk1g	Eln	Islr	Optc	Sgcd	
Cdh15	Miat	Vat1l	Camk2n1	Emp1	Itgb5	Osbpl5	Sgcz	
Celf4	Mmp17	Wnt7a	Car8	Enc1	Itpka	Osm	Sgk1	
Cemip	Mpp3	Zbtb20	Cartpt	Enpp1	Kalrn	Otof	Sh3pxd2a	
Cenpf	Mrgprf	Zdhhc22	Cbln4	Epha4	Kank4	P4ha2	Shh	
Cerkl	Mtss1	Zfhx2	Ccbe1	Epha5	Kcna6	Pam	Siglech	
Cipc	Myocd	Zfhx2os	Ccdc184	Epha8	Kcnb1	Paqr8	Sik1	
Cmss1	Ncam1	Zfhx4	Cd109	Esrrg	Kcne4	Pax3	Skor2	
Cntn2	Neurod1	Zfpm2	Cd44	Ets1	Kcnf1	Pcdh15	Slc14a2	
Col8a1	Neurod4	Zfyve28	Cd83	Etv5	Kcnip1	Pcdh19	Slc17a8	
Coro2b	Nfix	Zhx2	Cd93	Fam20c	Kcnip4	Pcdh20	Slc2a4	
Crabp1	Nos1		Cdh11	Fam43b	Kcnma1	Pcp2	Slc35f1	
Crhr1	Ntf3		Cdh20	Fam46a	Kcnn3	Pcp4	Slc41a3	

Csmd2	Ntrk3	1110015O18Rik	Cdh4	Fat4	Kcnv1	Pcsk5	Slc5a7	
D430041D05Rik	Nxpe3	1810011O10Rik	Cdh7	Fbln1	Kctd14	Pcsk6	Slc6a1	
D630010B17Rik	Olig3	2310015A10Rik	Cdh9	Fbln2	Kctd16	Pde1c	Slc6a11	
Dio2	Otx2	9630028H03Rik	Cdkn1c	Fbxo2	Kif26a	Pde2a	Slco2b1	
Dock4	Paqr6	A730017C20Rik	Cebpb	Fibcd1	Kit	Pdgfa	Slit1	
Efcab5	Pcdh7	Abcb6	Cend1	Fos	Klf15	Pdgfc	Smad3	
Ephb1	Pde3a	Abcb9	Chd5	Foxq1	Klf4	Pdzd2	Smoc1	
Etv1	Pde9a	Ackr3	Chl1	Frem1	Lamb1	Pdzrn4	Snph	
Exph5	Pik3c2b	Acot7	Chrna4	Frmpd4	Lamc2	Pecam1	Sorcs1	
Fam107a	Plxna2	Adamts1	Chrnb4	Fscn1	Lgr6	Pgf	Sorcs2	
Fat2	Ppfia4	Adamts14	Chst1	Fxyd7	Lhfpl3	Phactr2	Sorcs3	
Fbn1	Prkce	Adamts3	Chst8	Fzd9	Lhpp	Pkdcc	Sowaha	
Fgf14	Prox1	Adamtsl1	Cnr1	Gaa	Lhx5	Pla2g5	Sox7	
Foxo6	Prune2	Adarb2	Cntn5	Galnt10	Lifr	Plat	Spats2l	
Ftx	Rapgef3	Adcy2	Cntn6	Galnt14	Limch1	Plcxd3	Sstr2	
Gabbr2	Rbfox3	Adcyap1	Cntnap5a	Galnt18	Lingo2	Plxdc1	St6galnac5	
Gabra2	Rimkla	Agtrap	Cntnap5b	Gas6	Lingo3	Plxna4	Stac	
Gabra6	Rims1	AI593442	Col25a1	Gem	Lix1l	Ppp1r16b	Stac2	
Gabrd	Rnf112	Aif1	Col26a1	Gfod1	Lmx1a	Ppp1r1b	Stc1	
Galr1	Rnf165	Aif1l	Col27a1	Ghr	Loxl1	Prdm13	Sv2c	
Gfap	Rnf182	Ajap1	Col4a1	Gldc	Lpar1	Prkar1b	Sybu	
Gjb6	Ryr2	Ak1	Col4a2	Glis3	Lrig3	Prkch	Syt13	
Gm9899	Samd12	Akap2	Col5a1	Glyctk	Lrtm2	Pros1	Syt16	
Gpr158	Schip1	Akna	Col9a1	Gm14204	Lum	Prr5	Tenm3	
Gpr3	Scrt2	Aldh1l1	Col9a3	Gm5083	Luzp2	Prss23	Tenm4	
Grb10	Sept3	Aldoc	Cpxm2	Gm5089	Ly86	Ptpn3	Tex29	
Grin2a	Sel1l3	Alk	Crtac1	Gm5607	Lypd6	Ptprm	Thbs1	
Grin2c	Sema3d	Angpt1	Cryba4	Gm8909	Masp1	Ptpru	Thsd4	
Grm1	Sez6	Ankrd55	Csdc2	Gpr12	Mb21d2	Ptprz1	Thy1	
Grm4	Sfrp1	Ano1	Csgalnact1	Gpr153	Mcam	Pvalb	Tiam2	
Heg1	Sgsm1	Ano4	Csrnp1	Gpr26	Mcc	Pvrl1	Tmem130	
Hivep2	Sh3rf3	Apod	Csrp2	Gria1	Mdga2	Pxylp1	Tmem132b	
Hivep3	Slc25a22	Apold1	Cttnbp2	Grik3	Medag	Qpct	Tmem132c	
Hsd11b1	Slc4a4	Arap1	Cyp11a1	Grik4	Mgat5	Rab27b	Tmem132d	
Igsf10	Slc7a11	Arhgap15	Cyp26b1	Grm7	Mn1	Rab3b	Tmem176b	

Table A10: Directly regulated gene targets of NFIX from Chapter 3 (578)

Data was obtained by comparing RNA-seq in *Nfix*$^{+/+}$ and *Nfix*$^{-/-}$ in CGNPs, with ChIP-seq for NFIX binding sites, and filtering through DNaseI hypersensitive data to find genes in regions of accessible chromatin. Red = downregulated, Green = upregulated.

Epigenetic Label Count		% of binding events
Accessible	533	48.90%
Active Accessible	49	4.50%
Active Enhancer	41	3.76%
Active Promoter	14	1.28%
Active Regulatory	2	0.18%
Poised Enhancer	443	40.64%
Poised Promoter	3	0.28%
Poised Regulatory	5	0.46%
Location Count		% of binding events
Promoter	46	4.22%
Genic	583	53.49%
Distal	461	42.29%
Annotation Approach		% of binding events
NearestGene	792	72.66%
Cismapper	298	27.34%
Total Binding events	1090	
Total Genes Bound	578	

Table A11: Breakdown of NFIX ChIP-seq binding events for gene targets from Chapter 3

Analysis of histone marks using ChIP-seq reveals that a majority of NFIX binding evens are found in distal and genic regions, with only a small portion (4.22%) in the region of the promoter. For annotating binding events, a combination of NearestGene and Cismapper was used, with 1090 NFIX binding events associated with 578 gene targets. This analysis was published as part of the thesis*: "A computational analysis of transcription factor interactions and binding guided by epigenetics". Essebier, A. 2020. PhD Thesis, School of Chemistry and Molecular Biosciences, The University of Queensland .https://doi.org/10.14264/uql.2020.835.* and data is used here with permission.

Chapter 4

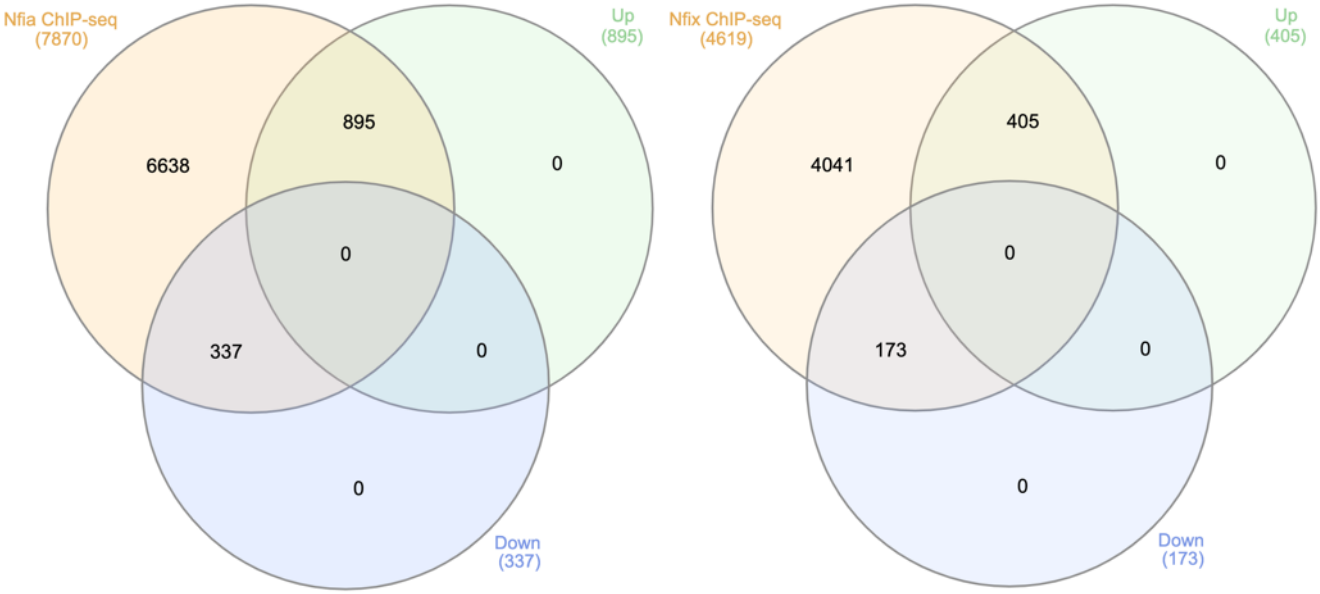

Figure A1: Venn diagrams comparing NFIA and NFIX ChIP-seq data with RNA-seq data, separated into up and downregulated genes (Chapter 3, 4).

NFIA ChIP-seq (left) found peaks associated with 7870 genes in accessible chromatin (orange), of which 1232 were identified as mis-regulated by RNA-seq in *Nfia*$^{fl/fl}$*; Math1*-Cre^{+} CGNPs compared to controls. Of these, 895 were upregulated (green) upon *Nfia* loss, and 337 were downregulated (blue). NFIX ChIP-seq (right) found peaks associated with 4619 genes in accessible chromatin (orange), of which 578 were identified as mis-regulated by RNA-seq in *Nfix*$^{-/-}$ CGNPs compared to controls. Of these, 405 were upregulated upon *Nfix* loss (green), and 173 were downregulated (blue). These data demonstrate that when NFIA or NFIX are lost, a larger proportion of genes are upregulated than are downregulated, that in normal tissue, both transcription factors function as repressors a majority of the time.

Downregulated targets		Upregulated targets					
Sept3	Neurod4	Adcy2	Chrna4	Fbxo2	Kif26a	Pcdh20	Slc35f1
Abcc8	Nfix	Adcyap1	Col26a1	Frem1	Kit	Pcsk5	Slc5a7
Adcy1	Nos1	Agtrap	Col27a1	Frmpd4	Klf15	Pcsk6	Slc6a1
Amer3	Otx2	Ak1	Col4a1	Fscn1	Lgr6	Pde1c	Slc6a11
Arpp21	Pde3a	Akap2	Col4a2	Gaa	Lhfpl3	Pde2a	Slit1
Atp2b3	Prkce	Akna	Col5a1	Galnt10	Lhpp	Pdgfa	Smad3
Barhl2	Rbfox3	Aldh1l1	Col9a3	Gas6	Lhx5	Pdgfc	Smoc1
Car10	Rimkla	Aldoc	Cpxm2	Glyctk	Lifr	Pdzd2	Sorcs1
Celf4	Rims1	Alk	Crtac1	Gm5607	Limch1	Pdzrn4	Sorcs2
Cerkl	Samd12	Angpt1	Csdc2	Gpr153	Lix1l	Pkdcc	Sowaha
Cntn2	Scrt2	Ano1	Cttnbp2	Gpr26	Loxl1	Pla2g5	Spats2l
D430041D05Rik	Sema3d	Apod	Cyp26b1	Gria1	Lpar1	Plat	Sybu
D630010B17Rik	Sez6	Arap1	Dab1	Grik3	Lrtm2	Plxna4	Syt13
Exph5	Sfrp1	Arl4a	Dhrs3	Grik4	Lum	Prdm13	Tenm4
Fat2	Sh3rf3	Asap1	Dkk3	Grm7	Luzp2	Prss23	Thbs1
Foxo6	Snap25	Ass1	Dlc1	Gsg1l	Masp1	Ptpn3	Thsd4
Gabra2	Sowahb	Atp13a4	Dnm3	Hdac11	Mcc	Ptprm	Thy1
Galr1	Spata13	Atp2b4	Dpp6	Hhip	Mn1	Ptprz1	Tmem132b
Grm1	Sphkap	B3gat1	Dpysl4	Hpca	Mxra7	Pvalb	Tmem132c
Grm4	Srcin1	Bcan	Dtx4	Hspa12a	Ncam2	Pxylp1	Tmem176b
Heg1	Syt9	Bcas1	Dync1i1	Icmt	Nckap5	Qpct	Tmem200a
Hivep3	Tenm1	Begain	Ebf2	Ier5	Nell1	Rab27b	Tnc
Igsf10	Tgfb2	Bmper	Egln3	Igfbp2	Ngfr	Rfx4	Tsc22d4
Il16	Tle2	Btbd11	Elk3	Il17rd	Nhlrc4	Rgs3	Tspan11
Jph4	Tmprss13	Cacna2d2	Emp1	Ildr2	Notch3	Rgs4	Tspan9
Kcna1	Unc5b	Cacng4	Enpp1	Iqsec1	Nptx1	Rhoj	Txlnb
Kcnj11	Vat1l	Calcrl	Epha4	Irx1	Ntng2	Robo1	Vim
Kcnk1	Zfpm2	Camk2n1	Epha5	Islr	Nuak2	Ryr3	Vit
Kcnq5	A730017C20Rik	Cartpt	Epha8	Itgb5	Ogdhl	Sall1	Wnt5a
Kcns2	Abcb6	Cbln4	Esrrg	Kalrn	Optc	Scml4	Wnt7b
Klf9	Abcb9	Cd44	Ets1	Kank4	Osbpl5	Scn3a	Zfp618
Lrrtm3	Ackr3	Cd93	Etv5	Kcna6	P4ha2	Scube2	
Map3k5	Acot7	Cdh11	Fam20c	Kcnb1	Pam	Serinc5	
Mpp3	Adamts1	Cdh20	Fat4	Kcnn3	Paqr8	Serpine2	
Mtss1	Adamts14	Cdkn1c	Fbln1	Kcnv1	Pax3	Sh3pxd2a	
Neurod1	Adarb2	Chl1	Fbln2	Kctd14	Pcdh15	Sik1	

Table A12: Co-ordinately regulated gene targets by NFIA and NFIX from Chapter 4

Data was obtained by combining RNA-seq in *Nfix*$^{-/-}$ and *Nfia*$^{fl/fl}$*;Math1*-Cre CGNPs, ChIP-seq for NFIA and NFIX, and filtering through DNaseI hypersensitive data to find genes in regions of accessible chromatin. Red = downregulated, Green = upregulated.

Common regulatory targets of NFIA, NFIX and NFIB during postnatal cerebellar development.

James Fraser[1,*], Alexandra Essebier[2,*], Alexander S. Brown[5], Raul Ayala Davila[1], Danyon Harkins[1], Oressia Zalucki[1], Lauren P. Shapiro[6], Peter Penzes[6], Brandon J. Wainwright[3], Matthew P. Scott[5], Richard M. Gronostajski[7], Mikael Bodén[2], Michael Piper[1,4,#] and Tracey J. Harvey[1,#]

[1]The School of Biomedical Sciences, [2]The School of Chemistry and Molecular Bioscience [3]Institute for Molecular Bioscience and [4]Queensland Brain Institute, The University of Queensland, Brisbane, 4072, Australia.

[5]Department of Developmental Biology, Stanford University School of Medicine, Stanford, CA, USA

[6]Department of Physiology, Northwestern University Feinberg School of Medicine, Chicago, IL, USA

[7]Department of Biochemistry, Program in Genetics, Genomics and Bioinformatics, Center of Excellence in Bioinformatics and Life Sciences, State University of New York at Buffalo, Buffalo, NY, USA

[Ψ] Authors for correspondence: Michael Piper
Email: m.piper@uq.edu.au
Tracey Harvey
Email: t.harvey1@uq.edu.au

[*, #] These authors contributed equally to this work.

Conflict of interest: None

Abstract

Transcriptional regulation plays a central role in controlling neural stem and progenitor cell proliferation and differentiation during neurogenesis. For instance, transcription factors from the nuclear factor I (NFI) family have been shown to co-ordinate neural stem and progenitor cell differentiation within multiple regions of the embryonic nervous system, including the neocortex, hippocampus, spinal cord and cerebellum. Knockout of individual *Nfi* genes culminates in similar phenotypes, suggestive of common target genes for these transcription factors. However, whether or not the NFI family regulate common suites of genes remains poorly defined. Here, we use granule neuron precursor cells (GNPs) of the postnatal murine cerebellum as a model system to analyse regulatory targets of three members of the NFI family; NFIA, NFIB and NFIX. By integrating transcriptomic profiling (RNA-seq) of *Nfia*- and *Nfix*-deficient GNPs with epigenomic profiling (ChIP-seq against NFIA, NFIB and NFIX, and DNase I hypersensitivity assays), we reveal that these transcription factors share a large set of potential transcriptional targets, suggestive of complementary roles for these NFI family members in promoting neural development.

Key words

NFIX, NFIA, NFIB, cerebellum, external granular layer, granule neuron.

Introduction

Transcription factors are integral to nervous system development, orchestrating a broad range of processes including cell proliferation, migration, differentiation, and maturation. The nuclear factor I (NFI) family of transcription factors (NFIA, NFIB, NFIC and NFIX) mediate several of these processes in the developing rodent nervous system [1-3]. For example, during embryogenesis, NFIs regulate cellular proliferation and differentiation in the neocortex, hippocampus, spinal cord and cerebellum [4-12]. Given these key roles of NFIs in the developing nervous system, it is perhaps unsurprising that their expression is highly overlapping. Indeed, NFIs are expressed by a broad range of cell types in the developing central nervous system, including radial glia, intermediate progenitors and neurons [3,13-16]. In the developing cerebellum, NFIA, NFIB and NFIX are expressed by GNPs at postnatal day (P) 6 [3]. Thus, the expression of NFIs across key cellular populations, and within multiple brain regions, enables these transcription factors to coordinate nervous system development.

The role of the NFIs in nervous system development is also evident through the analysis of knockout mouse models. The phenotypes of *Nfi* knockout mice are markedly similar. For example, neuroanatomical defects are evident in *Nfia*, *Nfib* and *Nfix* knockout mice, including aberrant development of the corpus callosum and hippocampus [8,10,13,17,18]. Midline glial populations also fail to develop correctly in *Nfia*, *Nfib* and *Nfix* knockout mice [13,17,18], reflecting altered astrocytic development. Indeed, with regards to the development of the neocortex and hippocampus, mice lacking *Nfia*, *Nfib* and *Nfix* show delayed differentiation of radial glial stem cells into mature neurons and glia [8-10,19], in part due to delayed generation of intermediate progenitor cells [7]. In the cerebellum, NFIX was recently shown to promote GNP differentiation [20], and, while the role of other NFI family members in GNP biology is unclear, the expression of NFIA and NFIB by GNPs at P6 [3] is indicative of a role in regulating GNP differentiation. Moreover, NFIs have been shown to bind to the same DNA recognition motif [21]. Collectively, these data suggest that these transcription factors regulate the expression of similar cohorts of genes.

Despite much work outlining the expression and proposed function of NFIs in brain development, whether NFI family members actually regulate similar gene targets is poorly defined. To date, there has been one published report highlighting overlapping NFIA and NFIB gene targets in the developing forebrain [22]. This analysis, whilst insightful, did not include epigenomic data to refine potential gene targets and was performed on a heterogeneous population of cells. We therefore sought to overcome these limitations, and examined if NFIs regulate similar gene targets using the developing cerebellum as a model system. In the rodent brain, cerebellar development begins at

approximately embryonic day (E) 12, when ATOH1-expressing granule neuron precursors (GNPs) are generated in the rhombic lip [23]. These GNPs then proliferate and migrate tangentially, forming a transient germinal zone called the external granule layer (EGL) [23-25]. Cerebellar development continues postnatally, with GNPs proliferating and differentiating into immature neurons, which ultimately migrate radially through the molecular layer, becoming mature granule cells within the internal granule layer (IGL) of the cerebellum [26]. Whilst NFIA, NFIB and NFIX are expressed in GNPs [3] it remains an open question whether or not the NFIs are co-expressed in these cells. Moreover, it is unclear whether these transcription factors share any common gene targets during cerebellar development. Here, we reveal co-expression of the NFI transcription factor family within GNPs of the EGL. Moreover, using a combination of transcriptomic and epigenomic profiling, we reveal that a significant proportion of potential target genes are common between the NFI family members, highlighting the functional complementarity within this group of transcription factors.

Materials and methods

Animals

All the mice used in this study were maintained on a C57Bl/6 background. *Nfia* null mice on this genetic background are embryonic lethal. As such, we used a conditional *Nfia* allele ($Nfia^{fl/fl}$) crossed to a *Atoh1 cre* line [27]. This line enabled the ablation of *Nfia* from ATOH1-expressing cells from embryonic day (9) [25] including the cells of the rhombic lip, that will ultimately give rise to GNPs within the EGL of the postnatal cerebellum. Knockout animals were $Nfia^{fl/fl}$; *Atoh1-cre*$^{+}$; controls were $Nfia^{fl/fl}$; *Atoh1-cre*$^{-}$. Animals were used with approval from the University of Queensland Animal Ethics Committee (AEC approval numbers: QBI/143/16/NHMRC/ARC and QBI/149/16/ARC). Animals were genotyped by PCR; primer sequences are available on request. All experiments were performed according to the Australian Code of Practice for the Care and Use of Animals for Scientific Purposes. Pregnant females were acquired by placing male and female mice together overnight. The next day, females were inspected for the presence of a vaginal plug and, if present, this day was designated as E0. The day of birth was designated as postnatal day (P) 0. Mice were housed in Optimice IVC caging, with double HEPA filters and built in ventilation. Food and water was available *ad libitum*, and materials were provided for nesting and enrichment.

Immunohistochemistry

To analyze the cell-type specific expression of NFIA, NFIB and NFIX, we performed co-immunofluorescence labelling, as described previously [14]. Briefly, postnatal mice at P3, P7 or P15 were anesthetized with pentobarbital and perfused transcardially with phosphate-buffered saline (PBS), followed by 4% paraformaldehyde, then post-fixed for 48-72 hours before long term storage in PBS at 4°C. Cerebella were isolated and embedded in Noble agar (3%) and sectioned (50 μm) in a sagittal plane using a vibratome. Sections were placed sequentially across the wells of a 6-well plate to ensure appropriate sampling from different medio-lateral regions of the cerebellum. Sections were mounted on SuperFrost Plus (Thermo Scientific) slides, before heat-mediated antigen retrieval was performed in 10 mM sodium-citrate solution (pH 6.0) at 95°C for 15 min. Sections were blocked for 2 hours in a solution containing 2% serum and 0.2% Triton-X-100 in PBS. Sections were then incubated overnight at 4°C with primary antibodies against the target proteins (Table 1). Subsequently, sections were rinsed in PBS, then incubated with the relevant secondary antibodies (Table 1) for 2 hours in the dark at room temperature. Sections were rinsed in PBS, then were counterstained with 4',6-diamidino-2-phenylindole (DAPI), and mounted in fluorescent mounting media (DAKO). For all experiments, at least three animals at each age were analyzed.

Cerebellar imaging

Fluorescent immunolabelling was visualized using a Nikon 20x Air objective on a spinning disk confocal microscope (Diskovery; Andor Technology, UK) on a Nikon Ti-E body (Nikon Corporation, Japan), equipped with a Zyla 4.2 10-tap sCMOS camera (Andor Technologies). For comparative sections identical imaging parameters were used including pinhole size (70 μm), laser power and exposure time. We took 10 consecutive 1 μm-thick optical sections to generate a 10 μm-thick z-stack. In all cases the 10 μm z-stack was taken from the middle of the section to minimize potential artefacts arising from the sectioning process such as damage to the tissue. Image acquisition, tiling and stitching was performed using NIS-elements Advanced Research Imaging Software (Nikon Corporation, Japan). All brightfield images were captured using a Aperio ScanScope XT Slide scanner (Leica Biosystems, Germany) with a doubled 20x objective (40x magnification overall, Nikon Corporation, Japan) and visualized using Aperio ImageScope software.

For analysis of wildtype, *Nfia*$^{fl/fl}$; *Atoh1 Cre*$^{+}$ and *Nfia*$^{fl/fl}$; *Atoh1 Cre*$^{-}$ mice, high magnification images were taken of the same lobule of the cerebellum, using at least three biological replicates at each of the ages assessed. For quantification of granule neuron and proliferative markers (PAX6 and Ki67, respectively), three 200 μm regions of the EGL were quantified for each section. This ensured more representative count of the EGL thickness across the whole lobule. 1 μm-thick optical sections were viewed in Fiji, and the 'cell counter' plugin used to mark and quantify cells expressing respective markers in each fluorescent channel. Cells co-expressing markers (for example PAX6 and Ki67) were also quantified this way, and DAPI was used to visualize the cell nucleus, to ensure accuracy, especially in areas of high cell density.

Granule cell isolation

To isolate GNPs from the cerebellum of P7 *Nfix*$^{+/+}$ and *Nfix*$^{-/-}$ mice, and of P7 *Nfia*$^{fl/fl}$*; Atoh cre*$^{+}$ and *Nfia*$^{fl/fl}$*; Atoh cre*$^{-}$ mice, we used a technique originally described by Lee and colleagues [28]. To do this, we isolated the cerebellum from wild-type and knockout mice, carefully removing the choroid plexus and meningeal tissue. Cerebellar tissue was dissociated using a 20 units/mL papain solution at 37°C for 15 mins. A single cell suspension was obtained by trituration with a serum-coated P1000 pipette tip and nuclear membranes were removed using an albumin-ovomucoid inhibitor gradient. GNPs were separated from other cells using a 30%-60% percoll gradient. GNPs were lysed using Trizol (Ambion). We next used an RNeasy miniprep kit (Qiagen) to isolate RNA from lyzed GNPs.

RNA-seq analysis

RNA-sequencing was performed on the samples using the Illumina NextSeq High Output system (Illumina; 150 base pair read length, paired-end reads). We isolated cells from three P7 *Nfia*$^{fl/fl}$*; Atoh cre*$^{-}$ mice and three P7 *Nfia*$^{fl/fl}$*; Atoh cre*$^{+}$ mice. RNA-seq analysis was performed on RNA isolated from P7 cerebella as described previously. Briefly, the three replicates for each cohort were aligned by TopHat2 (v2.0.9) [29] to the *Mus musculus*, UCSC, mm10 reference transcriptome and FASTA annotation downloaded from the TopHat index and annotations page (https://ccb.jhu.edu/software/tophat/igenomes.shtml). Cufflinks (v2.1.1) [29] was used to assemble each replicate's transcripts from the alignment file generated by TopHat. Cuffmerge was used to create a single assembly containing transcripts across all samples and replicates. Cuffdiff was run using the merged set of transcripts and the three replicate TopHat2 bam files from each sample.

ChIP-seq

ChIP-seq was performed on chromatin isolated from P7 wild-type C57Bl/6 GNPs as described [20]. We used antibodies against NFIA, NFIB or NFIX, for which specificity has previously been demonstrated [30]. For chromatin immunoprecipitation, litters of P7 pups were pooled for GNP isolation. Isolated GNPs were crosslinked with 1% formaldehyde for 10 minutes, then were quenched with glycine. Cells were lyzed in RIPA buffer supplemented with protease and phosphatase inhibitors (Roche) and sonicated with a Bioruptor (Diagenode) for six 15 minute intervals of 30 seconds on, 30 seconds rest. Chromatin immunocomplexes were isolated with protein G-agarose beads (Roche), washed once for 5 minutes with buffers 1 through 4. Crosslinking was reversed by incubation with proteinase K (Roche) at 60 degrees overnight. DNA was isolated by phenol-chloroform extraction then incubated with RNAse A (Roche) for 30 minutes before final cleanup with PCR columns (Qiagen). Sequencing libraries were constructed using the standard protocol for the NEB Next Ultra II DNA Library Prep Kit (New England BioLabs). Pooled libraries were sequenced on an Illumina HiSeq2000 (Illumina; 30 base pair single end read).

ChIP-seq analysis

Alignment was performed on the NFIA, NFIB and NFIX ChIP-seq data sets by bowtie2 [31] to mm10. Unaligned reads and reads which aligned to multiple locations were removed leaving only uniquely mapped reads. MACS2 [32] was used to call narrow peaks with default parameters for both datasets. Each experiment contained two biological replicates and if both biological replicates shared a peak, it was recorded using the maximum boundaries of the supporting peaks to generate a merged set of peaks for each experiment.

Annotation of ChIP-seq peaks

A set of target genes was identified for NFIA, NFIB and NFIX by the following method. A promoter region was defined as 2,000 base pairs either side of a transcription start site. ChIP-seq binding sites located in a promoter region were annotated as *proximal*, while sites outside the promoter region but overlapping gene boundaries (transcription start to stop site) were labelled as *genic*. All remaining binding sites were labelled as *distal*. A binding site annotated as proximal was assigned to the nearest gene as a target while genic binding sites were assigned to the overlapping gene as a target. Distal binding sites are difficult to assign target genes to, as they are not necessarily regulating the nearest gene (by genomic distance) and proximal and genic sites are also capable of regulating a gene other than the nearest. While distal binding sites were also annotated to the nearest gene, where available, CisMapper was used to provide a secondary annotation to all sites, with resulting links filtered to a threshold of 0.05 [33]. Both the CisMapper annotation and nearest gene annotation were used where available.

After identifying a gene target for each NFI binding site; the associated *p*-value from both the *Nfix* and *Nfia* RNA-seq differential expression analyses was recorded. Genes targeted by both NFIX and NFIA with a significant ($p < 0.05$) change in expression in both experiments were extracted. Genes showing coordinated positive or negative log fold change values across both experiments were selected to generate a putative set of genes under the control of NFIX and NFIA. Functional annotation was performed using DAVID (6.8) on target genes identified for NFIX, target genes identified for NFIA and target genes under the control of both NFIX and NFIA [34,35].

DNase I hypersensitivity analysis

The DNase I hypersensitivity (DHS) data from Frank et al. 2015 (GEO: GSE60731) [36] was accessed for comparison to our transcriptomic and epigenomic profiling. These data contain called peaks from whole cerebellar tissue at P7 across three replicates. UCSC liftover was used to convert the mm9 files to mm10. Maximum boundaries of the supporting peaks were used to generate a merged DHS peak file, with the stipulation that peaks need to be shared by at least two replicates. Given that transcription factors preferentially bind to regions of accessible chromatin [37,38], DHS was used to extract NFI ChIP-seq peaks occurring in accessible regions.

qPCR analysis of target genes

RNA isolated from P7 GNPs from the cerebella of *Nfix*$^{+/+}$, *Nfix*$^{-/-}$, *Nfia*$^{fl/fl}$*; Atoh cre*$^{-}$ or *Nfia*$^{fl/fl}$*; Atoh cre*$^{+}$ mice was used to prepare cDNA as described previously [9]. qPCR was performed with

Quantifast SYBR Green (Qiagen) to detect gene expression levels of the genes identified in the RNA-seq analysis. The primers for these genes are listed in Table 2. Gene expression was calculated using the $2^{-\Delta\Delta Ct}$ method relative to the housekeeping gene *glyceraldehyde 3-phosphate dehydrogenase* (*Gapdh*). All the samples were tested in triplicate within each experiment, and each experiment was repeated three times. qPCR was run using the QuantStudio 7 Flex Real-Time PCR system (Applied Biosystems, USA).

Results

NFIA and NFIX are co-expressed in the developing cerebellum

NFI transcription factors are expressed across the developing and adult central nervous system. This includes the cerebellum, where NFIX is broadly expressed in the embryonic, postnatal and adult cerebellum [11,14], and where it regulates postnatal GNP differentiation [20]. NFIA is also critical for cerebellar development, and is expressed by GNPs [3,39,40]. Given the broad roles of NFI transcription factors in progenitor cell differentiation and that their protein expression overlaps in other brain regions [22,41], we first examined whether NFIA and NFIX were co-expressed in GNPs. We used co-immunofluorescence to analyse NFIX and NFIA expression across postnatal cerebellar development (P3, P7 and P15). We found that not only do GNPs in the EGL express NFIX, in agreement with our previous data [14], but we also found that these cells co-express NFIA (Fig. 1). Indeed, analysis at P7 revealed that over 90% of cells within the EGL co-expressed NFIA and NFIX at this age. Expression of *Nfi* family members is also seen within the embryonic rhombic lip (Supp. Fig. 1).

NFIX expression is also detected within astrocytes within the emerging cerebellum [14]. We also labelled sections with an antibody against the astrocytic marker s100β, and revealed that astrocytes within the IGL were immunoreactive for both NFIX and NFIA (Figs. 1 and 2). Moreover, we also found co-expression of NFIX and NFIA in Bergmann glia across these ages (Fig. 2); indeed, we observed that over 95% of s100β-expressing Bergmann glia at P15 were also immunopositive for both NFIA and NFIX. These analyses also revealed that granule neurons within the IGL also co-express NFIA and NFIX (Fig. 2). Finally, to verify the expression of NFIA in GNPs in the EGL, we performed co-immunofluorescence labelling with the progenitor cell marker, PAX6, and the proliferation marker Ki67. We found co-expression of NFIA and PAX6 within the EGL (Fig. 3A-D). Consistent with this, those proliferating cells in the EGL were also immunopositive for NFIA (Fig. 3E-H). These data suggest that NFIA, in addition to driving the development of mature cerebellar neurons [3] may also contribute to GNP proliferation and differentiation. Collectively, these data demonstrate that NFIX and NFIA expression is overlapping in the developing cerebellum, with both transcription factors expressed by GNPs within the postnatal EGL. This led us to hypothesize that these transcription factors drive GNP differentiation in the postnatal cerebellum through regulation of common target genes. We sought to address this hypothesis via co-ordinate analysis of transcriptomic and epigenomic profiling datasets.

Nfia cKO mice exhibit cerebellar abnormalities

To determine the extent of overlap in function between NFI family members in cerebellar GNPs, we first sought to define the cohort of genes potentially under direct control of NFIA. To do this, we used a number of transcriptomic and epigenomic sequencing approaches, as well as utilising published DNase I hypersensitivity analyses detailing chromatin accessibility within the whole cerebellum at P7 [36]. As *Nfia* null mice on a C57Bl/6 are embryonic lethal [17], we employed a conditional *Nfia* allele (*Nfia*$^{fl/fl}$) crossed to a *Atoh1 cre* line [27]. ATOH1 is expressed by progenitor cells within the nascent rhombic lip from E9 [25], and thus enables the removal of *Nfia* from these cells, as well as their progeny, including GNPs. We crossed the *Nfia*$^{fl/fl}$ line to the *Atoh1 cre*, and analyzed NFIA expression in GNPs within the postnatal cerebellum (P7) to validate ablation of *Nfia*. Immunolabelling with NFIA, and PAX6, revealed that NFIA expression was still present within cells at the border of the IGL (likely Bergmann glia that are not derived from *Atoh1*-expressing progenitor cells within the embryonic brain) and within the IGL (Fig. 4). However, expression of NFIA was dramatically reduced within the EGL of *Nfia*$^{fl/fl}$; *Atoh1 cre*$^{+}$ mice (hereafter referred to as *Nfia cKO* mice). Interestingly, the ablation of *Nfia* was not fully penetrant within all of the lobes of the cerebellum, with GNPs within lobe X retaining a higher percentage of NFIA expression in comparison to lobes IV-V and VIII (Fig. 4 E-G). Incomplete ablation of a conditional *Nfib* allele was recently reported [7], suggesting that some cells may escape Cre-mediated depletion when this strategy is used to ablate *Nfi* family members. Thus, the NFIA-expressing cells within the IGL of *Nfia cKO* mice likely comprise astrocytes (Fig. 2) and granule neurons derived from EGL progenitors in which *Nfia* was not deleted. Despite this caveat, these data suggest that this is a valid model in which to study the role of NFIA in GNP biology.

The role of NFIA in cerebellar development has been studied almost exclusively through the prism of the migration and maturation of postmitotic granule neurons [39,40,42]. In other regions of the nervous system, such as the developing hippocampus, *Nfia*$^{-/-}$ mice exhibit very similar phenotypes to *Nfix*$^{-/-}$ mice [8,10]. Given that a delay in the differentiation of GNPs is evident in the cerebellum of P15 *Nfix*$^{-/-}$ mice, we posited that a similar delay would be evident in *Nfia cKO* mice. We firstly analysed the gross morphology of the cerebellum in *Nfia control* and *Nfia cKO* mice. In contrast to *Nfix*$^{-/-}$ mice [20], haematoxylin staining at the level of the vermis revealed increased foliation in *Nfia cKO* mice in comparison to the controls, with lobe VI showing the clearest phenotype (Fig. 4H, I). Critically, however, PAX6 and Ki67 labelling revealed there were more PAX6-positive cells within the EGL of the mutant at this age in comparison to controls (Fig. 4J-M), although the width of the EGL was comparable between mutant and control animals at this age (Fig. 4N). These data reveal

that the retention of PAX6-expressing GNPs within the EGL is a shared phenotype between mice lacking either *Nfia* or *Nfix*.

Transcriptomic profiling in GNPs reveals common gene targets of the NFI transcription factor family

The co-expression of NFIA and NFIX (Fig. 1), coupled with the retention of GNPs within the EGL at P15 in both strains (Fig. 4; [20]) led us to posit that these transcription factors may regulate a common set of genes during GNP development. We have recently detailed transcriptomic profiling (RNA-seq) of *Nfix*$^{-/-}$ P7 GNPs, coupled with genome-wide analysis of NFIX binding (ChIP-seq; [20]). To determine the extent of shared targets between NFIA and NFIX, we repeated these analyses with NFIA. Firstly, we isolated P7 control and *Nfia cKO* GNPs, and performed RNA-seq. Analysis of these datasets revealed 2,267 genes as being significantly misregulated in the absence of *Nfia* (Fig. 5A; Supp. Table 1). Profiling of these data using the Gene Ontology and Pathway tool in DAVID [34,35] revealed a suite of different biological processes (e.g. cell adhesion; nervous system development), cellular components (e.g. membrane; proteinaceous extracelluar matrix) and molecular functions (e.g. calcium ion binding; integrin binding) (Fig. 5B; Supp. Table 2).

To begin to refine this potential list of NFIA target genes, we performed ChIP-seq with an NFIA-specific antibody [30], using GNPs isolated from wildtype P7 cerebella. This profiling identified 14,025 NFIA binding peaks (Supp. Table 3). Cross correlation of these data with published chromatin accessibility data (DNase I hypersensitivity analysis) from P7 cerebellum [36] revealed that 12,539 of these NFIA binding peaks were in accessible regions of chromatin, whereas 1,486 were in closed regions of chromatin (Fig. 5C). Interestingly, the 12,539 NFIA ChIP-seq peaks in regions of accessible chromatin correlated to 7,870 NFIA-bound genes. When we took this cohort of 7,870 genes and compared it to the list of differentially regulated genes within *Nfia cKO* GNPs (Fig. 5A), we determined that 1,232 of the 2,267 genes that were significantly misregulated also contained a NFIA ChIP binding peak (Fig. 5D, Supp. Table 4), highlighting them as strong candidates for direct regulation by NFIA. Critically, DAVID analysis on this NFIA targetome of 1,232 genes identified many processes and functions previously identified in our analysis of *Nfix*-deficient GNPs [20], including many associated with neural function (e.g. axon guidance; neuronal cell body; cell adhesion; Fig. 5D; Supp. Table 2), indicative of potential shared functions of these transcription factors.

Finally, to define whether or not NFIA and NFIX regulate a common cohort of genes, we compared our refined NFIA targetome (1,232 targets; Fig. 5) with an analysis performed the same way but

targeting NFIX (578 targets; [20]). This analysis revealed that 304 genes were high-confidence targets for both NFIA and NFIX in P7 GNPs, and, moreover, that more than 93% of these (283 out of 304) were co-ordinately regulated by both NFIA and NFIX (i.e. gene was downregulated in both *Nfia cKO* and *Nfix*$^{-/-}$ datasets, or upregulated in both; Fig. 6, Supp. Table 5).

NFIB is also expressed by NFIX-expressing GNPs within the postnatal cerebellum (Supp. Fig. 1; [3]). Although we did not have access to the conditional strain crossed to a cerebellum-specific driver, we were able to gain insight into potential NFIB targets by performing ChIP-seq on isolated P7 GNPs using a specific NFIB antibody [30]. This analysis identified 24,950 NFIB ChIP-seq peaks (Supp. Table 3), of which 21,712 were in regions of accessible chromatin. Comparison of the accessible binding sites in each of the three NFI ChIP-seq datasets revealed that, of the 22,129 sites where at least one of NFIA, NFIB of NFIX had a binding event associated with it, ~25% were bound by all three of these transcription factors (Supp. Fig. 3). Furthermore, over 55% of sites were bound by two of the NFI family (Supp. Fig. 3). Importantly, when we overlaid our NFIB ChIP-seq results onto our combined NFIA/NFIX targetome (Fig. 6A), the analysis that revealed that 282 of the 283 co-ordinately regulated NFIA/NFIX targets genes also possessed an associated NFIB ChIP-seq peak. DAVID analysis revealed that categories enriched in this dataset included axon, neuron projection, neuronal cell body and nervous system development (Fig. 6B). This cohort of genes potentially targeted by NFIA, NFIB and NFIX included a number of genes known to mediate cerebellar development, including *Otx2, Epha4* and *Nfix* itself, as well as a number of factors whose role in cerebellar genesis is novel (Fig. 6C). Analysis of the proportion of NFI ChIP-seq peaks in proximal, genic or distal locations revealed that the majority of binding sites were in distal or genic locations (Fig. 6D). Finally, we validated six of these misregulated genes using qPCR, focussing on a mix of genes with known (*Wnt5a*) and novel (*Kalrn, FoxO6, Id3, Gas6* and *Etv5*) roles in cerebellar development. We confirmed that the levels of *Kalrn, Wnt5a, FoxO6, Id3, Gas6* and *Etv5* mRNAs were significantly higher in both *Nfia*$^{-/-}$ and *Nfix*$^{-/-}$ GNPs at P7 (Fig. 6E-J).

Discussion

The NFI proteins are transcription factors that exhibit conserved N-terminal DNA-binding domains, as well as a common DNA recognition motif [43]. Within the nascent mouse nervous system, neural stem and progenitor populations have been shown to co-express individual NFI family members [1], and, moreover, individual *Nfi* knockout mice exhibit broadly similar cortical phenotypes [4,8,10,12]. However, the extent to which these factors share common regulatory targets has not been investigated thoroughly, apart from a recent study that used RNA-seq in developing cortical tissue from both *Nfia*$^{-/-}$ and *Nfib*$^{-/-}$ mice to investigate potential overlap in gene regulation [30]. Here, we use a range of transcriptomic approaches to more clearly demarcate common targets of the broader NFI family, demonstrating that NFIA, NFIB and NFIX likely regulate a common suite of genes to promote the differentiation of GNPs within the postnatal cerebellum.

A coherent theme emerging from many of the studies on NFI function is their role in promoting differentiation and maturation. Within the cerebellum, NFIX is required for the timely differentiation of GNPs within the postnatal EGL [20], and NFIA has been reported to regulate a program of gene expression required for the migration and maturation of granule neurons [3,39,42]. Within the broader central nervous system, NFIB has also been shown to regulate neural stem cell differentiation within the cerebral cortex [5], a function also reported for NFIA and NFIX [44]. Outside the nervous system, NFIs have also been shown to regulate differentiation; for instance, NFIX has been shown to contribute to skeletal myogenesis by promoting a switch from embryonic to fetal-specific gene programs [45,46]. In line with this, our transcriptomic analyses suggest that the NFI family are key mediators of GNP differentiation within the postnatal cerebellum. Indeed, our DAVID analysis of the 282 genes we identified as potential NFI targets included a high proportion of terms associated with the nervous system (Supp. Table 2). For instance, of the 20 most enriched terms for Cellular Component in the DAVID analysis, 10 were directly associated with the nervous system (e.g. Neuron projection, Axon, Dendrite, Neuronal cell body), with a further seven associated with the plasma membrane and extracellular matrix, both of which are central to mature neural biology. These data reinforce the role for NFIs in promoting neural differentiation within the cerebellum.

The targetome identified for the NFI family within postnatal GNPs includes a number of specific factors that highlights their role in promoting differentiation. For example, *Wnt5a*, a factor known to regulate neural progenitor proliferation within the cerebellum [47], is upregulated in the absence of either *Nfia* or *Nfix*, consistent with the phenotype for delayed GNP differentiation in these strains. Conversely, factors known to promote neural differentiation, such as *Neurod1, Neurod4* and *Nfix* were reduced, as was the neuronal marker *Rbfox3*. In addition to these individual factors identified as

likely targets of co-regulation by the NFI family, a novel theme to arise from this multi-faceted analysis was that NFIs may regulate cohorts of genes related to similar processes. For example, within the NFI targetome we identified 6 collagen genes, 13 genes encoding potassium channel or glutamate receptor subunits, and a range of factors related to axon guidance (e.g. *Slit1, Robo1, Epha4, Epha5, Epha8*). These findings may point to previously unrecognised roles for the NFI family. For example, NFIs are widely expressed in neurons [30], but their role in these cells is unknown. The identification of potassium channel and glutamate receptor subunit genes in our target list suggests that NFIs may contribute to the process of neurotransmission. Looking forwards, more sophisticated approaches using multiple conditional *Nfi* alleles crossed to cell-type specific drivers (e.g. *CamK2a CreERT2*) may enable the role of the NFI family in specific functions such as neurotransmission to be investigated.

Our approach to determine shared NFI target genes also highlighted a number of other interesting elements of NFI biology whose significance has not been previously appreciated. For example, partitioning of reported ChIP-seq peaks for each of NFIA, NFIB and NFIX into defined regions (proximal, genic or distal) revealed that only 3-6% of binding peaks were in proximal regions (defined as ± 2000 base pairs from a transcriptional start site), whereas approximately 44% were found in genic regions (sites outside the promoter regions but overlapping gene boundaries), with the remaining ~50% of ChIP-seq peaks within distal regions. This implicates a large portion of NFI binding may be related to interactions with distal enhancers. The role of NFIs in distal binding is at this stage unclear, but a recent report of NFIB mediating chromatin accessibility in small cell lung cancer [48] may point to this family playing a much broader role in transcriptional architecture than regulating promoter activity. In future, the role of NFIs in mediating enhancer activity could be investigated using techniques including luciferase assays, whereas chromatin interaction analysis by paired-end tag sequencing (ChIA-PET) could be used to interrogate the role of NFIs in mediating long-range chromatin interactions *in vivo*. Our findings also suggest that numerous NFI binding sites can be found in regions of closed chromatin. Exactly what this means is, at this stage, unclear, but the possibility of the NFIs acting to promote chromatin accessibility in a developmental context, in addition to that seen in small cell lung cancer [48], is a tantalising possibility. One way in which could be analysed would be to combine ChIP-seq on GNPs at different developmental stages with DNase I hypersensitivity analyses at the same age. From this, the capacity of NFIs to bind to, and potentially open, regions of previously compressed chromatin, could be ascertained.

Our analyses also raise a number of questions. For instance, our analysis revealed a high proportion of ChIP-seq peaks that were common between NFIA, NFIB and NFIX. One interpretation of this

could be that the NFI proteins promiscuously form heterodimers to bind DNA. Although heterodimerization of the NFIs has long been known to occur *in vitro* [49], its prevalence *in vivo* is less clear. NFIA and NFIB were recently reported to co-immunoprecipitate in lysates from embryonic day 13 mouse cerebral cortical tissue [22]; our data suggest that heterodimerization between NFIA, NFIB and NFIX may be a common theme in the way this family regulates development, a theory supported by the similar neural phenotypes observed following knockout of individual *Nfi* genes [4,8,10]. Despite this, our analyses revealed that the role of *Nfia* and *Nfix* may not be entirely overlapping. Indeed, there were a number of genes identified as NFIA targets that were not identified as NFIX targets (Fig. 6A). Although care needs to be taken when interpreting the differences in our targetomes, as experimental conditions may underlie this (e.g. variations in antibody affinity for ChIP-seq), the fact that the *Nfia cKO* mutant cerebellum exhibited increased foliation (Fig. 4I), whereas the *Nfix* mutant does not [20], provides a morphological indication of some distinct functions between these transcription factors. Potential differences in the targets of NFIA and NFIX (and, potentially, NFIB) could relate to the capacity of different family members to bid to co-factors. The C-terminal region of each family member is less well conserved [43], indicative of potentially different affinity for protein-binding partners. There is surprisingly little known regarding other proteins that the NFIs interact with. One recent study performed in HEK298T cells used tandem affinity purification followed by mass spectrometry to reveal an interaction between NFIX and CREB1 [50] In future, the use of sophisticated approaches like this, in conjunction with specific cellular populations like GNPs, could be ways in which proteins that interact with NFIs could be identified. In conclusion, our study has enhanced our understanding of neural development specifically, and NFI biology more broadly, using molecular and transcriptomic assays to reveal that the NFI family share a large number of targets during the differentiation of the postnatal cerebellum.

Acknowledgements

This work was supported by Australian Research Council grants (DP160100368, DP180100017 to MP) and NYSTEM grants (CO30133 and C30290GG to RMG). JF and AE were supported by Research Training Program scholarships from the Australian Government. ASB was supported by Ruth L. Kirschstein NRSA F32 GM105227. Imaging was carried out in The School of Biomedical Sciences Microscopy and Imaging Facility. We thank the facility manager, Dr. Shaun Walters, for his assistance.

Tables

Antibody	*Source species*	*Company*	*Catalogue number*	*Dilution used*
NFIX	Mouse	Sigma-Aldrich	SAB1401263	1/200
NFIA	Rabbit	Sigma-Aldrich	HPA008884	1/400
NFIB	Rabbit	Sigma-Aldrich	HPA003956	1/400
S100β-Alexa647	Rabbit	ABCAM	AB196175	1/400
PAX6	Rabbit	DAKO	Z0334	1/400
Ki67	Mouse	BD Pharmigen	550609	1/400

Table 1: Antibodies used in this study.

Gene	*Forward*	*Rev*
Id3	CTGTCGGAACGTAGCCTGG	GTGGTTCATGTCGTCCAAGAG
Wnt5a	CAACTGGCAGGACTTTCTCAA	CCTTCTCCAATGTACTGCATGTG
Gas6	GACCCCGAGACGGAGTATTTC	TGCACTGGTCAGGCAAGTTC
Kalrn	AAGACCTACGGAAACTTGTGACG	CCCCGCATGTCGATGATGAC
Etv5	TCAGTCTGATAACTTGGTGCTTC	CTACAGGACGACAACTCGGAG
FoxO6	TCATGGACAGTGACGAAATGG	ACCCAGCTCTGGTTAGGGG
Gapdh	GCACAGTCAAGGCCGAGAAT	GCCTTCTCCATGGTGGTGAA

Table 2: qPCR primers used in this study.

Figures

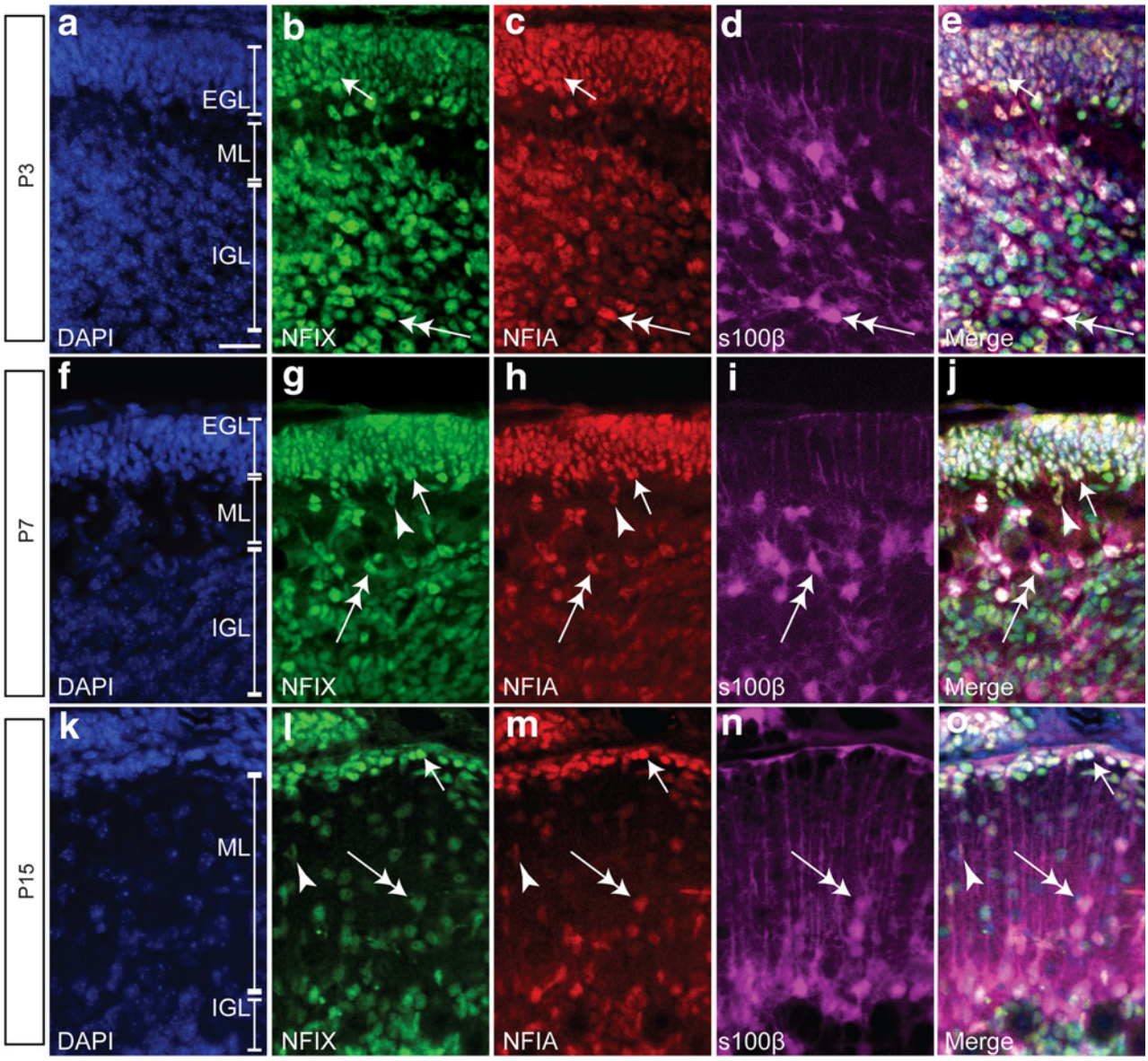

Figure 1. NFIX and NFIA are co-expressed by various cellular populations in the developing mouse postnatal cerebellum.

Sagittal cerebellar sections showing the nuclear marker DAPI (blue), NFIX (green), NFIA (red) and s100β expression (magenta) in P3 (A-E), P7 (F-J) and P15 (K-O) wild-type mice. NFIX and NFIA are co-expressed by GNPs within the external granule layer (EGL; arrows in B-E, G-J, L-O). NFIX and NFIA are also co-expressed by s100β-positive glial cells (double-headed arrows in B-E, G-J, L-O). These transcription factors are also expressed by cells leaving the EGL (arrowheads in G-J, L-O); these are likely immature neurons migrating to the internal granule layer (IGL). ML = molecular layer. Scale bar (in A): 20 μm.

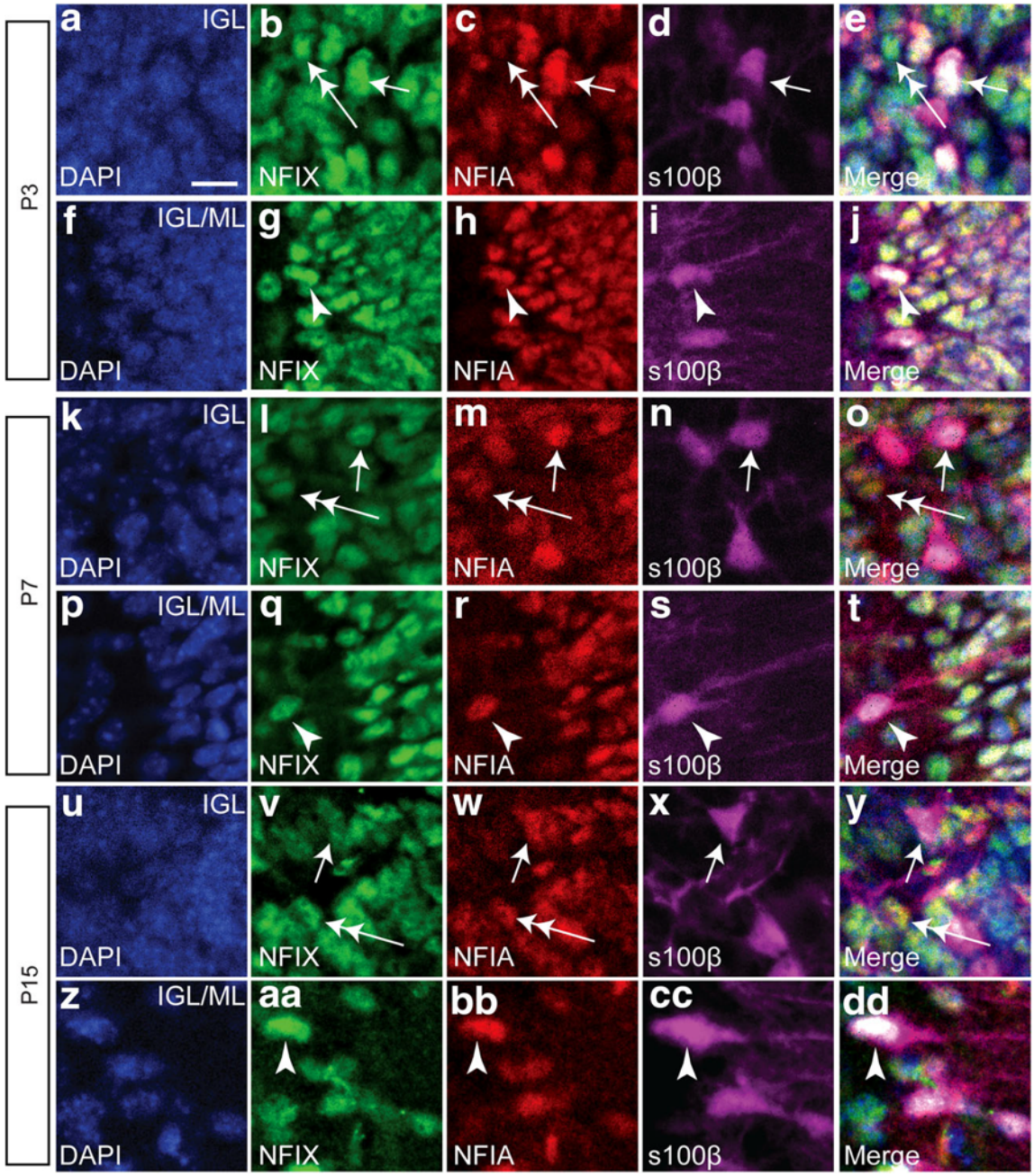

Figure 2. NFIX and NFIA are co-expressed in Bergmann glia and astrocytes in the developing cerebellum.

High magnification sagittal cerebellar sections showing the nuclear marker DAPI (blue), NFIX (green), NFIA (red) and s100β expression (magenta) in P3 (A-J), P7 (K-T) and P15 (U-DD) wild-type mice. NFIX and NFIA are co-expressed in IGL white matter astrocytes at these ages (arrows in B-D, L-O, V-Y). NFIX and NFIA are also co-expressed in Bergmann glia at P3, P7 and P15 (arrowheads in G-J, Q-T, AA-DD). The NFI factors are also co-expressed in mature granule neurons within the IGL (double-headed arrows in B-D, L-O, V-Y). IGL = inner granule layer, ML = molecular layer. Scale bar (in A): 10 μm.

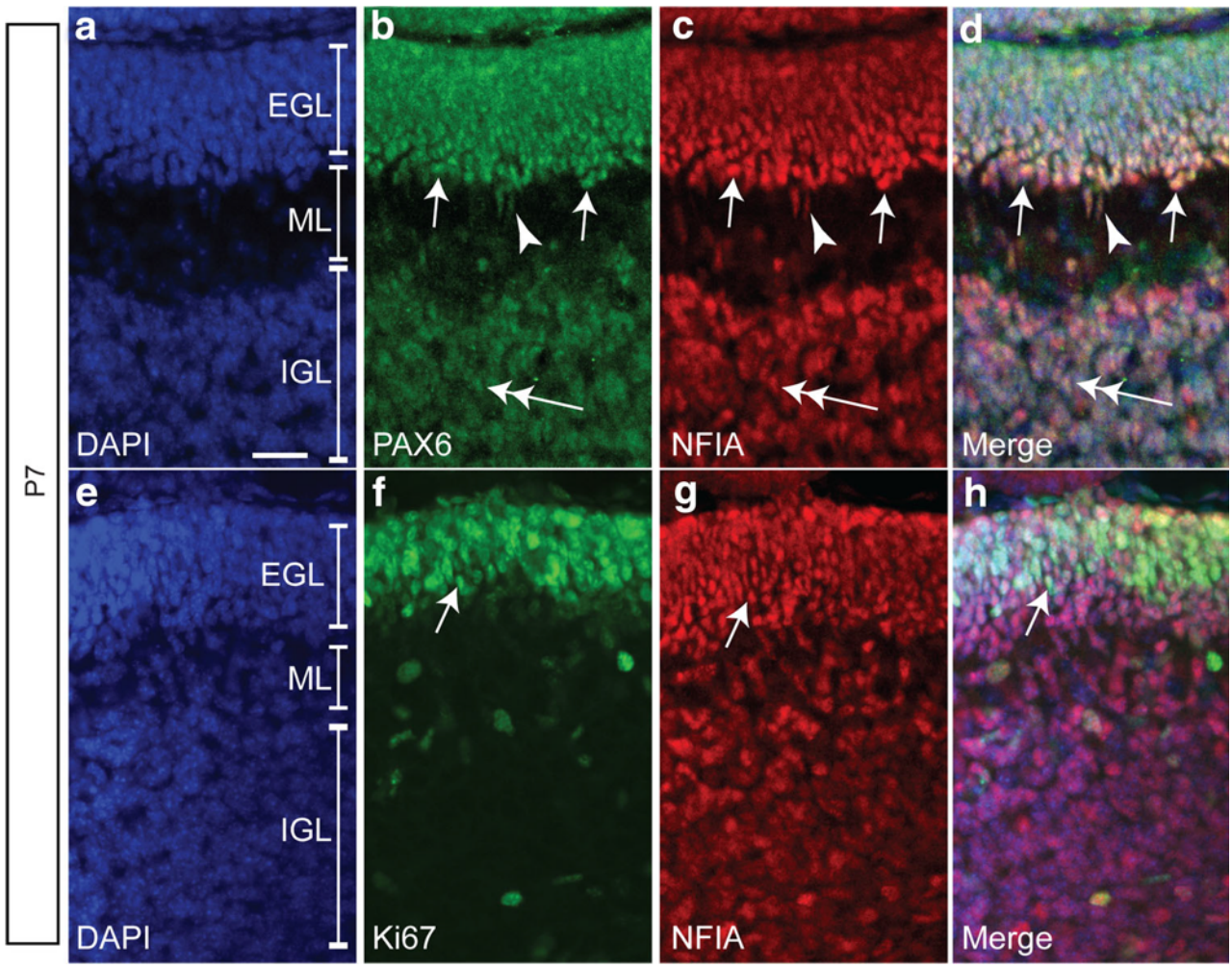

Figure 3. PAX6-positive EGL progenitors express NFIA.

(A-D) Expression of the nuclear marker DAPI (blue, A), PAX6 (green, B), and NFIA (red, C) reveals NFIA expression in PAX6-positive EGL progenitor cells (arrows in B-D). NFIA is also expressed in IGL granule neurons (double-headed arrows in B-D) and migrating cells exiting the EGL (arrowheads in B-D). (E-H) Expression of the nuclear marker DAPI (blue, E), Ki67 (green, F), and NFIA (red, G) also shows NFIA expression in proliferating EGL progenitor cells (arrows in F-H). EGL = external granule layer, ML = molecular layer, IGL = inner granule layer. Scale bar (in A): 20 μm.

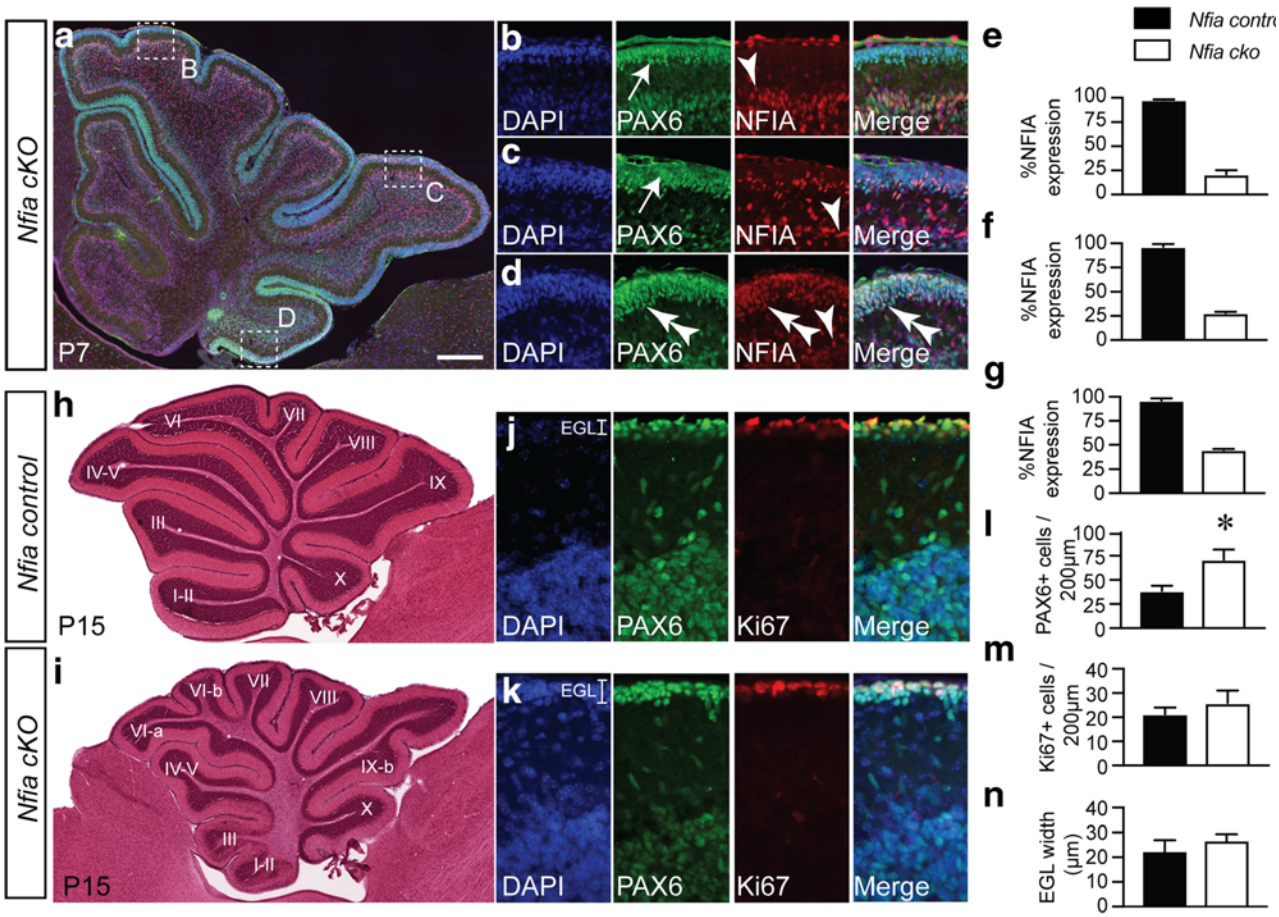

Figure 4. Conditional ablation of NFIA from EGL progenitors using *Atoh1-cre*.

(A) Sagittal cerebellar section in a P7 *Nfia*$^{fl/fl}$*; Atoh1-cre*$^{+}$ mouse (*Nfia cKO*). Co-expression of PAX6 and NFIA was examined in different cerebellar lobes and is shown in the respective high-magnification panels (B-D). (B-D) DAPI (blue), PAX6 (green) and NFIA (red) expression revealed that cells at the margin of the molecular layer and IGL expressed NFIA (arrowheads in B-D). Importantly, the majority of cells in the EGL of lobes VI and IX were immunopositive for PAX6, but did not express NFIA (arrows in B, C). Within lobe X, there were more cells within the EGL that had not undergone Cre-mediated ablation, and hence retained NFIA expression (double arrowheads in D). (E-G) Quantification of the percentage of cells within the EGL of lobes VI (E), IX (F) and X (G) that expressed NFIA. (H, I) Hematoxylin staining of *Nfia control* and *Nfia cKO* cerebella at P15. The cerebellum of mice lacking *Nfia* was dysmorphic, with elevated foliation of the cerebellar lobes evident. Expression of DAPI, PAX6 and Ki67 in *Nfia control* (J) and *Nfia cKO* (K) cerebella at P15 revealed significantly more PAX6-positive cells within the EGL of the mutant (L), although the number of proliferating cells (M), and the width of the EGL (N), was not significantly different between sample groups . * $p < 0.05$, *t*-test. Scale bar (in A): 250 µm, A; 400 µm, H, I; 30 µm, B-D; 25 µm, J, K.

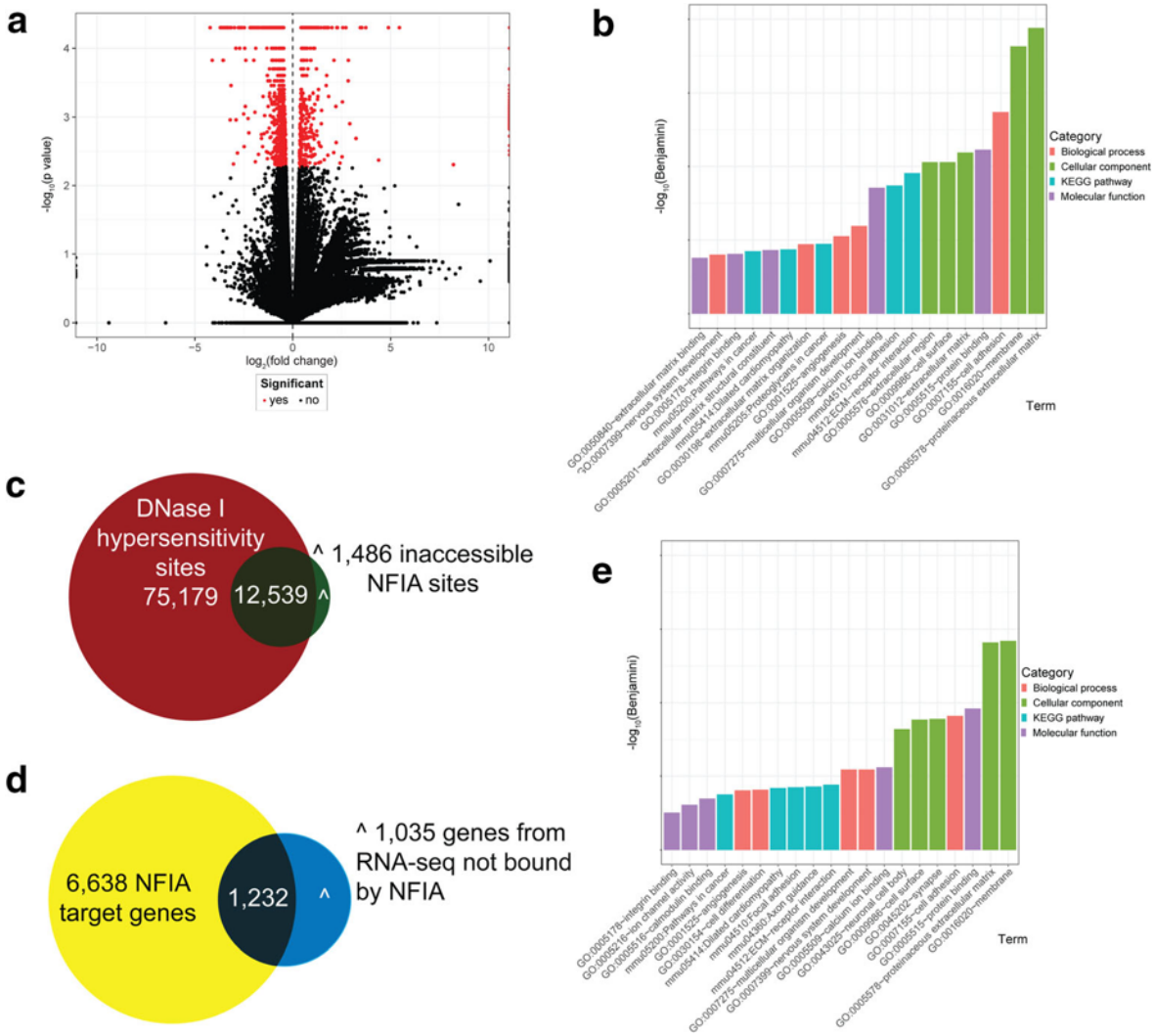

Figure 5. Transcriptomic profiling of GNPs in *Nfia*$^{fl/fl}$; *Atoh1-cre*$^{+}$ mice.

(A) Volcano plot of misregulated genes following RNA-seq in P7 *Nfia cKO* mice GNPs in comparison to *Nfia controls*. Red dots represent the 2,267 genes misregulated in *Nfia* mutant GNPs. (B) Gene Ontology (DAVID 6.8) analysis identifying Biological processes, Cellular components, KEGG pathways and Molecular functions as misregulated in P7 *Nfia cKO* mice GNPs in comparison to controls. Only the top five items for each category are shown; full details can be found in Supp. Table 2. The *p* value was corrected using the Benjamani-Hochberg method. (C) To narrow the list of potential NFIA target genes, we performed ChIP-seq on wild-type P7 GNPs with an anti-NFIA antibody. This revealed 14,025 NFIA binding peaks (green circle). We compared this with a published DNase I hypersensitivity analysis of P7 cerebellar tissue (red circle [36]). Of the 14,025 NFIA ChIP peaks, 12,539 were in regions of accessible chromatin. (D) We then compared the 7,870 genes (yellow circle) associated with these 12,539 NFIA peaks with our RNA-seq data (blue circle). This analysis identified 1,232 potential direct NFIA target genes. (E) DAVID Gene Ontology analysis was performed again following refinement of our target gene list. The top five categories for the NFIA targetome from each of Biological processes, Cellular components, KEGG pathways and Molecular functions identified are shown; full details can be found in Supp. Table 2.

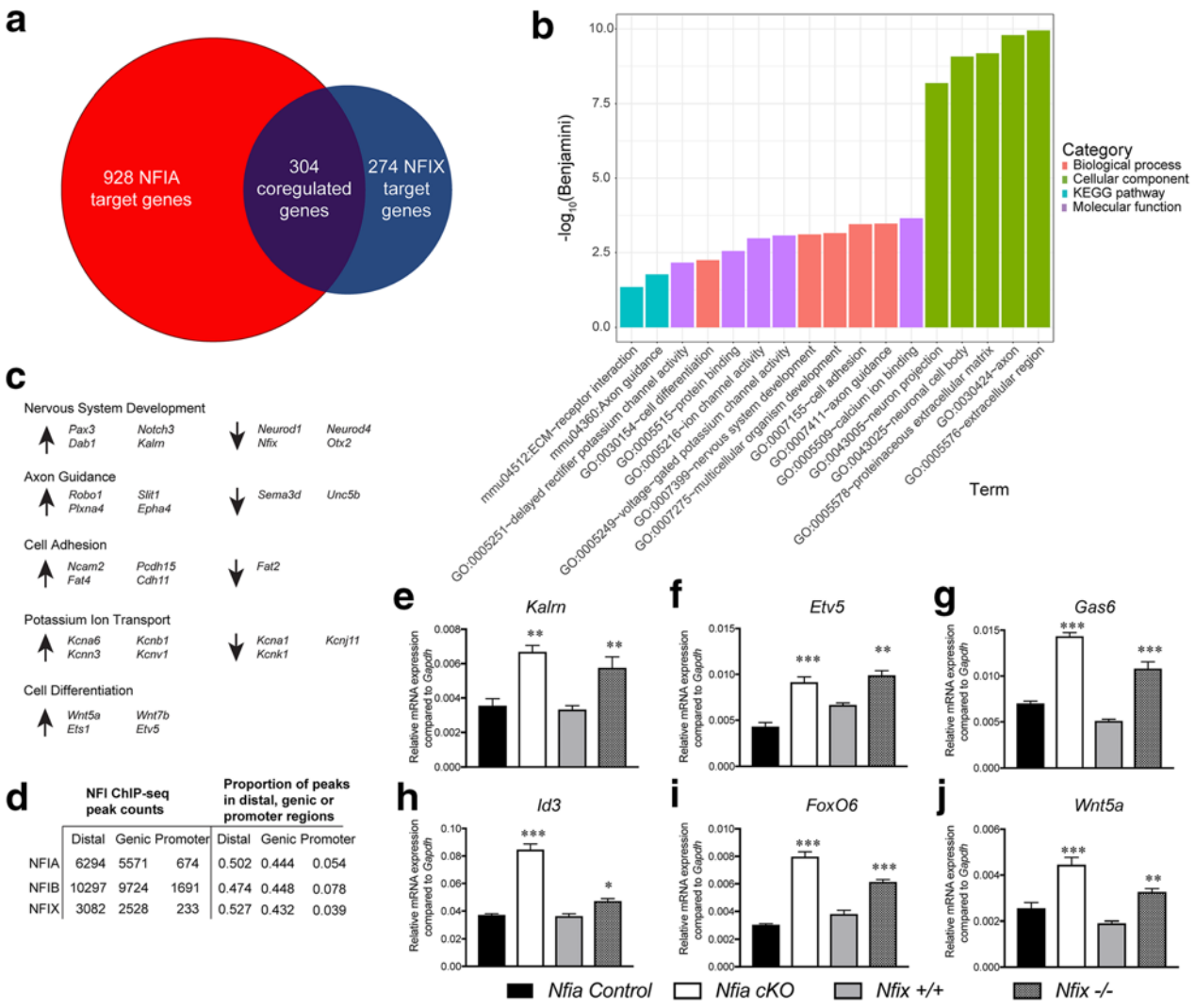

Figure 6. Identification of coregulated targets of NFI family members in GNP development.

(A) Cross comparison of our NFIA targetome (red circle) with a similar analysis performed against NFIX (blue circle; [20]) revealed that there were 304 coregulated genes (i.e. identified in both datasets). Of these, 283 demonstrated coordinated regulation (i.e. either upregulated in RNA-seq experiments from P7 GNPs in both *Nfia cKO* GNPs and *Nfix*-deficient GNPs, or downregulated in both). Of these 283 coordinated targets, 282 also possessed an associated NFIB ChIP-seq peak (Supp. Table 3), indicative of shared regulatory roles for all three NFI family members in GNP biology. (B) DAVID Gene Ontology analysis was performed on these 282 genes. The top five categories from each of Biological processes, Cellular components, KEGG pathways and Molecular functions identified are shown; full details can be found in Supp. Table 2. The *p* value was corrected using the Benjamani-Hochberg method. (C) Curated list of genes from DAVID analysis (Biological Processes), highlighting downstream NFI targets (upwards pointing arrow denotes mRNA upregulation in mutant GNPs, downwards pointing arrow denotes mRNA downregulation in mutant GNPs). (D) Analysis of ChIP-seq binding events for NFIA, NFIB and NFIX, showing the proportion of distal, promoter and genic binding. (E-J) Validation of potential NFI targets using qPCR. * $p < 0.05$; ** $p < 0.01$; *** $p < 0.001$, *t*-test.

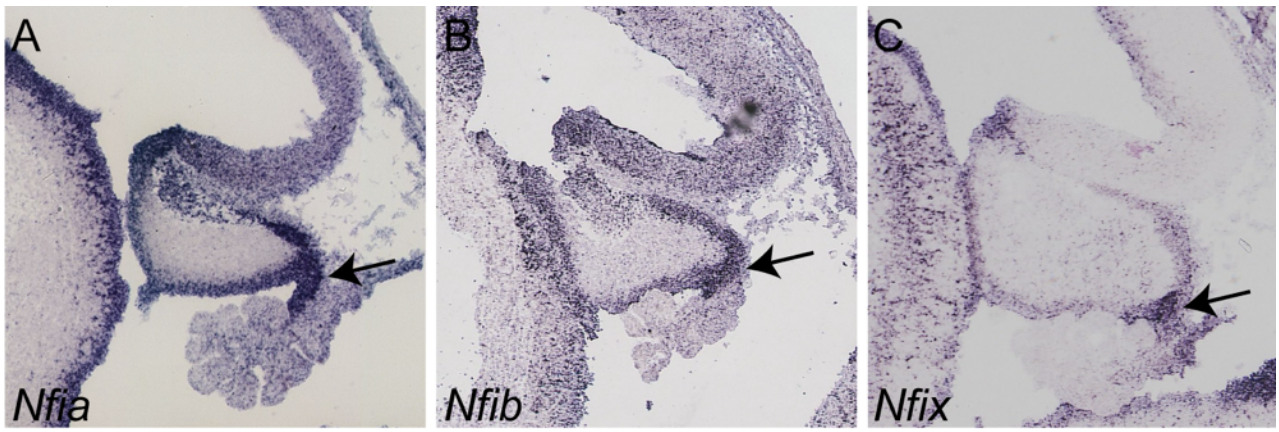

Supplementary Figure 1. Expression of Nfia, Nfib and Nfix within the embryonic rhombic lip.

Sagittal sections of E14.5 mouse brains, showing the expression of Nfia (A), Nfib (B) and Nfix (C) within the rhombic lip (arrows in A-C). These data are derived from the online repository, GenePaint - https://gp3.mpg.de/.

References

1. Harris L, LA Genovesi, RM Gronostajski, BJ Wainwright and M Piper. (2015). Nuclear factor one transcription factors: Divergent functions in developmental versus adult stem cell populations. Dev Dyn 244:227-38.
2. Harris L, O Zalucki, M Piper and JI Heng. (2016). Insights into the Biology and Therapeutic Applications of Neural Stem Cells. Stem Cells Int 2016:9745315.
3. Wang W, D Mullikin-Kilpatrick, JE Crandall, RM Gronostajski, ED Litwack and DL Kilpatrick. (2007). Nuclear factor I coordinates multiple phases of cerebellar granule cell development via regulation of cell adhesion molecules. J Neurosci 27:6115-27.
4. Barry G, M Piper, C Lindwall, R Moldrich, S Mason, E Little, A Sarkar, S Tole, RM Gronostajski and LJ Richards. (2008). Specific glial populations regulate hippocampal morphogenesis. J Neurosci 28:12328-40.
5. Betancourt J, S Katzman and B Chen. (2014). Nuclear factor one B regulates neural stem cell differentiation and axonal projection of corticofugal neurons. J Comp Neurol 522:6-35.
6. Deneen B, R Ho, A Lukaszewicz, CJ Hochstim, RM Gronostajski and DJ Anderson. (2006). The transcription factor NFIA controls the onset of gliogenesis in the developing spinal cord. Neuron 52:953-68.
7. Harris L, O Zalucki, I Gobius, H McDonald, J Osinki, TJ Harvey, A Essebier, D Vidovic, I Gladwyn-Ng, TH Burne, JI Heng, LJ Richards, RM Gronostajski and M Piper. (2016). Transcriptional regulation of intermediate progenitor cell generation during hippocampal development. Development 143:4620-4630.
8. Heng YH, RC McLeay, TJ Harvey, AG Smith, G Barry, K Cato, C Plachez, E Little, S Mason, C Dixon, RM Gronostajski, TL Bailey, LJ Richards and M Piper. (2014). NFIX regulates neural progenitor cell differentiation during hippocampal morphogenesis. Cereb Cortex 24:261-79.
9. Piper M, G Barry, TJ Harvey, R McLeay, AG Smith, L Harris, S Mason, BW Stringer, BW Day, NR Wray, RM Gronostajski, TL Bailey, AW Boyd and LJ Richards. (2014). NFIB-mediated repression of the epigenetic factor Ezh2 regulates cortical development. J Neurosci 34:2921-30.
10. Piper M, G Barry, J Hawkins, S Mason, C Lindwall, E Little, A Sarkar, AG Smith, RX Moldrich, GM Boyle, S Tole, RM Gronostajski, TL Bailey and LJ Richards. (2010). NFIA controls telencephalic progenitor cell differentiation through repression of the Notch effector Hes1. J Neurosci 30:9127-39.
11. Piper M, L Harris, G Barry, YH Heng, C Plachez, RM Gronostajski and LJ Richards. (2011). Nuclear factor one X regulates the development of multiple cellular populations in the postnatal cerebellum. J Comp Neurol 519:3532-48.
12. Piper M, RX Moldrich, C Lindwall, E Little, G Barry, S Mason, N Sunn, ND Kurniawan, RM Gronostajski and LJ Richards. (2009). Multiple non-cell-autonomous defects underlie neocortical callosal dysgenesis in Nfib-deficient mice. Neural Dev 4:43.
13. Campbell CE, M Piper, C Plachez, YT Yeh, JS Baizer, JM Osinski, ED Litwack, LJ Richards and RM Gronostajski. (2008). The transcription factor Nfix is essential for normal brain development. BMC Dev Biol 8:52.
14. Fraser J, A Essebier, RM Gronostajski, M Boden, BJ Wainwright, TJ Harvey and M Piper. (2017). Cell-type-specific expression of NFIX in the developing and adult cerebellum. Brain Struct Funct 222:2251-2270.
15. Matuzelski E, J Bunt, D Harkins, JWC Lim, RM Gronostajski, LJ Richards, L Harris and M Piper. (2017). Transcriptional regulation of Nfix by NFIB drives astrocytic maturation within the developing spinal cord. Dev Biol 432:286-297.

16. Plachez C, C Lindwall, N Sunn, M Piper, RX Moldrich, CE Campbell, JM Osinski, RM Gronostajski and LJ Richards. (2008). Nuclear factor I gene expression in the developing forebrain. J Comp Neurol 508:385-401.
17. Shu T, KG Butz, C Plachez, RM Gronostajski and LJ Richards. (2003). Abnormal development of forebrain midline glia and commissural projections in Nfia knock-out mice. J Neurosci 23:203-12.
18. Steele-Perkins G, C Plachez, KG Butz, G Yang, CJ Bachurski, SL Kinsman, ED Litwack, LJ Richards and RM Gronostajski. (2005). The transcription factor gene Nfib is essential for both lung maturation and brain development. Mol Cell Biol 25:685-98.
19. Cerminara NL, EJ Lang, RV Sillitoe and R Apps. (2015). Redefining the cerebellar cortex as an assembly of non-uniform Purkinje cell microcircuits. Nat Rev Neurosci 16:79-93.
20. Fraser J, A Essebier, AS Brown, RA Davila, AS Sengar, Y Tu, KS Ensbey, BW Day, MP Scott, RM Gronostajski, BJ Wainwright, M Boden, TJ Harvey and M Piper. (2019). Granule neuron precursor cell proliferation is regulated by NFIX and intersectin 1 during postnatal cerebellar development. Brain Struct Funct 224:811-827.
21. Acampora D, M Gulisano, V Broccoli and A Simeone. (2001). Otx genes in brain morphogenesis. Prog Neurobiol 64:69-95.
22. Bunt J, J Osinki, J Lim, D Vidovic, Y Ye, O Zalucki, T O'Connor, L Harris, R Gronostajski, LJ Richards and M Piper. (2017). Combined allelic loss of Nfia and Nfib causes an increased severity of cortical developmental defects. Brain and Neuroscience Advances 1:1-21.
23. Machold R and G Fishell. (2005). Math1 is expressed in temporally discrete pools of cerebellar rhombic-lip neural progenitors. Neuron 48:17-24.
24. Chizhikov V and KJ Millen. (2003). Development and malformations of the cerebellum in mice. Mol Genet Metab 80:54-65.
25. Machold R, C Klein and G Fishell. (2011). Genes expressed in Atoh1 neuronal lineages arising from the r1/isthmus rhombic lip. Gene Expr Patterns 11:349-59.
26. Leto K, M Arancillo, EB Becker, A Buffo, C Chiang, B Ding, WB Dobyns, I Dusart, P Haldipur, ME Hatten, M Hoshino, AL Joyner, M Kano, DL Kilpatrick, N Koibuchi, S Marino, S Martinez, KJ Millen, TO Millner, T Miyata, E Parmigiani, K Schilling, G Sekerkova, RV Sillitoe, C Sotelo, N Uesaka, A Wefers, RJ Wingate and R Hawkes. (2015). Consensus Paper: Cerebellar Development. Cerebellum.
27. Schuller U, Q Zhao, SA Godinho, VM Heine, RH Medema, D Pellman and DH Rowitch. (2007). Forkhead transcription factor FoxM1 regulates mitotic entry and prevents spindle defects in cerebellar granule neuron precursors. Mol Cell Biol 27:8259-70.
28. Lee HY, LA Greene, CA Mason and MC Manzini. (2009). Isolation and culture of post-natal mouse cerebellar granule neuron progenitor cells and neurons. J Vis Exp.
29. Trapnell C, A Roberts, L Goff, G Pertea, D Kim, DR Kelley, H Pimentel, SL Salzberg, JL Rinn and L Pachter. (2012). Differential gene and transcript expression analysis of RNA-seq experiments with TopHat and Cufflinks. Nat Protoc 7:562-78.
30. Chen KS, L Harris, JWC Lim, TJ Harvey, M Piper, RM Gronostajski, LJ Richards and J Bunt. (2017). Differential neuronal and glial expression of nuclear factor I proteins in the cerebral cortex of adult mice. J Comp Neurol 525:2465-2483.
31. Langmead B and SL Salzberg. (2012). Fast gapped-read alignment with Bowtie 2. Nat Methods 9:357-9.
32. Feng J, T Liu, B Qin, Y Zhang and XS Liu. (2012). Identifying ChIP-seq enrichment using MACS. Nat Protoc 7:1728-40.
33. O'Connor T, M Boden and TL Bailey. (2017). CisMapper: predicting regulatory interactions from transcription factor ChIP-seq data. Nucleic Acids Res 45:e19.
34. Huang da W, BT Sherman and RA Lempicki. (2009). Bioinformatics enrichment tools: paths toward the comprehensive functional analysis of large gene lists. Nucleic Acids Res 37:1-13.

35. Huang da W, BT Sherman and RA Lempicki. (2009). Systematic and integrative analysis of large gene lists using DAVID bioinformatics resources. Nat Protoc 4:44-57.
36. Frank CL, F Liu, R Wijayatunge, L Song, MT Biegler, MG Yang, CM Vockley, A Safi, CA Gersbach, GE Crawford and AE West. (2015). Regulation of chromatin accessibility and Zic binding at enhancers in the developing cerebellum. Nat Neurosci 18:647-56.
37. Guertin MJ and JT Lis. (2013). Mechanisms by which transcription factors gain access to target sequence elements in chromatin. Curr Opin Genet Dev 23:116-23.
38. Hughes TR. (2011). Introduction to "a handbook of transcription factors". Subcell Biochem 52:1-6.
39. Wang W, Y Shin, M Shi and DL Kilpatrick. (2011). Temporal control of a dendritogenesis-linked gene via REST-dependent regulation of nuclear factor I occupancy. Mol Biol Cell 22:868-79.
40. Wang W, RE Stock, RM Gronostajski, YW Wong, M Schachner and DL Kilpatrick. (2004). A role for nuclear factor I in the intrinsic control of cerebellar granule neuron gene expression. J Biol Chem 279:53491-7.
41. Plachez C, K Cato, RC McLeay, YH Heng, TL Bailey, RM Gronostasjki, LJ Richards, AC Puche and M Piper. (2012). Expression of nuclear factor one A and -B in the olfactory bulb. J Comp Neurol 520:3135-49.
42. Wang W, JE Crandall, ED Litwack, RM Gronostajski and DL Kilpatrick. (2010). Targets of the nuclear factor I regulon involved in early and late development of postmitotic cerebellar granule neurons. J Neurosci Res 88:258-65.
43. Gronostajski RM. (2000). Roles of the NFI/CTF gene family in transcription and development. Gene 249:31-45.
44. Piper M, R Gronostajski and G Messina. (2019). Nuclear factor one X in development and disease. Trends Cell Biol 29:20-30.
45. Messina G, S Biressi, S Monteverde, A Magli, M Cassano, L Perani, E Roncaglia, E Tagliafico, L Starnes, CE Campbell, M Grossi, DJ Goldhamer, RM Gronostajski and G Cossu. (2010). Nfix regulates fetal-specific transcription in developing skeletal muscle. Cell 140:554-66.
46. Pistocchi A, G Gaudenzi, E Foglia, S Monteverde, A Moreno-Fortuny, A Pianca, G Cossu, F Cotelli and G Messina. (2013). Conserved and divergent functions of Nfix in skeletal muscle development during vertebrate evolution. Development 140:1528-36.
47. Subashini C, SB Dhanesh, CM Chen, PA Riya, V Meera, TS Divya, R Kuruvilla, K Buttler and J James. (2017). Wnt5a is a crucial regulator of neurogenesis during cerebellum development. Sci Rep 7:42523.
48. Denny SK, D Yang, CH Chuang, JJ Brady, JS Lim, BM Gruner, SH Chiou, AN Schep, J Baral, C Hamard, M Antoine, M Wislez, CS Kong, AJ Connolly, KS Park, J Sage, WJ Greenleaf and MM Winslow. (2016). Nfib Promotes Metastasis through a Widespread Increase in Chromatin Accessibility. Cell 166:328-342.
49. Kruse U and AE Sippel. (1994). Transcription factor nuclear factor I proteins form stable homo- and heterodimers. FEBS Lett 348:46-50.
50. Li X, W Wang, J Wang, A Malovannaya, Y Xi, W Li, R Guerra, DH Hawke, J Qin and J Chen. (2015). Proteomic analyses reveal distinct chromatin-associated and soluble transcription factor complexes. Mol Syst Biol 11:775.

UQ Research and Innovation
Director, Research Management Office
Nicole Thompson

Animal Ethics Approval Certificate

16-May-2017

Please check all details below and inform the Animal Welfare Unit within 10 working days if anything is incorrect.

Activity Details

Chief Investigator: Associate Professor Michael Piper, Biomedical Sciences

Title: Breeding colonies for Piper lab: Cerebellar development project

AEC Approval Number: SBMS/149/16/ARC/BREED

Previous AEC Number:

Approval Duration: 23-May-2016 to 23-May-2019

Funding Body: ARC

Group: Anatomical Biosciences

Other Staff/Students: Tracey Harvey, Rebecca Mills, Trish Hitchcock

Location(s): St Lucia Bldg 79 - Queensland Brain Institute

Summary

Subspecies	Strain	Class	Gender	Source	Approved	Remaining
Mice - genetically modified	NfiX +/- (Breed)	Adults	Mix	Institutional Breeding Colony	36	26
Mice - genetically modified	Nfix delta neo Flox/Flox (breed)	Adults	Mix	Institutional Breeding Colony	36	36
Mice - genetically modified	Math1 Cre ER+/- (breed)	Adults	Mix	Institutional Breeding Colony	36	36
Mice - genetically modified	Nfix delta neo Flox/+ ; Math1 Cre ER+/- (breed)	Adults	Mix	Institutional Breeding Colony	36	31
Mice - genetically modified	Nfix delta neo flox/flox; Math1 Cre ER+/- (breed)	Adults	Mix	Institutional Breeding Colony	72	72
Mice - genetically modified	tdTomato +/- (Breed)	Adults	Mix	Institutional Breeding Colony	36	36
Mice - genetically modified	Nfix delta neo Flox/+; tdTomato +/- (breed)	Adults	Mix	Institutional Breeding Colony	36	36
Mice - genetically modified	NfiX delta neo flox/flox; tdTomato +/+ (Breed)	Adults	Mix	Institutional Breeding Colony	36	36
Mice - genetically modified	NfiX delta neo flox/+; tdTomato +/-; Math1 Cre ER+/- (breed)	Adults	Mix	Institutional Breeding Colony	36	33

Mice - genetically modified	Nfix delta neo flox/flox; tdTomato+/-; Math1 Cre ER+/- (breed)	Adults	Mix	Institutional Breeding Colony	72	72
Mice - genetically modified	tdTomato +/-; Math1 Cre ER+/- (breed)	Adults	Mix	Institutional Breeding Colony	36	36
Mice - genetically modified	NfiX +/- (Cull)	Adults	Mix	Institutional Breeding Colony	516	357
Mice - genetically modified	Nfix delta neo Flox/Flox (cull)	Adults	Mix	Institutional Breeding Colony	468	468
Mice - genetically modified	Math1 Cre ERT2+/- (cull)	Adults	Mix	Institutional Breeding Colony	522	522
Mice - genetically modified	Nfix delta neo Flox/+ ; Math1 Cre ERT2+/- (cull)	Adults	Mix	Institutional Breeding Colony	558	487
Mice - genetically modified	Nfix delta neo flox/flox; Math1 Cre ERT2+/- (cull)	Adults	Mix	Institutional Breeding Colony	846	846
Mice - genetically modified	tdTomato +/- (Cull)	Adults	Mix	Institutional Breeding Colony	540	540
Mice - genetically modified	Nfix delta neo Flox/+; tdTomato +/- (cull)	Adults	Mix	Institutional Breeding Colony	540	540
Mice - genetically modified	NfiX delta neo flox/flox; tdTomato +/+ (Cull)	Adults	Mix	Institutional Breeding Colony	558	558
Mice - genetically modified	NfiX delta neo flox/+; tdTomato +/-; Math1 Cre ERT2+/- (cull)	Adults	Mix	Institutional Breeding Colony	558	529
Mice - genetically modified	Nfix delta neo flox/flox; tdTomato+/-; Math1 Cre ERT2+/- (cull)	Adults	Mix	Institutional Breeding Colony	846	846
Mice - genetically modified	tdTomato +/-; Math1 Cre ERT2+/- (cull)	Adults	Mix	Institutional Breeding Colony	288	288
Mice - genetically modified	Nfia flox/flox (breed)	Adults	Mix	Institutional Breeding Colony	36	32
Mice - genetically modified	Nfia flox/flox (cull)	Adults	Mix	Institutional Breeding Colony	540	512
Mice - genetically modified	Math1 Cre +/- (breed)	Adults	Mix	Institutional Breeding Colony	36	36
Mice - genetically modified	Math1 Cre +/- (cull)	Adults	Mix	Institutional Breeding Colony	558	558
Mice - genetically modified	Nfia flox/+:Math1 Cre +/- (breed)	Adults	Mix	Institutional Breeding Colony	36	36
Mice - genetically modified	Nfia flox/+:Math1 Cre +/- (cull)	Adults	Mix	Institutional Breeding Colony	558	558

Mice - genetically modified	Nfia flox/flox:Math1 Cre +/- (breed)	Adults	Mix	Institutional Breeding Colony	72	62
Mice - genetically modified	Nfia flox/flox:Math1 Cre +/- (cull)	Adults	Mix	Institutional Breeding Colony	846	767
Mice - genetically modified	NSD1 +/- (breed)	Adults	Mix	Institutional Breeding Colony	36	34
Mice - genetically modified	NSD1 +/- (cull)	Adults	Mix	Institutional Breeding Colony	720	720
Mice - non genetically modified	C57BL/6 (breed)	Adults	Mix	Institutional Breeding Colony	18	18

Permits

Provisos

Breeding Proviso:
1) The amount of animals shown on this certificate only includes your Breeders(s) and projected culled (ie wrong genotype, incorrect gender etc) limit.
2) Progeny used for Colony maintenance should be reported on this project.
3) Whilst estimated progeny are required on the application however the final numbers of progeny transferred to Research Project(s) must be reported only on the Research Project.

Approval Details

Description		Amount	Balance
Mice - genetically modified (Math1 Cre +/- (breed), Mix, Adults, Institutional Breeding Colony)			
11 May 2016	Mod #1	36	36
31 Dec 2016	Use in 2016 (from 2017 MAR; AEMAR22717)	0	36
Mice - genetically modified (Math1 Cre +/- (cull), Mix, Adults, Institutional Breeding Colony)			
11 May 2016	Mod #1	558	558
31 Dec 2016	Use in 2016 (from 2017 MAR; AEMAR22717)	0	558
Mice - genetically modified (Math1 Cre ER+/- (breed), Mix, Adults, Institutional Breeding Colony)			
11 May 2016	Initial Approval	36	36
31 Dec 2016	Use in 2016 (from 2017 MAR; AEMAR22717)	0	36
Mice - genetically modified (Math1 Cre ERT2+/- (cull), Mix, Adults, Institutional Breeding Colony)			
11 May 2016	Initial Approval	522	522
31 Dec 2016	Use in 2016 (from 2017 MAR; AEMAR22717)	0	522
Mice - genetically modified (Nfia flox/+:Math1 Cre +/- (breed), Mix, Adults, Institutional Breeding Colony)			
11 May 2016	Mod #1	36	36
31 Dec 2016	Use in 2016 (from 2017 MAR; AEMAR22717)	0	36
Mice - genetically modified (Nfia flox/+:Math1 Cre +/- (cull), Mix, Adults, Institutional Breeding Colony)			
11 May 2016	Mod #1	558	558
31 Dec 2016	Use in 2016 (from 2017 MAR; AEMAR22717)	0	558
Mice - genetically modified (Nfia flox/flox (breed), Mix, Adults, Institutional Breeding Colony)			
11 May 2016	Mod #1	36	36
31 Dec 2016	Use in 2016 (from 2017 MAR; AEMAR22717)	-4	32
Mice - genetically modified (Nfia flox/flox (cull), Mix, Adults, Institutional Breeding Colony)			

11 May 2016	Mod #1	540	540
31 Dec 2016	Use in 2016 (from 2017 MAR; AEMAR22717)	-28	512

Mice - genetically modified (Nfia flox/flox:Math1 Cre +/- (breed), Mix, Adults, Institutional Breeding Colony)

11 May 2016	Mod #1	72	72
31 Dec 2016	Use in 2016 (from 2017 MAR; AEMAR22717)	-10	62

Mice - genetically modified (Nfia flox/flox:Math1 Cre +/- (cull), Mix, Adults, Institutional Breeding Colony)

11 May 2016	Mod #1	846	846
31 Dec 2016	Use in 2016 (from 2017 MAR; AEMAR22717)	-79	767

Mice - genetically modified (NfiX +/- (Breed), Mix, Adults, Institutional Breeding Colony)

11 May 2016	Initial Approval	36	36
31 Dec 2016	Use in 2016 (from 2017 MAR; AEMAR22717)	-10	26

Mice - genetically modified (NfiX +/- (Cull), Mix, Adults, Institutional Breeding Colony)

11 May 2016	Initial Approval	516	516
31 Dec 2016	Use in 2016 (from 2017 MAR; AEMAR22717)	-159	357

Mice - genetically modified (Nfix delta neo Flox/+ ; Math1 Cre ER+/- (breed), Mix, Adults, Institutional Breeding Colony)

11 May 2016	Initial Approval	36	36
31 Dec 2016	Use in 2016 (from 2017 MAR; AEMAR22717)	-5	31

Mice - genetically modified (Nfix delta neo Flox/+ ; Math1 Cre ERT2+/- (cull), Mix, Adults, Institutional Breeding Colony)

11 May 2016	Initial Approval	558	558
31 Dec 2016	Use in 2016 (from 2017 MAR; AEMAR22717)	-71	487

Mice - genetically modified (NfiX delta neo flox/+; tdTomato +/-; Math1 Cre ER+/- (breed), Mix, Adults, Institutional Breeding Colony)

11 May 2016	Initial Approval	36	36
31 Dec 2016	Use in 2016 (from 2017 MAR; AEMAR22717)	-3	33

Mice - genetically modified (NfiX delta neo flox/+; tdTomato +/-; Math1 Cre ERT2+/- (cull), Mix, Adults, Institutional Breeding Colony)

11 May 2016	Initial Approval	558	558
31 Dec 2016	Use in 2016 (from 2017 MAR; AEMAR22717)	-29	529

Mice - genetically modified (Nfix delta neo Flox/+; tdTomato+/- (breed), Mix, Adults, Institutional Breeding Colony)

11 May 2016	Initial Approval	36	36
31 Dec 2016	Use in 2016 (from 2017 MAR; AEMAR22717)	0	36

Mice - genetically modified (Nfix delta neo Flox/+; tdTomato+/- (cull), Mix, Adults, Institutional Breeding Colony)

11 May 2016	Initial Approval	540	540
31 Dec 2016	Use in 2016 (from 2017 MAR; AEMAR22717)	0	540

Mice - genetically modified (Nfix delta neo Flox/Flox (breed), Mix, Adults, Institutional Breeding Colony)

11 May 2016	Initial Approval	36	36
31 Dec 2016	Use in 2016 (from 2017 MAR; AEMAR22717)	0	36

Mice - genetically modified (Nfix delta neo Flox/Flox (cull), Mix, Adults, Institutional Breeding Colony)

11 May 2016	Initial Approval	468	468
31 Dec 2016	Use in 2016 (from 2017 MAR; AEMAR22717)	0	468

Mice - genetically modified (Nfix delta neo flox/flox; Math1 Cre ER+/- (breed), Mix, Adults, Institutional Breeding Colony)

11 May 2016	Initial Approval	72	72
31 Dec 2016	Use in 2016 (from 2017 MAR; AEMAR22717)	0	72

Mice - genetically modified (Nfix delta neo flox/flox; Math1 Cre ERT2+/- (cull), Mix, Adults, Institutional Breeding Colony)

11 May 2016	Initial Approval	846	846
31 Dec 2016	Use in 2016 (from 2017 MAR; AEMAR22717)	0	846

Mice - genetically modified (NfiX delta neo flox/flox; tdTomato +/+ (Breed), Mix, Adults, Institutional Breeding Colony)

11 May 2016	Initial Approval	36	36
31 Dec 2016	Use in 2016 (from 2017 MAR; AEMAR22717)	0	36

Mice - genetically modified (NfiX delta neo flox/flox; tdTomato +/+ (Cull), Mix, Adults, Institutional Breeding Colony)

11 May 2016	Initial Approval	558	558
31 Dec 2016	Use in 2016 (from 2017 MAR; AEMAR22717)	0	558

Mice - genetically modified (Nfix delta neo flox/flox; tdTomato+/-; Math1 Cre ER+/- (breed), Mix, Adults, Institutional Breeding Colony)

11 May 2016	Initial Approval	72	72
31 Dec 2016	Use in 2016 (from 2017 MAR; AEMAR22717)	0	72

Mice - genetically modified (Nfix delta neo flox/flox; tdTomato+/-; Math1 Cre ERT2+/- (cull), Mix, Adults, Institutional Breeding Colony)

11 May 2016	Initial Approval	846	846
31 Dec 2016	Use in 2016 (from 2017 MAR; AEMAR22717)	0	846

Mice - genetically modified (NSD1 +/- (breed), Mix, Adults, Institutional Breeding Colony)

8 Jun 2016	Mod #2	36	36
31 Dec 2016	Use in 2016 (from 2017 MAR; AEMAR22717)	-2	34

Mice - genetically modified (NSD1 +/- (cull), Mix, Adults, Institutional Breeding Colony)

8 Jun 2016	Mod #2	480	480
31 Dec 2016	Use in 2016 (from 2017 MAR; AEMAR22717)	0	480
10 May 2017	Mod #3	240	720

Mice - genetically modified (tdTomato +/- (Breed), Mix, Adults, Institutional Breeding Colony)

11 May 2016	Initial Approval	36	36
31 Dec 2016	Use in 2016 (from 2017 MAR; AEMAR22717)	0	36

Mice - genetically modified (tdTomato +/- (Cull), Mix, Adults, Institutional Breeding Colony)

11 May 2016	Initial Approval	540	540
31 Dec 2016	Use in 2016 (from 2017 MAR; AEMAR22717)	0	540

Mice - genetically modified (tdTomato +/-; Math1 Cre ER+/- (breed), Mix, Adults, Institutional Breeding Colony)

11 May 2016	Initial Approval	36	36
31 Dec 2016	Use in 2016 (from 2017 MAR; AEMAR22717)	0	36

Mice - genetically modified (tdTomato +/-; Math1 Cre ERT2+/- (cull), Mix, Adults, Institutional Breeding Colony)

11 May 2016	Initial Approval	288	288
31 Dec 2016	Use in 2016 (from 2017 MAR; AEMAR22717)	0	288

Mice - non genetically modified (C57BL/6 (breed), Mix, Adults, Institutional Breeding Colony)

10 May 2017	Mod #3	18	18

Please note the animal numbers supplied on this certificate are the total allocated for the approval duration

Please use this Approval Number:

1. When ordering animals from Animal Breeding Houses
2. For labelling of all animal cages or holding areas. In addition please include on the label, Chief Investigator's name and contact phone number.
3. When you need to communicate with this office about the project.

It is a condition of this approval that all project animal details be made available to Animal House OIC.
(UAEC Ruling 14/12/2001)

The Chief Investigator takes responsibility for ensuring all legislative, regulatory and compliance objectives are satisfied for this project.

This certificate supercedes all preceeding certificates for this project (i.e. those certificates dated before 16-May-2017)

THE UNIVERSITY OF QUEENSLAND
AUSTRALIA

Office of Research Ethics
Director
Nicole Shively

Animal Ethics Approval Certificate

23-Feb-2018

Please check all details below and inform the Animal Ethics Unit within 10 working days if anything is incorrect.

Activity Details

Chief Investigator: Associate Professor Michael Piper, Biomedical Sciences

Title: Assessing the role of NFIX in cerebellar development

AEC Approval Number: QBI/143/16/NHMRC/ARC

Previous AEC Number:

Approval Duration: 17-May-2016 to 17-May-2019

Funding Body:

Group: Anatomical Biosciences

Other Staff/Students: Tracey Harvey, Kim Woolley, Oressia Zalucki, Michelle Sanchez Vega, James Fraser, Kevin Mutemi, Raul Ayala Davila, Danyon Harkins, David Hollingsworth, Suzy Alexander, Raquelle Ludwig, Thomas Burne, Maria Kashermann, Jack Wood, Sazia Sharmin

Location(s): St Lucia Bldg 79 - Queensland Brain Institute

Summary

Subspecies	Strain	Class	Gender	Source	Approved	Remaining
Mice - genetically modified	Nfix delta neo flox/flox; Math1 Cre ER+/-	Adults	Mix		168	168
Mice - genetically modified	Nfix delta neo flox/flox; Math1 Cre ER+/-	Juvenile / Weaners / Pouch animal	Mix		920	920
Mice - genetically modified	Nfix ko	Juvenile / Weaners / Pouch animal	Mix		920	920
Mice - genetically modified	Nfix ko	Prenatal / Embryo	Mix		336	336
Mice - genetically modified	Nfix delta neo flox/flox; tdTomato+/-; Math1 Cre ER+/-	Juvenile / Weaners / Pouch animal	Mix		1050	1050
Mice - genetically modified	Nfix ko	Adults	Female		56	56
Mice - genetically modified	Nfia flox/flox:Math1 Cre +/-	Adults	Mix	Institutional Breeding Colony	84	84
Mice - genetically modified	Nfia flox/flox:Math1 Cre +/-	Juvenile / Weaners / Pouch animal	Mix	Institutional Breeding Colony	460	390
Mice - genetically modified	NSD1 +/-	Adults	Mix	Institutional Breeding Colony	20	20
Mice - genetically modified	NSD1 +/-	Juvenile / Weaners / Pouch animal	Mix	Institutional Breeding Colony	110	110

Mice - genetically modified	NSD1 +/-	Prenatal / Embryo	Mix	Institutional Breeding Colony	40	40
Mice - genetically modified	Intersectin Knockout (Tissue Only)	Adults	Mix	Institutional Breeding Colony	10	10
Mice - non genetically modified	C57BL/6J	Juvenile / Weaners / Pouch animal	Mix		1842	1829

Permits

Provisos

Approval Details

Description		Amount	Balance
Mice - genetically modified (Intersectin Knockout (Tissue Only), Mix, Adults, Institutional Breeding Colony)			
18 Apr 2017	Mod #5	10	10
Mice - genetically modified (Nfia flox/flox:Math1 Cre +/- , Mix, Adults, Institutional Breeding Colony)			
11 May 2016	Mod #2	84	84
31 Dec 2016	Use in 2016 (from 2017 MAR; AEMAR22705)	0	84
Mice - genetically modified (Nfia flox/flox:Math1 Cre +/- , Mix, Juvenile / Weaners / Pouch animal, Institutional Breeding Colony)			
8 Jun 2016	Mod #2	460	460
31 Dec 2016	Use in 2016 (from 2017 MAR; AEMAR22705)	-70	390
Mice - genetically modified (Nfix delta neo flox/flox; Math1 Cre ER+/-, Mix, Adults,)			
11 May 2016	Initial approval	168	168
31 Dec 2016	Use in 2016 (from 2017 MAR; AEMAR22705)	0	168
Mice - genetically modified (Nfix delta neo flox/flox; Math1 Cre ER+/-, Mix, Juvenile / Weaners / Pouch animal,)			
11 May 2016	Initial approval	920	920
31 Dec 2016	Use in 2016 (from 2017 MAR; AEMAR22705)	0	920
Mice - genetically modified (Nfix delta neo flox/flox; tdTomato+/-; Math1 Cre ER+/-, Mix, Juvenile / Weaners / Pouch animal,)			
11 May 2016	Initial approval	1050	1050
31 Dec 2016	Use in 2016 (from 2017 MAR; AEMAR22705)	0	1050
Mice - genetically modified (Nfix ko, Female, Adults,)			
11 May 2016	Initial approval	56	56
31 Dec 2016	Use in 2016 (from 2017 MAR; AEMAR22705)	0	56
Mice - genetically modified (Nfix ko, Mix, Juvenile / Weaners / Pouch animal,)			
11 May 2016	Initial approval	920	920
31 Dec 2016	Use in 2016 (from 2017 MAR; AEMAR22705)	0	920
Mice - genetically modified (Nfix ko, Mix, Prenatal / Embryo,)			
11 May 2016	Initial approval	336	336
31 Dec 2016	Use in 2016 (from 2017 MAR; AEMAR22705)	0	336
Mice - genetically modified (NSD1 +/- , Mix, Adults, Institutional Breeding Colony)			
8 Jun 2016	Mod #3	20	20
31 Dec 2016	Use in 2016 (from 2017 MAR; AEMAR22705)	0	20
Mice - genetically modified (NSD1 +/- , Mix, Juvenile / Weaners / Pouch animal, Institutional Breeding Colony)			

8 Jun 2016	Mod #3	110	110
31 Dec 2016	Use in 2016 (from 2017 MAR; AEMAR22705)	0	110
Mice - genetically modified (NSD1 +/- , Mix, Prenatal / Embryo, Institutional Breeding Colony)			
8 Jun 2016	Mod #3	40	40
31 Dec 2016	Use in 2016 (from 2017 MAR; AEMAR22705)	0	40
Mice - non genetically modified (C57BL/6J , Mix, Juvenile / Weaners / Pouch animal,)			
11 May 2016	Initial approval	1842	1842
31 Dec 2016	Use in 2016 (from 2017 MAR; AEMAR22705)	-13	1829

Please note the animal numbers supplied on this certificate are the total allocated for the approval duration

Please use this Approval Number:

1. When ordering animals from Animal Breeding Houses
2. For labelling of all animal cages or holding areas. In addition please include on the label, Chief Investigator's name and contact phone number.
3. When you need to communicate with this office about the project.

It is a condition of this approval that all project animal details be made available to Animal House OIC. (UAEC Ruling 14/12/2001)

The Chief Investigator takes responsibility for ensuring all legislative, regulatory and compliance objectives are satisfied for this project.

This certificate supercedes all preceeding certificates for this project (i.e. those certificates dated before 23-Feb-2018)